# PS LOGGING FOR
# SITE RESPONSE ANALYSIS IN DHAKA CITY

**A. S. M. FAHAD HOSSAIN**

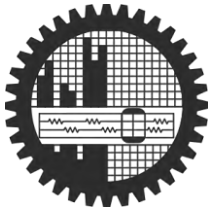

**DEPARTMENT OF CIVIL ENGINEERING**
**BANGLADESH UNIVERSITY OF ENGINEERING AND TECHNOLOGY**
**DHAKA, BANGLADESH**

**JANUARY, 2015**

# PS LOGGING FOR
# SITE RESPONSE ANALYSIS IN DHAKA CITY

A THESIS SUBMITTED BY

A. S. M. FAHAD HOSSAIN

IN PARTIAL FULFILLMENT OF THE REQUIREMENTS FOR THE DEGREE OF

MASTER OF SCIENCE IN

CIVIL AND GEOTECHNICAL ENGINEERING

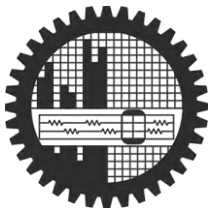

**DEPARTMENT OF CIVIL ENGINEERING**
**BANGLADESH UNIVERSITY OF ENGINEERING AND TECHNOLOGY**
**DHAKA, BANGLADESH**

**JANUARY, 2015**

The thesis titles –**PS LOGGING FOR SITE RESPONSE ANALYSIS IN DHAKA CITY**" submitted by A S M Fahad Hossain, Roll No. 0412042201; Session: April 2011 has been accepted as satisfactory in partial fulfillment for the requirement of the degree of Master of Science in Civil and Geotechnical Engineering on January, 2015

## BOARD OF EXAMINERS

| | |
|---|---|
| **Dr. Mehedi Ahmed Ansary**<br>Professor<br>Department of CE, BUET, Dhaka | **:** Chairmen<br>(Supervisor) |
| **Dr. A. M. M. Taufiqul Anwar**<br>Professor and Head<br>Department of CE, BUET, Dhaka | : Member |
| **Dr. Abu Siddique**<br>Professor<br>Department of CE, BUET, Dhaka | : Member |
| **Dr. Md. Abu Taiyab**<br>Associate Professor<br>Department of CE, DUET, Gazipur | : Member<br>(External) |

# DECLARATION

Declared that, except for the contents where specific reference has been made to the work of others, the studies embodied in this thesis is the result of research work, carried by the author.

Neither the thesis nor any part thereof has been submitted or is being concurrently submitted to any other educational institute for the award of any degree or diploma, except for publication.

January, 2015

_____

Author

# ACKNOWLEDGEMENT

First of all, thanks to the Almighty Great Allah for his kindness and blessings for allowing me to do this research work under supervision of Dr. Mehedi Ahmed Ansary and completing the thesis.

The author wishes to express his profound gratitude and sincere appreciation to his supervisor, Dr. Mehedi Ahmed Ansary, Professor, Department of Civil Engineering, Bangladesh University of Engineering & Technology (BUET), Dhaka. It would not be possible for the author to carry out this study without his continuous guidance and inspiration.

The author wishes to expresses special thanks to Professor Dr. Tahmeed Malik-Al Hussaini, Director of BUET-JIDPUS (Japanese Institute of Disaster Prevention and Urban Safety); for providing the instrumentations required for the test. The author also thanks the staffs of BUET-JIDPUS for their field supports for conducting the test.

The author wishes to express his sincere thanks to Mr. Naveel Islam, Graduate Student, Faculty of Engineering and Applied Science, Memorial University of Newfoundland, Canada, for field support. Without his support it would be very difficult for the author to conduct some tests in field.

Finally, the author wishes to express his gratitude to his parents, brother and all other family members for their continuous support and utmost sacrifice without which this thesis work would not come into reality.

# ABSTRACT

The purpose of this research is to measure shear wave velocity of different areas of Dhaka city using PS Logging and estimate the site amplification of those areas based on shear wave velocity. For this purpose, seventeen locations were selected in Dhaka city. Among them, PS logging was carried out at ten locations by the author and data of rest seven locations were collected from CDMP. Most of the sites are located on reclaimed areas which have filling sand up to a depth of 15 to 20m. Original soil is encountered at the surface in some places. In every location, Standard Penetration Test was carried out up to a depth of 30m and later in the same hole a 3inch PVC pipe was installed. Finally, shear wave velocities were estimated using Suspension PS Logging equipment in Down-hole technique.

Using 189 pairs of values of corrected SPT N and Shear Wave Velocity from seventeen locations, a correlation among Shear Wave Velocity, SPT N Value and Depth was developed and proposed for Dhaka city. Perfect correlation between variables would result in an "r" of 1.0. The coefficient of determination ($r^2$) is 0.45, which indicates a "r" value of 0.67. This means a significant amount of scatter exists in the measured data.

For estimating site amplification for those seventeen locations, acceleration computer program DEEPSOIL was used. With soil layer depth, unit weight ($\gamma$) and shear wave velocity ($V_s$) as inputs, soil amplification by equivalent linear analysis was estimated. Four input motions (The Imperial Valley Earthquake; the Kobe Earthquake; the Kocaeli Earthquake and the Northridge Earthquake) were used in these analyses, which were scaled to 0.19g value for bedrock in the Dhaka region. From the detailed site specific analysis, it was observed that Imperial Valley Earthquake produces the highest (2.46g) peak spectral acceleration (PSA) for the site East Nandipara and the Northridge Earthquake produces the lowest (0.002g) peak spectral acceleration (PSA) for most of the sites. The peak ground acceleration values at surface were observed to be in the range of 0.11g (Kocaeli) for the site Ashulia Jubok Project to as high as 0.66g (Northridge) for the site East Nandipara. The Amplification Factor of different locations were found in the range of 0.47 (Kocaeli) for the site Gulsan-2 to as high as 4.69 (Northridge) for the site East Nandipara. Four Site Amplification maps were prepared for Dhaka City for the above four input motions.

# Notations

| | | |
|---|---|---|
| SPT N | = | Standard Penetration Resistance number |
| $V_s$ | = | Shear Wave Velocity |
| $V_p$ | = | Compression Wave Velocity |
| E | = | Young‘s Modulus |
| K | = | Bulk Modulus |
| G | = | Shear Modulus |
| M | = | Constrained Modulus |
| $\rho$ | = | Density |
| $\nu$ | = | Poisson‘s Ratio |
| f | = | Frequency of vibration |
| $\lambda_R$ | = | Rayleigh wave length |
| $\phi(f)$ | = | Phase difference for a given frequency in radians |
| $l_R$ | = | Surface wave length |
| $m_s$ | = | Surface wave magnitude |
| $\mu$ | = | vertical particle displacement |
| PGA | = | Peak Ground Acceleration |
| PSA | = | Peak Spectral Acceleration |

# TABLE OF CONTENTS

## LIST OF TABLES



## LIST OF FIGURES

# CHAPTER ONE
# INTRODUCTION

## 1.1 General

Bangladesh did not suffer any damaging large earthquakes in the recent past, but in the past few hundred years, several large catastrophic earthquakes struck this area. The 1897 Great Indian Earthquake with a magnitude of 8.7, which is one of the strongest earthquake in the world killed 1542 and affected almost the whole of Bangladesh (Oldham, 1899). Recently, Bilham et al. (2001) pointed out that, there is a very high possibility that a huge earthquake will occur around the Himalayan region based on the difference between energy accumulation in this region and historical earthquake occurrence. The population increase around this region is the last 50 times than the population of 1897 and city like Dhaka has population exceeding several millions. It is a cause for great concern that the next great earthquake may occur in this region at any time.

## 1.2 History of Suspension PS Logging

P-S suspension velocity logging was first developed in the mid-1970s to measure seismic shear wave velocities in deep, uncased boreholes; it was originally used by researchers at the OYO Corporation of Japan (**Kaneko et al., 1990).** It gained acceptance in Japan in the mid-1980s and was used for other velocity measurement methods to characterize earthquake site response. Public Works Research Institute (PWRI) of Japan has measured S-wave velocities in boreholes using the PS suspension logging tool since 1980. Since the early 1990s it has gained acceptance in the United States, especially among earthquake engineering researchers of US .

## 1.3 Worldwide Use of Suspension PS Logging

PS Logging techniques are being used worldwide. Some example of some research works are shown below. Tomio Inazaki (2006) investigations; where shear wave velocities of surficial unconsolidated sediments was o correlate with geotechnical properties determined by laboratory testing. The S-wave velocity data, all of them were accurately measured in boreholes using the PS suspension logging tool. N-values

obtained by in situ Standard Penetration Test (SPT), bulk densities, solidities, and mean grain sizes measured by the standard soil test, and elastic constants determined by tri-axial dynamic loading tests were correlated with the S-wave velocities at the same horizons in the same boreholes. However the dynamic range and measurement accuracy of SPT was too low to compare with S-wave velocity data obtained using the suspension logging tool. So it was possible to estimate N-values from S-wave velocity data using his empirically synthesized equation.

Ming-Hung Chen et al. (2012) showed that 175 strong-motion station sites were investigated by National Center for Research on Earthquake Engineering (NCREE) and Central Weather Bureau (CWB) to characterize the subsurface conditions that affect measured ground motions measuring in soil, gravel and rock layers throughout Taiwan. The suspension P-S Logging method was applied at most sites because of its high accuracy and resolution. He showed that that the frequencies and wave lengths of receiving signals varied with different subsoil materials. The investigated shear wave velocity profiles of an alluvial deposit in southwestern Taiwan were introduced. Based on the abundant and reliable shear wave velocities, an empirical formula for alluvial deposits was developed. Depth and corrected SPT-N value were chosen to be two major parameters of the empirical formula. For some specific sites, surface wave, seismic refraction, or down-hole velocity measurements were also executed. The results of various tests are generally very close and increase the reliability of the measurements.

Emre Biringen and John Davie (2011) made correlations between the values of P-wave velocity and dynamic elastic modulus through in-situ dynamic testing (suspension P-S logging) and the values of uniaxial compressive strength (UCS) and static elastic modulus through laboratory static testing (uniaxial compressive) of sound rock from two sites located in South Carolina and Virginia. For both sites, the bedrock, which classified as good to excellent, is hard fresh to slightly discolored metamorphic rock, or igneous rock with numerous metamorphic inclusions. Suspension P-S logging tests were performed in 12 uncased fluid-filled boreholes, to rock depths of over 120 m.
Ming-Hung Chen and Bing-Ru Wu (2003) showed in another paper that, the site investigation at 175 TSMIP stations was completed by National Center for Research on Earthquake Engineering (NCREE) cooperating with Central Weather Bureau (CWB) in Taiwan. By sampling soils in the borehole and using the Suspension P-S Logger

Technique, specific geological and geotechnical data are obtained including the soil profile, the physical properties of soils, and the wave velocities of the stratum. This database is helpful to the site effect analysis and the earthquake-resistant design.

Michael W. Asten and David M. Boore (2005) showed that measurement or estimation of the shear wave velocity (Vs) profile of sediments overlying geological basement is a vital part of site zonation studies for earthquake hazard prediction, and more generally for geotechnical studies. A series of boreholes drilled in the Santa Clara Valley Water District provide opportunity for the comparison of geophysical methods (PS Logging, SASW, and MASW) with known geological data. The author compared the shear-wave velocity profiles obtain from fourteen invasive and non-invasive methodologies obtained in and near a single 300 m borehole.

Itzair Perez et al. (2011) compared SASW and PS-logging (in-hole) seismic techniques with the relatively new ReMi (Refraction Micro tremor) method at a common site with a well-known soil profile: a recently constructed high-speed railway embankment. The author showed that the PS-Logging is the most accurate technique in identifying the soil profile of the embankment followed by Re-Mi and SASW. Mean shear wave velocity estimations are also higher for PS-logging, followed by SASW and ReMi, while mean deviation is similar in each technique.

### 1.4 Information of the Study Area

Dhaka City is almost flat, with many depressions, bounded by rivers on all four sides topographically. The surface elevation of the city ranges between 1.7 and 14 meters above mean sea level, but is generally around 6.5 meters. The average depth of the groundwater table is 3 meters. The seasonal variation of the water table ranges from 1 to 2 meters. The urban area is situated in a seismic zone, which has experienced earthquake intensities of up to IX at the Modified Mercalli scale. Geologically, nine units can be distinguished. The depressions and abandoned channels are dominated by organic clay and peat. The main part of the city lies either on Madhupur Clay, old natural levees, high flood plains, or filled-in gullies. The Madhupur Clay, with its average thickness of 8 meters, consists of over-consolidated clayey silt and is underlain by the Plio-Pleistocene Dupi Tila Formation.

The area investigated is divided into seven engineering geological units based on their physical properties, homogeneity, and distribution of subsurface strata. Engineering geological units I, II and III consist generally of consolidated clayey silt layers at the top, underlain by dense Dupi Tila sand, found above the normal flood level, a favorable condition for urban settlement. However, the present expansion of the city is towards the low-lying areas, notably in depressions and flood plains. In general, the fill layer in depressions is about 5 meters thick. Fine-grained sand, clayey silt, organic clay, even peat and garbage are being used as fill materials.

Unfortunately, most of the natural drainage systems are currently obstructed due to these filling activities. Every rainy season, the city faces problems due to stagnant water. As part of the city's flood control measures, the construction of a flood-protection embankment under way, along the rivers, mainly in depressions, using locally excavated sediments without any core.

### 1.4.1 Location, Extent and Accessibility

Dhaka is situated in the centre of Bangladesh, between longitude 90°20' E and 90°30' E and latitude 23°40' N and 23°55' N. It is covered by the Survey of Bangladesh topographical sheet numbers 79 1/5 and 79 1/6. Figure 1.1 shows the location map of the Dhaka City.

The present area of the city is 256 square kilometers, bounded by the Demra in the east, the Turag River in the west, the Tongi Khal in the north and the Burhiganga River in the south. In and around the city, an area of 280 square kilometers has been mapped.

The city is well connected with other parts of the country, as well as the rest of the world with its roads, railways, airways and waterways. Kamalapur Station is the main railway station and Sadarghat the main water-transport terminal, while Hazrat Shahjalal International Airport is Dhaka's main airport, situated at Kurmitola.

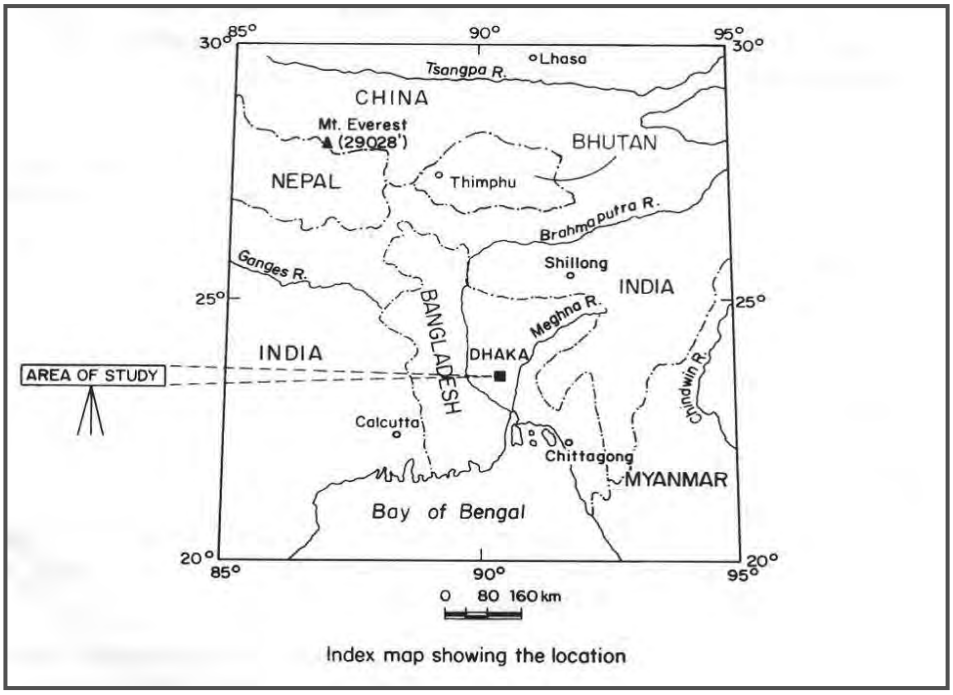


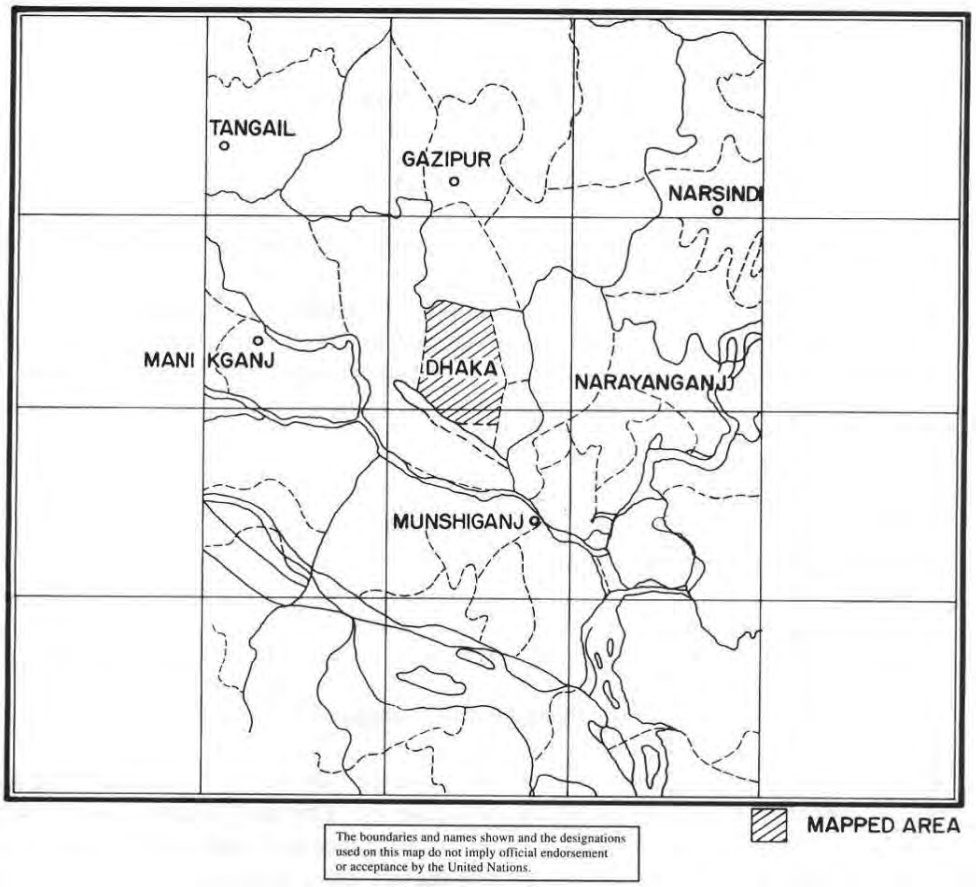


Figure 1.1 Location map of the study area

### 1.4.2 Geomorphology of the Study Area

Regionally, the study area lies in the extreme southern part of the Madhupur Tract. This tract is situated in the central-eastern part of Bangladesh, with an overall elevation of more than 16 meters above mean sea level, lowering gradually towards the south. The area is surrounded by the old Brahmaputra flood plain in the north and east, by the Ganges-Meghna flood plain in the south and by the Jamuna flood plain in the west. The regional geomorphology around Dhaka is shown in Figure1.2 and the elevation in Figure1.3.

The main city is situated on the Madhupur Tract. This is bounded by the flood plains of the Ganges and the Brahmaputra system. Geomorphologically, the study area is divided into the following units based on surface morphology and elevation (Figure 1.4):

- high land (AH)
- mixed high and low lands (AM)
- low land (AL)
- abandoned channel (AC)
- natural levee (NL)
- depression (D)
- sand bar (SB)
- point bar (PB)

The elevation of the area investigated ranges from 2 meters to 14 meters above mean sea level. The highest elevation is 14 meters above mean sea level at the Pallabi area and the lowest is 1.8 meters above mean sea level found in a depression behind Rampura TV station. The elevation of mapping unit All ranges from 4 meters to 15 meters; AL ranges from 2 meters to 4 meters and areas less than 2 meters are depressions (D).

The city is bounded by rivers on all sides, the Burhiganga in the south, the Balu River in the east and the Turag in the west and north. The depressions are north-south trending in both the eastern and western parts of the city. The city is divided by an abandoned channel named Begunbari Khal, trending east-west. The general slope of the city is towards both east and west. A sharp boundary between the high Madhupur Clay and depressions is observed both in the eastern and western side of the city area.

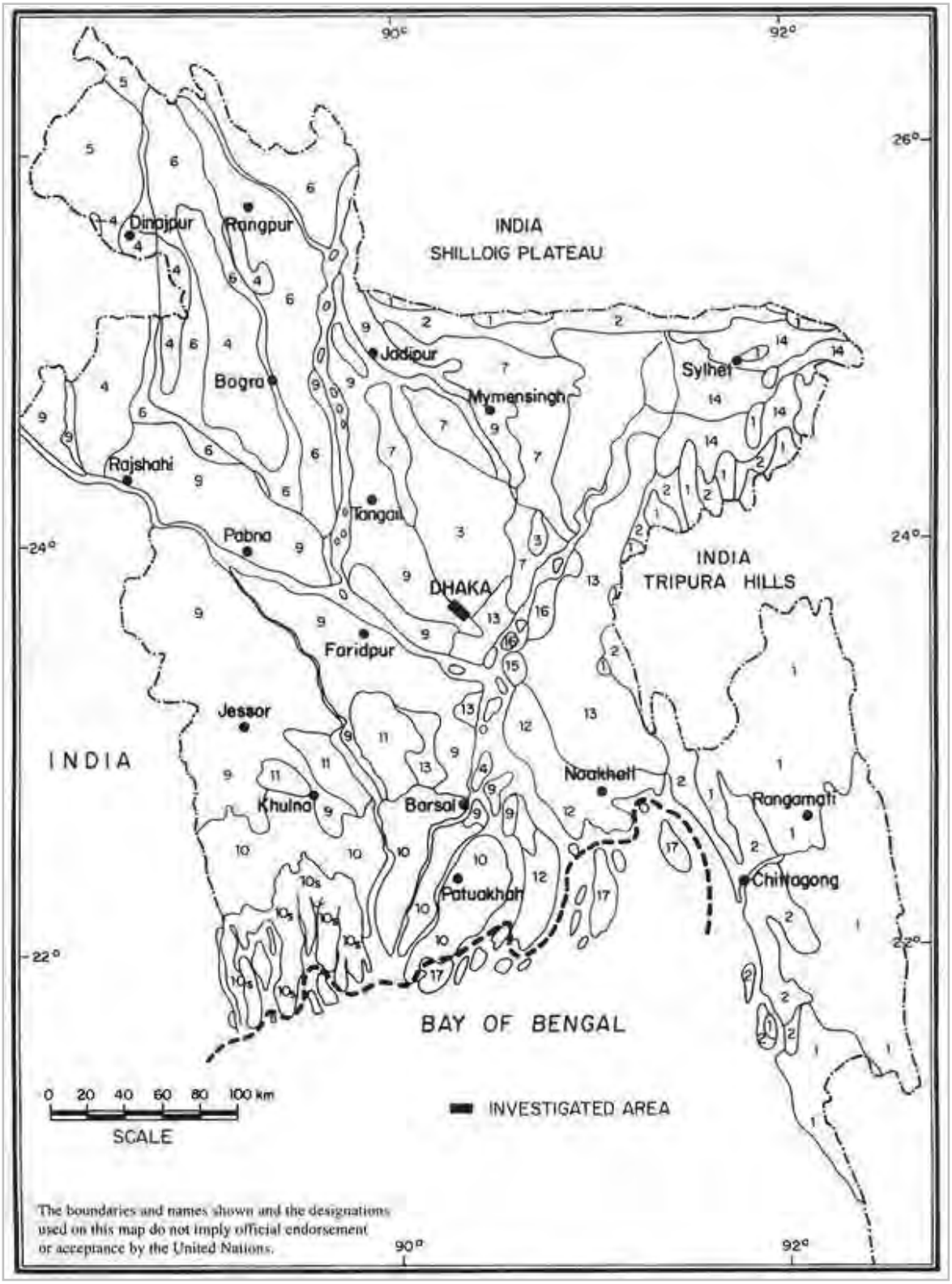


Figure 1.2 Preliminary geomorphologic subdivision of Bangladesh.

(Source: Modified from Brammer, 1971)


Figure 1.3 Generalized contour map of Bangladesh.

(Source: Master Plan Organization, 1985)

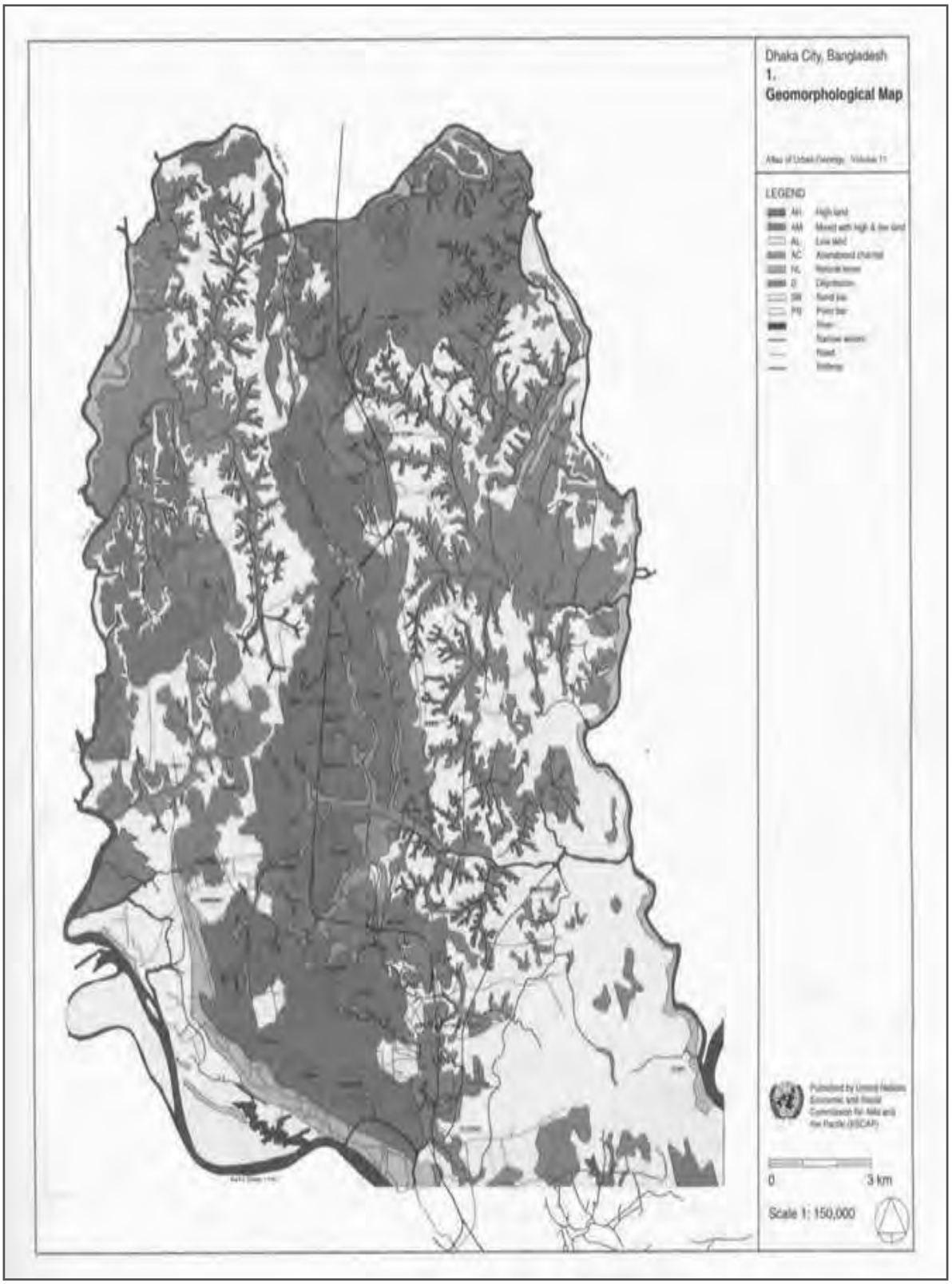


Figure 1.4 Geomorphologic map of Dhaka

(Source: United Nations Economic and Social Commission of Asia and the Pacific)

### 1.4.3 Geology of the Study Area

Dhaka City lies on the southeastern corner of Madhupur Tract along the Burhiganga River on a regional basis. This tract is made of sediments of Pleistocene age, which is underlain by the Plio-Pleistocene Dupi Tila Formation. The Madhupur Tract is bounded by the Ganges flood plain in the south, the Brahmaputra-Meghna flood plain in the east, the Brahmaputra flood plain in the north and the Jamuna flood plain in the west. Figure 1.5 shows the general regional geology of the area.

On the basis of geomorphological expression and sediment characteristics, the area has been divided into nine geological units having deposits of the following:

- Sand bar/point bar
- Active natural levee
- Flood plain
- Depression
- Abandoned channel
- Gully fill
- High flood plain
- Old natural levee
- Madhupur Clay.

**Sand bar/point bar deposits**

These deposits consist mainly of loose and fresh sand and are medium to fine grained. Some yellowish-brown sand patches are observed at many places. Few laminations of silty materials are found in the sand. At places, the percentage of silt is comparatively high.

**Active natural levee deposits**

These deposits consist dominantly of sand with many discontinuous thin laminations of sandy silt and clayey silt. The sand is light brown to light gray in color, fine to course grained and moderately compact. This unit is more elevated than its surrounding areas.

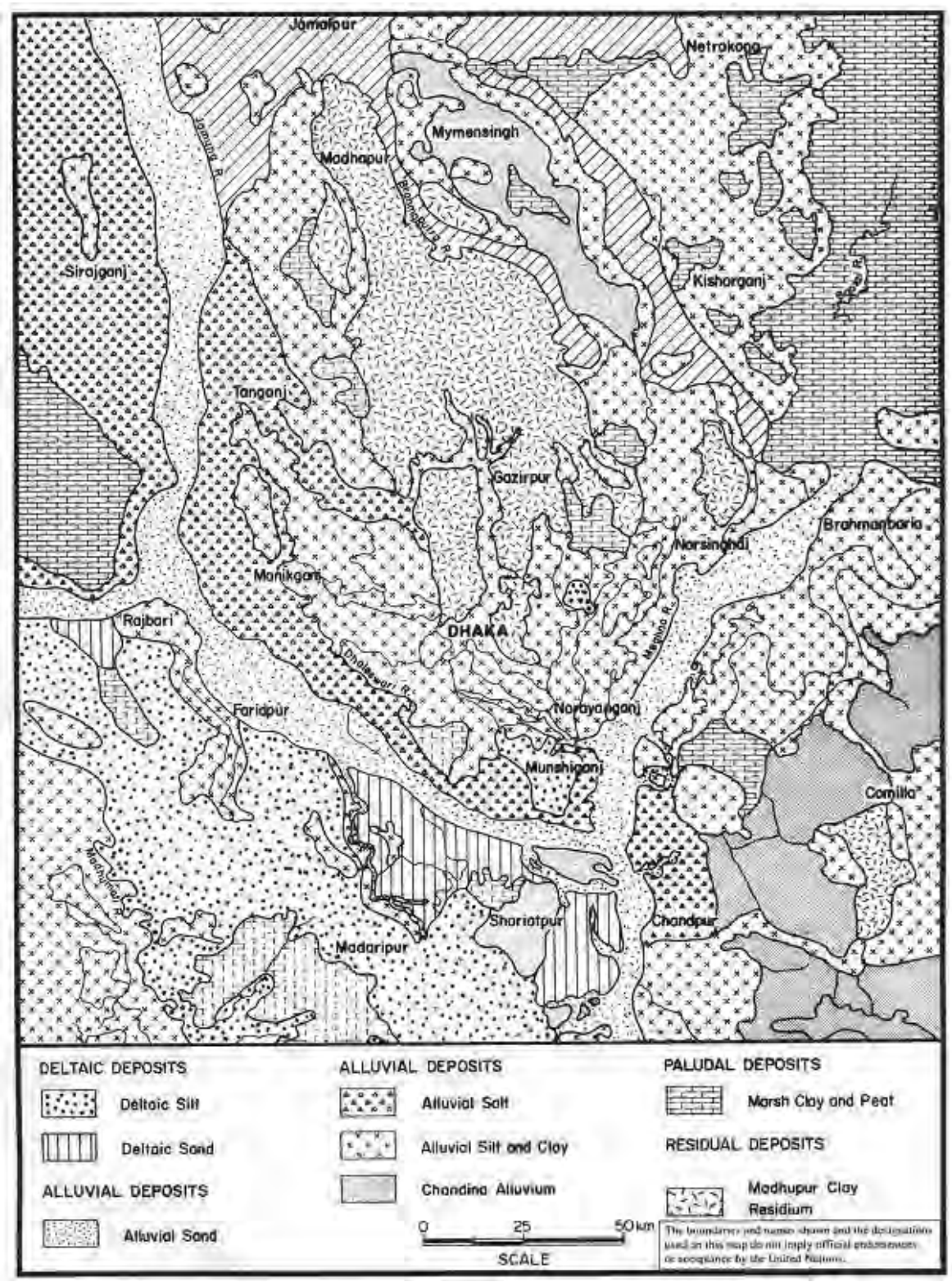


Figure 1.5 Geological map of the Dhaka Region.

(1988)

**Flood plain deposits**

The flood plain is the extended flat, poorly drained land that is flooded annually. These deposits consist of alternating silt, clay, fine sand and peaty clay. At many

places, peat layers are a few centimeters to 0.3 meters thick within 1 meter from the surface. Generally, the upper 1 meter is silty clay to clayey silt, which is light gray to light yellowish brown in color. Below this, thick layers of light gray to yellowish-brown silty clay with mottling and ferruginous concretions are found. Alternating layers of blackish-gray organic clay and blackish-brown silty clay are generally found in the unit in down slope areas near depressions. At places, alternating fine-sand layers are found irrespective of depth, where peat layers from a few centimeters to 0.3 meters thick are found in near surface. Decomposed and partially decomposed grass roots and animal burrows are common at the upper part of the unit.

**Depression deposits**

Depressions are the deepest part of the area situated above 1.3-2 meters above mean sea level. Most of the area is usually covered with water year round but occasionally dry during the winter. In aerial photographs, the area shows dark-gray tone. The deposit consists of gray to light-gray organic clay, dark gray to blackish-gray peaty clay and blackish to dark-brown peat. Decomposed and partially decomposed vegetal matters are common. The sediments are highly sticky and plastic with high natural moisture content A few patches of reddish- to yellowish-brown silty clay with orange-red mottling are sporadically present. This silty clay is medium to high plastic and compacted. Some blackish-gray, thin, fine-sand layers (+0.6 meters) with a large amount of silicified tree branches (0.26 centimeters mean diameter and 2 centimeters length) coated with yellowish-brown, fine sand are present near the reddish to yellowish-brown, silty clay patches.

Generally, two layers of peat with average thickness of 1 meter were found. These layers are present within 1-4 meters below the surface. These peats, containing fibers from decomposed and partially decomposed tree branches, are spongy, medium to light weight when dry and mixed with some clay. According to local people and field investigation, buried partially decomposed tree trunks are found 3-5 meters below the surface at many places in depressions.

### Abandoned channel deposits

Channel segments that are abandoned by avulsion or cut-off process become flood plain lakes of identifiable origin. Surface deposits are silty clay or clayey silt that are dark gray, greenish gray to yellowish gray with yellow and brown mottling in many localities. Below the near surface, thick layers of organic clay and peat are common.

### Gully fills deposits

Along the edge of the high Madhupur Clay unit, several small drainage channels of dendrite patterns have formed to drain out water to low-lying areas. Due to partial or complete obstruction of the main channel of the drainage system, the amount and velocity of the water flow decreases; as a result, sedimentation starts on the channel base and the channels are filled up. The main sediments constituting this unit are light-gray to dark-gray sticky, clayey silt. A few thin layers of yellowish-brown, fine sand and blackish-gray organic clay are present. Occasionally, garbage and thin bands of sand layers are also found at some places. The thickness of the top layer ranges from 1.5 to 2.5 meters, which is underlain by Madhupur Clay.

### High flood plain deposits

The top layer of this unit is light-gray to yellowish-brown sandy silt and bluish-gray silty clay, which is underlain by yellowish-brown to reddish-brown Madhupur Clay. Thickness of the top layer is 1.7-3 meters. Worm burrows, root tubes and vegetal matters are common.

### Old natural levee deposits

The sediments are mainly grayish-brown, sandy silt and silty clay with thin lamination of yellowish-brown, fine sand. Few peaty matter and small pieces of wood are present at places. The sediments are well compacted and oxidized along rootlets and fractures. The thickness of the sediment is generally 2-3 meters, underlain by Madhupur Clay. The area gently slopes towards the city side. This unit generally lies above high-flood level and general elevation is more than 6.5 meters above mean sea level. The old natural levee sediments were deposited on Madhupur Clay unit.

**Madhupur clay**

This unit mainly consists of yellowish-brown to reddish-brown, highly oxidized, silty clay. The main characteristics of this unit are orange-red mottling, high oxidation and a metallic-black iron oxide accumulation in nodular form with a nucleus. This black nucleus might have been formed by manganese. Some yellowish-brown ferruginous nodules are also present. The reddening of color increases with depth. Some sand and mica are present in this unit. The clays are mainly kaolinite and illite (Chowdhury and others, 1989). Secondary light-bluish gray, plastic silty clay is deposited along fractures and animal burrows. The sediments of this unit are highly compacted, medium plastic and sticky. The average thickness of this unit is about 8 metres. This unit is underlain by Dupi Tila Formation and is probably a residual deposit.

### 1.4.4 Tectonic Activities of the study area

Bangladesh is surrounded by regions of high seismicity, including the Himalayan Arc and the Shillong Plateau in the north, the Burmese Arc and the Arakan Yoma Anticlinorium in the east and the complex Naga-Disang-Haflong thrust zones in the northeast (Hussain, 1989). Northern and eastern Bangladesh and adjoining regions lie in one of the most seismically active zones in the world. Historical records show that Bangladesh has been shaken by at least 9 major earthquakes during the past 250 years and at least 159 small to medium earthquakes from 1906-1988, of which 48 events had magnitudes of $M_b$ 4.0 to 7.5 between 1962 and 1988.

Dhaka City falls in earthquake zone II of the seismic-zoning map of Bangladesh. The probable maximum intensity predicted for this zone is 6.0 to 6.5, with a seismic coefficient of 0.05 (Geological Survey of Bangladesh; pers. comm., 1979), but according to Kaila and Sarkar (1978), Dhaka experienced a maximum earthquake on 12 June 1897, with an intensity of IX at the Modified Mercalli scale (Figure 1.6, Table 1.1). The great earthquake of 1897 did much damage to Dhaka but, luckily, it caused comparatively little loss of life (Rizvi, 1975).

Before this great earthquake, Dhaka experienced six medium to large earthquakes: in April 1762 and 1775; on April 10 and May 11, 1812; in December 1876; and on July 14, 1885.The earthquake of 1762 proved to be very violent in the city and along the eastern bank of the Meghna River as far as Chittagong. At Dhaka, the rivers and depressions were agitated and raised high above their usual levels. The shocks were accompanied by subterranean hollow noises, destroyed many civil structures and killed over 500 people. The earthquakes of 1812 also damaged and destroyed many civil structures in the city, especially at the Tejgaon area (Rizvi, 1975). In the last decade, Dhaka felt many small tremors but no major damage of civil structures was reported. After the earthquake of 1967, many sand boils were formed in and around Dhaka. Many cracks on roads and civil structures were also found after the earthquake (personal communication, Coleman, 1990)

Table 1.1 Major historical earthquakes in and around Bangladesh

| *Date* | *Location* | *Magnitude [Richter scale]* | *Maximum intensity** | *Deaths* | *Damage [US$] in million* | *Maximum intensity* in Dhaka* |
|---|---|---|---|---|---|---|
| 1/10/1737 | Calcutta, India | — | — | 300,000 | >1 | — |
| 2/4/1762 | Chittagong, | — | VII | 500 in Dhaka | >5 | — |
| 10/4/1812 | Dhaka, Bangladesh | — | — | | — | — |
| 10/6/1869 | Assam, India | — | — | | | — |
| 12/6/1897 | Assam, India | 8.7± | XII | >1,542 | >25 | IX |
| 8/7/1918 | Srimangal, | 7.6 | X | | 1 | VI |
| 3/7/1930 | Dhubri, India | 7.1 | IX | | — | V |
| $1^{5}/_{1}$/1934 | Bihar, India-Nepal | 8.1 | X | 10,000 | >25 | VI |
| 15/8/1950 | Assam, India | 8.7 | X | | — | V |
| 1967 | Koyna, Assam , India | 6.5 | — | — | — | — |

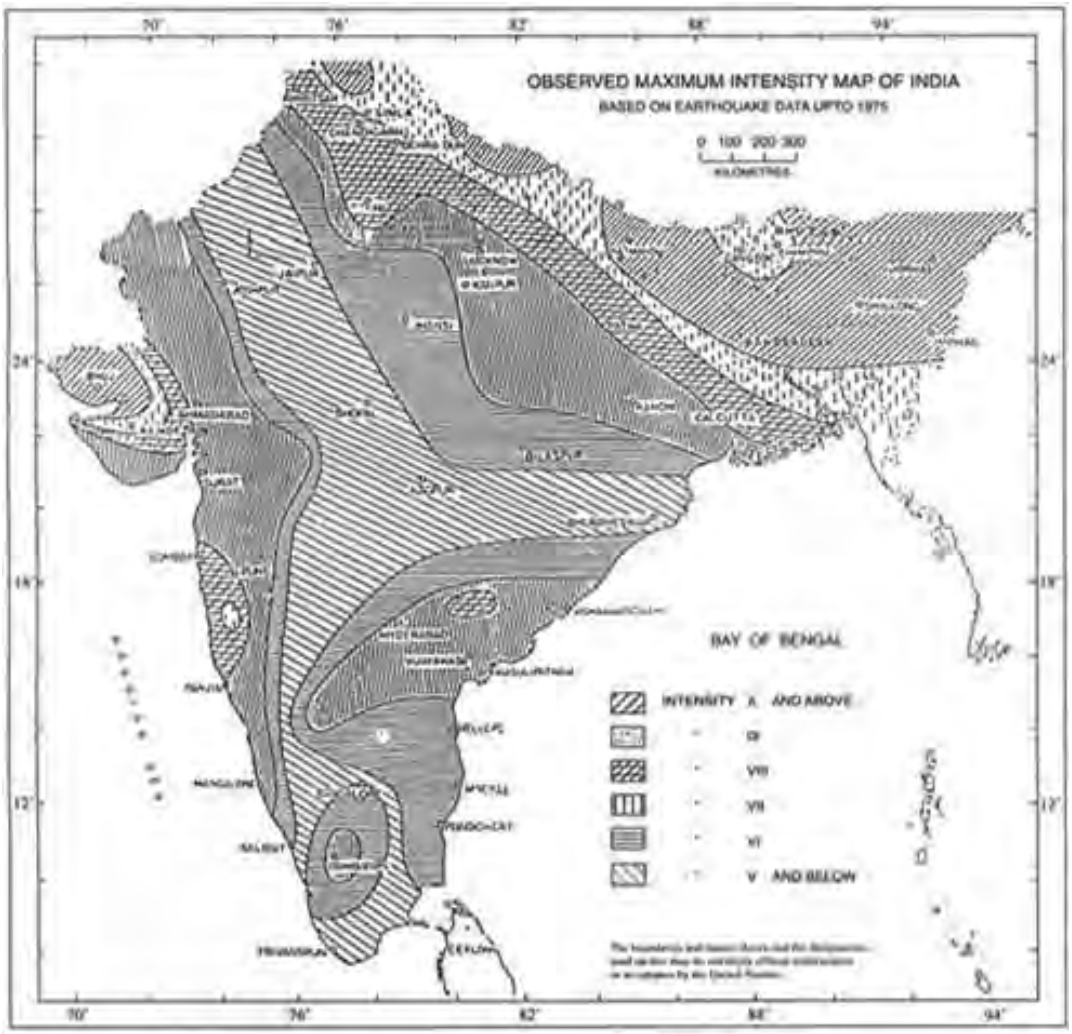


Figure 1.6 Observed maximum intensity map of the Indian subcontinent.
(Source: Kaila and Sarkar, 1978)

## 1.5 Objectives of the Research

Based on the problems identified in the above sections, the main objectives of the present study are:

- To use PS Logging to estimate shear-wave velocity of soils using seismic down-hole technique at different locations of Dhaka city.
- To develop correlation between shear-wave velocity (Vs), SPT N value and depth.
- Propose velocity profile for different locations of Dhaka city.
- To estimate site amplification through ground response analysis of those locations of Dhaka city using the program DEEPSOIL.

## 1.6 Outline of the Study

The thesis comprised of five chapters.

Chapter One (Introduction) is the presentation of a brief introduction to the subject states the major objects of the study and need for ground response analysis.

Chapter Two (Literature Review) presents a brief review of the existing literature on Seismic Down-hole, Up-hole and Cross-hole techniques, methodology of PS Logging, Determination of Seismic wave velocities from the data obtained, different dynamic properties of soil and their determination, site amplification procedures using DEEPSOIL.

Chapter Three (Field Investigation) presents the SPT N Value and Shear Wave Velocity at different locations.

Chapter Four (Results Ground Response Analysis) presents detailed site response analysis using DEEPSOIL software. Using the software, response spectra, amplification factor and peak ground acceleration at different locations is estimated. Also amplification maps were prepared.

Chapter Five (Conclusions and Recommendations) presents a summary of the results and findings resulting from this work. It includes recommendations for future research. List of references and appendices follows.

# Chapter Two
# Literature Review

## 2.1 General

This chapter deals with, Earthquake, its different waves, Richter and Intensity scales. Different dynamic properties of soil and different tests for determination of these properties are discussed. This chapter also deals with detail procedure of PS Logging technique. Seismicity and seismic zoning of Bangladesh is described. At the last portion of this chapter, the site amplification of soil and its different analysis is included.

## 2.2 Earthquake and Seismic Waves

An earthquake is the result of a sudden release of energy in the Earth's crust that creates seismic waves. The elastic rebound theory is an explanation for how energy is spread during earthquakes. As rocks on opposite sides of a fault are subjected to force and shift, they accumulate stress energy and slowly deform (strain) until their internal strength is exceeded. At that time, a sudden movement occurs along the fault, releasing the accumulated energy, and the rocks snap back to their original undeformed shape.

During the earthquake, the portions of the rock around the fault that were locked and had not moved 'spring' back, relieving the strain (accumulated over several years) in a few seconds. Like an elastic band, the more the rocks are strained the more elastic energy is stored and the greater potential for an event. The stored energy is released during the rupture partly as heat, partly in damaging the rock, and partly as elastic waves. Modern measurements using GPS largely support Reid‘s theory as the basis of seismic movement, though actual events are often more complicated.

We can define earthquake as: a sudden and violent motion of the earth caused by volcanic eruption, plate tectonics, or manmade explosions which lasts for a short time, and within a very limited region.

Seismic waves are generated by the release of energy during an earthquake. They travel through the earth like waves travel through water. The location within the Earth where the rock actually breaks is called the focus of the earthquake. Most foci are located within 65 km of the Earth's surface; however, some have been recorded at depths of 700 km. The location on the Earth's surface directly above the focus is called the epicenter. The study of seismic waves and earthquake is called seismology, which is a branch of geophysics.

Two types of seismic waves are generated at the earthquake focus:

1. Body waves spread outward from the focus in all directions.
2. Surface waves spread outward from the epicenter to the Earth's surface, similar to ripples on a pond. These waves can move rock particles in a rolling motion that very few structures can withstand. These waves move slower than body waves

There are two types of Body Waves:

### 2.2.1 Primary Wave (P wave)

The P-wave, where P stands for Primary wave or Pressure wave and it is formed from alternating compressions and rarefactions the particles in the solid have vibrations along (or parallel to) the travel direction of the wave energy. P wave can pass through a fluid (gas or liquid) and arrives at recording station first. Figure 2.1 shows the P wave.

### 2.2.2 Secondary Wave (S wave)

The S-wave, where S stands for Secondary wave or Shear wave, moves as a shear or transverse wave, so motion is perpendicular to the direction of wave propagation S-waves are like waves in a rope. S-waves are slower than P waves, and speeds are typically around 60% of that of P waves in any given material. This wave cannot pass through a fluid (gas or liquid). Figure 2.2 shows the S wave.

Surfaces waves are produced when earthquake energy reaches the Earth's surface. Surface wave moves rock particles in a rolling and swaying motion, so that the earth

moves in different directions and waves are the most destructive for structures on earth. Surface waves are of two types- Rayleigh and Love waves - are generated by the interaction of P- and S- waves at the surface of the earth, and travel with a velocity that is lower than the P-, S- wave velocities.

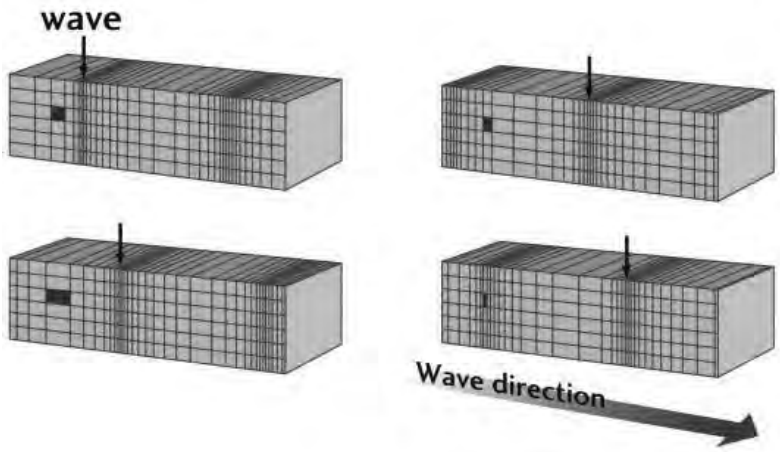


Figure 2.1 P Wave

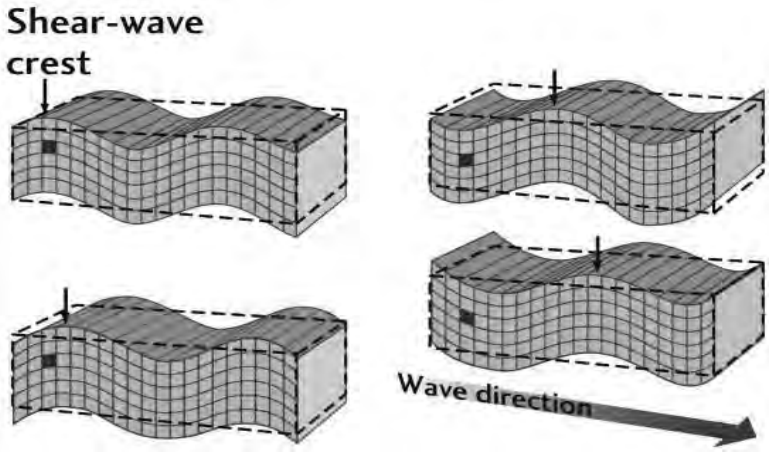


Figure 2.2 S wave

### 2.2.3 Rayleigh waves

Rayleigh waves also called ground roll, are surface waves that are confined to the Earth‘s surface where they travel as ripples with motions that are similar to those of waves on the surface of water. The surface particles move in ellipses in planes normal to the surface and parallel to the direction of propagation. At the surface and at shallow depths this motion is retrograde (unlike water waves). Particles deeper in the material move in smaller ellipses with an eccentricity that changes with depth. The speed of

Rayleigh waves on bulk solids, of the order of 2–5 km/s, is slightly less than the S-waves velocity. Figure 2.3 shows the Rayleigh wave.

### 2.2.4 Love waves

Love waves are surface seismic waves that cause horizontal shifting of the earth during an earthquake. The particle motion of a Love wave forms a horizontal line perpendicular to the direction of propagation (i.e. are transverse waves). The amplitude, or maximum particle motion, often decreases rapidly with depth. Figure 2.4 shows the Love wave.

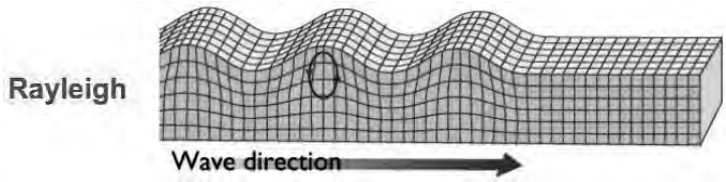


Figure 2.3 Surface Waves (Rayleigh Wave)

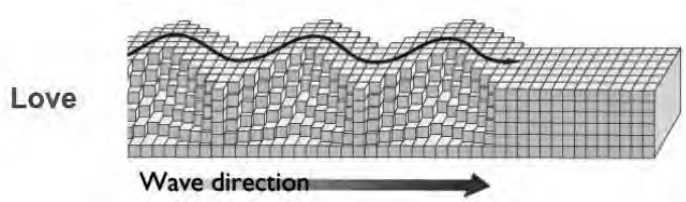


Figure 2.4 Surface Waves (Love Wave)

## 2.3 Dynamic Soil Properties and Tests

The analysis of foundation vibrations and geotechnical earthquake engineering problems in civil engineering requires characterization of dynamic soil properties using geophysical methods.

Structural analysis of the superstructures also requires knowledge of the dynamic response of the soil-structure, which, in turn relies on dynamics soil properties. Machine vibrations, blasting and seismic events are example so the type of dynamic input that an engineered systems may be subjected to. Geophysical methods are often used to characterize the dynamic soil properties of the subsurface

The response of soils to cyclic loading is controlled mostly by the mechanical properties of the soil. There are several types of geotechnical engineering problems associated with dynamic loading, some examples include: wave propagation, machine vibrations, seismic loading, liquefaction and cyclic transient loading, etc. The mechanical properties associated with dynamic loading are shear wave velocity (Vs), shear modulus (G), damping ratio (D), and Poisson‘s ratio (n) etc. The customary name for this type of properties is –dynamic soil properties”, even though they are also used in many non-dynamic type problems. The engineering problems governed by wave propagation effects induce low levels of strain in the soil mass. On the other hand, when soils are subjected to dynamic loading that may cause a stability problem then, large strains are induced.

The usual dynamic soil properties of soil are

- Dynamic modulli- Young‘s modulus E, Shear modulus G, Bulk modulus K.
- Poisson‘s ratio ν.
- Damping ratio D or h.
- Liquefaction factors- Cyclic shear stress, cyclic deformation and pore pressure response.
- Shearing strength in terms of strain rate effects.

Shear Modulus, Constrained Modulus, Poisson‘s Ratio, Young‘s Modulus and Bulk Modulus can be determined from the equation 2.1, 2.2, 2.3, 2.4 and 2.5.

The equations for determining the dynamic properties are as follows,

$$G = \rho V_S^2 \quad (2.1)$$

$$M = \rho V_P^2 \quad (2.2)$$

$$\nu = [0.5(\frac{V_p}{V_S})^2 - 1]/[(\frac{V_P}{V_S})^2 - 1] \quad (2.3)$$

$$E = 2G(1+\nu) \quad (2.4)$$

$$K = \frac{E}{3(1-2\nu)} \quad (2.5)$$

*Here,*

G = Shear Modulus

M = Constrained Modulus

ρ = Density

$V_s$ = Shear Wave Velocity

$V_p$ = Compression Wave Velocity

ν = Poisson's Ratio

E = Young's Modulus

K=Bulk Modulus

### 2.3.1 Tests for measurement of Dynamic soil properties

**Field test**

The dynamic properties of soil can be obtained from the following field tests.

- Seismic reflection test
- Seismic refraction test
- Seismic cone penetration test
- Suspension logging test
  - Seismic down-hole technique
  - Seismic up-hole technique
  - Seismic cross-hole technique
- Steady State Vibration Test/ Surface Wave Technique
- Spectral Analysis of Surface waves Test

**Laboratory Test**

The dynamic properties of soil can be obtained from the following laboratory tests.

- Cyclic Triaxial Test
- Cyclic direct simple shear test
- Resonant Column test
- Ultrasonic pulse test
- Cyclic tortional shear test
- Piezoelectric bender element test
- Shake table Test
- Centrifugal test

## 2.4 Different Geophysical Methods

Geophysical methods have been used for many years by engineers in soils and foundation applications. Geophysics not only provides means to probe the properties of soils, sediments and rock outcrops, but is also used to determine dynamic properties of soils, particularly the soil‘s compression and shear wave velocities, as well as the soil‘s elastic and shear moduli. These properties are key parameters in predicting the response of soils and soil-structure systems to dynamic loading. The geophysical methods used in determining dynamic properties of soils are mainly field or in-situ tests based on measurement of velocities of waves propagating through the soil. The most common tests used for such purposes are presented subsequently.

### 2.4.1 Seismic Reflection Test

The seismic reflection test allows the wave propagation velocity and thickness of surficial layer to be determined from the ground surface. For the simple profile shown in Figure 2.5 the test is performed by producing an impulse (usually rich in P wave) at the source S, and measuring the arrival time at the receiver, R. The impulse produces stress wave that radiate away from the sources in all direction with a hemispherical wave front. Some of the wave energy follows a direct path from S to R and arrives at R at:

$$t_d = \frac{x}{v_{pl}}$$

Where, x is distance of travel and $v_{pl}$ is wave velocity.

By measuring x and $t_d$, the wave velocity of the upper layer, $V_{pl}$, can easily determined. Another portion of the impulse energy travels downward and strikes the horizontal layer boundary at an angle of incidences (eq-2.6).

$$i = \tan^{-1}\frac{x}{2H} \tag{2.6}$$

The part of that wave that is reflected back toward the ground surface arrives at the receiver at time (eq-2.7):

$$t_r = \frac{2\sqrt{H^2+(x/2)^2}}{v_{pl}} = \frac{\sqrt{4H^2+x^2}}{v_{pl}} \tag{2.7}$$

By measuring tr and knowing vpl from the direct wave calculation, the thickness (eq-2.8) of the upper layer can be calculated as:

$$H = \frac{1}{2}\sqrt{t_r^2 v_{pl}^2 - x^2} \tag{2.8}$$

### 2.4.2 Seismic Refraction Test

The seismic refraction method is well suited for general site investigations for soil dynamics and earthquake engineering purposes. This technique provides for the determination of elastic wave velocities of a layered soil profile. Wave velocities and thickness of each layer are determined as long as the wave velocities increase with each successively deeper layer. The test aims to accurately measure the arrival-times of the seismic body waves, which consists of Compression P and shear S waves, produced by a near-surface seismic source. The source travels through the soil to a linear array of detectors placed at the ground surface. Compression P -waves arrive at a receiver faster than shear S waves, thus obscuring the arrival of the latter waves i.e. the S -waves. Therefore the P-waves have been widely used in seismic refraction tests (Woods, 1978; Whiteley, 1994). Figure 2.6 and Figure 2.7 shows the Seismic Refraction test.

However, in most dynamic soils problems, the shear wave velocity and shear moduli are the most important properties of the soils. As such, direct measurement of the shear wave velocities, by using a rich source of shearing energy that is able to propagate over long distances, is in advantage for geotechnical earthquake engineering problems. In addition, P-wave velocities at or below the water table depend on the degree of saturation of the soil, whereas the S-wave velocities are independent (Woods, 1978).

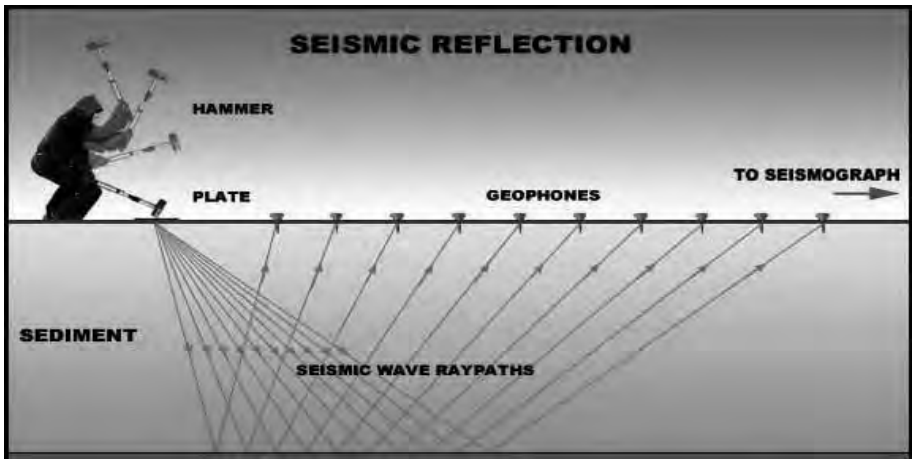


Figure 2.5 Seismic Reflection Test

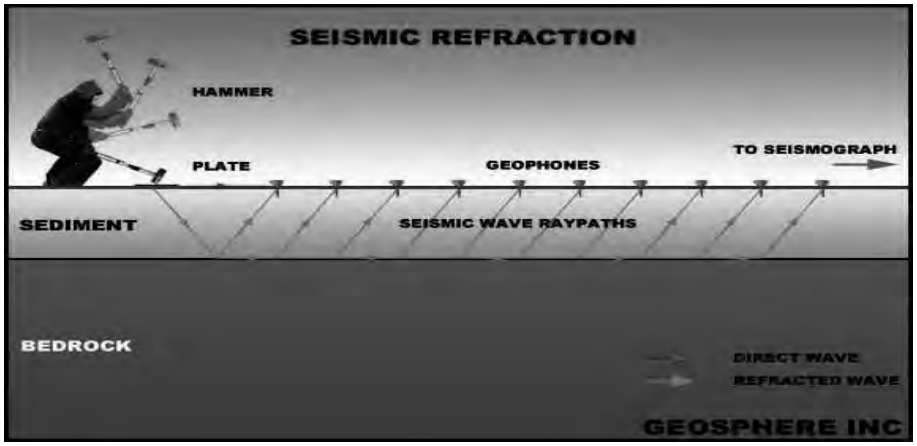


Figure 2.6 Seismic Refraction Test

Figure 2.7 Seismic Refraction survey in BUET.

### 2.4.3 Steady-State Surface Wave Technique

The steady state surface wave technique does not require boreholes and is another in-situ method used to measure the shear modulus (G) of all types of soils. In this test, an electromagnetic oscillator at high frequency (30 to 1000 cycles/second, cps) or a rotating mass type oscillator to produce low frequency vibrations (less than 30 cps) are used. These surface vibrators generate Rayleigh R -waves, which at low strains have nearly the same velocity as the shear waves. The ground surface can be deformed as shown in Figure 2.8. The shear wave velocity is computed from the Rayleigh wave-length measured with receivers placed along the ground surface, and the frequency of vibration at the source using the following equation 2.9 (SW-AJA, 1972; Gazetas, 1991):

$$V_S \sim V_R = f \lambda_R \qquad (2.9)$$

Where,

f = Frequency of vibration

$\lambda_R$= Rayleigh wave length

### 2.4.4 Spectral Analysis of Surface Waves (SASW)

The SASW method evolved from the steady-state vibration test discussed in the previous section. The purpose of the SASW test is to determine a detailed shear wave velocity profile working entirely from the ground surface. The method involves using a series of successively longer source-receiver arrays to measure the propagation of Rayleigh waves over a wide range in wavelengths. A vertical impact is applied at the ground surface generating transient Rayleigh R -waves. Two or more receivers placed at the surface, at known distances apart monitor the passage of these waves (Stokoe, et. al., 1994; Gazetas, 1991). Figure 2.9 shows a schematic of the field setup of this test. The receivers or vibration transducers produce signals that are digitized and recorded by a dynamic signal analyzer, and each recorded time signal is transformed to the frequency domain using a fast Fourier transform algorithm. The phase difference $\phi(f)$ between two signals is then determined for each frequency, and the travel time (t(f)) (eq-2.10) between receivers is obtained for each frequency as follows:

$$t(f) = \phi(f) / 2\pi f \qquad (2.10)$$

Where,

$\phi$ (f)= Phase difference for a given frequency in radians

f= frequency in cycle per seconds (cps)

The velocity of R-waves (eq-2.11) is determined as:

$$V_R = \Delta d / t(f) = \lambda_R f \quad (2.11)$$

Where,

$l_R$= Surface wave length

$\Delta d$ = distance between receivers

### 2.4.5 Seismic Cone Penetration Test (SCPT)

The SCPT has been more recently developed (Campanella and Robertson 1984). The test combines the seismic down-hole technique with the standard Cone Penetration test. A seismic pick-up or receiver is added to the cone, then the similar procedure as the one followed with the seismic down-hole test is used. At the surface, a shear force is induced while the penetration is paused momentarily In order to compare the intensity of signals arriving at the receiver at various depths; a source that is capable of generating repeatable signals is used. This is insured by the use of a single hammer weight and height of fall (Campanella and Davies, 1994). Typical test set up of the SCPT is presented as Figure 2.10. The shear wave velocity, VS, is calculated by dividing the difference in travel path between two depths by the time difference between the two signals recorded.

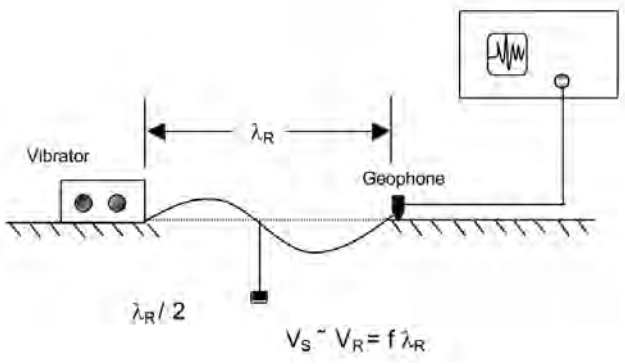


Figure 2.8 Steady-State Surface Wave Test

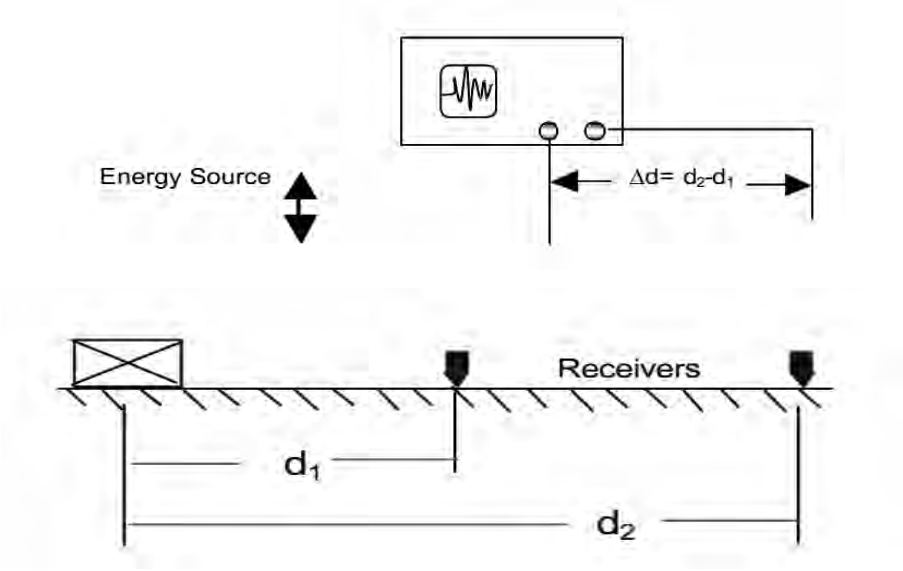


Figure 2.9 Spectral Analysis of Surface Wave Test

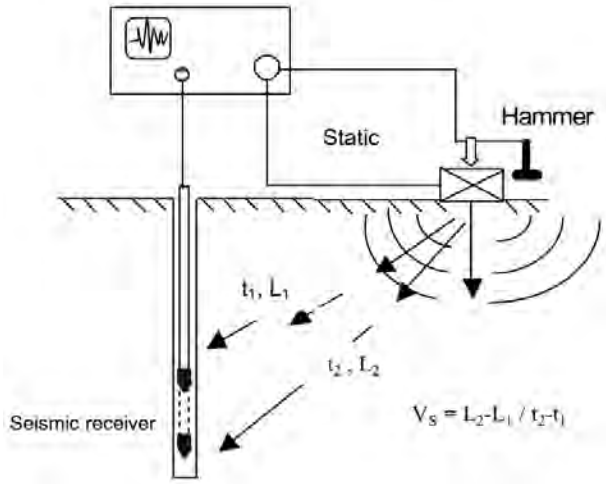


Figure 2.10 Seismic Cone Penetration Test

### 2.4.6 Cross-Hole Technique

The cross-hole technique is one of the best methods used for determining the variation with depth of low strain shear wave velocity. In this test, a source of seismic energy (mainly S-waves) is generated in or at the bottom of one borehole and the time for that energy to travel to another borehole through the soil layer is measured. From the borehole spacing and travel time, the velocity of the seismic wave is computed. Both body waves P -waves, and S-waves can be utilized in this test (Woods, 1978, 1994). At least two boreholes are required, one for the impulse and one or more for receivers as shown in Figure 2.11.

For the success of a cross-hole test there are several requirements. (1) Although a minimum of two boreholes is sufficient to perform the test, three or more boreholes improve the capabilities of the cross-hole method. (2) The energy source should be rich in shearing energy (S-waves) and poor in compressional energy (P-waves) such that the arrival of S-waves can be detected easily. (3) Geophones in the receiver boreholes should have proper frequency response and be oriented in the direction of particle motion. The geophones should also be in contact with the soil, either directly in case of cohesive soils, or indirectly in case of granular soils. Finally, the coupling between geophone transducers and vertical wall should be accomplished with specially designed packers. (4) Travel time measurement of shear waves should be measured accurately using direct or indirect resolution techniques. Often a direct time measurement is made by dual channel oscilloscopes or by digital oscilloscopes. Indirect time resolution involves cross-correlation functions generated from wave trains recorded at two receiver boreholes, and automated frequency domain techniques, which calculate travel time based on the cross spectral density function of wave trains obtained at the receiver borehole(s) (Gazetas, 1991; Woods, 1978, 1994). Figure 2.12 shows the cross hole test at BUET.

### 2.4.7 Down-Hole and Up-Hole Techniques

The up-hole and down-hole techniques are a more economical alternative to the cross-hole technique; only one borehole is needed. In the down-hole technique, the impulse source of energy is generated at the ground surface near the top of the borehole, in which one or multiple geophones are lowered at predetermined depths, whereas in the up-hole test, waves are generated at various depths in the borehole and receivers are located along the ground surface. Figure 2.13, shows schematics of down-hole tests. Travel time of the body waves (S- and P-waves) between each geophone and the source are recorded. Recorded travel time is then plotted versus depth as in the seismic refraction test. These plots are then used to determine the maximum compression and shear wave velocities; $V_{C\ max}$ and $V_{Smax}$ of all soil layers (SW-AJA, 1972; Woods, 1994; Gazetas, 1991).

In the seismic down-hole test, low velocity layers can be detected even if they are between high velocity layers if geophone spacing is sufficiently close. Sources of S -

wave used in seismic refraction can be used for the seismic up- and down-hole testing. Depending on the depth of the soil layers investigated, the source of seismic waves will vary from hand generated sources to the use of large mechanical equipment. In addition, in the seismic up-hole and down-hole tests, the difficulty of picking up the first arrival of shear waves from compression waves is resolved, by reversing the polarity of the source generating the wave pattern. The wave pattern is measured twice, using a horizontally directed sledge hammer blow on a firmly embedded post, which is struck in a direction parallel to the ground surface at first, then struck 180 degrees out of phase a second time (in the opposite direction). Reversing the direction of the energy blow, allows for the shear wave pattern to be recorded in the reverse direction while the compression wave pattern is essentially unchanged. In this manner, the shear wave patterns are distinguished from compression wave patterns. However, in the up-hole test, it is more difficult to generate selected shear waves. P -waves tend to be predominant within the source generated (SW-AJA, 1972; Woods, 1994; Gazetas, 1991). Figure 2.14 shows down-hole test at MIST.

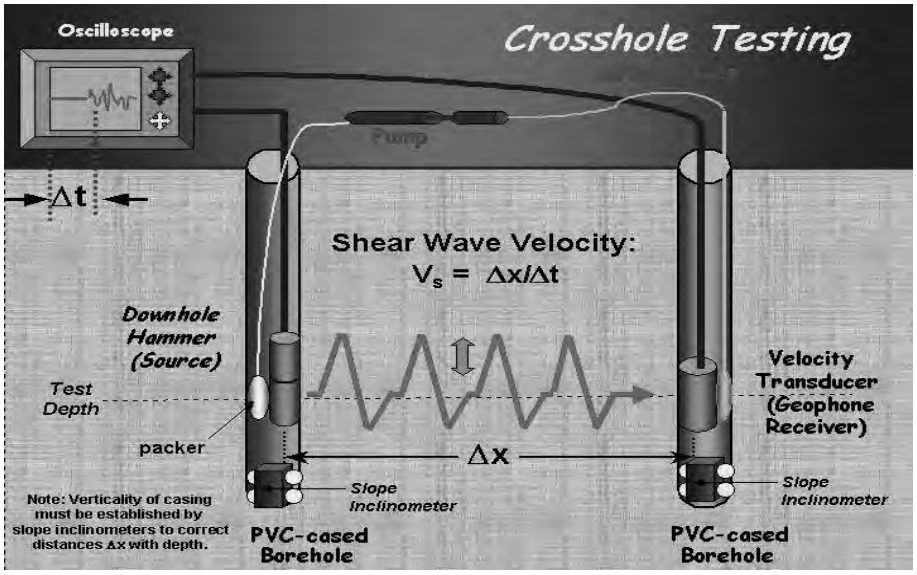


Figure 2.11 Seismic cross-hole test.

Figure 2.12 Seismic cross-hole test at BUET

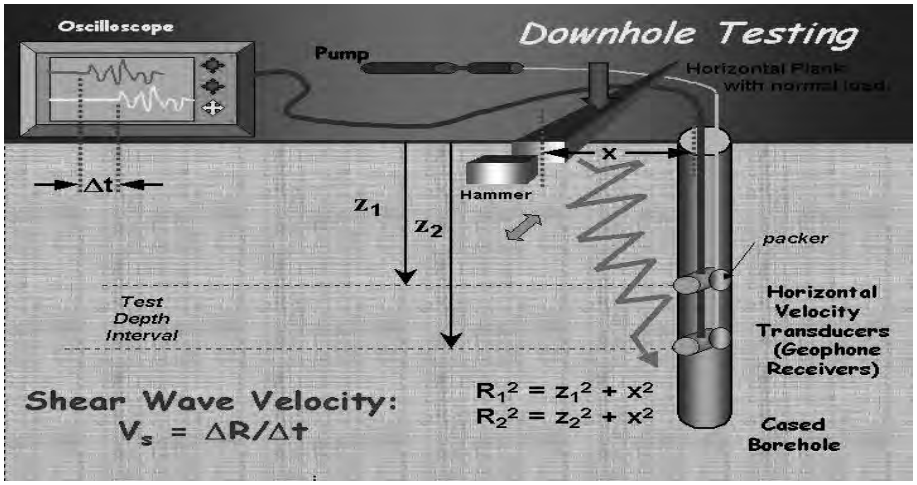


Figure 2.13 Seismic down-hole test

Figure 2.14 Seismic down-hole test at MIST

## 2.5 Standard Penetration Test (SPT)

In the early 1900s, penetration resistance testing and sampling with an open ended pipe was started. In 1927 the Raymond Concrete Pile Company developed the Standard Penetration Test with the split barrel sampler. Since then, the SPT has been performed worldwide. The SPT or variations of the test are the primary means of collecting geotechnical design data in the United States. An estimated 80-90 percent of geotechnical investigations consist of SPTs. The SPT consists of driving a 2-3 inch outside diameter "split barrel" sampler (Figure 3.2) at the bottom of an open borehole with a 140-pound (63.6-kg) hammer dropped 30 inches (75 cm). The "N" value is the number of blows to drive the sampler the last 1 foot (30 cm), expressed in blows per foot. After the penetration test is completed, the sampler is retrieved from the hole. The split barrel is opened, the soil is classified, and a moisture specimen is obtained. After the test, the borehole is extended to the next test depth and the process is repeated. SPT soil samples are disturbed during the driving process and cannot be used as undisturbed specimens for laboratory testing.

The ASTM (American Society of Testing and Materials) standardized the test in the 1950s. The procedure required a freefalling hammer, but the shape and drop method were not standardized. Many hammer systems can be used to perform the test, and many do not really free fall. The predominant hammer system used in the United States is the safety hammer (Figure 2.15) that is lifted and dropped with a rope and cat head. Donut hammers (Figure 2.16) are operated by rope and cat head or mechanical tripping. Donut hammers are not recommended because the hammers are more dangerous to operate and are less efficient than safety hammers. Automatic hammer systems are used frequently and are preferred because the hammers are safer and offer close to true free fall conditions, and the results are more repeatable.

In Bangladesh maximum case manual hammer system are used for low cost. But there are many companies, who use automatic hammers. In the research work, the manual hammer system was used in all locations.

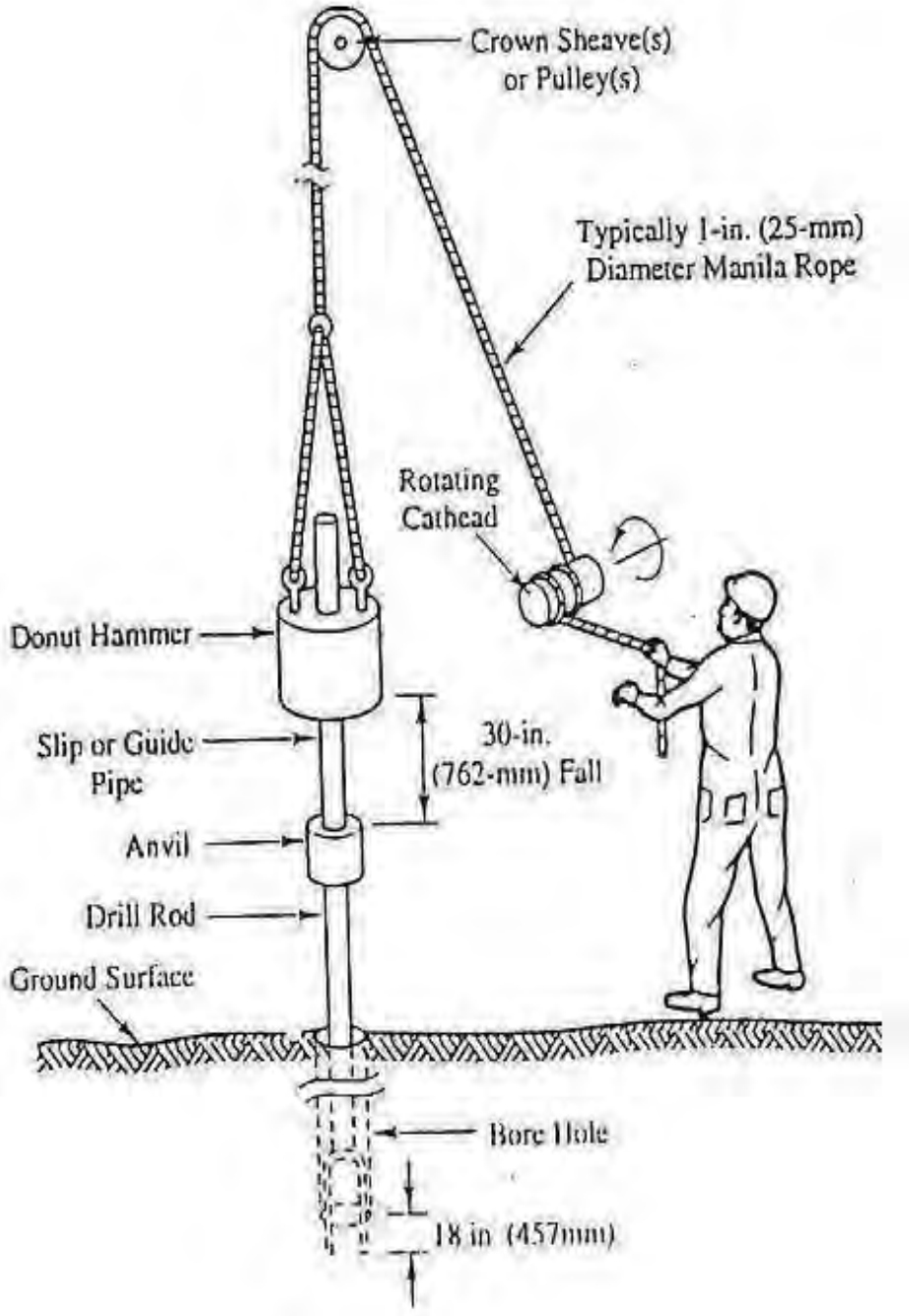


Figure 2.15 The SPT Sampler in place in the boring with hammer, rope and cathead in place

(Adapted from Korvaes et al., 1981)

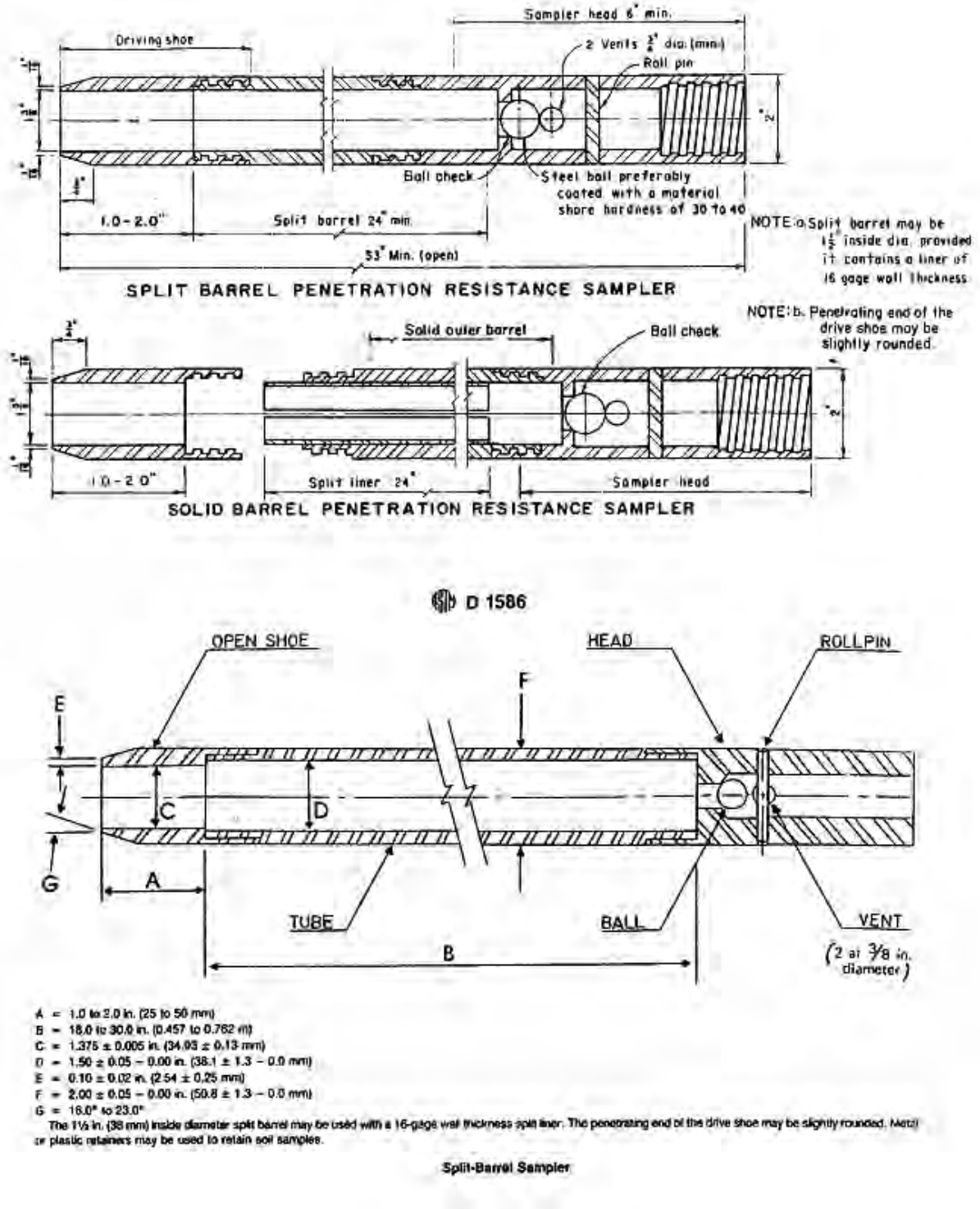


Figure 2.16 ASTM and Reclamation SPT sampler requirements.

## 2.6 Empirical Relations

Shear wave velocity is a basic engineering tool required to define dynamic properties of soils. In many instances it may be preferable to determine Vs indirectly by common in-situ tests, such as the Standard Penetration Test. Many empirical correlations based on the Standard Penetration Test are broadly classified as regression techniques shear wave velocity (*Vs*) is a principal geotechnical soil property for site response analysis. A summary of established correlation in half of the past century is given in Table 2.1. The published regression was divided into three groups, namely all soil types, cohesionless soil and cohesive soil.

Table 2.1: Correlation of Vs = ANB (After Jafari *et al.* (2002); Hanumantharao and Ramana (2008); Uma Maheswari *et al.* (2010); Kuo *et al.* (2011); Akin *et al.* (2011); Anbazhagan *et al.* (2012))

| Year | Researcher | All soil | Cohesionless soil | Cohesive soil |
|---|---|---|---|---|
| 1966 | Kanai | $Vs = 19N^{0.6}$ | - | - |
| 1970 | Ohba and Toriumi | $Vs = 84N^{0.31}$ | - | - |
| | Shibata | | $Vs = 32N^{0.5}$ | - |
| | Imai and Yahimura | $Vs = 76N^{0.33}$ | | - |
| 1972 | Ohta et al | | $Vs = 87N^{0.36}$ | - |
| | Fujimara | $Vs = 92.1N^{0.337}$ | | - |
| 1973 | Ohsaki and Iwasaki | $Vs = 81.4N^{0.39}$ | $Vs = 59.4N^{0.47}$ | - |
| 1975 | Imai and Yoshimura | $Vs = 92N^{0.329}$ | - | - |
| | Imai et al | $Vs = 89.9N^{0.341}$ | - | - |
| 1977 | Imai | $Vs = 91N^{0.337}$ | $Vs = 80.6N^{0.331}$ | $Vs = 102N^{0.292}$ |
| 1978 | Ohta and Goto | $Vs = 85.35N^{0.348}$ | $Vs = 88N^{0.34}$ | |
| 1980 | JRA | | $Vs = 80N^{0.33}$ | $Vs = 100N^{0.33}$ |
| 1981 | Seed and Idriss | $Vs = 61.4N^{0.5}$ | - | - |
| 1982 | Imai and Tonouchi | $Vs = 97N^{0.314}$ | - | - |
| 1983 | Seed et al | - | $Vs = 56.4N^{0.5}$ | - |
| | Sykora and Stokoe | - | $Vs = 100.5N^{0.29}$ | - |
| 1989 | Okamoto et al | - | $Vs = 125N^{0.3}$ | - |
| 1990 | Lee | - | $Vs = 57.4N^{0.49}$ | $Vs = 114.43N^{0.31}$ |
| | Imai and Yoshimura | $Vs = 76N^{0.33}$ | - | - |
| 1991 | Yokota et al | $Vs = 121N^{0.27}$ | - | - |
| 1992 | Kalteziotis et al | $Vs = 76.2N^{0.24}$ | $Vs = 49.1N^{0.50}$ | $Vs = 76.6N^{0.45}$ |
| 1995 | Raptakis et al | | $Vs = 100N^{0.24}$ | $Vs = 184.2N^{0.17}$ |
| | Athanasopoulos | $Vs = 107.6N^{0.36}$ | - | - |
| | Sisman | $Vs = 32.8N^{0.51}$ | - | - |
| 1996 | Iyisan | $Vs = 51.5N^{0.516}$ | - | - |
| 1997 | Jafari et al | $Vs = 22N^{0.85}$ | - | - |
| 2000 | Chien et al | - | $Vs = 22N^{0.76}$ | - |
| 2001 | Kiku et al. | $Vs = 68.3N^{0.292}$ | - | - |
| 2002 | Jafari et al | $Vs = 22N^{0.85}$ | $Vs = 19N^{0.85}$ | $Vs = 27N^{0.73}$ |
| 2007 | Hasancebi and Ulusay | $Vs = 90N^{0.309}$ | $Vs = 90.82N^{0.319}$ | $Vs = 97.89N^{0.269}$ |
| 2008 | Hanumantharao and Ramana | $Vs = 82.6N^{0.43}$ | $Vs = 79N^{0.434}$ | |
| 2008 | Lee and Tsai | $Vs = 137.153N^{0.229}$ | $Vs = 98.07N^{0.305}$ | $Vs = 163.15N^{0.192}$ |
| 2009 | Dikmen | $Vs = 58N^{0.39}$ | $Vs = 73N^{0.33}$ | $Vs = 44N^{0.48}$ |
| 2010 | Brandenberg et al | | | |
| | Uma Maheswari et al. | $Vs = 95.64N^{0.301}$ | $Vs = 100.53N^{0.265}$ | $Vs = 89.31N^{0.358}$ |
| 2011 | Tsiambaos and Sabatakakis | $Vs = 105.7N^{0.327}$ | $Vs = 79.7N^{0.365}$ | $Vs = 88.8N^{0.370}$ |
| 2012 | Anbazhagan et al | $Vs = 68.96N^{0.51}$ | $Vs = 60.17N^{0.56}$ | $Vs = 106.63N^{0.39}$ |

## 2.7 Seismicity in Bangladesh and Hazards

Significant historical earthquakes have occurred in and around Bangladesh. The country's position adjacent to the very active Himalayan front and ongoing deformation in nearby parts of south-east Asia expose it to strong shaking from a variety of earthquake sources that can produce tremors of magnitude 8 or greater. Large earthquakes occur less frequently than serious floods, but they can affect much larger areas and can have long lasting economic, social and political effects. According to the report on time predictable fault modeling (2009), earthquake and tsunami preparedness component of CDMP have identified five tectonic fault zones which may produce damaging earthquakes in Bangladesh. These are:

a) Madhupur fault zone
b) Dauki fault zone.
c) Plate boundary fault zone-1
d) Plate boundary fault zone-2
e) Plate boundary fault zone-3

Considering fault length, fault characteristics, earthquake records etc, the maximum magnitude of earthquakes that can be produced in different tectonic blocks have been given in Table 2.2.

**Table 2.2** Maximum estimated earthquake magnitude in different tectonic faults (Report of CDMP, 2009)

| **Fault zone** | **Earthquake events** | **Estimated magnitude, $m_w$** |
|---|---|---|
| Madhupur fault zone | AD 1885 | 7.5 |
| Dauki fault zone | AD 1897. AD 1500 to 1630(AD 1548) | 8.0 |
| Plate Boundary-1 | AD 1762, AD 680 to 980, BC 150 to AD 60, BC 395 to 740 | 8.5 |
| Plate Boundary-2 | Before 16$^{th}$ century | 8.0 |
| Plate Boundary-3 | Before 16$^{th}$ century | 8.3 |

Figure 2.18 shows the generalized tectonic map of Bangladesh.The distribution of epicenters has been found to be linear along the Dauki fault system and random in other regions of Bangladesh. The investigation of the map demonstrates that the epicenters are lying in the weak zones comprising surface or subsurface faults. Figure 2.17 shows the major fault lines which affect the seismicity in Bangladesh. Most of the events are of moderate rank (magnitude 4~6) and lie at a shallow depth, which suggests that the recent movements occurred in the sediments overlying the basement rocks. In the northeastern region (Surma basin), major events have been controlled by the Dauki fault system. The events located in and around the Madhupur tract also indicate shallow displacement in the faults separating the block from the alluvium.

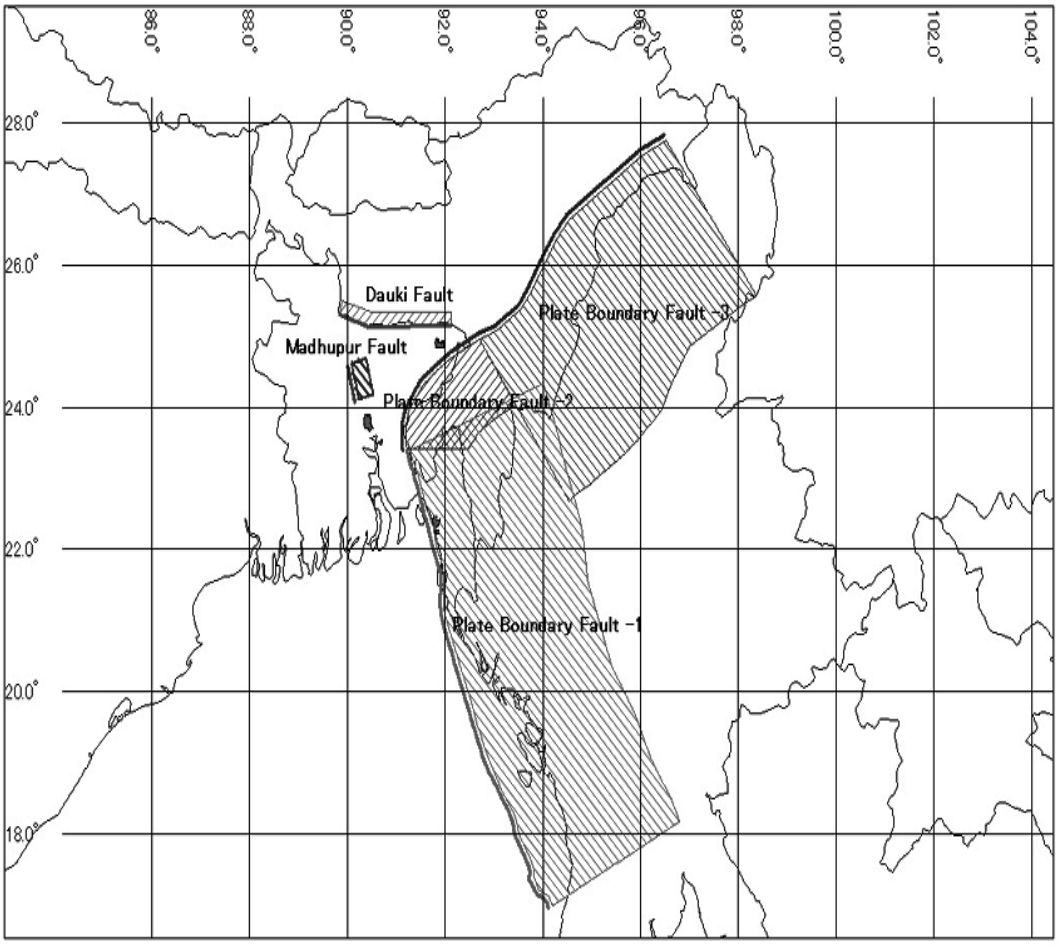


Figure 2.17 The major fault lines which affect seismicity in Bangladesh

(Source: Report on time predictable fault modeling, 2009, earthquake and tsunami preparedness component, CDMP)

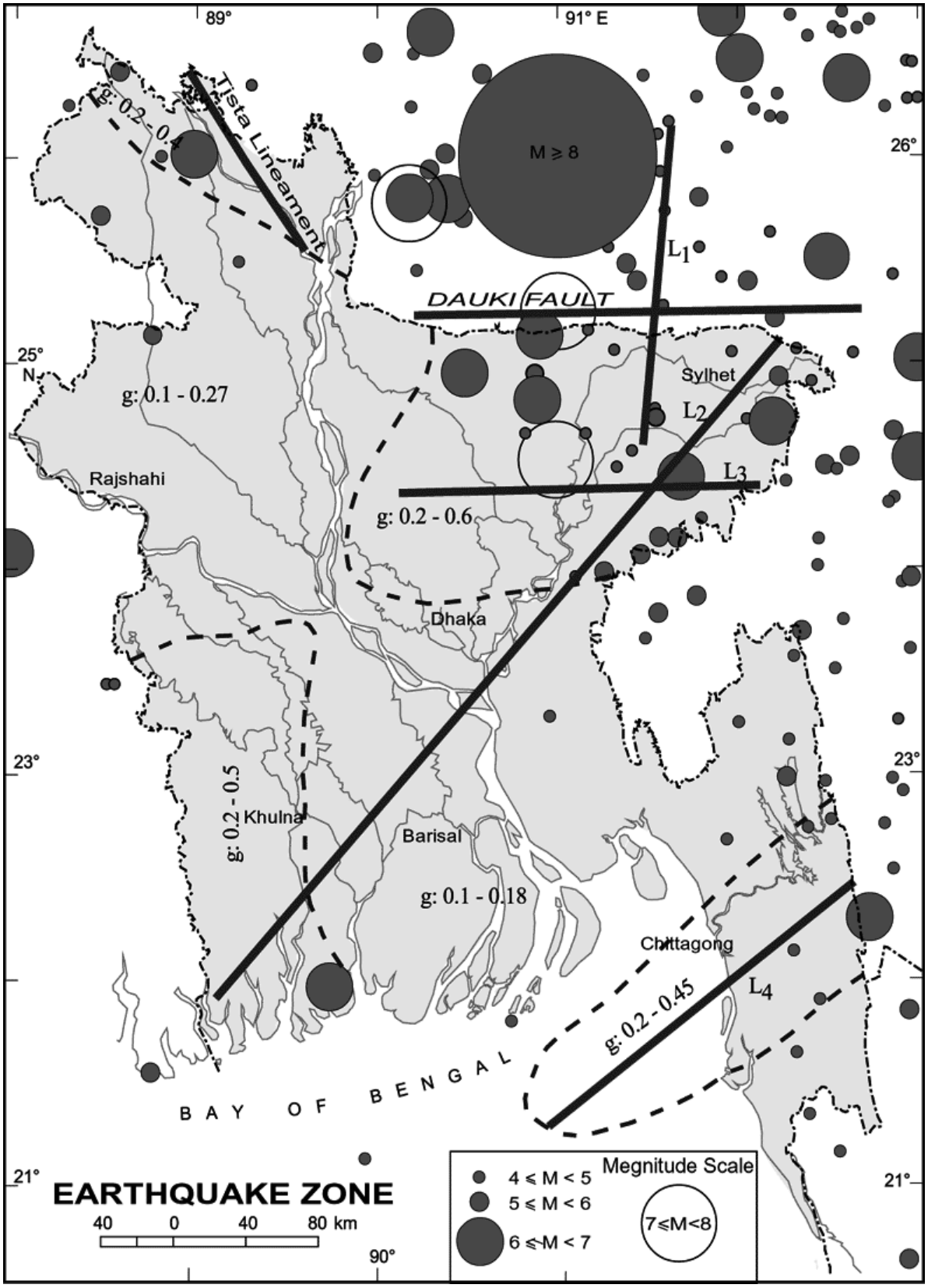


Figure 2.18 Seismo-tectonic lineaments capable of producing damaging earthquakes

During the last 150 years, seven major earthquakes have affected Bangladesh. The surface wave magnitude, maximum intensity according to European Macroseismic scale (EMS) and epicentral distance from Dhaka has been presented in Table 2.3.

**Table 2.3** List of major earthquake affecting Bangladesh during last 150 years (Ms>7) (*After Sabri, 2002*)

| Date | Name of Earthquake | Surface wave magnitude ($m_s$) | Maximum intensity (EMS) | Epicentral distance from Dhaka(km) | Basis |
|---|---|---|---|---|---|
| 10 January, 1869 | Cachar Earthquake | 7.5 | IX | 250 | Back calculation from intensity |
| 14 july,1885 | Bengal Earthquake | 7.0 | VII to IX | 170 | Directly from seismograph |
| 12 June, 1897 | Great Indian Earthquake | 8.7 | X | 230 | |
| 8 July,1918 | Srimongal Earthquake | 7.0 | VII to IX | 150 | |
| 2 July, 1930 | Dhubri Earthquake | 7.1 | IX | 250 | |
| 15 January, 1934 | Bihar-Nepal Earthquake | 8.3 | X | 510 | |
| 15 August, 1950 | Assam Earthquake | 8.5 | X | 780 | |

## 2.8 Seismic Zoning Map of Bangladesh

From the earthquake magnitude for various return periods and the acceleration attention relationship, the seismicity zones and the zone coefficients may be determined. It is required for design of superstructures.

Bangladesh National Building code (BNBC) presented Seismic zoning map for Bangladesh in 1993. There are three zones in the map- zone 1, zone 2 and zone3. The seismic coefficients of the zones are 0.075g, 0.15g and 0.250g for zone 1, zone 2 and zone 3 respectively. Bangladesh National Building Code (1993) placed Dhaka city area in seismic zone 2 as shown in Figure 2.19. However, the seismic zones in the code are not based on the analytical assessment of seismic hazard and are mainly based on the location of historical data.

**Zone-1**

Zone-1 comprising the southwestern part of Bangladesh is seismically quiet, with an estimated basic seismic zoning co-efficient of 0.075.

**Zone-2**

Zone-2 comprising the central part of Bangladesh represents the regions of recent uplifted Pleistocene blocks of the Barind and Madhupur Tracts, and the western extension of the folded belt. The zone extends to the south covering Chittagong and Cox‘s Bazar. Seismic zoning coefficient for Zone II is 0.15.

**Zone-3**

Zone-3 comprising the northern and eastern regions of Bangladesh with the presence of the Dauki Fault system of eastern Sylhet and the deep seated Sylhet Fault, and proximity to the highly disturbed southeastern Assam region with the Jaflong thrust, Naga thrust and Disang thrust, is a zone of high seismic risk with a basic seismic zoning co-efficient of 0.25. Northern Bangladesh comprising greater Rangpur and Dinajpur districts is also a region of high seismicity because of the presence of the Jamuna Fault and the proximity to the active east-west running fault and the Main Boundary Fault to the north in India. The Chittagong-Tripura Folded Belt experiences

frequent earthquakes, as just to its east is the Burmese Arc where a large number of shallow depth earthquakes originate.

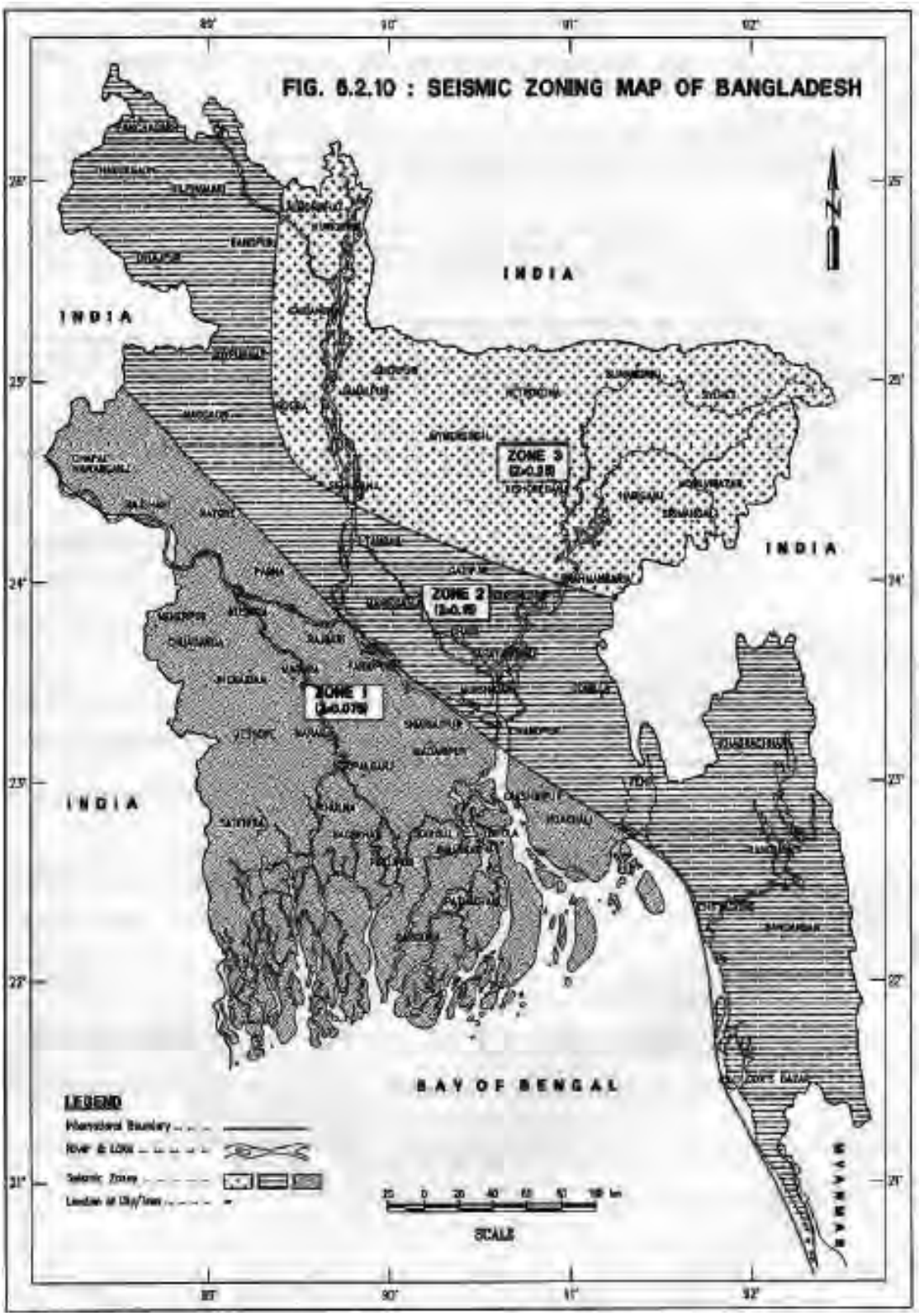


Figure 2.19 Seismic Zoning Map of Bangladesh

(BNBC, 1993)

## 2.9 Site Amplification

To estimate the effect of an earthquake, it is necessary to assess the expected ground motion characteristics, and the subsequent response of soil and structures to those ground motions. A site amplification phenomenon is dependent on frequency of input motion. The characteristics of earthquake motions are influenced by a number of mechanisms related to the local soil and rock properties. Site amplification is quantified using Eq. 2.12, known as the amplification factor (Kramer, 1996).

$$Amplification\ Factor = \frac{\mu\ ground}{\mu rock} \tag{2.12}$$

Where, μ= vertical particle displacement

## 2.10 Methods of Site Response Analysis

Primarily site response is influenced by properties that influence wave propagation, particularly stiffness and damping. Ground failure is mainly influenced by the shear strength of soil. Soil is the most nonlinear material and its behavior during strong shaking is very complex. Seismologists have traditionally treated soil as a linear material and rarely considered soil nonlinearity in the assessment of site conditions (Finn, W.D.L., 1991). Soil nonlinearity is prevalent even at low strain values (strains less than 10-2). The pioneering work of Seed, H.B. and Idriss, I.M., (1969) brought attention to the nonlinear behavior of soils during seismic shaking. Observations during 1964 Alaska, Niigata earthquakes and the 1967 Caracas earthquake formed the basis for the work. Since then, site response has become an integral part of geotechnical earthquake engineering.

Not until the 1985 Michoacan earthquake, soft soils were thought to deamplify motions at peak ground accelerations larger than 0.1 to 0.2 g (Seed, H.B. et al., 1983), while motions at stiff soils were thought to be largely unaffected by the ground motion intensity. The Mexico City earthquake (1985) also brought attention to the need for a better understanding of the dynamic properties of soft clays (Finn, W.D.L., 1991). The development of design codes has followed the advancements in understanding of site response. The use of spectral shapes without amplification factors for peak acceleration

reflected the observations by Seed, H.B. et al., (1976) that accelerations in soils and rocks were approximately equal. Factors that underlain the ground response are peak ground acceleration, predominant frequency and amplitude. Techniques used widely to quantify site response include the following:

i. Experimental Methods

a. Standard Spectral Ratio(SSR)
b. Microtremor Measurements
- H/V noise ratio ( Nogoshi-Nakamura technique)
- H/V spectral ratio of weak motion

ii. Numerical Methods

a. One dimensional site response analysis
- Transfer functions
- Equivalent linear approximation of nonlinear response
- Deconvolution

b. Advanced Methods

iii. Empirical and Semi-Empirical Methods

a. Empirical attenuation laws

### 2.10.1 Experimental Methods

**Standard Spectral Ratio (SSR) Method**

Borcherdt, R.D., introduced (1970) this method for recordings at nearby site to compare which are subjected to source and path effects. This method provides a reliable estimate of site response possible only if the reference site is free from site effects. The recording site has to be unaffected by any site effects and the reference site must be justifiable for the assumption of behavioral difference unaffected by source radiation or travel path. For this reason, reference site has to be located near to the location of testing to ensure that the difference in the records is due to only site effects

but not due to source or path effects (caused when hypocentral distance is more than 10 times of array aperture). SSR technique gives an upper bound of actual site effects at high frequencies and under estimation at frequencies below fundamental frequency for site effects.

### *Microtremor Measurements*

Microtremors are caused by artificial disturbances in the ground such as traffic, industrial machines and so on. Their amplitude of motions is 0.1-1microns. Kanai, K. and Tanaka, T., (1960) from systematic measurements of microtremors carried out at several thousands of places in Japan have inferred that the properties of ground can be identified from the characteristics of microtremors and can be utilized for determining the seismic factor for estimating seismic hazard. The spectral analysis of microtremors is an alternate way to characterize site response. The relationship between local site response and microtremor characteristics, such as predominant period or resonant frequency, site amplification and liquefaction vulnerability, was first studied many years ago (Gutenberg,B., 1957; Kanai,K., and Tanaka,T., 1961). Kanai,K. et al., (1954) proposed a method to classify the ground into four categories, which is used by the Japan Building Code.

#### *H/V Noise Ratio method*

Many researchers (Ohmachi, et. al., 1991; Lermo, et al., 1992; Field,. and Jacob, 1993, 1995) shown that, how H/V ratio of noise can be used to identify the fundamental resonant frequency and amplification factor of sediments. This method doesn‘t depend on reference site. It is also called as Nogoshi-Nakamura technique which was introduced in early seventies. ‗H‘ represents the horizontal component of the Fourier Spectra of microtremors and ‗V‘ is the corresponding vertical component. H/V is more stable than the raw noise spectra. It exhibits a clear peak in soft soils which could be correlated with the fundamental resonant frequency. Field observations combined with several theoretical investigations corroborate the randomly distributed near surface source lead to H/V ratios. Though the frequency of the peak correlated to the peak frequency of the ground, amplitude of this peak is not well correlated with the S wave amplification at the site's resonant frequency. Amplitude is highly sensitive to poisons

ratio near the surface. This technique is rather inexpensive and noninvasive in character. Figure 2.20 represents the H/V method and SSR method of recording.

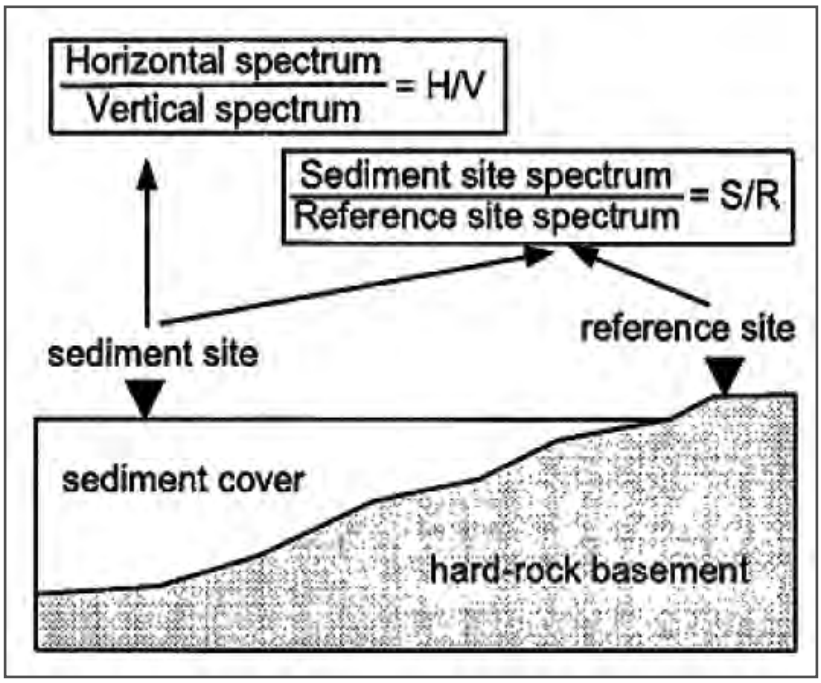


**Figure 2.20** Different methods for estimating site frequency using ambient noise vibrations (after IbsvonSeht, M. and Wohlenberg, J., 1999)

***H/V spectral ratio of weak motion***

The H/V spectral ratio (HVSR) method is an experimental technique for evaluating characteristics of soft sedimentary (soil) deposits. HVSR technique is a combination of Langston‘s receiver function method and Nakamura‘s proposal to use HVSR ratio with recordings of ambient vibrations. Receiver function method was used for determining the velocity structure of the crust from the horizontal to vertical spectral ratio (HVSR) of the seismic P-waves. H/V method is based on the records of the ambient noise (microtremors) in environment. Microtremor consists of both body and surface waves. Suzuki, T. (1933) pointed out that H/V spectrum ratio of Rayleigh waves reflects the surface structure. Nogoshi, M., and Igarashi, T. (1971) in their paper distinguished the components of the microtremor whether body waves or surface waves. Nakamura, Y., (1989) estimated that some site characteristics are related with the site transfer function, using microtremor measurements. It consists in deriving the ratio between the Fourier spectra of the horizontal and the vertical components of the microtremor recording obtained at the surface; this ratio is called thereafter the H/V ratio. It was first applied

to the S wave portion of the earthquake recordings obtained at three different sites in Mexico by Lermo, J. and Chavez Garcia, F.J. (1994a).

The horizontal to vertical spectral ratio is also termed as Quasi transfer spectra (QTS). The purpose of Nakamura,Y., (1989) was to estimate the amplification factor caused by multiple reflected vertical incident SH waves and peak frequency. Microtremor can be divided into two parts, Rayleigh wave and the other wave. A typical geological structure has been shown in Fig.2.21

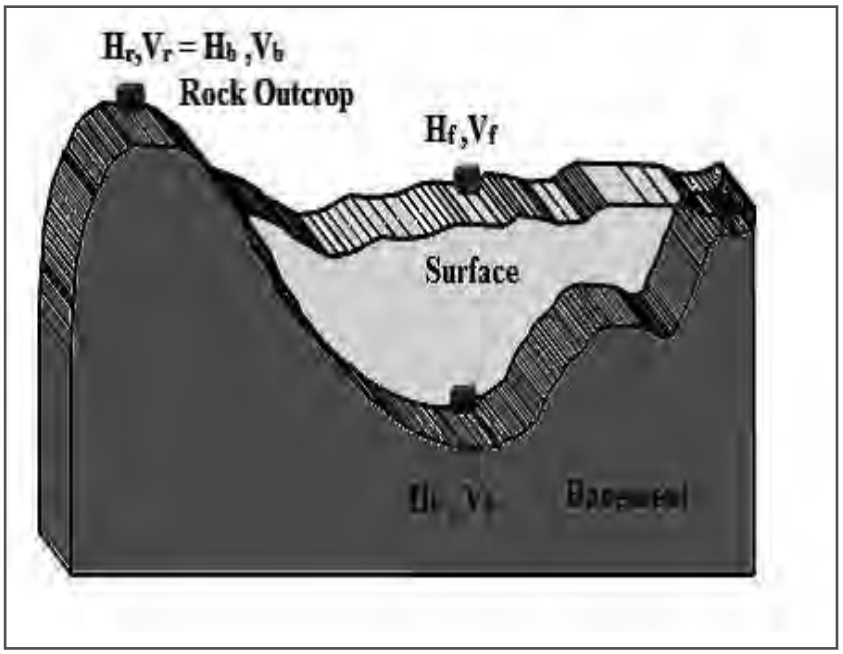


Figure 2.21 Typical geological structure of sedimentary basin
(modified from Nakamura, Y., 2000)

### 2.10.2 Numerical Methods

When high quality geotechnical data is available, site effects can be estimated using numerical analysis if the site characteristics are well known. Numerically based zoning can be done when sufficient density of boreholes and geotechnical information is available. But, such approach requires an in depth understanding of both analytical models and of the numerical schemes that are used. Lack of such expertise in numerical analyses may lead to less reliable results.

**One Dimensional Analysis**

The most general method of site response analysis is one dimensional analysis. Two dimensional and three dimensional analyses can be employed using finite element method, finite difference method and thin layer methods that even assess the effect of topography and basin structure on wave propagation (Bielak, et al., 1999; Law and Lam, 1999). This method is widely used for response analysis as it provides conservative results, evaluated from case histories of different earthquakes. In this analysis 1D propagation of the seismic waves are considered. One of the basic assumption in one dimensional analysis is that all boundaries are horizontal and response of soil is reliant on vertical propagation of SH wave from the bedrock below. The soil and bedrock are assumed to be infinite in horizontal direction. The assumptions are justified as velocity of wave generally decreases from the earth‘s interior towards the surface, and hence stress waves from the focus are bent by successive refractions into a nearly vertical path. By Snell‘s law of refraction, the waves trapped in the soil by refraction at the interface of firm ground and soil will propagate nearly vertical even though the waves are propagating in a shallow inclined direction from the firm ground. Vertical ground motions are generally not as important from the standpoint of structural design as horizontal ground motions. Soil properties generally vary more rapidly in the vertical direction than in the horizontal direction.

The methods of one dimension analysis can be broadly categorized as follows:

1. Linear analysis
2. Equivalent linear analysis
3. Nonlinear analysis

Linear analysis

Linear approach is the simplest approach to evaluate ground response in one dimensional analysis. Nonlinear behavior of soil is approximated by iterative procedure with equivalent linear soil properties. Linear approach has been implemented in the following procedures, which are commonly used for ground response analysis (Kramer, 1996).

- Transfer functions
- Equivalent linear approximation of non linear response
- Deconvolution

Many packages are available for one dimensional analysis such as SHAKE, DEEPSOIL, EDUSHAKE, PROSHAKE, Cyber Quake, EERA etc.

Nonlinear Approach

Nonlinear response of soil cannot be evaluated precisely like the linear approach. This limitation can be overcome by using the nonlinear response of soil using direct numerical integration in small time intervals in time domain. Nonlinear analysis is usually performed by using a discrete model such as finite element and lumped mass models, and performing time domain step-by-step integration of equations of motion. For nonlinear analysis to give meaningful results, the stress-strain characteristics of the particular soil must be realistically modeled. The integration of motion in small time intervals will permit the use of any linear or nonlinear stress-strain models. The data from borings or measurements of shear wave velocity are used to construct the soil model. When such data are not available, generic ground conditions can be used (Shima, and Imai, 1982). Since all soils have highly nonlinear properties, nonlinearity in site characterization and analysis has to be taken under serious consideration.

There are many types of software, which can incorporate the nonlinear response of soils such as PLAXIS, SASSI2000, FLAC, QUAKE/W, DEEPSOIL etc.

**Two Dimensional Analysis**

The one dimensional site response analysis is useful for sloping ground with parallel soil layers. Since these conditions are not so common, one dimensional analysis may not give very accurate results in most of the cases. In the case of sites where embedded structures like pipe lines or tunnels are present, one dimensional analysis will not yield desired results. Two dimensional analyses can be done either based on frequency domain or time domain methods.

This analysis can be done using dynamic finite element methods adopting either equivalent linear approach or nonlinear approach (Kramer, 1996). For modeling two dimensional cases, numerical modeling software like PLAXIS, FLAC, QUAKE/W etc. can be used. Various researchers proposed number of alternatives to this approach such as shear beam approach and layered inelastic shear beam approach for high computational cost. Shear beam approach is widely used for the analysis of earthen dams.

**Three Dimensional Analysis**

There may be cases in which, two dimensional approach may not adequate, there is variation in soil profile in three dimensions. This is better for studying the response of three dimensional structures. The method and the approaches are similar to the two dimensional approach. Equivalent linear finite element approach, nonlinear finite element approach etc. are the adopted approaches.

## 2.11 Ground Response Analysis

During an earthquake, propagation of seismic waves through soil column alters the amplitude, frequency and duration of ground motion by the time it reaches the surface. The effects of ground motion are propagated in the form of waves from one medium to another. The evaluation of such response of the site to dynamic loading is termed as ground response analysis. Site effects can be quantified by empirical correlations between rock outcrop motion and motion at soil sites. Different correlations are used for stiff soils and deep cohesionless soils. Depending on the geometry and loading conditions different analysis i.e., one, two and three dimensional are suggested.

Ground response analysis also termed as soil amplification study comprises the calculation of site natural periods, ground motion amplification, evaluation of liquefaction potential, stability analysis etc. The important features that are considered for analysis are characteristics of soil overlying bedrock, bedrock location and inclination, topography of bedrock and soil deposits, faults in the soil deposits. A complete ground response analysis considers source, path and site amplification effects.

Damping factors of the soil are difficult to be assessed. Important steps in site specific ground response analysis are dynamic characterization of the site and selection of rock motions. Empirical relationships are useful when large area is considered for response analysis and time is constrained. But due to scanty data and the range of applicable site conditions, empirical relationships cannot be applied to all situations. Numerical simulations are practical in such situations as they cover a range of ground motions and site effects for the locations where previous information is not available.

### 2.11.1 Equivalent linear Analysis

Equivalent linear analysis has been developed by Schnabel, et al., 1972 to capture the nonlinear cyclic response of soil within frequency domain solution. This method is widely used for engineering applications as the results well converged with the field recordings. Schnabel, et al., (1972) addressed nonlinear hysteretic stress–strain properties of sand by using an equivalent linear method of analysis. The method was originally based on the lumped mass model of sand deposits resting on rigid base to which the seismic motions were applied. Later, this method was generalized to wave propagation model with an energy transmitting boundary. The seismic excitation could be applied at any level in the new model. Up to a strain of $10^{-3}$soil model can be simplified to an equivalent linear model. Equivalent linear method implies that strain always returns to a value of zero after cyclic loading and failure cannot occur. In a frequency domain analysis it is assumed that modulus and damping properties are constant.

## 2.12 Analysis using DEEPSOIL

A computer program DEEPSOIL (Hashash et al, 2011), is used to compute the seismic response of horizontally layered soil deposits of the study area. It is a one-dimensional site response analysis program that can perform linear, equivalent linear and non-linear approach of analysis. The linear analysis can be done either in frequency domain or time domain. Frequency domain methods are the most widely used to estimate site effects due to their simplicity, flexibility and low computational requirements. However, in cases of high seismic intensities at rock base and/or high strain levels in the soil layers, an equivalent soil stiffness and damping for each layer cannot represent

the behavior of the soil column over the entire duration of a seismic event. In such cases also ground motion propagation through deep soil deposits can be simulated using this tool. The equivalent linear approach implemented in DEEPSOIL is similar to that in SHAKE (Schnabel et al., 1972). Any number of material properties and layers can be used and the user can choose frequency dependent or independent complex shear modulus formulations (Park, and Hashash, 2004).

For performing 1D equivalent linear analysis following inputs about soil are required i.e., number of layers of the profile, thickness of layer, shear wave velocity/shear modulus, % of damping, unit weight and water table depth. The steps involved in the analysis are:

- Selection of analysis method
  - Frequency Domain
  - Linear
  - Equivalent Linear
  - Time Domain
  - Linear
  - Nonlinear
- The method to define the soil curve:
  - Discrete Points
  - Pressure-Dependent Hyperbolic Model
- Defining of soil properties and soil model properties
  - Layer thickness, damping, shear property, unit weight
  - Soil model – Sand/Clay
- Defining of rock properties
  - Elastic/rigid half space
  - Rock properties such as shear property, unit weight, damping
- Analysis control
  - Fourier transform type
  - Type of complex shear modulus
- Input ground motion
- Output

For the input ground motion, array recordings or rock outcrop records are used to simulate field response. In the absence of such records, synthetic motions can be used. For evaluation of 1D response, the generated input ground motions are propagated through the soil profiles. Damping and shear modulus properties can be selected from the database or user defined curves can be inputted.

# CHAPTER THREE
# FIELD INVESTIGATION

## 3.1 General

The objective of this chapter is to describe detail procedure of the test for this research work. So PS Logging Test is described briefly in this chapter. It also describes the procedure for determination of Shear Wave Velocity. The Shear Wave and SPT N value at selected locations of Dhaka City has been presented in this chapter.

## 3.2 PS Logging Test (Down-hole Technique)

PS Logging test can be performed in both up-hole and down-hole techniques. The Cross hole and Down hole techniques were described briefly at Chapter Two (Literature Review). For the research work, PS Logging equipment of BUET-JIDPUS was used. It was bought from the OLSON INSTRUMENTS. The testing system consists of several basic components packaged into a padded carrying case plus the Freedom Data PC in its own case. The padded case stores the down-hole source, tri-axial geophones, down-hole links, dummy probes, compressor, pressure gage, cables and battery charger. Different components of the test system are shown in Figure 3.1.

The down hole seismic test requires only 1 borehole (preferably a 2.5-3 inch diameter hole with PVC pipe installed up to the depth in which competent soil or rock is reached) to be used for the geophone receiver. Usually PVC pipes are used to permanently stabilize the hole. The standard for the test technique is set forth in the ASTM D4428/D4428M. An installed cased borehole in the JIDPUS, BUET is shown in Figure 3.5.

For preparing the boreholes for Suspension PS Logging Test at all ten selected areas of the Dhaka City, Standard Penetration Test (SPT) was conducted according to ASTM D1586(ASTM, 2000). In every location 3in borehole was prepared by SPT method and N value was observer at every 5ft and in some places every 10ft interval. Figure 3.3 shows the SPT test at MIST, Mirpur. After preparing the borehole, a PVC pipe was for

protecting the hole from caving. Figure 3.4 shows the installation of the PVC pipe at Aftabnagar.


Data Pc

Cables from Freedom Data PC to Receivers

Tri-axial Geophone Receiver

Dummy Probes

Pressure Gage

Rope cleat

Figure 3.1 Different components of Suspension PS Logging Test Equipment used in this study

Disturbed and undisturbed sample were collected during the test. After preparing the borehole using the SPT test, installation of the PVC pipe was the most difficult of the test procedure, because in sand caving is sever. It was shown in many places that after performing a 100ft SPT boring, PVC pipe was installed only 50-80ft depending on the time and method of pipe installation. In some places second boring was performed because of caving of soil. The SPT test is described below.

In the Research work, N value was taken 5ft interval in some places and 10ft interval in others. Undisturbed and disturbed samples were collected where N value was taken. After performing the borehole, 3in diameter PVC pipe (20ft each pipe) installed along the borehole for protecting the soil from caving. Firstly the bottom of the first pipe was burnt (Figure 3.4) and sealed before installing for protecting the soil from hydraulic or soil heaving from bottom. Each pipe had socket system at both end for connecting each other. So when one pipe was penetrated, another pipe was connected with the previous pipe using the socket and then penetrated. For a 100ft borehole, 5 pipes were needed.

For the test, a wooden plank source of 6 in x 30 in area and 3 m (10 ft) in length was used. Figure 3.6 shows the wooden plank used for the test at Kamrangichor. A vehicle was placed on the plank, to hold the plank tightly. Figure 3.6 shows PS Logging test at Gulsan-2. The setup of the equipment shown below as flow chart in Figure 3.10

There was a sensor attached to the wooden plank. The plank was hit separately on both ends to generate shear wave energy in two different directions. It was also hit vertically in the downward vertical direction to generate vertically polarized compression wave energy. The shear wave energy was polarized in the direction parallel to the plank as is the transverse component. The transverse component was used to measure the shear wave energy. The vertical component was used to measure the vertically polarized compression wave energy. Typically 3-5 records are taken for each type of wave –east going, west going shear wave and vertical compression wave. Using the test plans that come with the Freedom Data PC down-hole Seismic / Cross Hole Seismic – 2 system, 8 records were taken for each wave type. Figure 3.2 shows the flowchart of installation of PS Logging test. Figure 3.7 shows PS logging test at Gulshan-2.

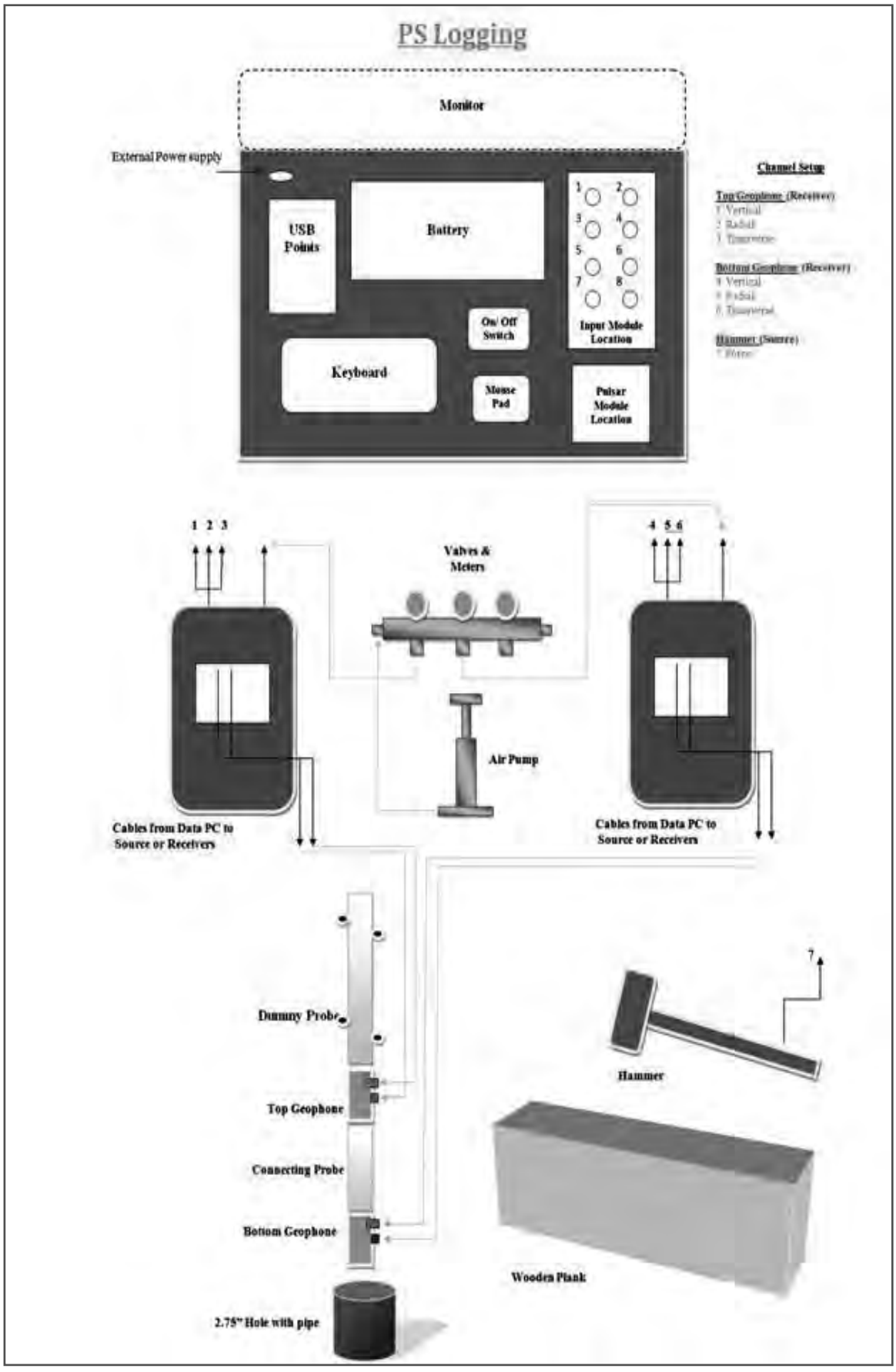


Figure 3.2 Installation of PS Logging test (Down-hole seismic method)

Figure 3.3 SPT Test at MIST.

Figure 3.4 Burning of PVC pipe at bottom, before installation

Figure 3.5 PVC pipe cased borehole on the testing location on west side of BUET JIDPUS, BUET.

Figure 3.6 A heavy wooden plank used for PS Logging Test at Kamrangichor, Dhaka

Figure 3.7 PS Logging Test Setup at Gulshan-2, Dhaka.

Sample of data obtained from test is shown in Figure 3.8 and Figure 3.9 for calculating compression wave and shear wave. Figure 3.8, shows the data of compression wave. For computing the arrival time of the compression wave, we have to take the first point of the time domain data of the vertical component when the response starts for both geophones. Figure 3.9 shows the data of shear wave generated by giving blow with hammer in both horizontal directions. For computing the arrival time of the shear wave, take the first point of the time domain data of the radial and transverse component when both wave generated from both horizontal direction just overlap each other.

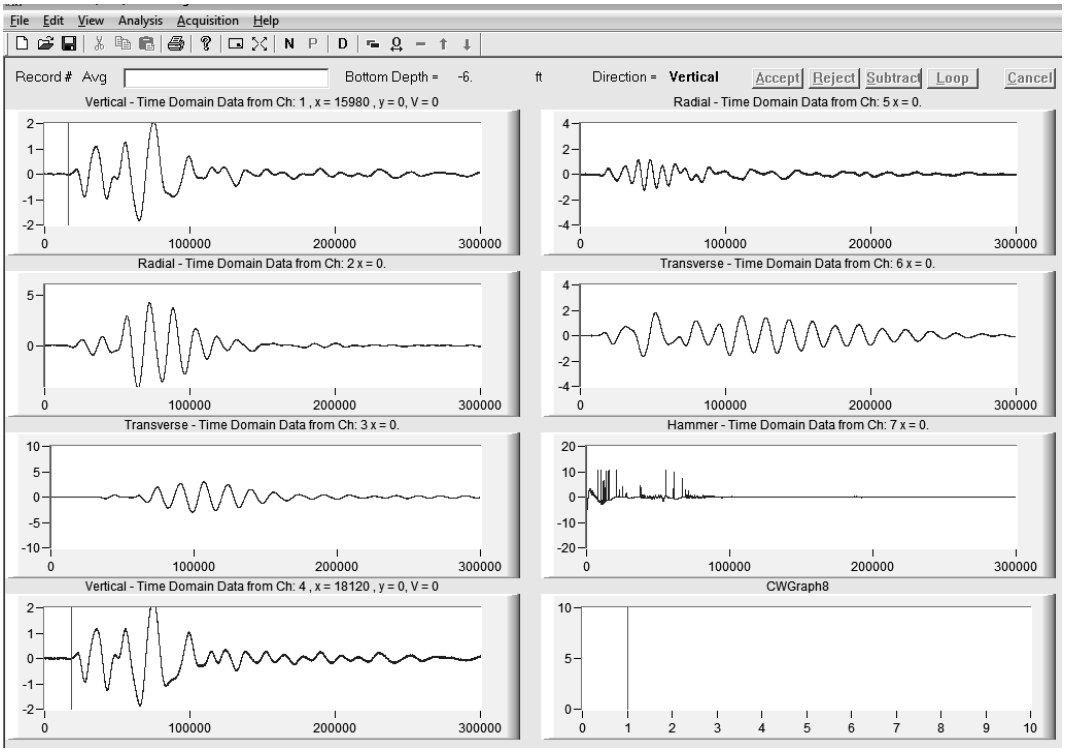


Figure 3.8 Time Domain data for compression wave.

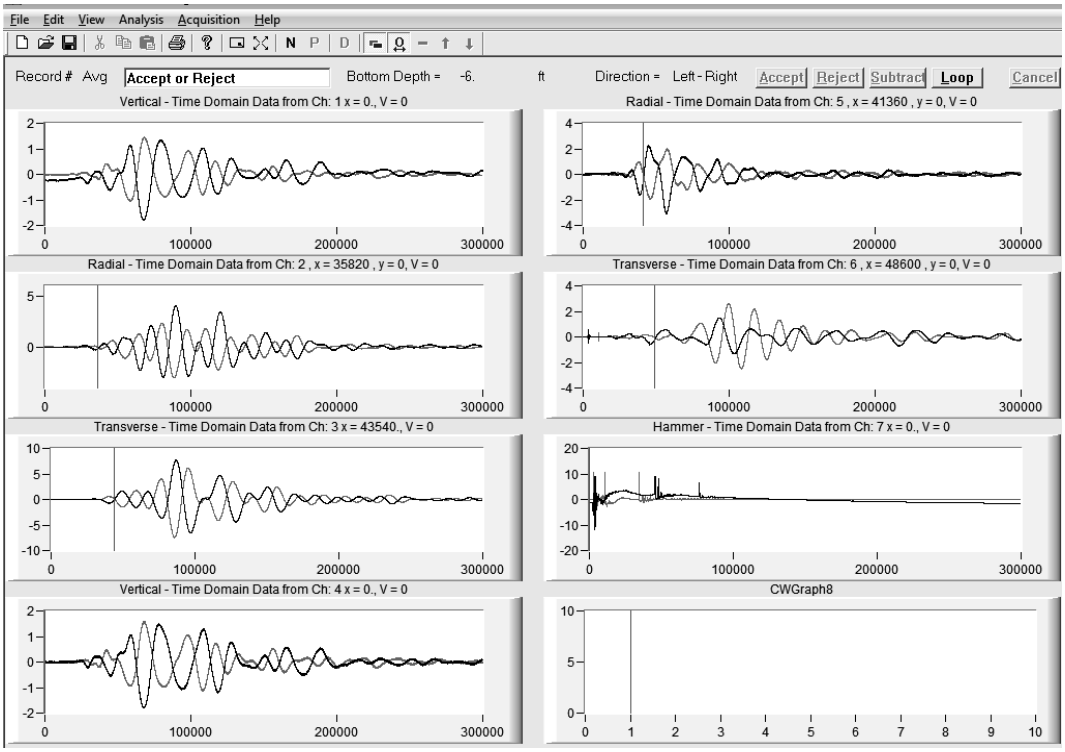


Figure 3.9 Time Domain data for shear wave.

From the calculated travel time of the compression and shear wave, the velocity can be determined by dividing the distance of the source to receiver by the travel time. Both compression wave and shear wave velocity were determined in this method. Figure 3.10 shows the different distances between source and receivers.

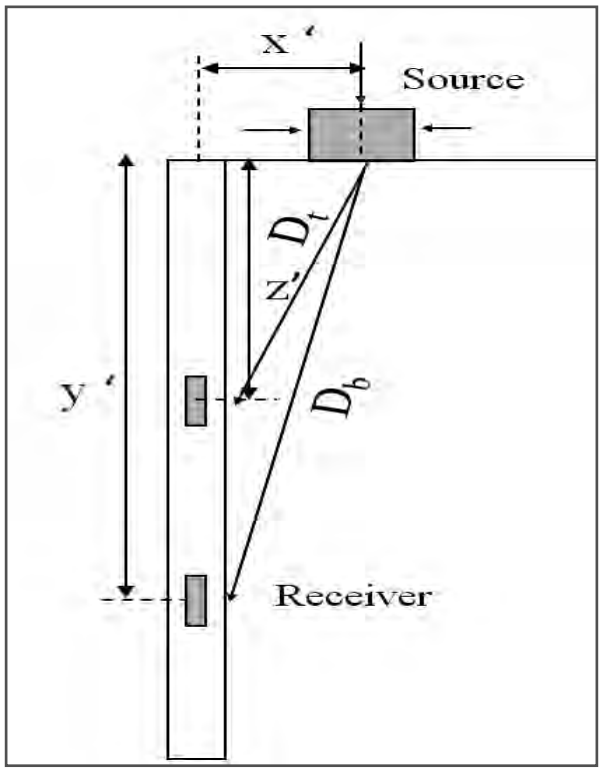


Figure 3.10 PS Logging test in Seismic Down-hole method.

Equations used,

$$D_t = \sqrt{(z^2 + x^2)} \quad (4.1)$$

$$D_b = \sqrt{(y^2 + x^2)} \quad (4.2)$$

$$V_p = \frac{D_b - D_t}{t_b - t_t} \quad (4.3)$$

*Here,*

$D_t$ = Distance between top receiver to source

$D_b$ = Distance between bottom receiver to source

$T_t$ = Travel time of wave to top geophone

$T_b$ = Travel time of wave to bottom geophone

The arrival times of S wave for the test at JIDPUS, BUET and from them, the wave velocity calculation is shown in Table 3.1 below

Table 3.1 Calculation of S wave from the arrival times

| Depth ft | Geophone-1 | | | Geophone-2 | | | S wave Velocity ft/s |
|---|---|---|---|---|---|---|---|
| | Arrival time μs | Arrival time sec | Distance ft | Arrival time μs | Arrival time sec | Distance ft | |
| **6** | 32880 | 0.03288 | 15.86 | 40740 | 0.04074 | 16.93 | **136** |
| **11** | 39560 | 0.03956 | 16.93 | 44980 | 0.04498 | 19.28 | **433** |
| **16** | 39340 | 0.03934 | 19.28 | 43604 | 0.043604 | 22.51 | **758** |
| **21** | 45760 | 0.04576 | 22.51 | 48640 | 0.04864 | 26.30 | **1316** |
| **26** | 48200 | 0.0482 | 26.30 | 62220 | 0.06222 | 30.44 | **295** |
| **31** | 54440 | 0.05444 | 30.44 | 57740 | 0.05774 | 34.81 | **1324** |
| **36** | 59840 | 0.05984 | 34.81 | 64180 | 0.06418 | 39.33 | **1041** |
| **41** | 66340 | 0.06634 | 39.33 | 69280 | 0.06928 | 43.95 | **1572** |
| **46** | 69300 | 0.0693 | 43.95 | 76460 | 0.07646 | 48.65 | **656** |
| **51** | 75920 | 0.07592 | 48.65 | 79400 | 0.0794 | 53.40 | **1366** |
| **56** | 80100 | 0.0801 | 53.40 | 85940 | 0.08594 | 58.20 | **821** |
| **61** | 81540 | 0.08154 | 58.20 | 90600 | 0.0906 | 63.02 | **533** |
| **66** | 102720 | 0.10272 | 63.02 | 109620 | 0.10962 | 67.87 | **703** |
| **71** | 94580 | 0.09458 | 67.87 | 101240 | 0.10124 | 72.74 | **731** |
| **76** | 95300 | 0.0953 | 72.74 | 99100 | 0.0991 | 77.63 | **1286** |
| **81** | 101120 | 0.10112 | 77.63 | 104780 | 0.10478 | 82.53 | **1339** |

### 3.3 Selected Areas:

Ten locations of Dhaka city were selected for conducting the test. Also Test data of seven more locations of Dhaka city were collected from CDMP. The locations are shown below in Figure 3.11.

**Tested by Author**

Site-1: BUET JIDPUS
Site-2: MIST, Mirpur
Site-3: Hazaribag
Site-4: Gulshan 2
Site-5: Kamrangichor
Site-6: Dakhin Kafrul
Site-7: Maniknagar
Site-8: Aftabnagar
Site-9: Lake City Concord, Khilkhet
Site-10: RHD, Tejgaon

**Tested by CDMP**

Site-11: Mehernagar, Uttara
Site-12: Jubok Project, Ashulia
Site-13: Mirpur-1, Avenue-2
Site-14: Akash Nagar, Mohammadpur, Beribadh
Site-15: United City Project, Beraidh
Site-16: East Nandipara
Site-17: Asian City, Dokhinkhan


Figure 3.11 Map showing different locations of research area

### 3.4 Results of Field Investigation

#### 3.4.1 Site-1

The Field SPT N values and, the shear wave velocity obtained are shown in Figure 3.12 and in Appendix B, the data is presented in tabular form. According to the figure, it was observed that- from surface to 20 ft clay soil found and shear wave velocity and SPT N value increased gradually according to dept. But after 20 ft rest soil were sand. SPT N value slightly decreased at 25ft but again gradually increased according to depth up to 65 ft then again increased. The shear wave velocity raised same where and also decreased somewhere up to full depth.

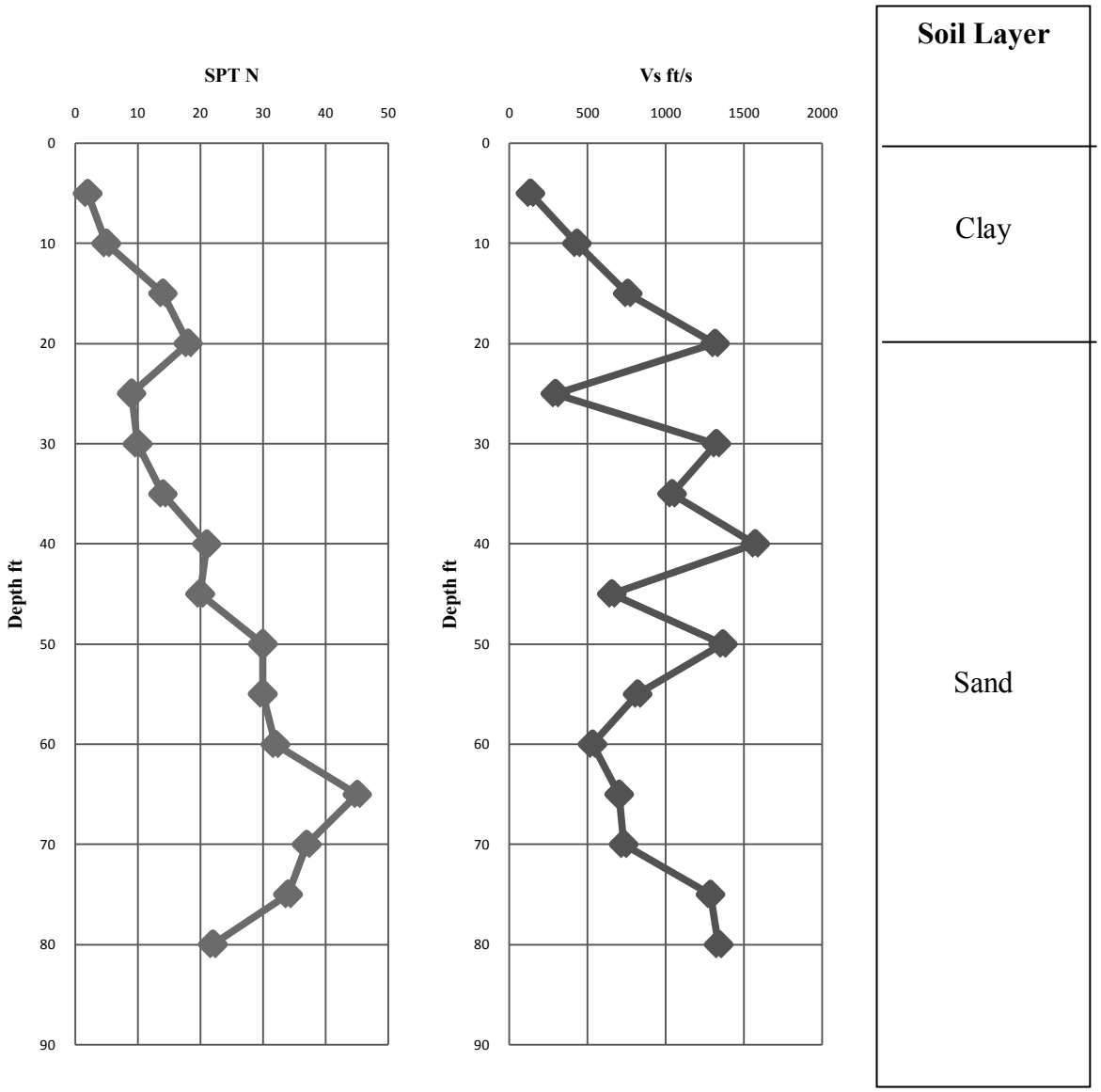


Figure 3.12 Different Test results at Site BUET-JIDPUS

### 3.4.2 Site-2

The Field SPT N Value, the shear wave and compression wave velocity obtained are shown in Figure 3.13 and in Appendix B, the data is presented in tabular form. According to the figure, it was observed that- from surface to 28 ft clay soil found and after 28 ft rest soil were sand. SPT N value decreased up to 18ft and after that increased gradually according to depth. Shear wave velocity also increased according to depth but at some depth it decreased.

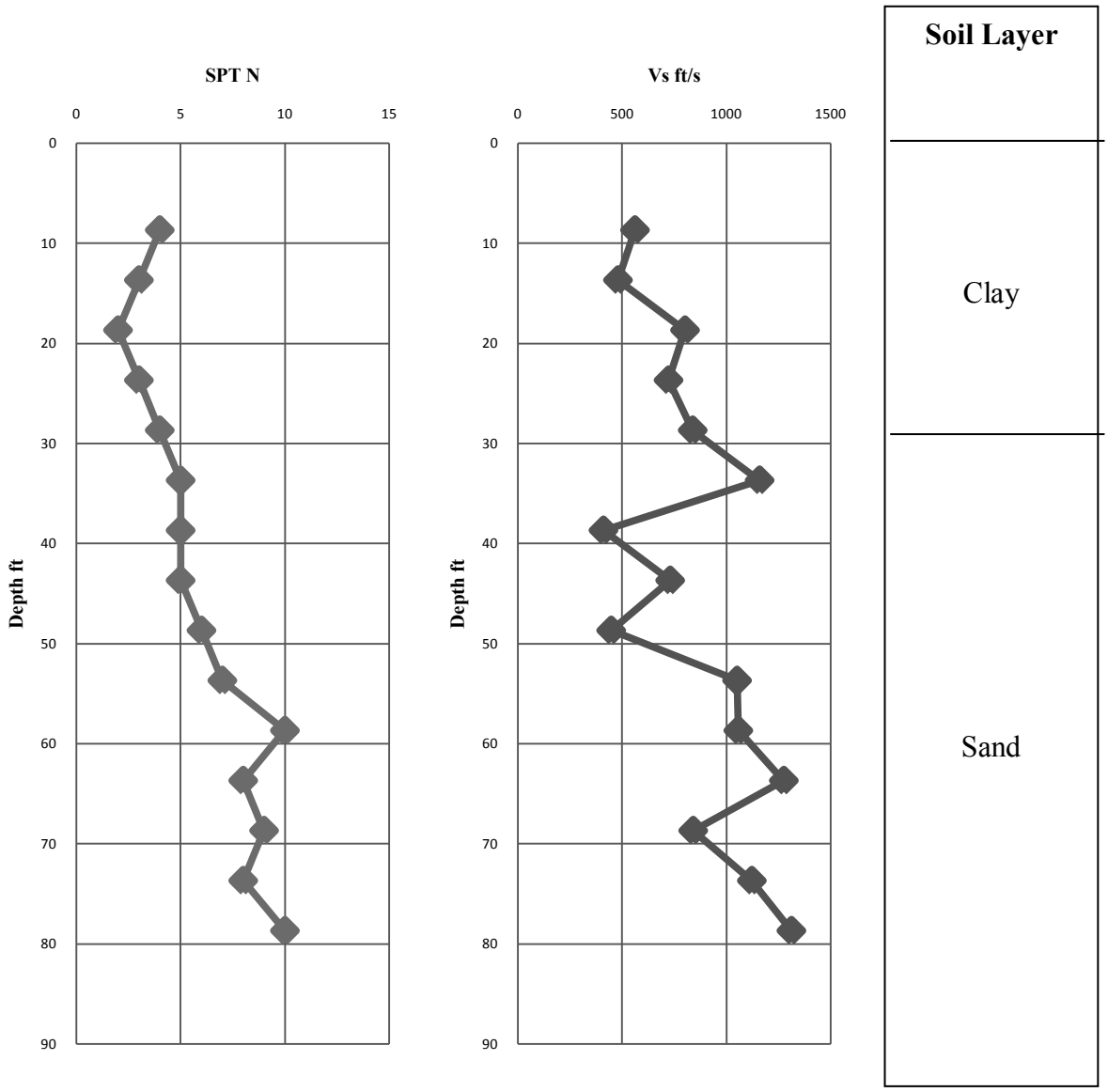


Figure 3.13 Different Test results at Site MIST, Mirpur.

### 3.4.3 Site-3

The Field SPT N values and, the shear wave velocity obtained are shown in Figure 3.14 and in Appendix B, the data is presented in tabular form. According to the figure, it was observed that- from surface to 17 ft organic soil found and rest soil was sand. SPT N value increased gradually according to depth. Shear wave velocity also increased according to depth but at some depth it decreased.

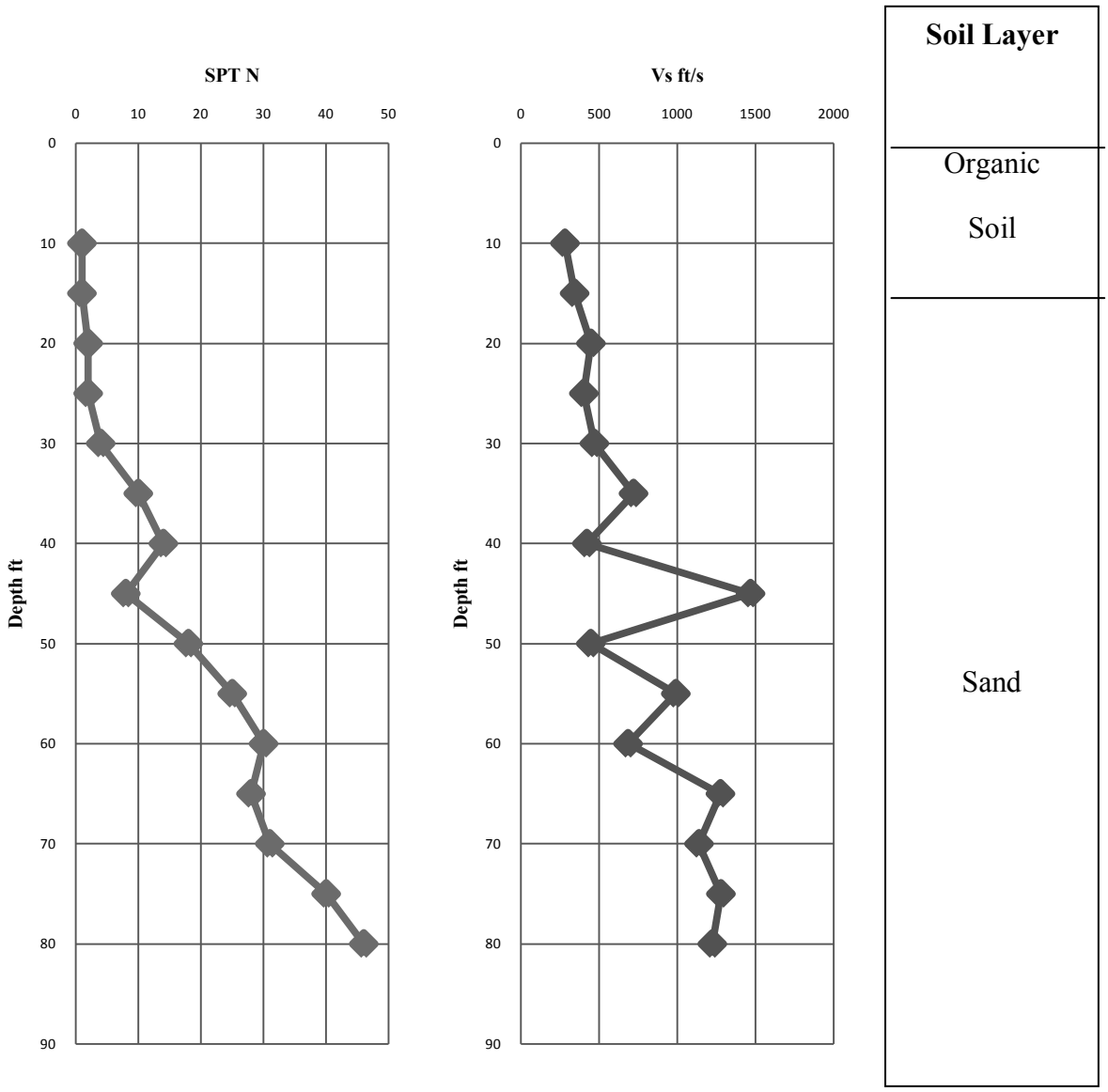


Figure 3.14 Different Test results at site Hazaribag.

### 3.4.4 Site-4

The Field SPT N values and, the shear wave velocity obtained are shown in Figure 3.15 and in Appendix B, the data is presented in tabular form. According to the figure, it was observed that- from surface to 44 ft clay soil found and rest soil was sand. SPT N value increased gradually according to depth. Shear wave velocity also increased according to depth but at some depth shear wave velocity decreased.

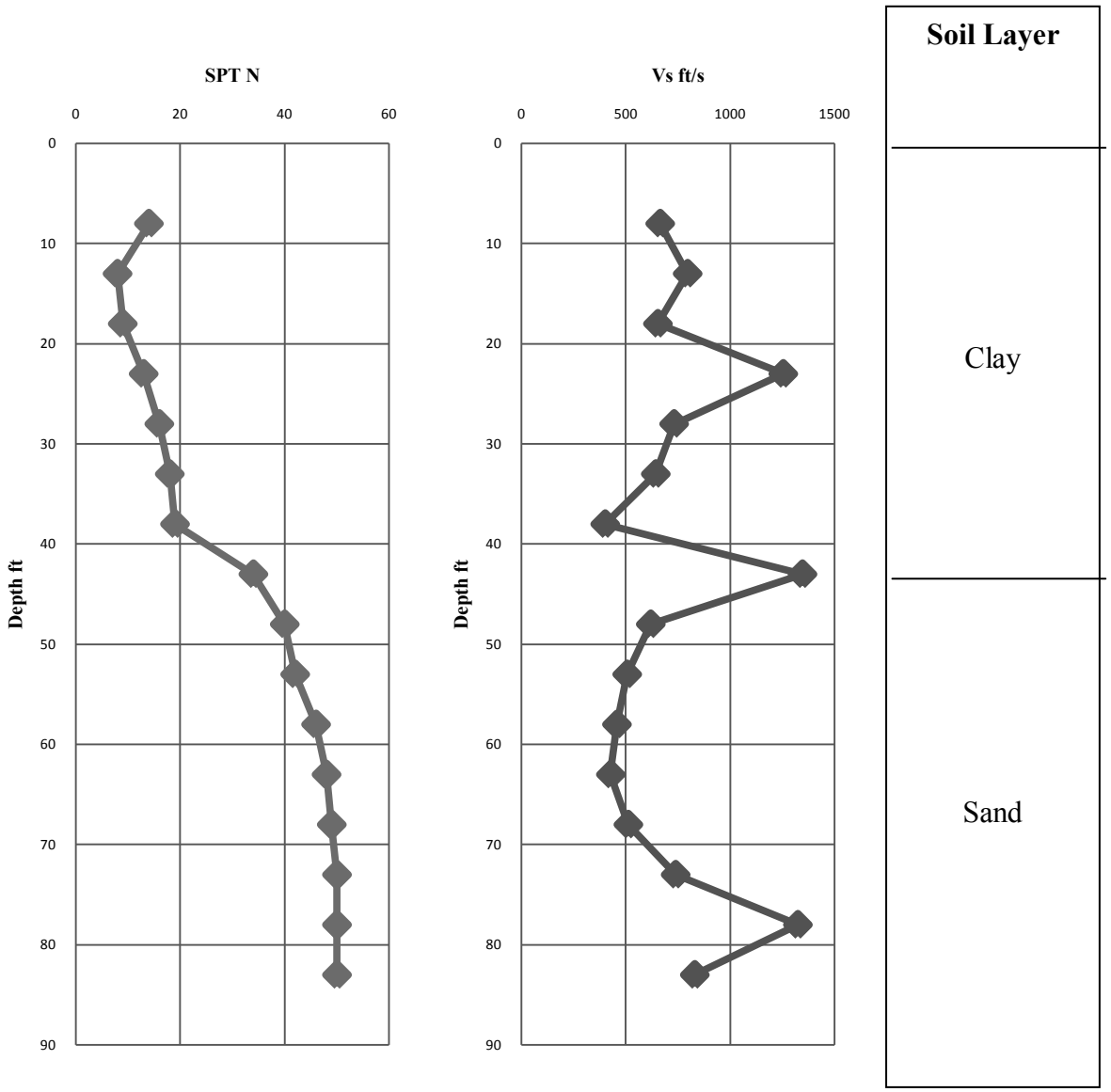


Figure 3.15 Different Test results at site Gulshan 2.

### 3.4.5 Site-5

The Field SPT N values and, the shear wave velocity obtained are shown in Figure 3.16 and in Appendix B, the data is presented in tabular form. According to the figure, it was observed that- from surface to last depth of soil was sand. SPT N value and shear wave velocity increased gradually according to depth.

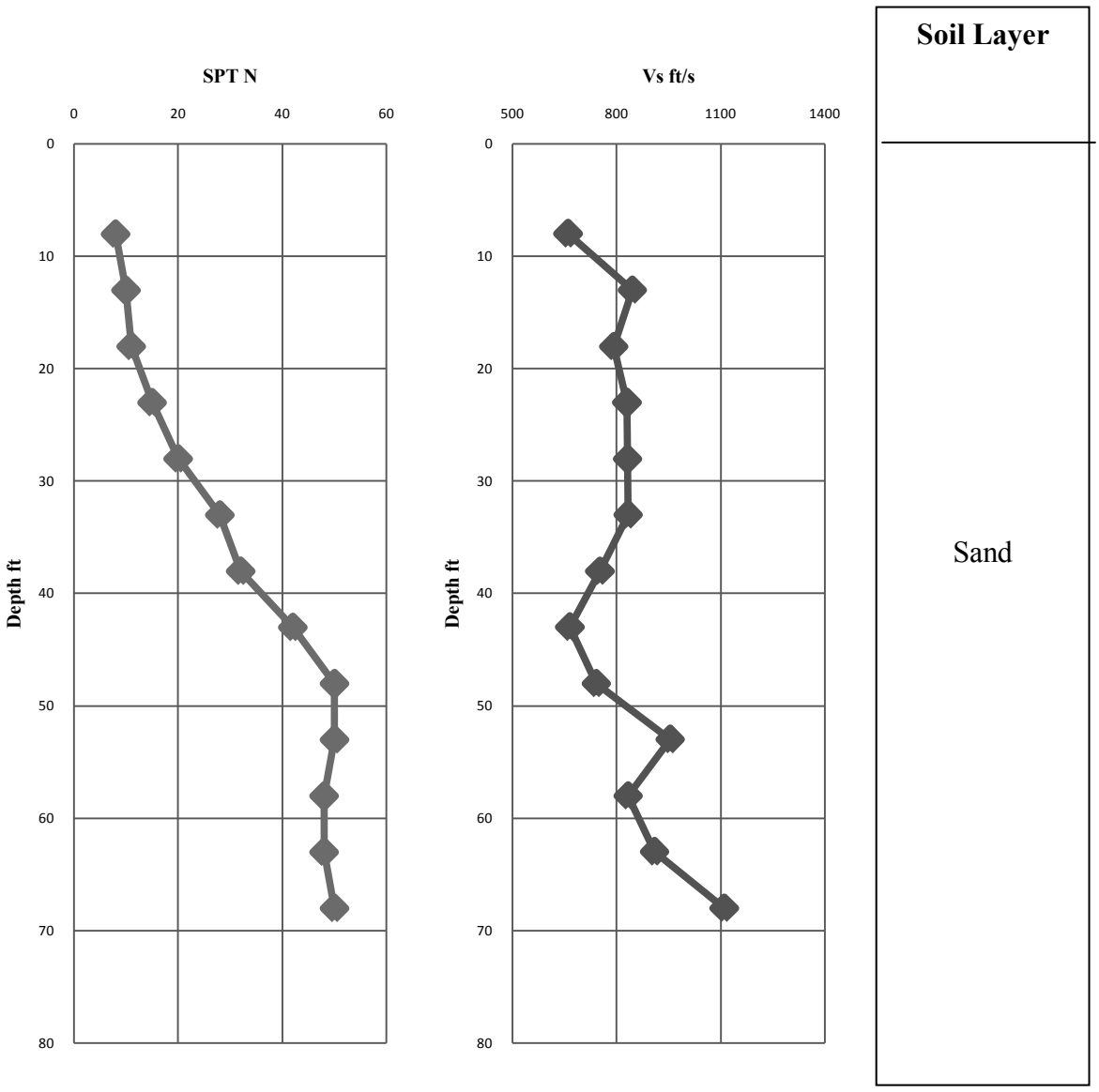


Figure 3.16 Different Test results at site Kamrangichor

### 3.4.6 Site-6

The Field SPT N values and, the shear wave velocity obtained are shown in Figure 3.17 and in Appendix B, the data is presented in tabular form. According to the figure, it was observed that- from surface to 20 ft clay soil found and rest soil was sand. SPT N value increased gradually according to depth. Shear wave velocity also increased according to depth but at some depth shear wave velocity decreased.

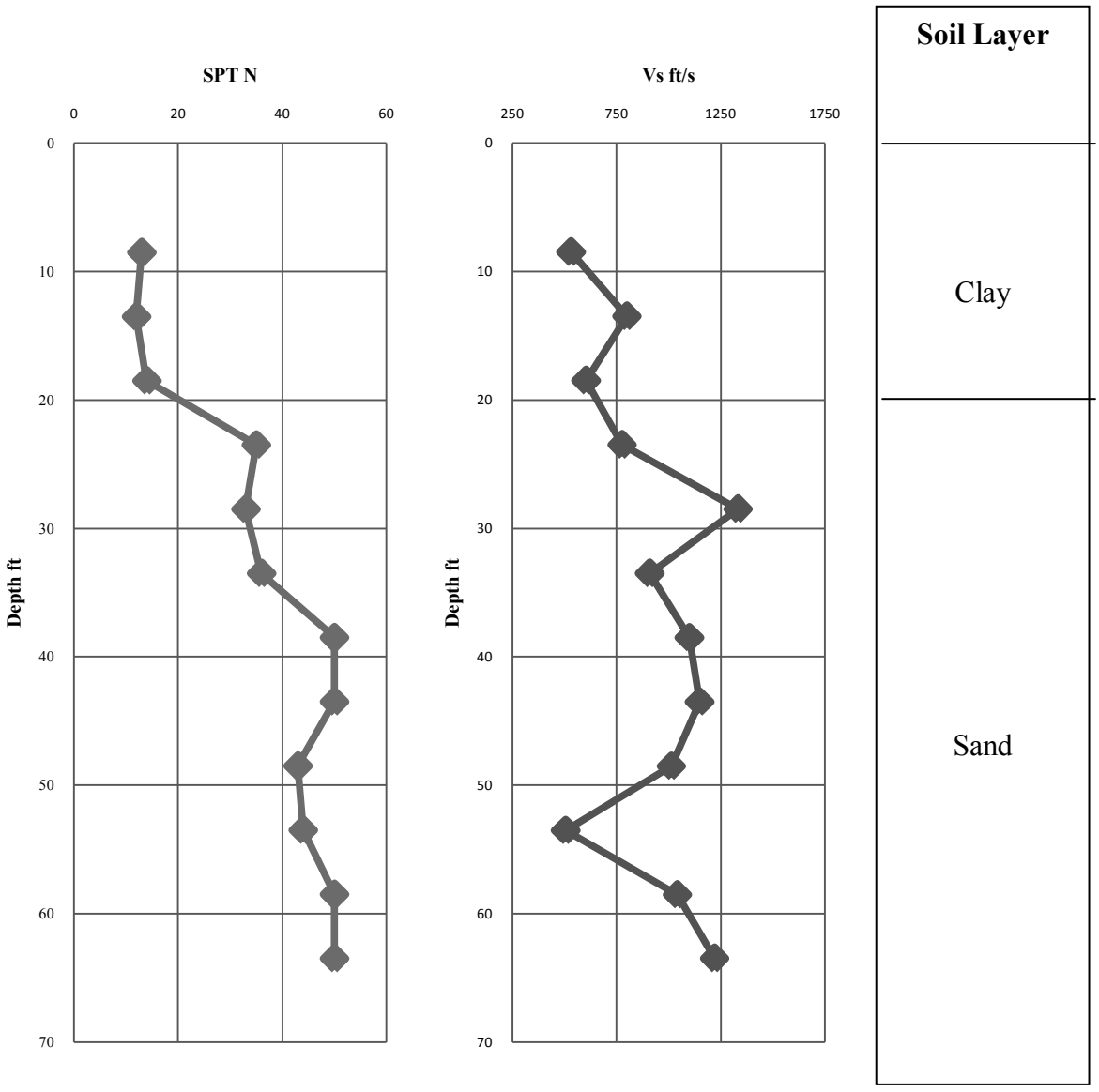


Figure 3.17 Different Test results at site Dakhin Kafrul.

### 3.4.7 Site-7

The Field SPT N values and, the shear wave velocity obtained are shown in Figure 3.18 and in Appendix B, the data is presented in tabular form. According to the figure, it was observed that- from surface to 30 ft clay soil found and rest soil was sand. SPT N value increased gradually according to depth. Shear wave velocity also increased according to depth.

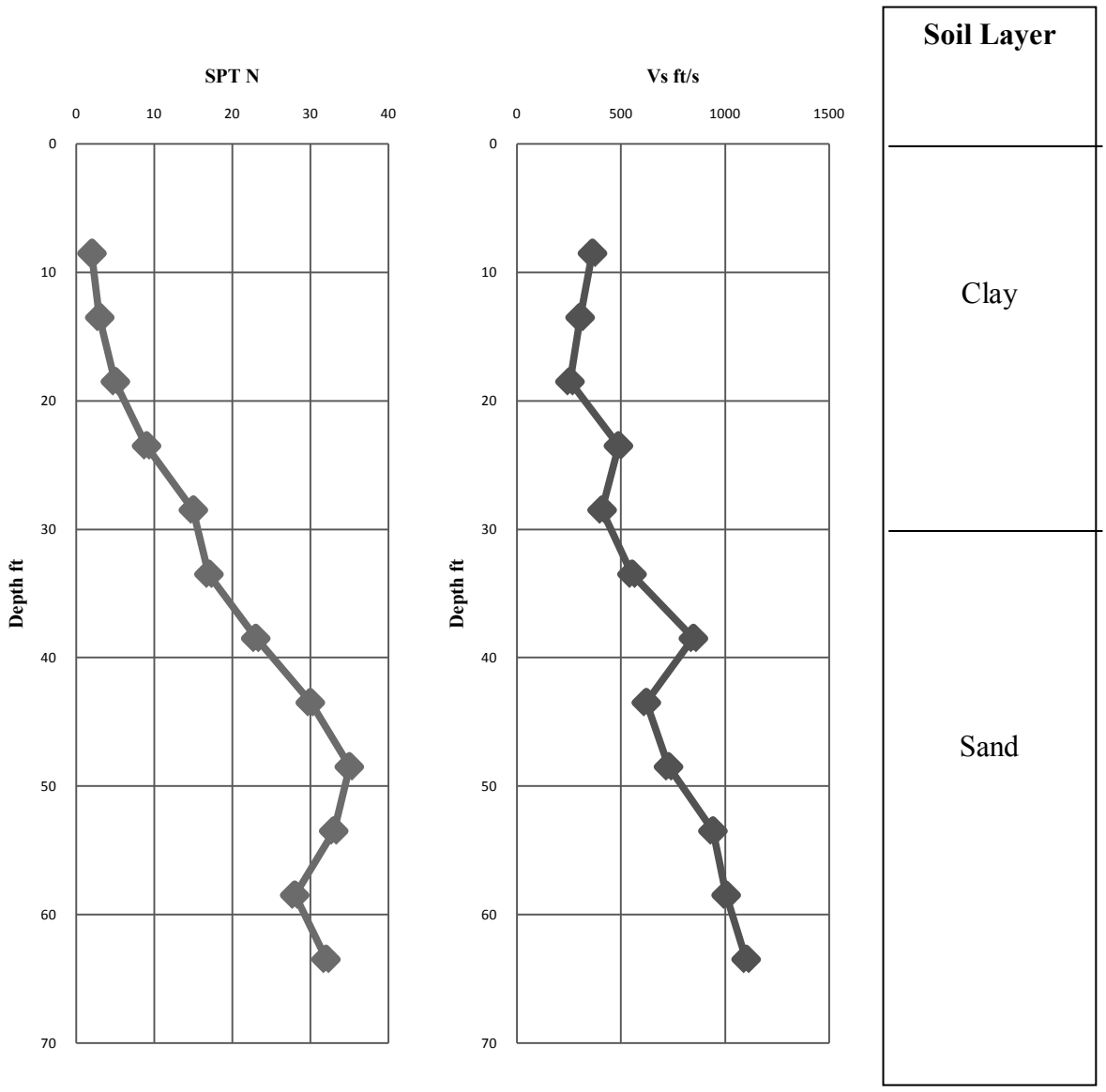


Figure 3.18 Different Test results at site Manikbagar.

### 3.4.8 Site-8

The Field SPT N values and, the shear wave velocity obtained are shown in Figure 3.19 and in Appendix B, the data is presented in tabular form. According to the figure, it was observed that- from surface to last depth of soil was sand. SPT N value increased gradually according to depth. Shear wave velocity also increased according to depth.

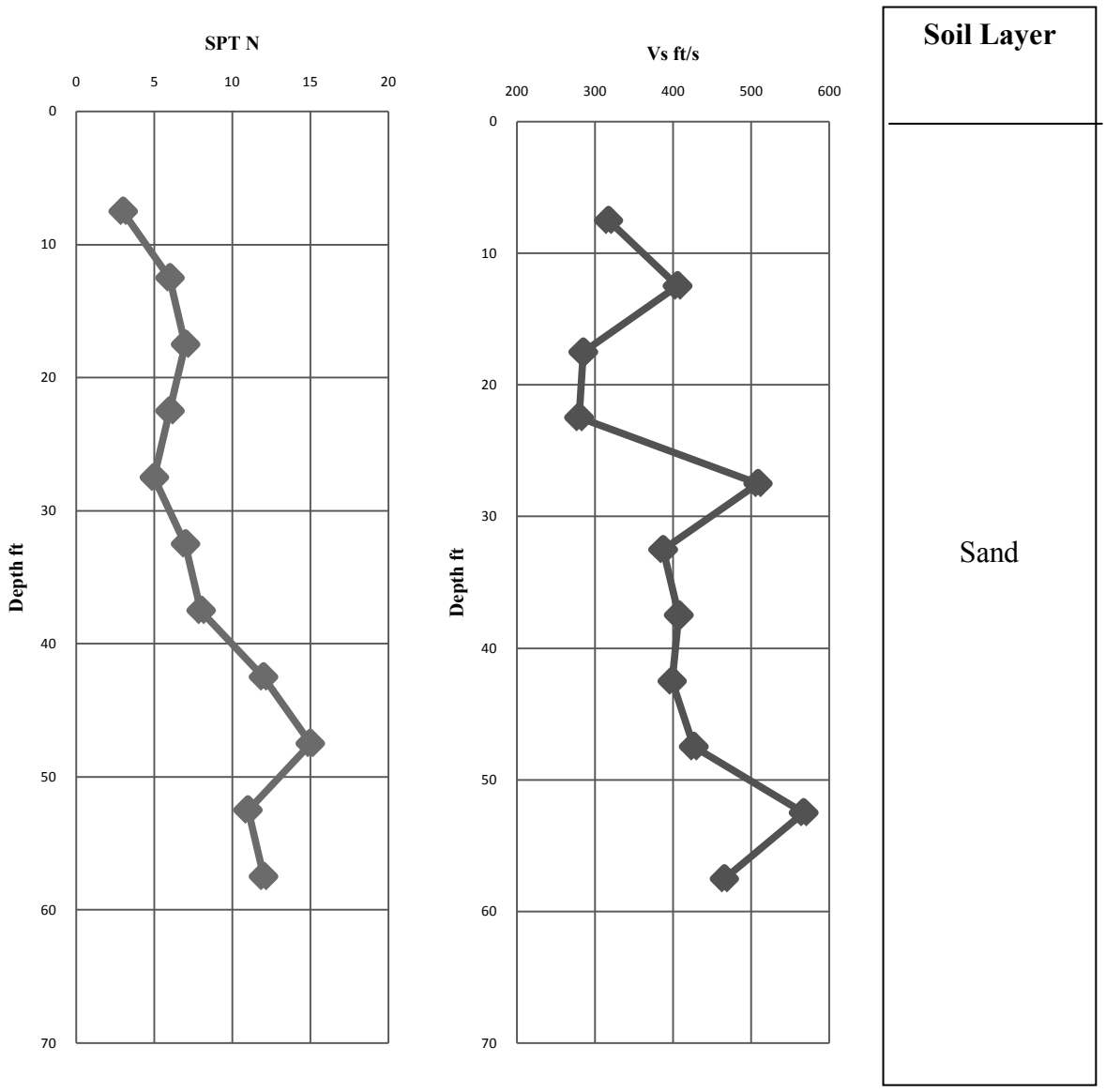


Figure 3.19 Different Test results at site Aftabnagar.

### 3.4.9 Site-9

The Field SPT N values and, the shear wave velocity obtained are shown in Figure 3.20 and in Appendix B, the data is presented in tabular form. According to the figure, it was observed that- from surface to 20 ft clay soil found and rest soil was sand. SPT N value increased gradually according to depth. Shear wave velocity also increased according to depth but at some depth shear wave velocity decreased.

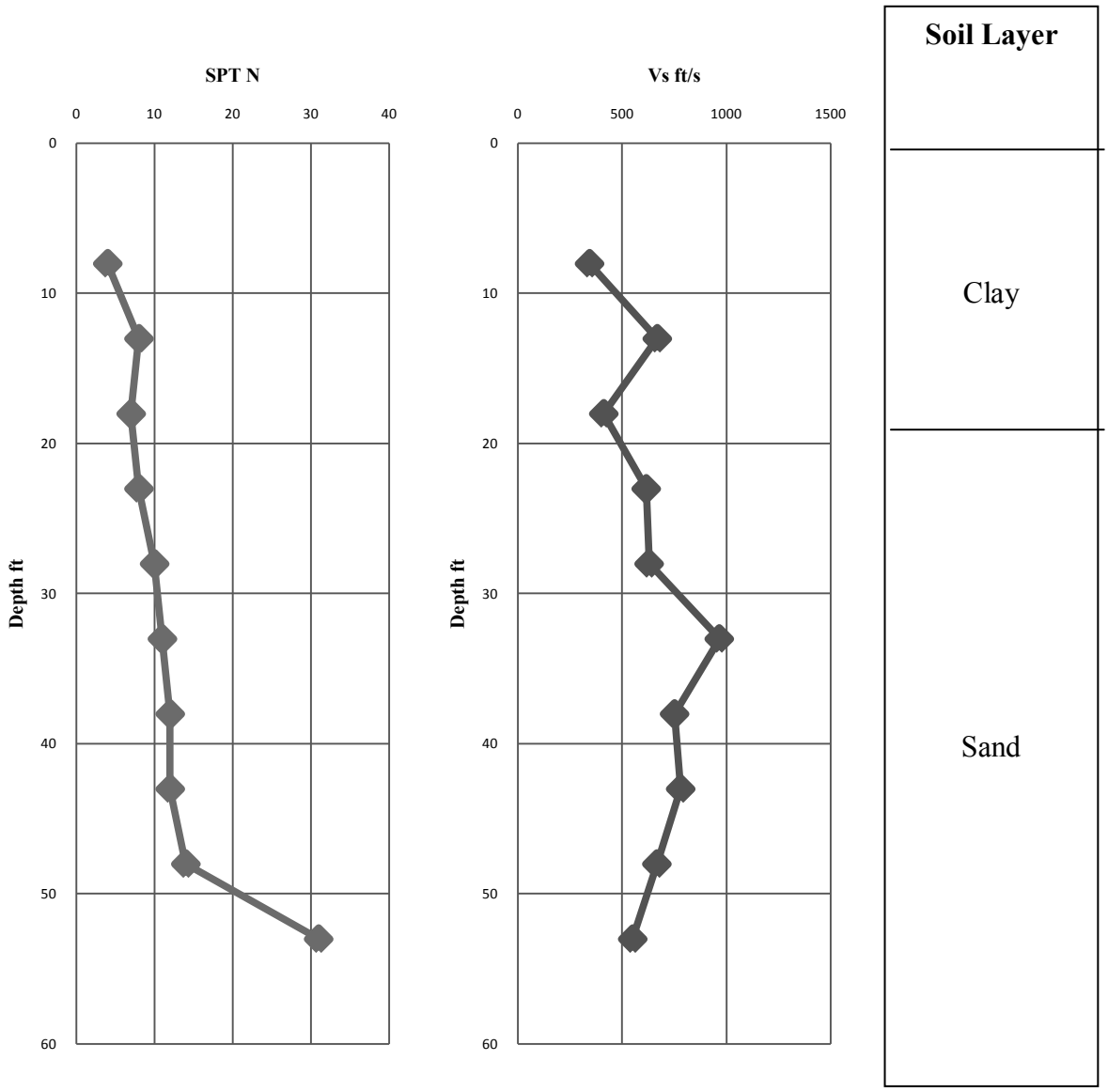


Figure 3.20 Different Test results at site Lake City Concord, Khilkhet

### 3.4.10 Site-10

The Field SPT N values and, the shear wave velocity obtained are shown in Figure 3.21 and in Appendix B, the data is presented in tabular form. According to the figure, it was observed that- from surface to 25 ft clay soil found and rest soil was sand. SPT N value increased gradually according to depth. Shear wave velocity also increased according to depth.

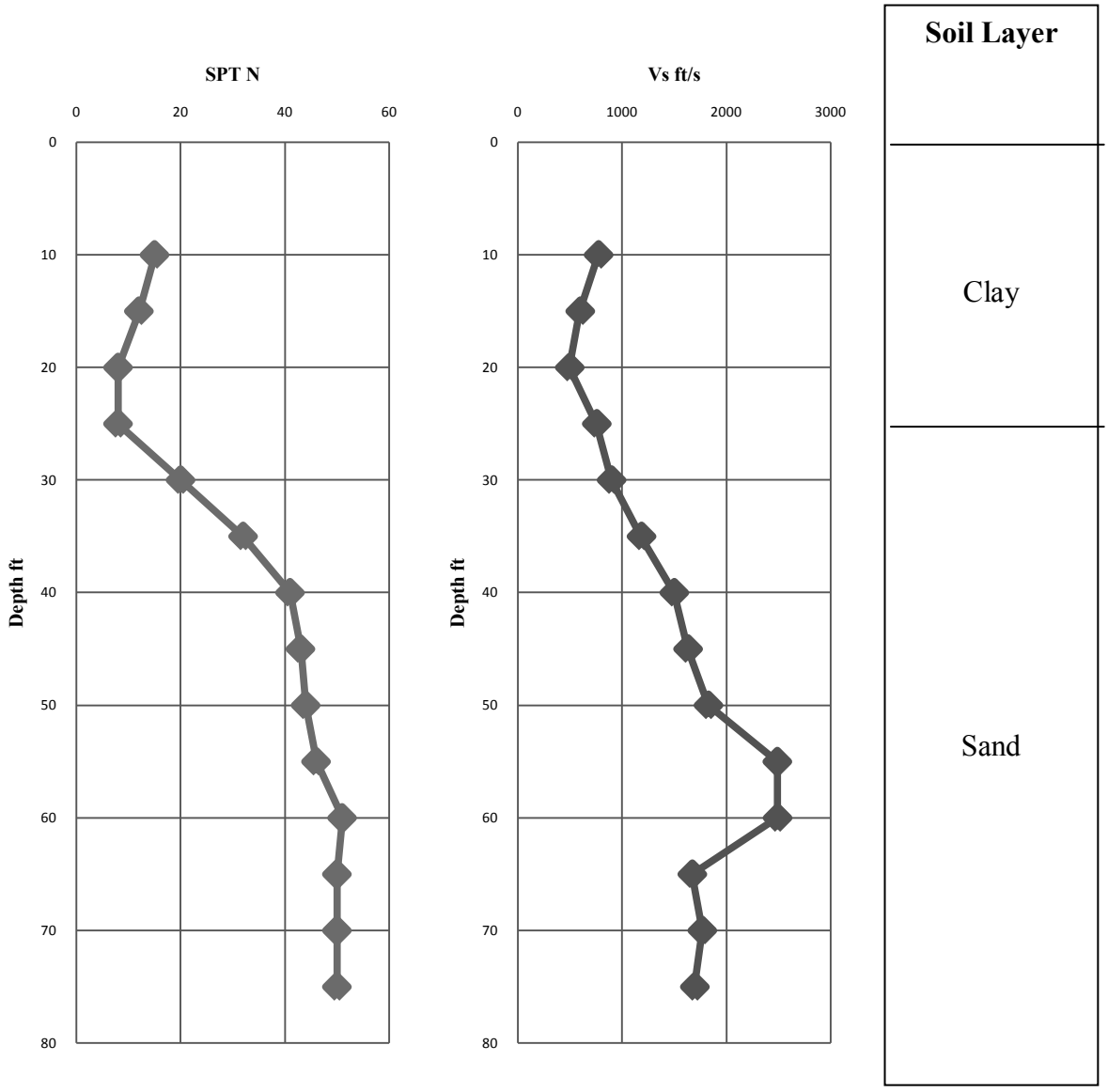


Figure 3.21 Different Test results at site RHD, Tejgaon.

### 3.5 Collected Data of Different Locations

#### 3.5.1 Site-11

The Field SPT N values and, the shear wave velocity obtained are shown in Figure 3.22 and in Appendix B, the data is presented in tabular form. According to the figure, it was observed that- from surface to 20 ft clay soil found and rest soil was sand. SPT N value increased gradually according to depth. Shear wave velocity also increased according to depth but at some depth shear wave velocity decreased.

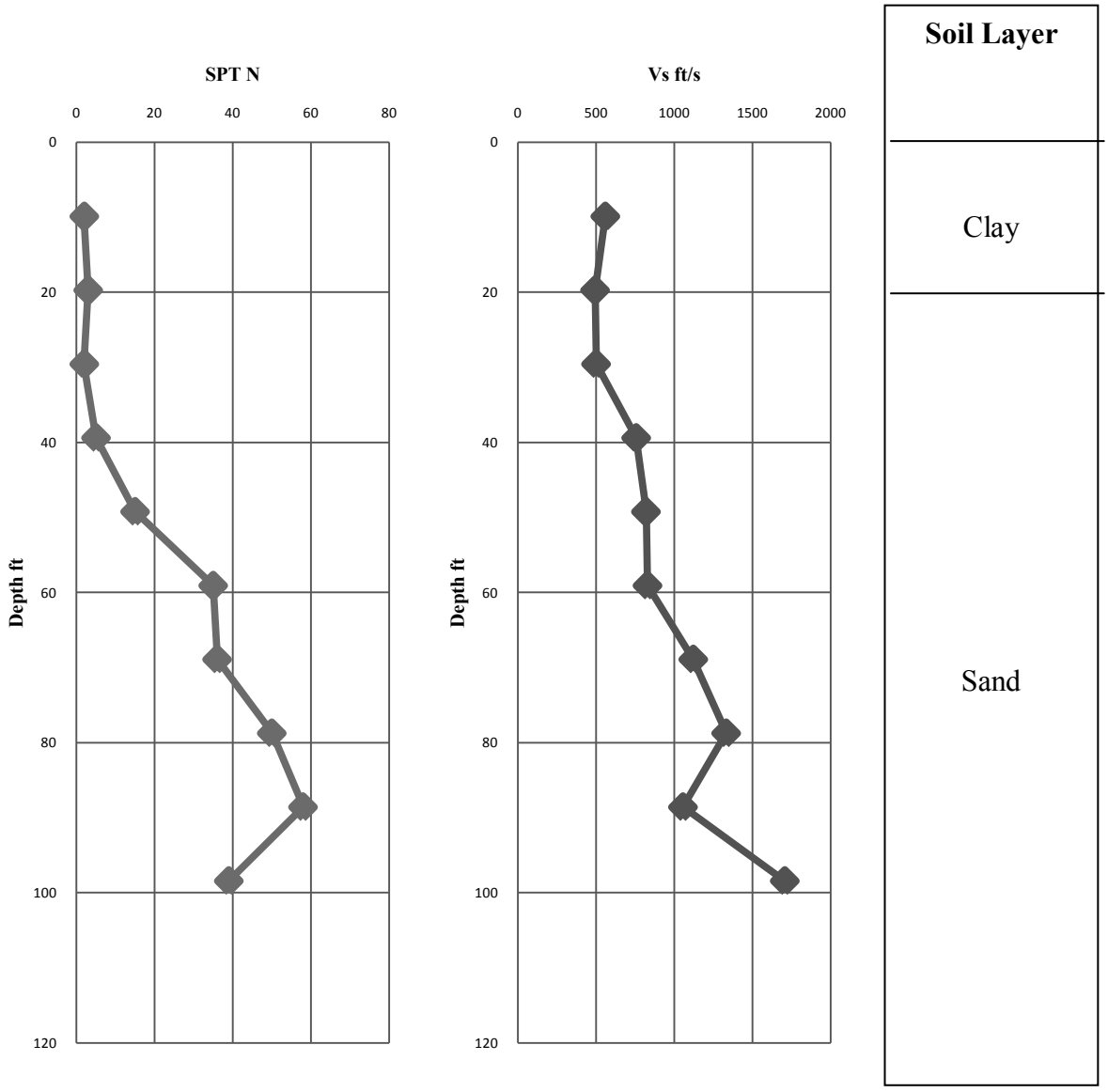


Figure 3.22: Different Test results at Site Mehernagar Uttara.

### 3.5.2 Site-12

The Field SPT N values and, the shear wave velocity obtained are shown in Figure 3.23 and in Appendix B, the data is presented in tabular form. According to the figure, it was observed that- from surface to 45 ft clay soil found and rest soil was sand. SPT N value increased gradually according to depth. Shear wave velocity also increased according to depth.

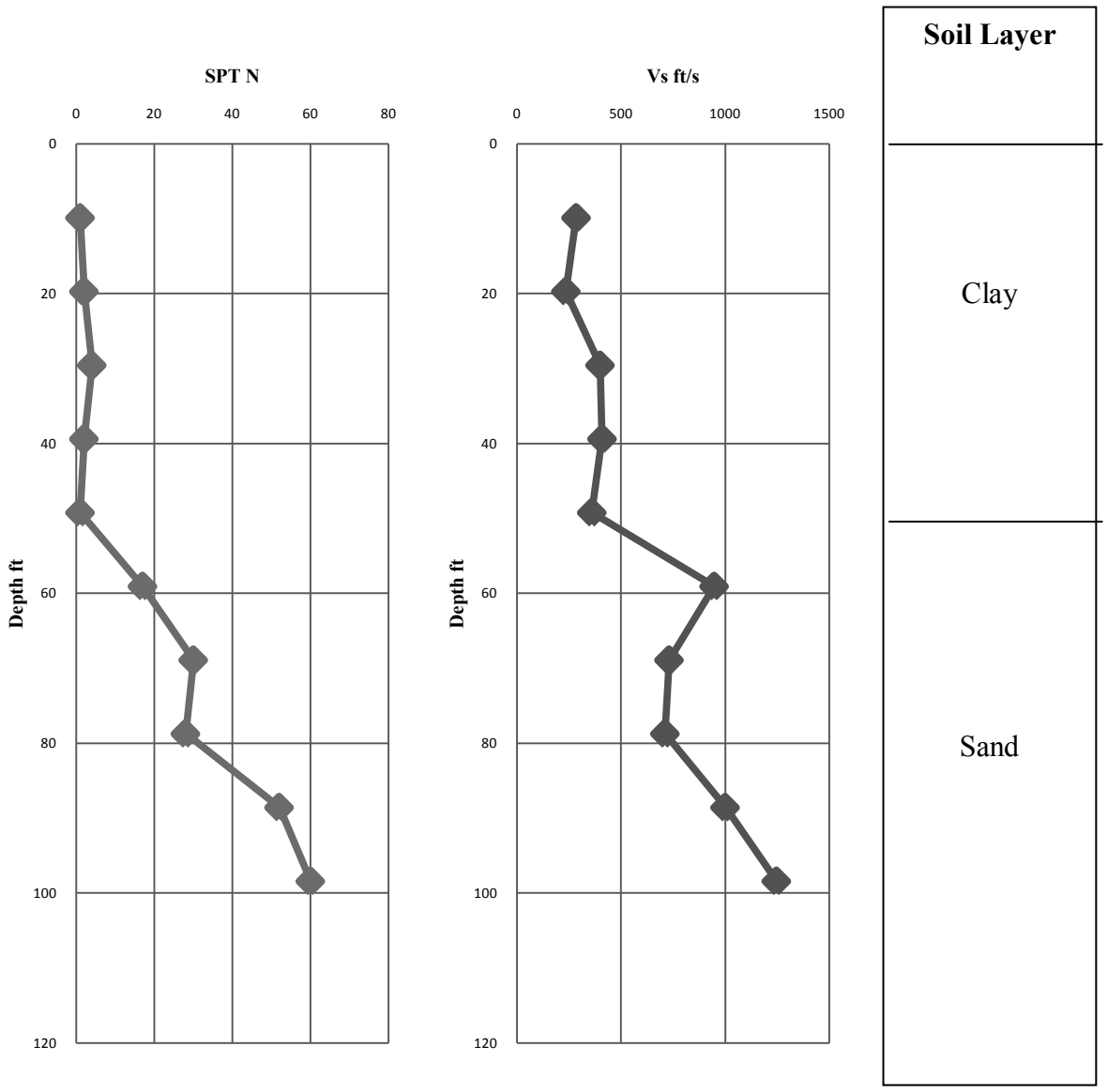


Figure 3.23 Different Test results at Site Ashulia, Jubok Project

.

### 3.5.3 Site-13

The Field SPT N values and, the shear wave velocity obtained are shown in Figure 3.24 and in Appendix B, the data is presented in tabular form. According to the figure, it was observed that- from surface to 10 ft it was sand; from 10 ft to 30 ft clay; from 30 ft to rest soil was sand. SPT N value increased gradually according to depth. Shear wave velocity also increased according to depth but at some depth shear wave velocity decreased.

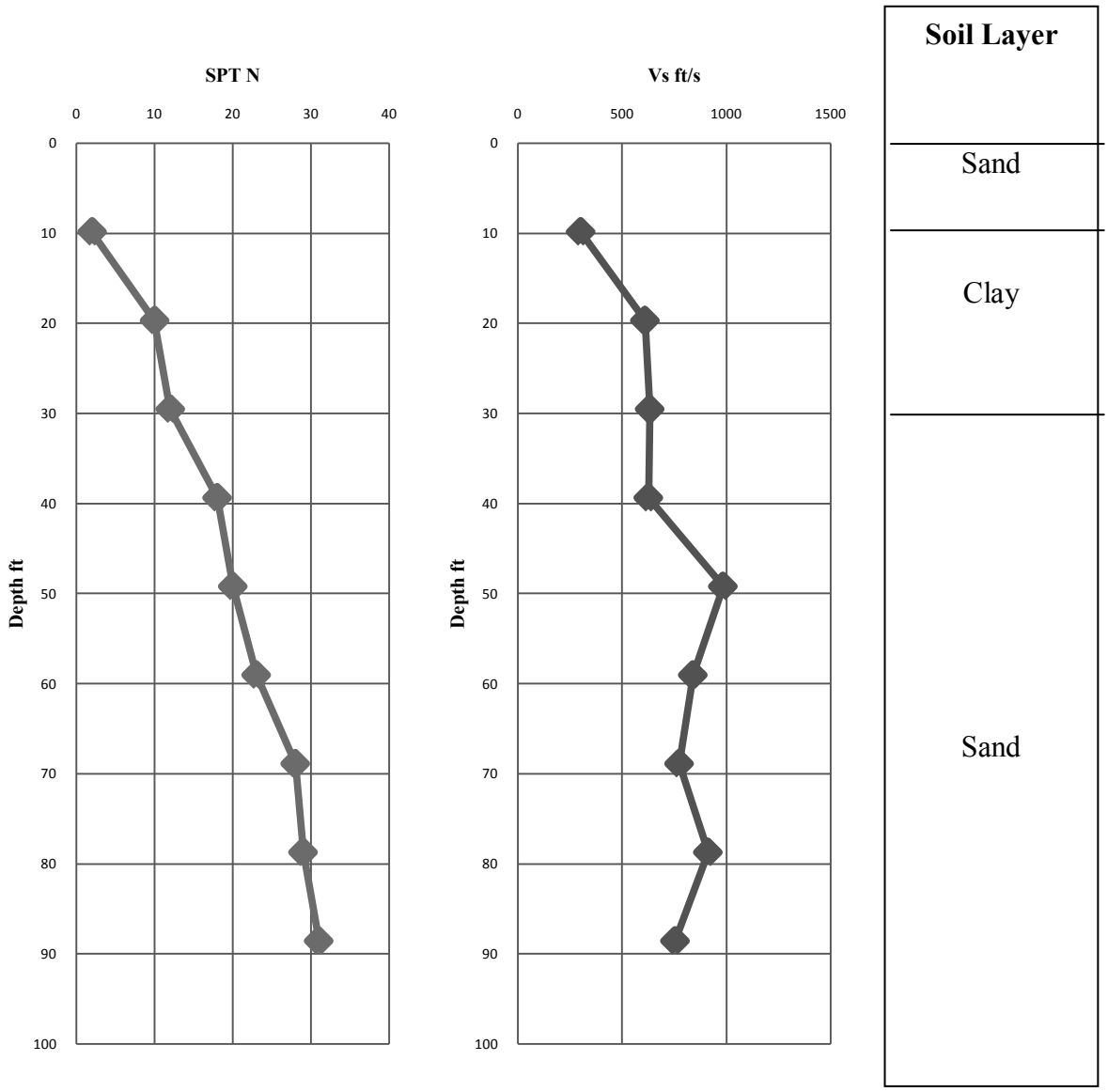


Figure 3.24 Different Test results at Site Mirpur-1, Avenue-2

### 3.5.4 Site-14

The Field SPT N values and, the shear wave velocity obtained are shown in Figure 3.25 and in Appendix B, the data is presented in tabular form. According to the figure, it was observed that- from surface to 10 ft it was sand; from 10 ft to 50 ft clay; from 50 ft to rest soil was sand. SPT N value increased gradually according to depth. Shear wave velocity also increased according to depth.

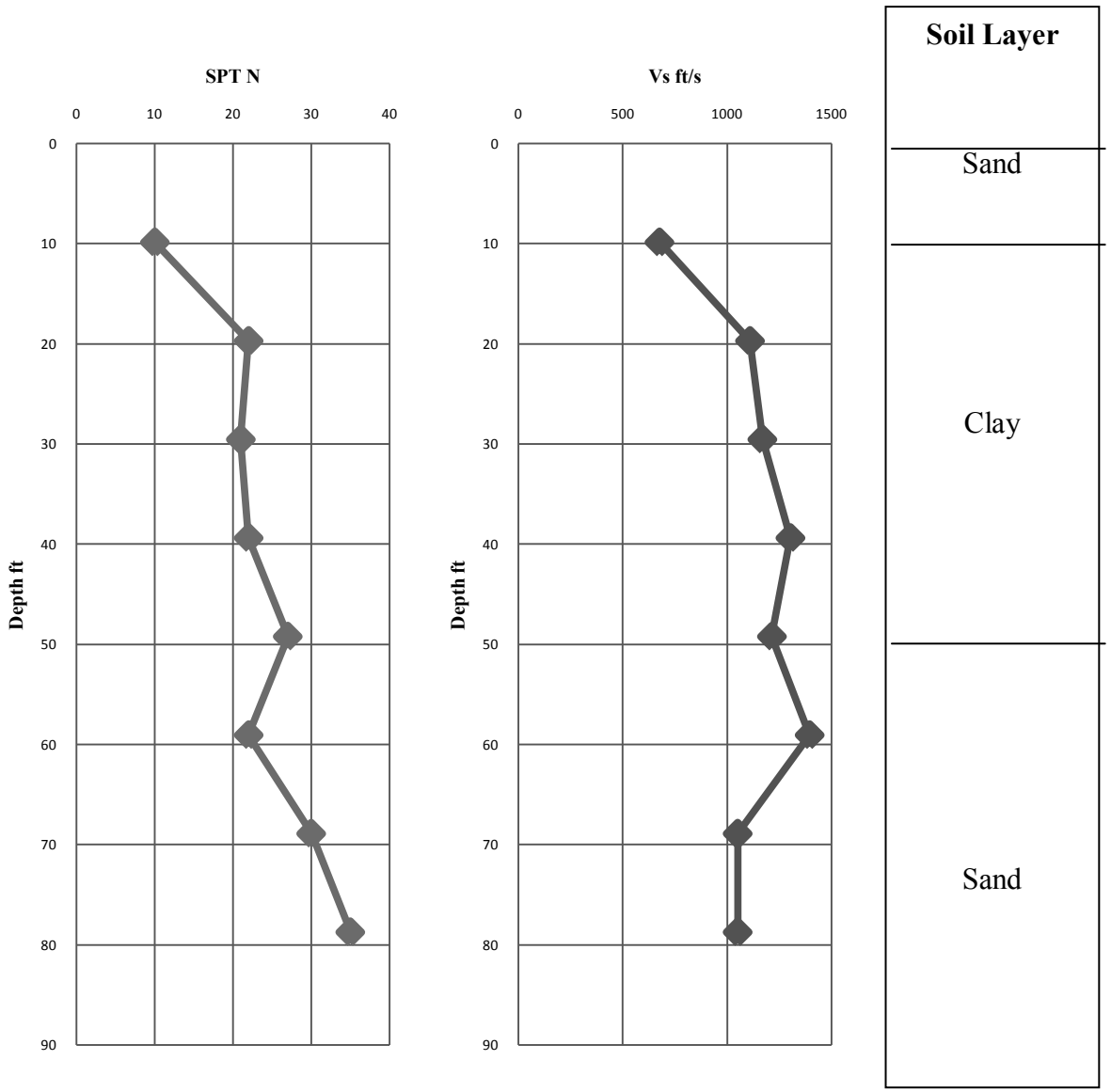


Figure 3.25 Different Test results at Site Akash Nagar, Mohammadpur, Beribadh

### 3.5.5 Site-15

The Field SPT N values and, the shear wave velocity obtained are shown in Figure 3.26 and in Appendix B, the data is presented in tabular form. According to the figure, it was observed that- from surface to 10 ft it was sand; from 10 ft to 50 ft clay; from 50 ft to 60 ft was sand and rest soil was clay. SPT N value and shear wave velocity was same up to depth 60 ft.

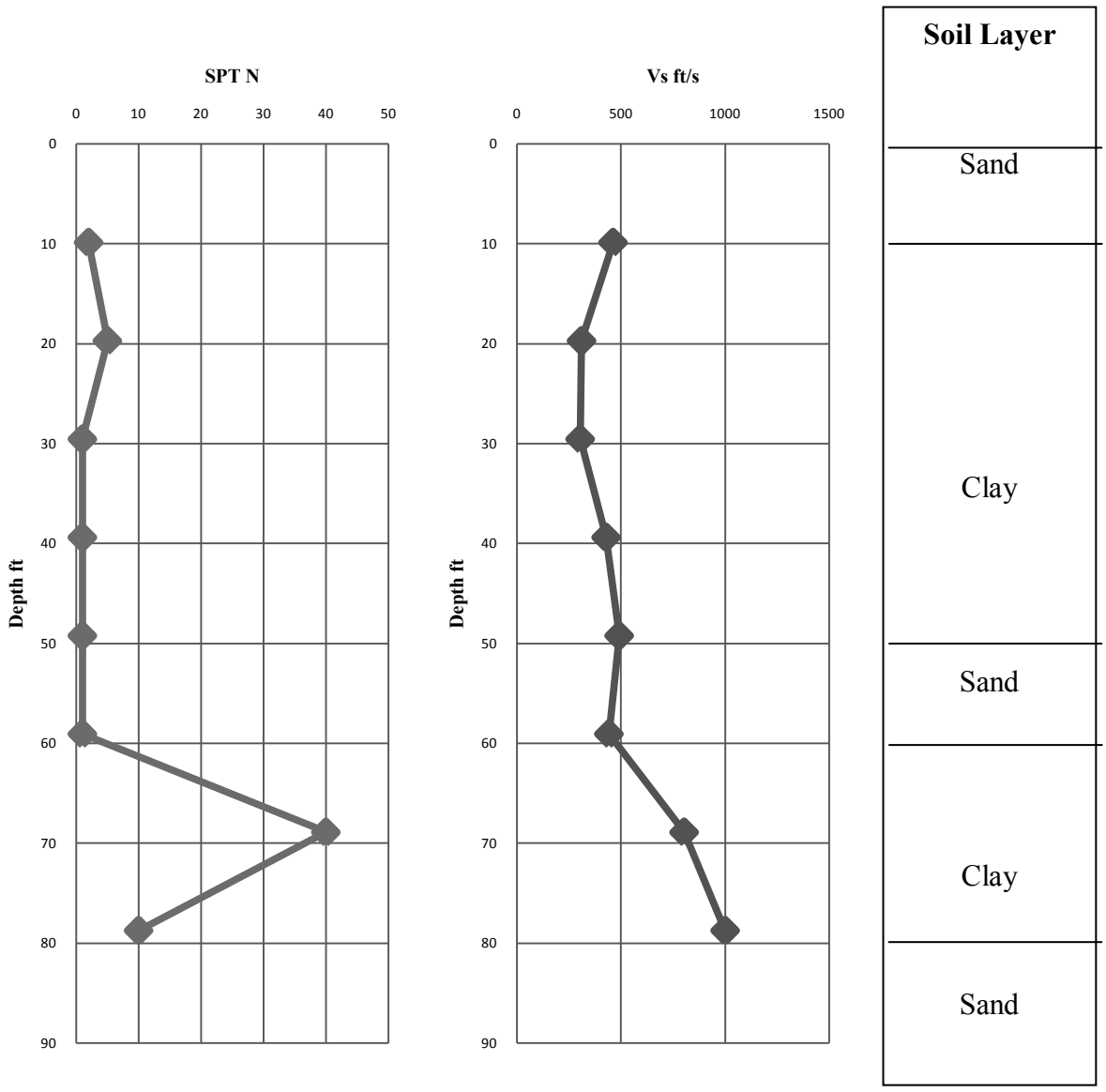


Figure 3.26 Different Test results at Site United City Project, Beraidh

### 3.5.6 Site-16

The Field SPT N values and, the shear wave velocity obtained are shown in Figure 3.27 and in Appendix B, the data is presented in tabular form. According to the figure, it was observed that- from surface to 10 ft clay soil found and rest soil was sand. SPT N value increased gradually according to depth. Shear wave velocity also increased according to depth.

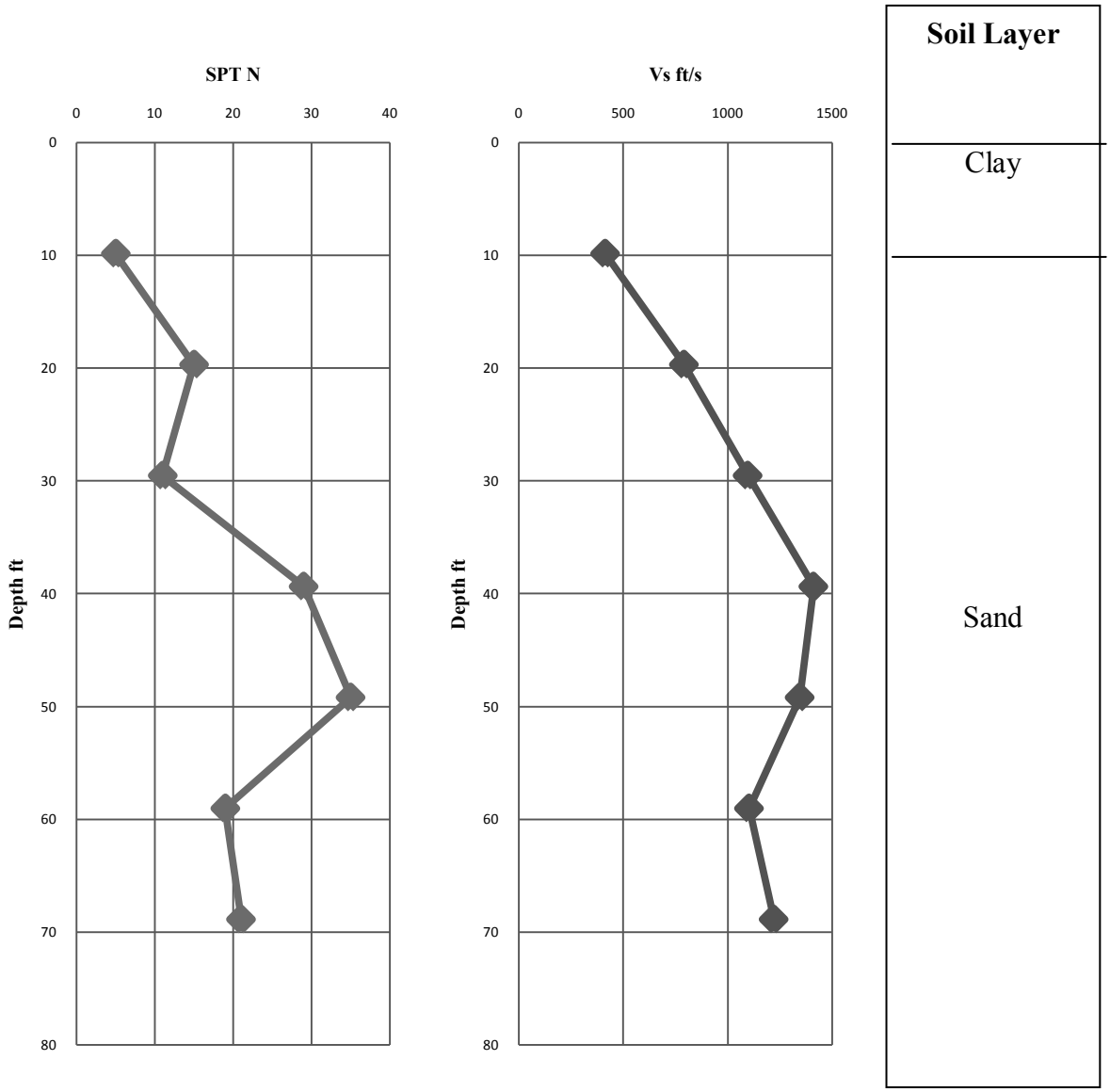


Figure 3.27: Different Test results at Site East Nandipara

### 3.5.7 Site-17

The Field SPT N values and, the shear wave velocity obtained are shown in Figure 3.28 and in Appendix B, the data is presented in tabular form. According to the figure, it was observed that- from surface to 45 ft clay soil found and rest soil was sand. SPT N value and Shear wave velocity decreased gradually according to depth.

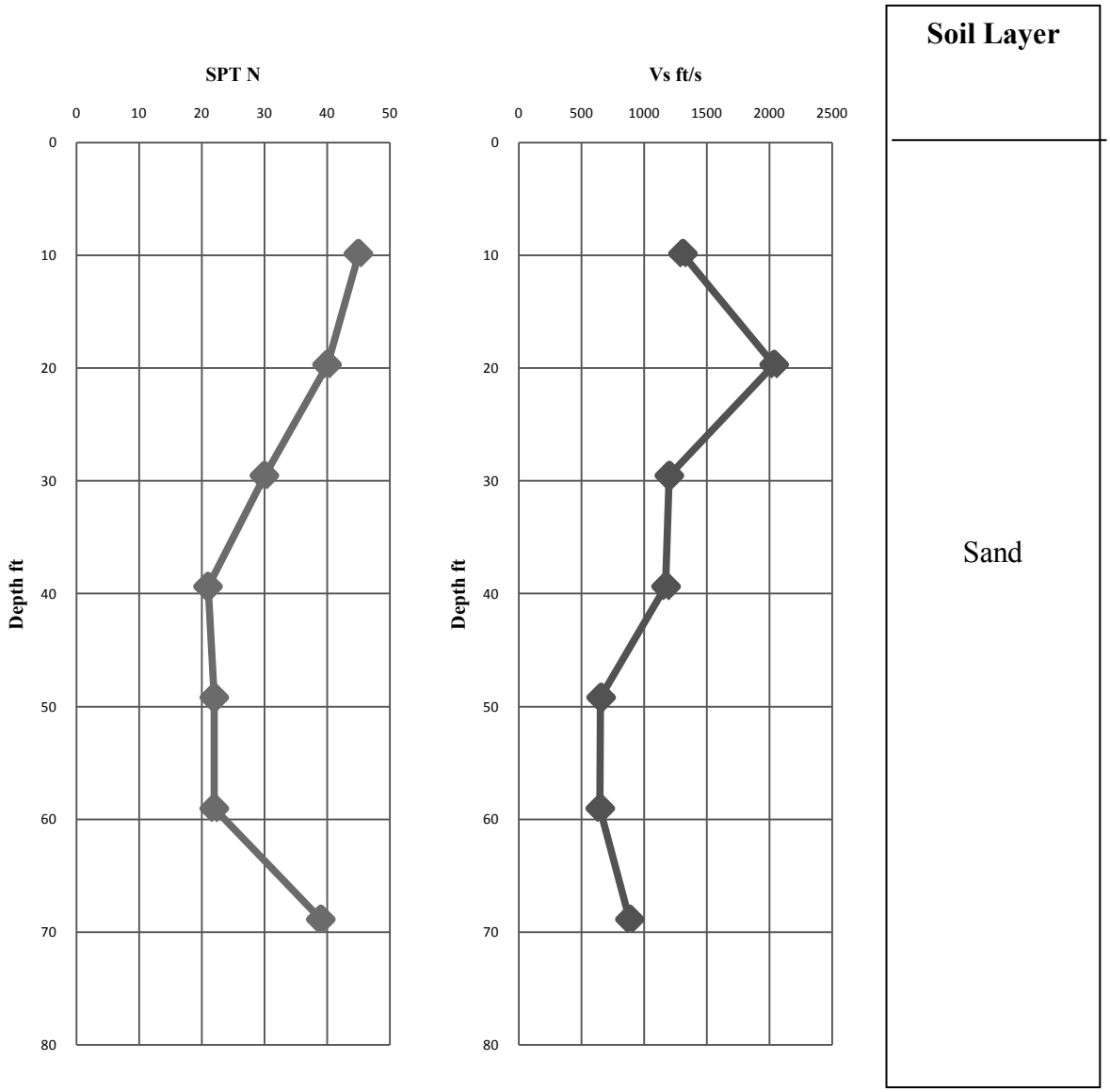


Figure 3.28 Different Test results at Site Asian City, Dokhinkhan

### 3.6 Correlations between SPT N – Shear Wave Velocity (Vs) and Depth

The SPT has historically been the most widely used in situ geotechnical test throughout the world. Researchers have studied the relationship between $V_S$ and SPT N values since the 1960s. A correlation was suggested using 189 set of data of depth, SPT N value and shear wave velocity. Figure 3.29 and Figure 3.30 shows the relation between the $V_s$ and depth and $V_s$ and SPT N value.

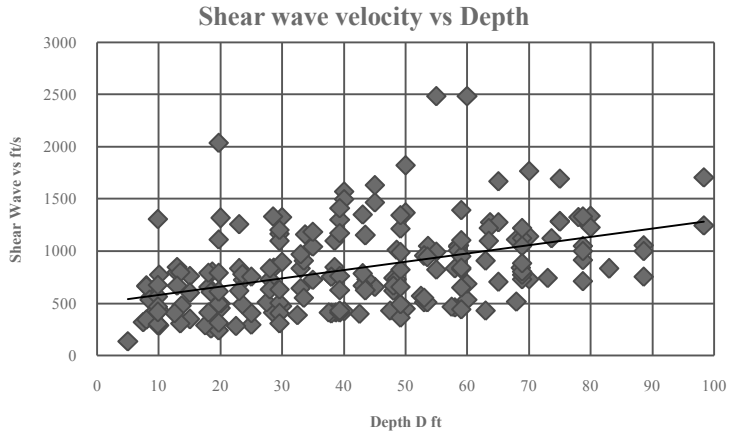


Figure 3.29: Graph of Shear Wave Velocity (Vs) and Depth

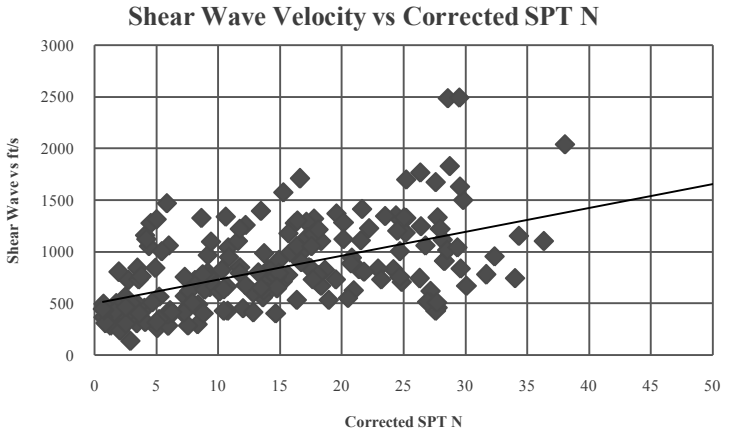


Figure 3.30 Graph of Shear Wave Velocity (Vs) and Corrected SPT N

Considering $V_S$ as the dependent variable and depth and the SPT N value as the independent variable following correlation was obtained for top soil at Dhaka City.

$$V_s = 169\ N^{0.2638}\ D^{0.2396}\ [r^2=0.45]$$

Here,

Vs = Shear wave velocity in ft/sec

N = Corrected Standard penetration Number

D = Depth in ft.

# CHAPTER FOUR

# RESULTS OF GROUND RESPONSE ANALYSIS

## 4.1 General

Generally earthquake effects are considered on the basis of degree of damage in addition to the recorded ground motions at a site. During the Northridge earthquake (M 6.7) in 1994, high ground motions were recorded (PGA 1.82g) whereas the predicted PGA at 100m was 0.46g (Silva, 2000). The curvature of a sediment-filled basin structure in particular can confine body waves and can cause some incident body waves to propagate through the alluvium as surface waves resulting stronger shaking effects and longer duration of strong ground motion (Kramer, S.L., 1996). Such is the effect of seismic wave propagation and amplification. So, for the estimation of seismic hazard, estimation of site specific dynamic response is important. The results of ground response analysis form an important parameter in case of performance based design. Cramer, and Real, (1992) concluded that variability in the geotechnical model associated with uncertainty in stiffness and damping characteristics more significantly impacted the predicted motions than variability between different methods of analysis utilizing relatively consistent velocity profiles (i.e., from preferred versus standard geotechnical models).

Most of the places of Dhaka city are underlain by loose sandy silts and silty clay which makes it vulnerable during an earthquake due to the ground motion amplification of the young, loose soil deposits in the area. Site response analysis consists of estimation of local site effects and surface ground motion. This chapter deals with the estimation of surface ground motion for Dhaka city. This chapter presents the ground responses analysis outputs of the selected locations in Dhaka city.

## 4.2. Ground Response Analysis

During earthquake, propagation of seismic waves through soil column alters the amplitude, frequency and duration of ground motion by the time it reaches the surface. The effects of ground motion are propagated in the form of waves from one medium to another. So, physically it is problem of prediction of ground motion characteristics whereas mathematically it is a problem of the wave propagation in continuous medium. The

evaluation of such response of the site to dynamic loading is termed as ground response analysis.

The Shear wave velocity ($V_s$) is one of the most important input parameter to represent the stiffness of the soil layers. Total ten locations were selected for Site Amplification Analysis in Dhaka city in this research. The Shear wave velocity ($V_s$) was measured in ten selected locations of Dhaka city by using Suspension PS Logging equipment.

In Dhaka City the depth of bedrock was unavailable due to lack of deep boreholes. In DEEPSOIL (Hashash, et al., 2011), rock depth was assumed to be below the last layer, so to prevent erroneous results the last layer was assumed to be the same up to a depth of 100m.

For site response analysis by equivalent linear method the results are considered to be accurate for estimating PGA up to 3sec for general projects (Finn, 1995; Martin, 1994; Durward, 1996; Dobry, 2000; Dickenson, 1995). Input ground motion have to be selected in such way that they represent the regional seismicity and must incorporate the anticipated earthquakes. The selection of ground motion can be done based on expected magnitude and distance, soil profile, strong motion duration, seismic-tectonic environment, acceleration to vertical ratio, spectral matching etc. In this study, The Kobe Earthquake in South-Central Japan on January 17, 1995 (Mb-7.2);The Imperial Valley earthquake in Mexico–United States border on October 15, 1979; The Northridge earthquake in the north-central San Fernando Valley region of Los Angeles, California on January 17 1994 (Mb-6.7) and The Kocaeli Earthquake at Kocaeli, Turkey on August 17, 1999(Mb-7.4) were selected as input motion for ground response analysis. The time history of the earthquake input motions are shown in Figure 4.1 to Figure 4.4. All input motions were converted to Site class A, to be imposed on the bottom of the bed rock. Then it was scaled to 0.19g. The spectral acceleration of the converted input motions are shown in Figure 4.5.

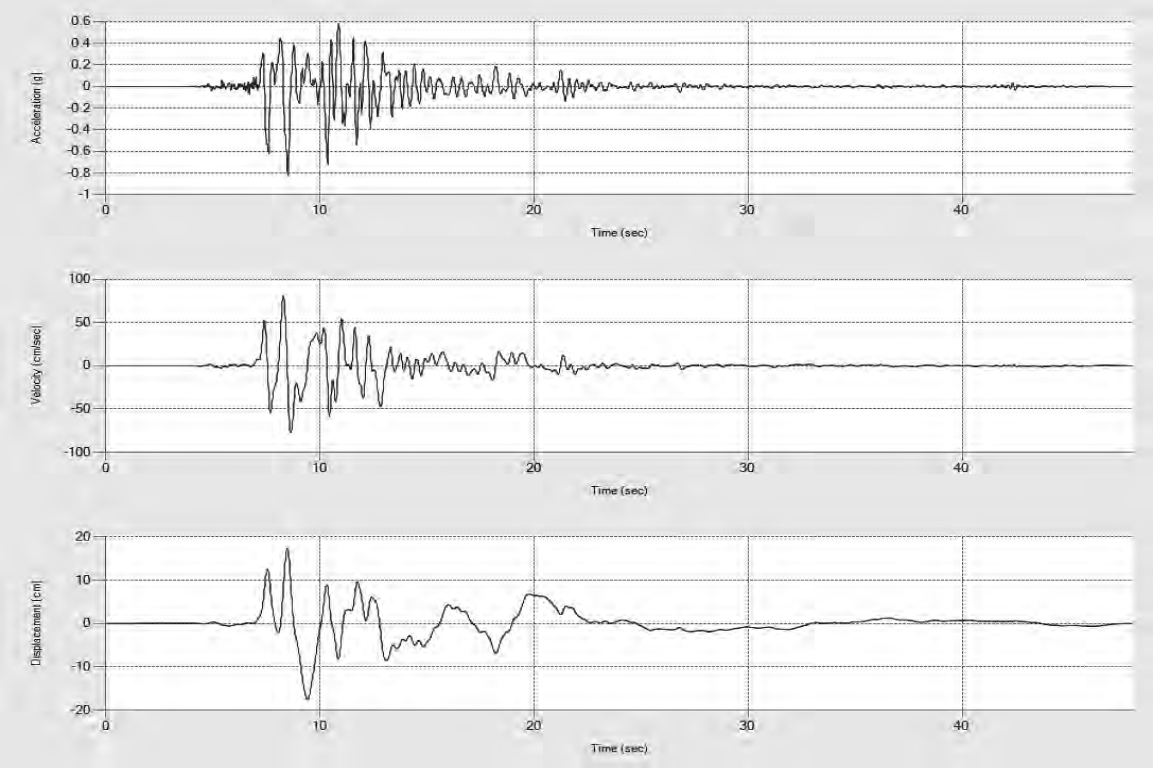


Figure 4.1 Time history of Kobe Earthquake

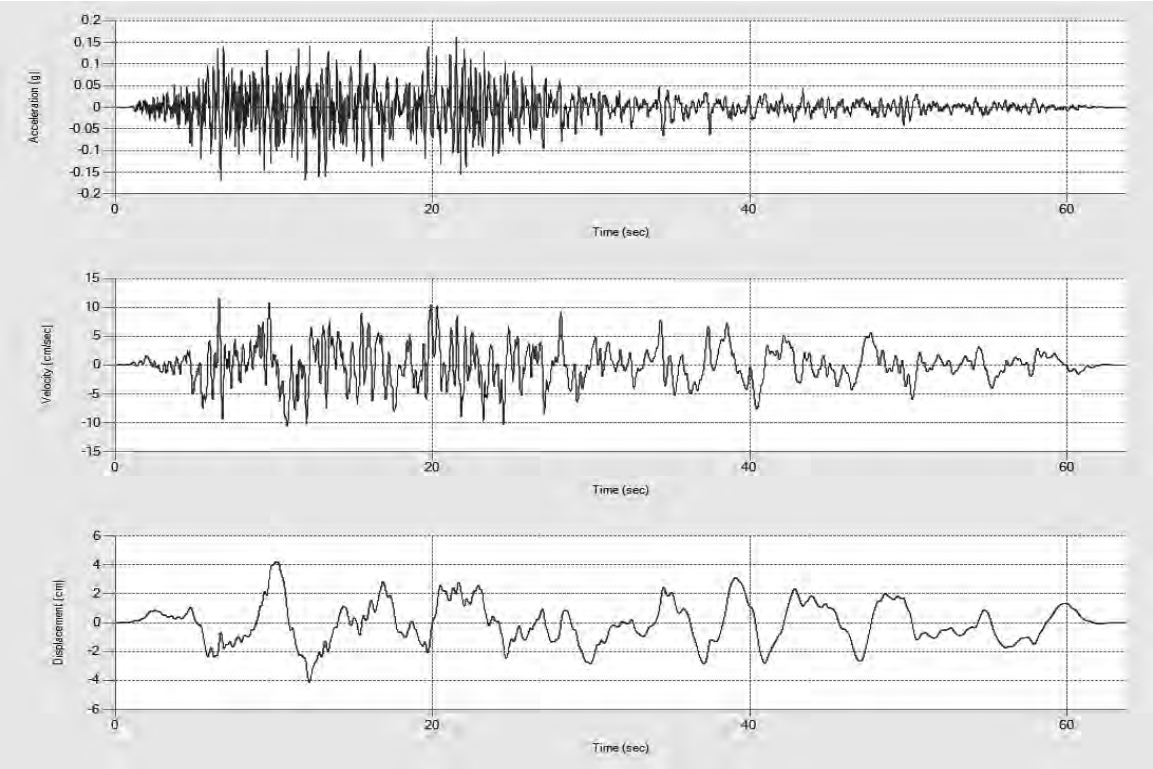


Figure 4.2 Time history of Imperial Valley Earthquake

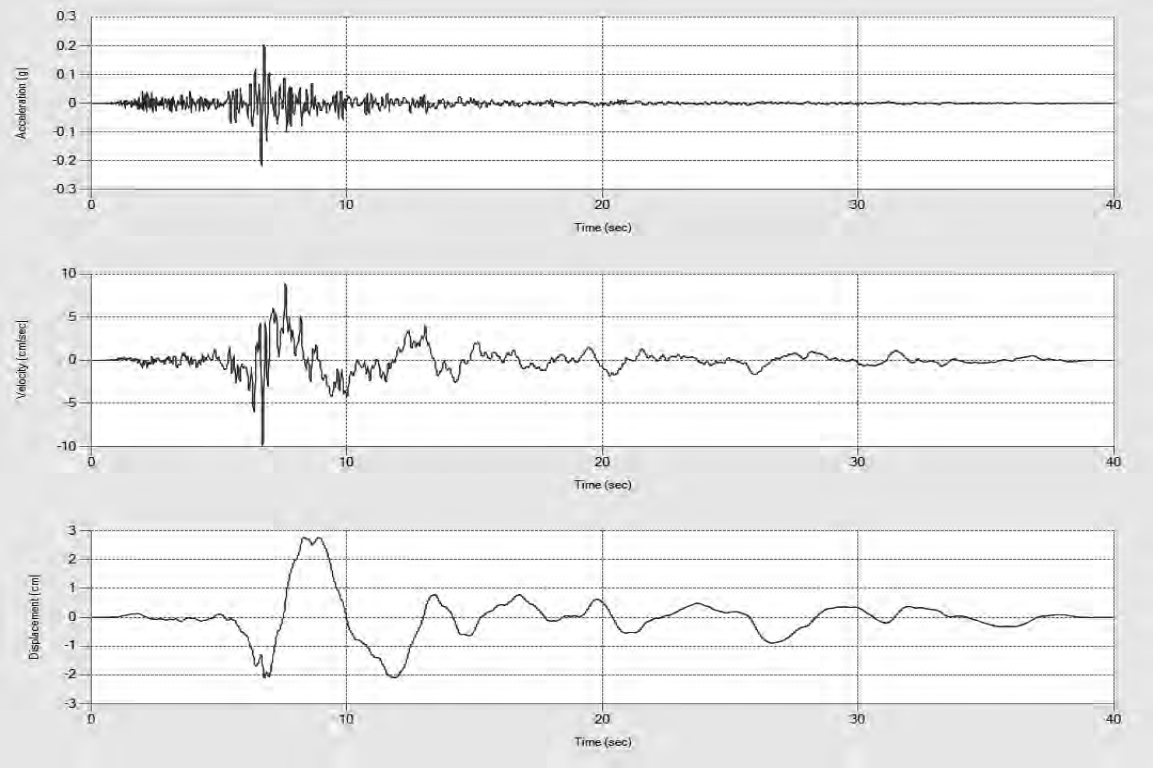


Figure 4.3 Time history of Northridge Earthquake

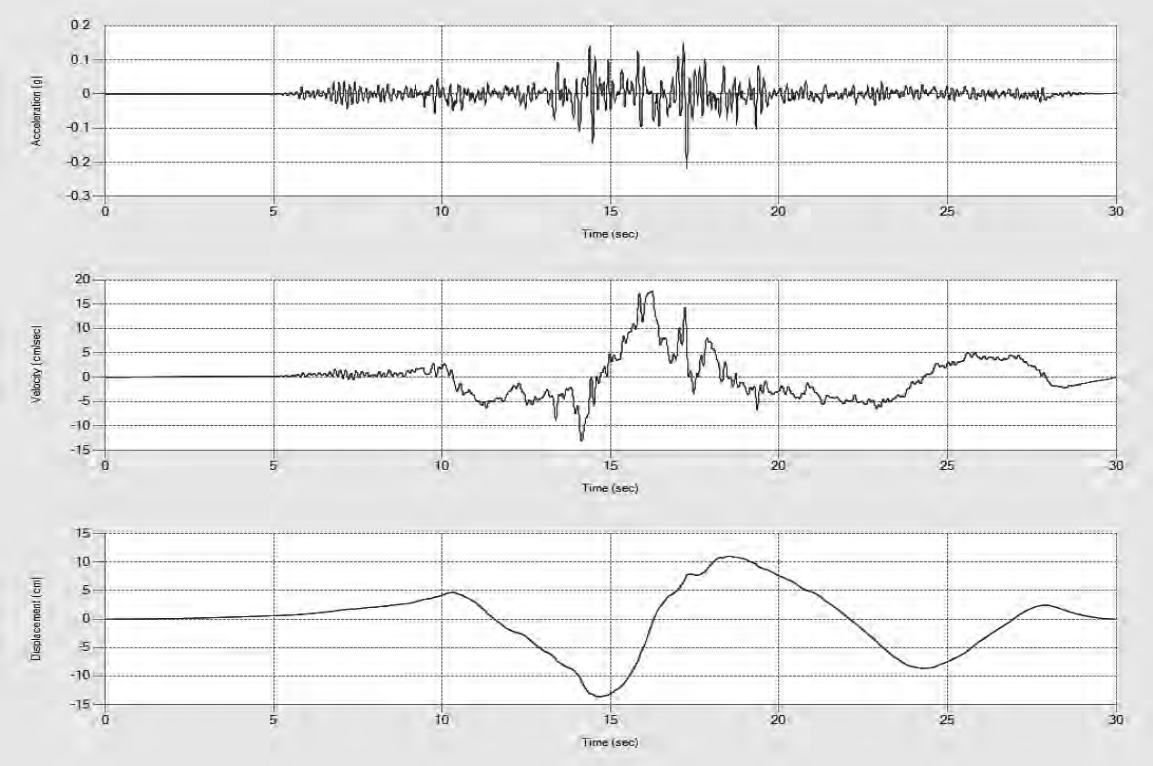


Figure 4.4 Time history of Kocaeli Earthquake

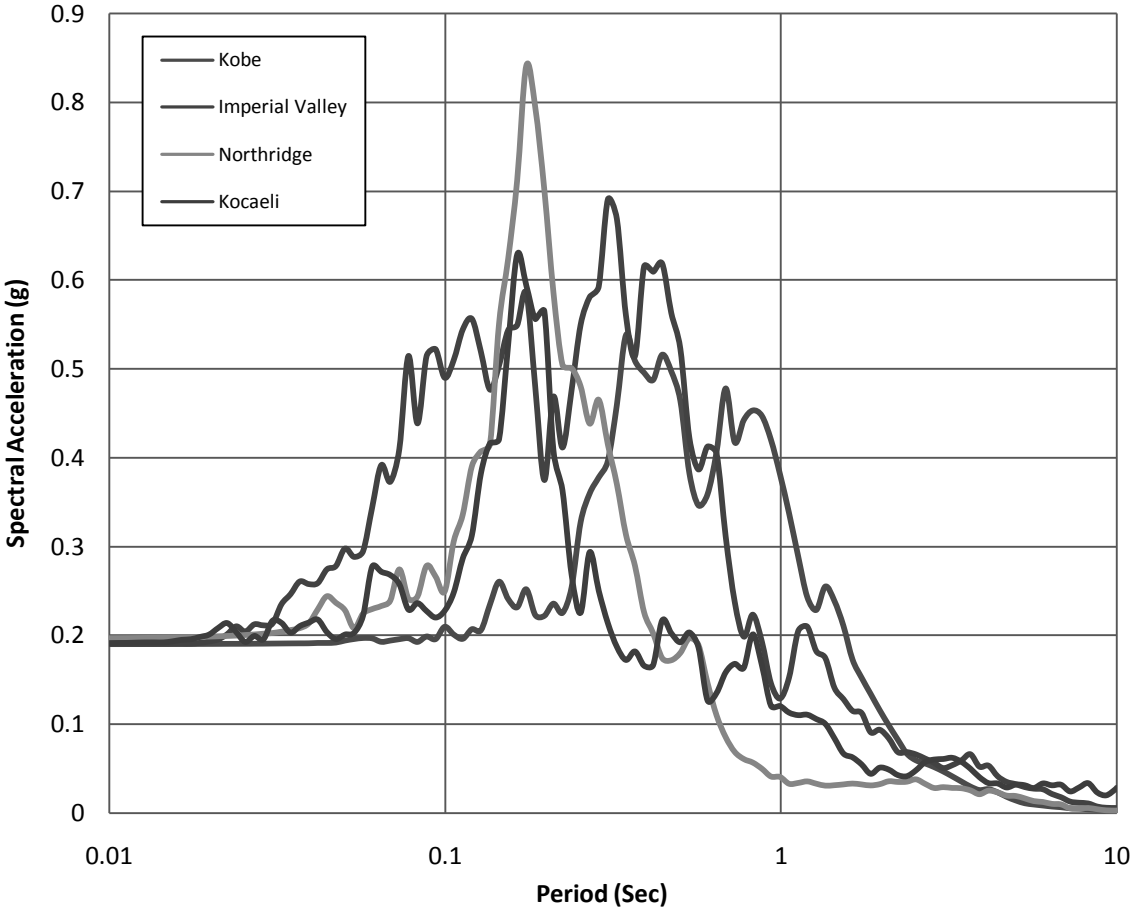


Figure 4.5 The spectral acceleration variation of the different input motions.

### 4.2.1 Ground Response Analysis of Site-1

This site was situated beside Palashi Bazar at JIDPUS field. The test was performed at 23rd October, 2013. A 110ft borehole was done and test performed near 100ft.

**Response Spectra**

Response spectra of four earthquakes are shown in Figure 4.6. Among the four earthquakes, Imperial Valley earthquake produces highest (1.103g) peak spectral acceleration (PSA) for this site and Kocaeli earthquake produces lowest (0.609g) peak spectral acceleration (PSA). It was observed that initially soil surface response was more than input response for some earthquakes for this site.

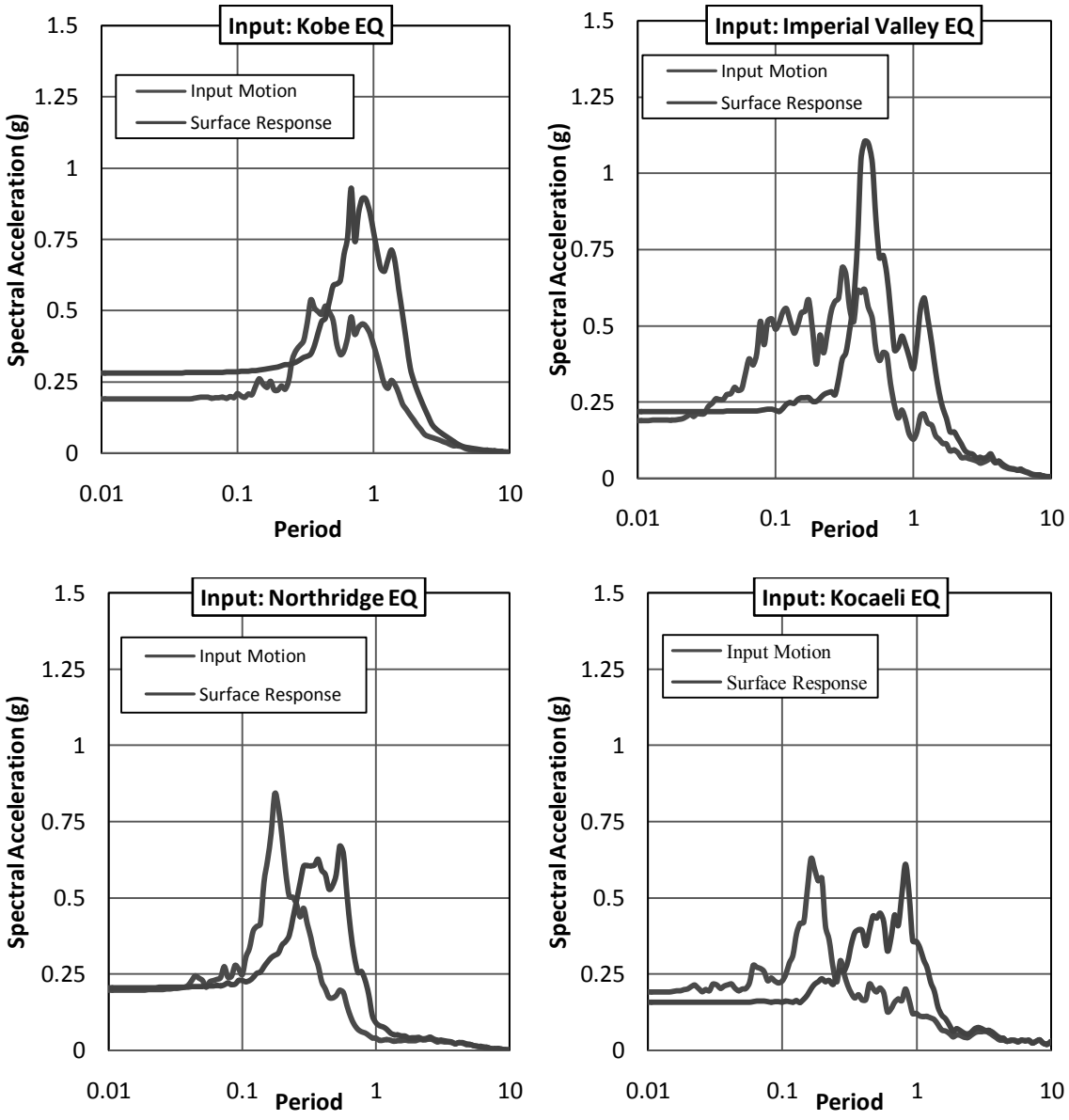


Figure 4.6 Response Spectra for the Site-1, JIDPUS, BUET.

**Maximum Peak Ground Acceleration (PGA)**

Maximum Peak Ground Acceleration (PGA) at different depths of four earthquakes for this site is shown in Figure 4.7. PGA at surface and that at bedrock is obtained from the analysis. The peak ground acceleration values at surface are observed to be in the range of 0.157g (Kocaeli) to 0. 281g (Kobe) and that of the bedrock were observed to vary from 0.181g (Kobe) to 0.189 g (Northridge).

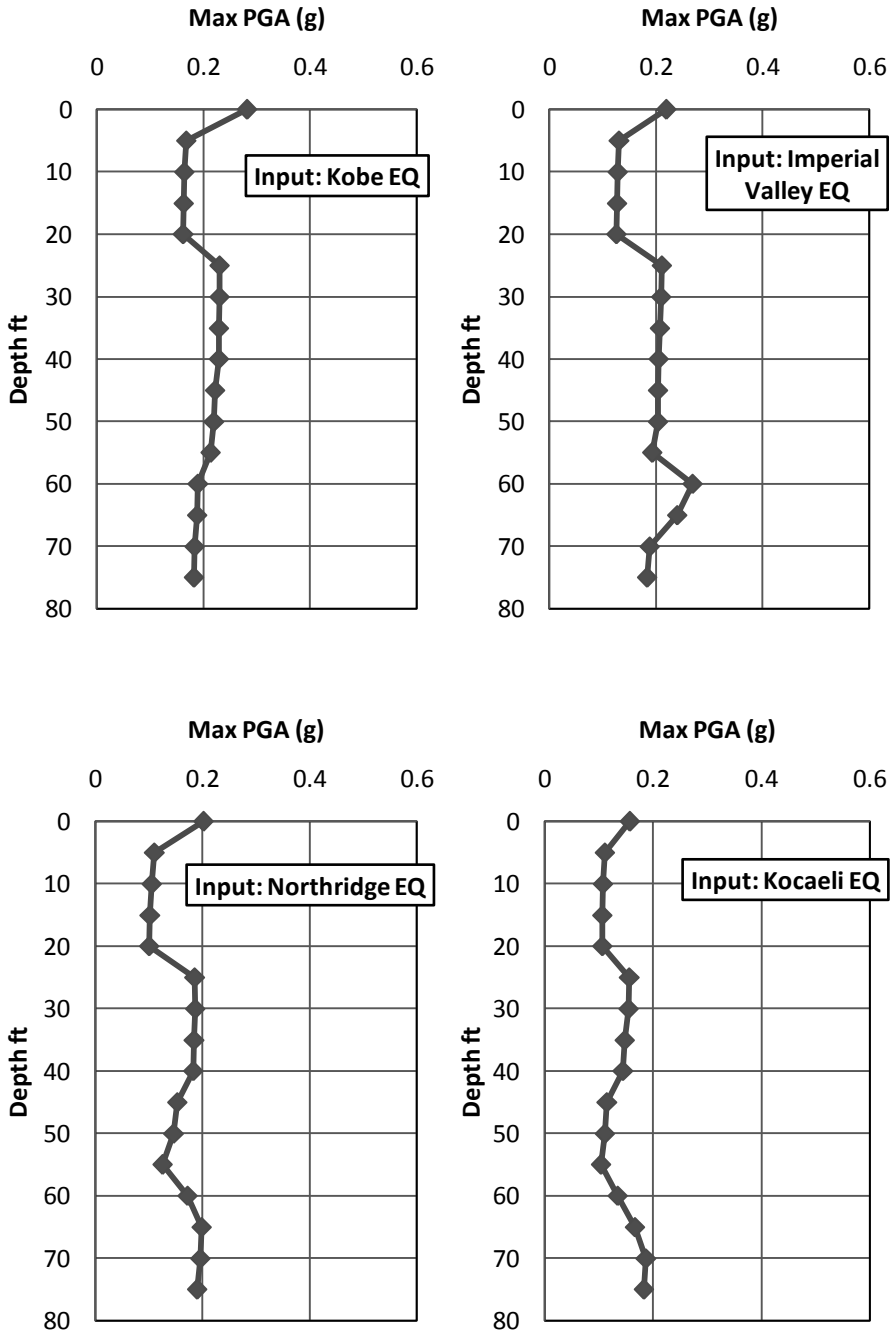


Figure 4.7 Maximum peak ground acceleration for the site-1 JIDPUS, BUET

Site amplification factors at sub surface layers are often used as one of the parameters for estimation of ground response. The amplification factor is the ratio of peak ground acceleration at surface to that of acceleration at hard rock. The amplification factors are determined as;

Amplification Factor = PGA recorded at ground surface / PGA recorded at hard rock

Amplification Factor (Kobe earthquake) = 1.547

Amplification Factor (Imperial Valley earthquake) = 1.192

Amplification Factor (Northridge earthquake) = 1.066

Amplification Factor (Kocaile earthquake) = 0.856

Hence, the amplification factors have also been computedand it was identified that similar to the peak ground acceleration values, the variation was within 0.856 (Kocaile) to 1.547 (Kobe).

The comparison of PSA is given in Figure 4.8 and the comparison of mean and standard deviation for surface PSA is given in Figure 4.9.

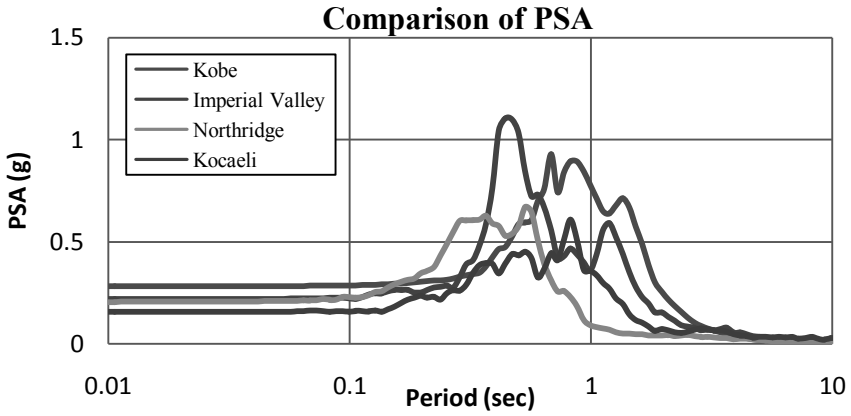


Figure 4.8: Comparison of PSA for different input motion for the site-1 JIDPUS, BUET.

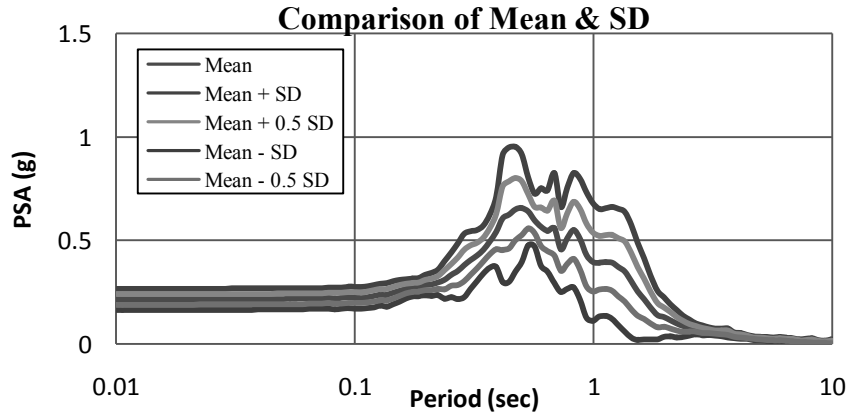


Figure 4.9: Comparison of mean and standard deviation for surface PSA.

### 4.2.2 Ground Response Analysis of Site-2

This site was situated beside the MIST Faculty building-1. The test was performed at 3rd March, 2014. A 100ft borehole was done and test performed near 80ft.

### Response Spectra

Response spectra of four earthquakes are shown in Figure 4.10. Among the four earthquakes, Northridge earthquake produces highest (1.47g) peak spectral acceleration (PSA) for this site and Kocaeli earthquake produces lowest (0.002g) peak spectral acceleration (PSA). It was observed that initially soil surface response is more than input response for this site.

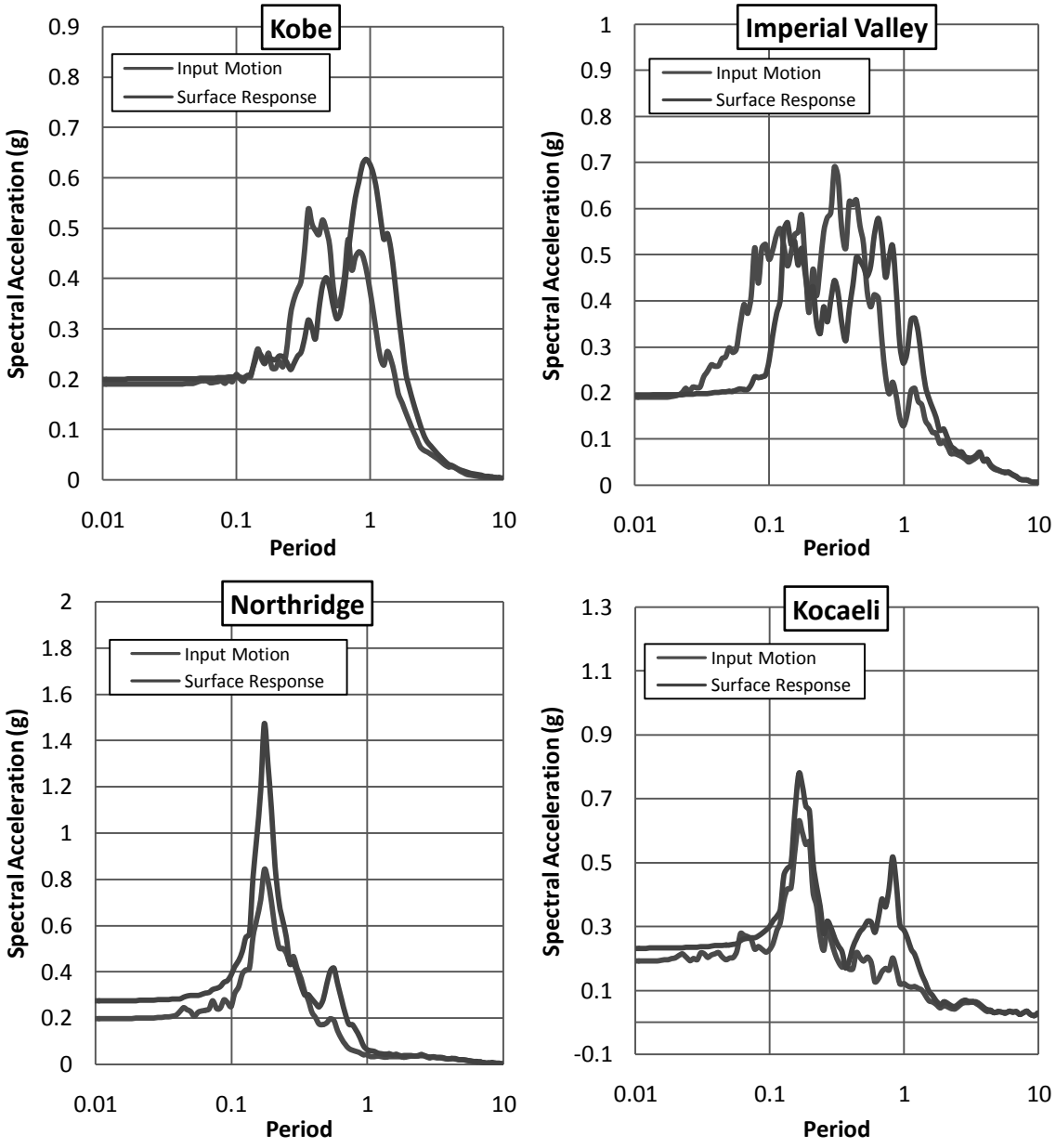


Figure 4.10 Response spectra for the site-2 MIST, Mirpur

**Maximum Peak Ground Acceleration (PGA)**

Maximum Peak Ground Acceleration (PGA) at different depths of four earthquakes for this site is shown in Figure 4.11. PGA at surface and that at bedrock was obtained from the analysis. The peak ground acceleration values at surface were observed to be in the range of 0.194g (Imperial Valley) to 0. 272g (Northridge) and that of the bedrock were observed to vary from 0.179g (Kocaeli) to 0.196 g (Imperial Valley).

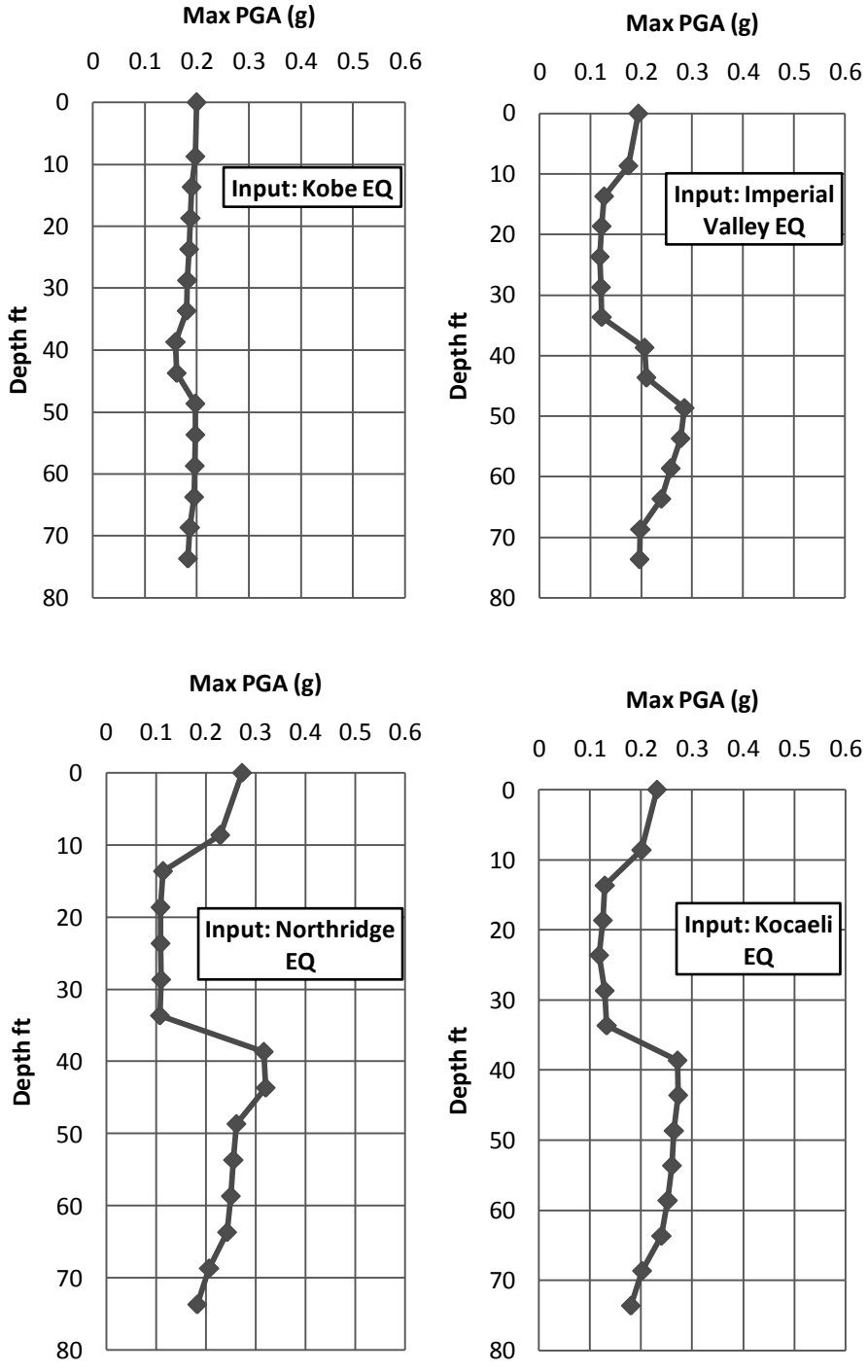


Figure 4.11 Maximum peak ground acceleration for the site-2, MIST, Mirpur.

**Site amplification factors**

Amplification Factor (Kobe earthquake) = 1.09

Amplification Factor (Imperial Valley earthquake) = 0.99

Amplification Factor (Northridge earthquake) = 1.49

Amplification Factor (Kocaile earthquake) = 1.28

It was identified that similar to the peak ground acceleration values, the variation of amplification factor was within 0.99 (Imperial Valley) to 1.49 (Northridge).

The comparison of PSA is given in Figure 4.12 and the comparison of mean and standard deviation for surface PSA is given in Figure 4.13.

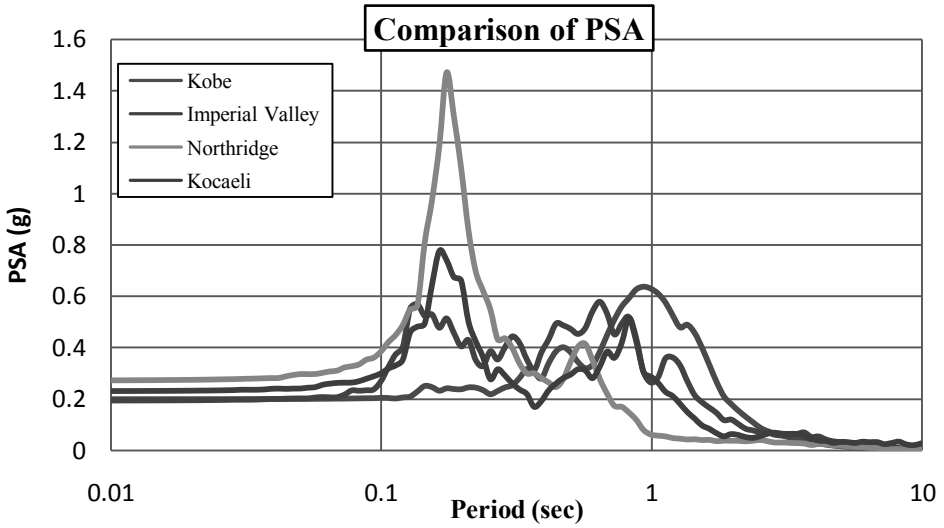


Figure 4.12 Comparison of PSA for different input Motion for the site-2, MIST, Mirpur.

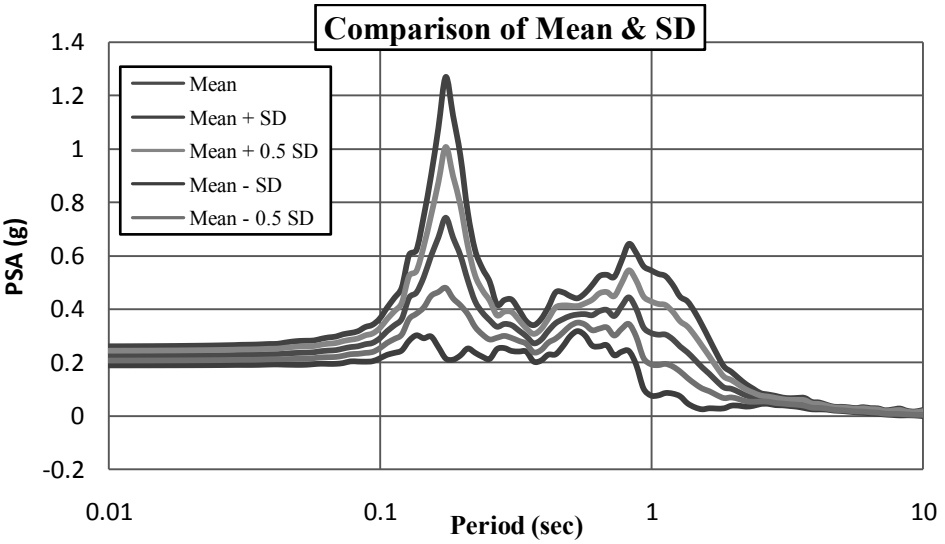


Figure 4.13 Comparison of mean and standard deviation for surface PSA for the site-2, MIST, Mirpur

### 4.2.3 Ground Response Analysis of Site-3

This site was situated at Hazaribag near Shikder Medical. This test was performed at 7th July, 2014. A 100ft borehole was done and test performed near 80ft.

**Response Spectra**

Response spectra of four earthquakes are shown in Figure 4.14. Among the four earthquakes, Imperial Valley earthquake produces highest (1.20g) peak spectral acceleration (PSA) for this site and Northridge earthquake produces lowest (0.002g) peak spectral acceleration (PSA). It was observed that initially soil surface response is less than input response for this site.

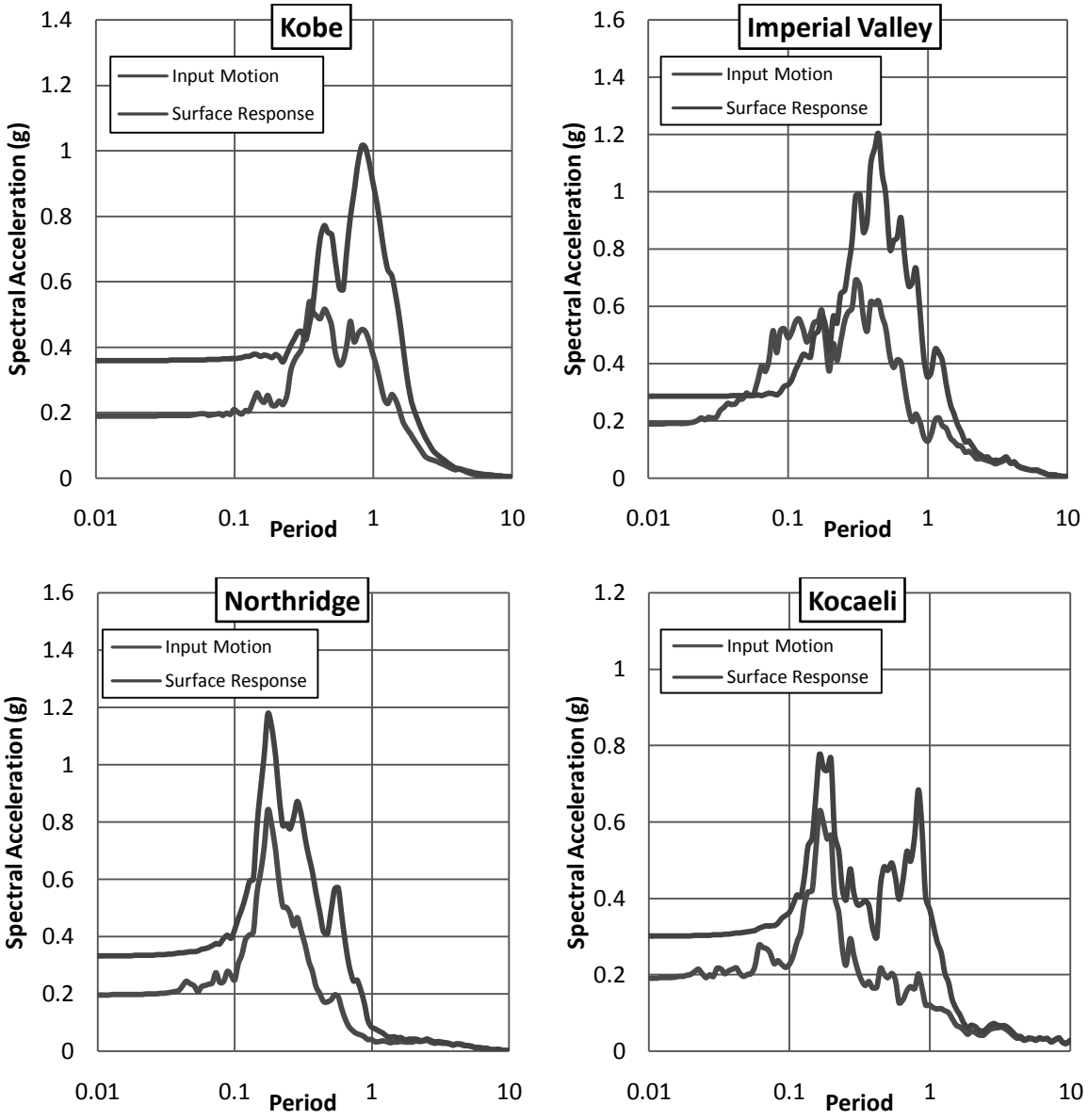


Figure 4.14 Response spectra for the Site-3, Hazaribag.

**Maximum Peak Ground Acceleration (PGA)**

Maximum Peak Ground Acceleration (PGA) at different depths of four earthquakes for this site is shown in Figure 4.15. PGA at surface and that at bedrock is obtained from the analysis. The peak ground acceleration values at surface were observed to be in the range of 0.28g (Imperial Valley) to 0. 36g (Kobe) and that of the bedrock were observed to vary from 0.183g (Kobe) to 0.184 g (Northridge).

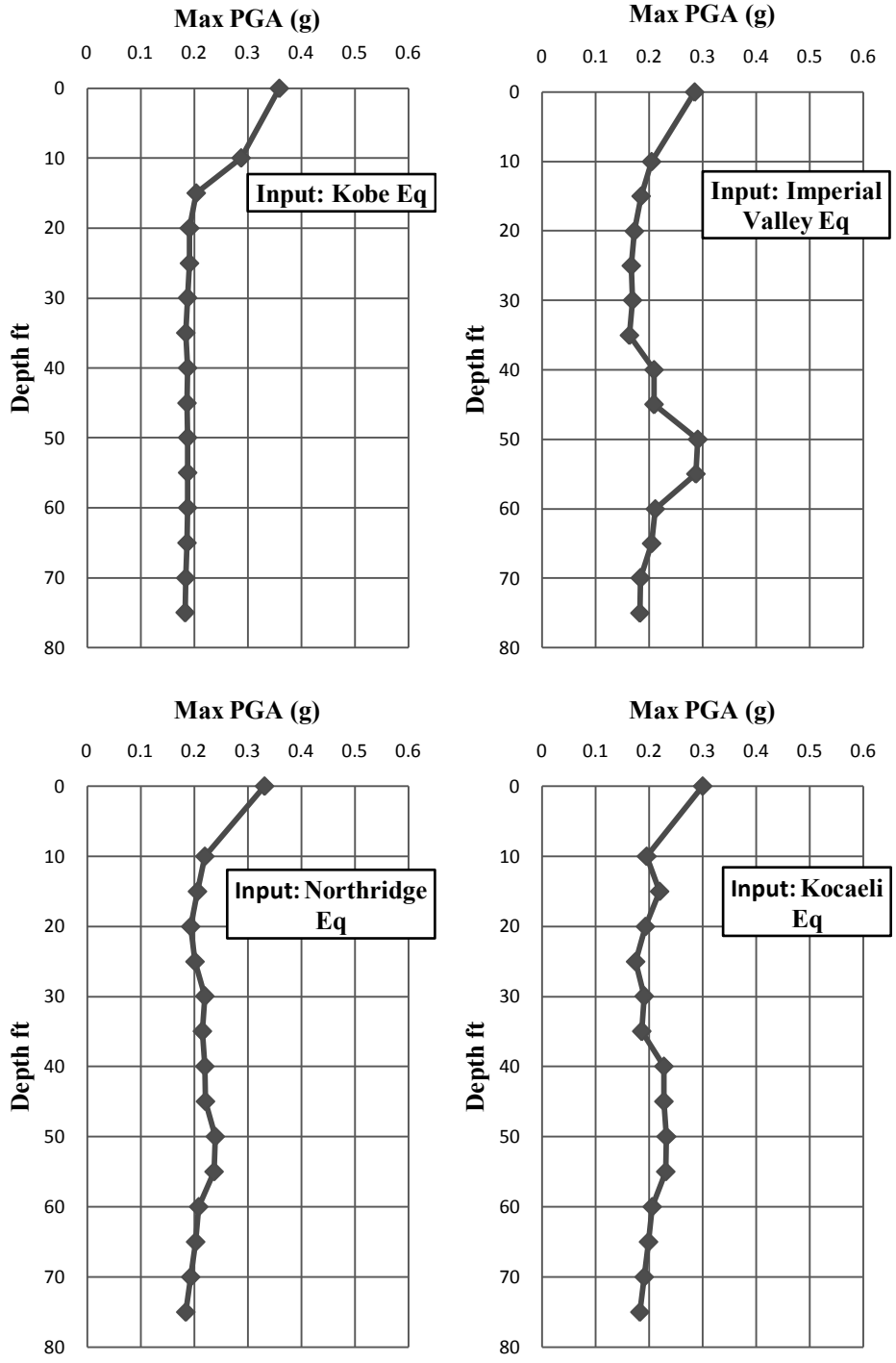


Figure 4.15 Maximum peak ground acceleration for the Site-3, Hazaribag.

**Site amplification factors**

Amplification Factor (Kobe earthquake) = 1.96

Amplification Factor (Imperial Valley earthquake) = 1.56

Amplification Factor (Northridge earthquake) = 1.80

Amplification Factor (Kocaile earthquake) = 1.64

It was identified that similar to the peak ground acceleration values, the variation of amplification factor was within 1.56 (Imperial Valley) to 1.96 (Kobe).

The comparison of PSA is given in Figure 4.16 and the comparison of mean and standard deviation for surface PSA is given in Figure 4.17.

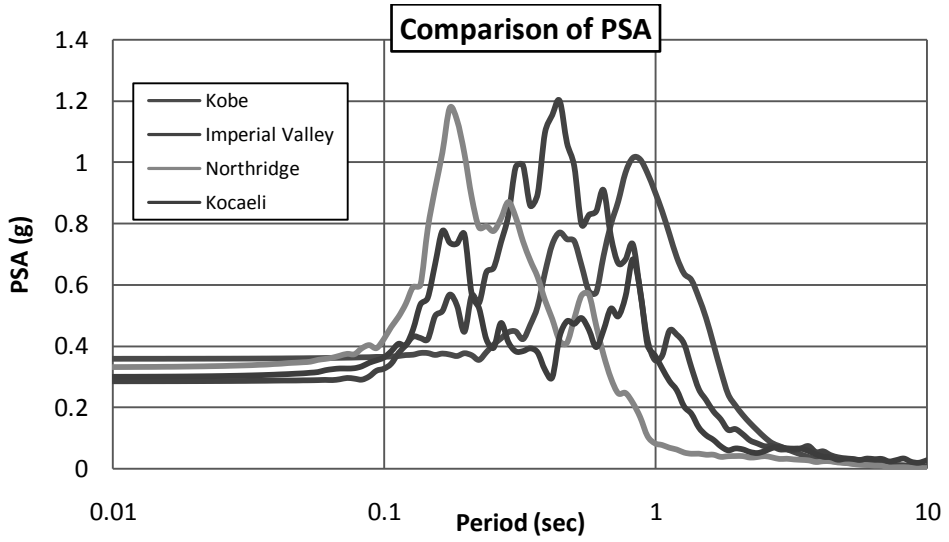


Figure 4.16 Comparison of PSA for different input motion for the Site-3, Hazaribag.

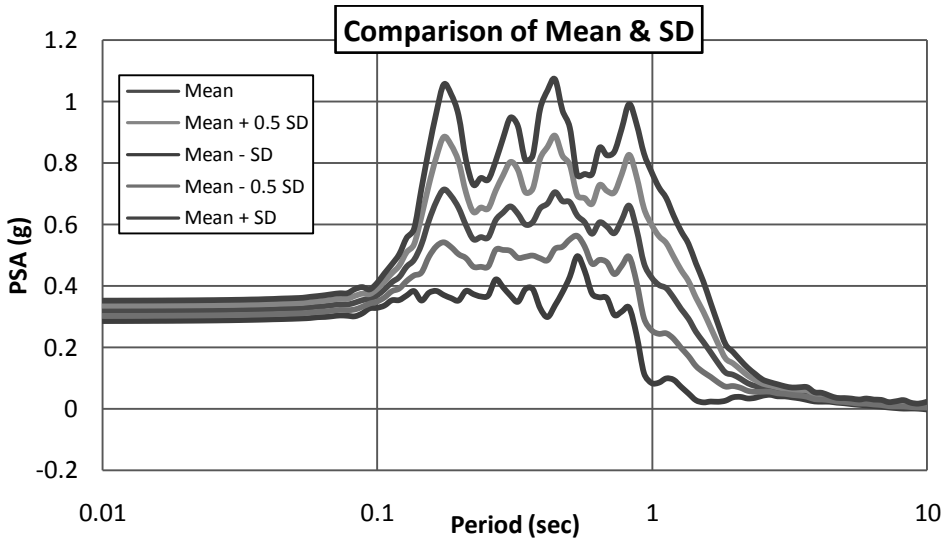


Figure 4.17 Comparison of mean and standard deviation for surface PSA for the Site-3, Hazaribag.

### 4.2.4 Ground Response Analysis of Site-4

This site was situated at Gulsan-2. The test was performed at 31st October, 2014. A 100ft borehole was done and test performed near 68 ft.

**Response Spectra**

Response spectra of four earthquakes are shown in Figure 4.18. Among the four earthquakes, Kobe earthquake produces highest (0.546g) peak spectral acceleration (PSA) for this site and Northridge earthquake produces lowest (0.002g) peak spectral acceleration (PSA). It was observed that initially soil surface response is less than input response for some earthquakes for this site.

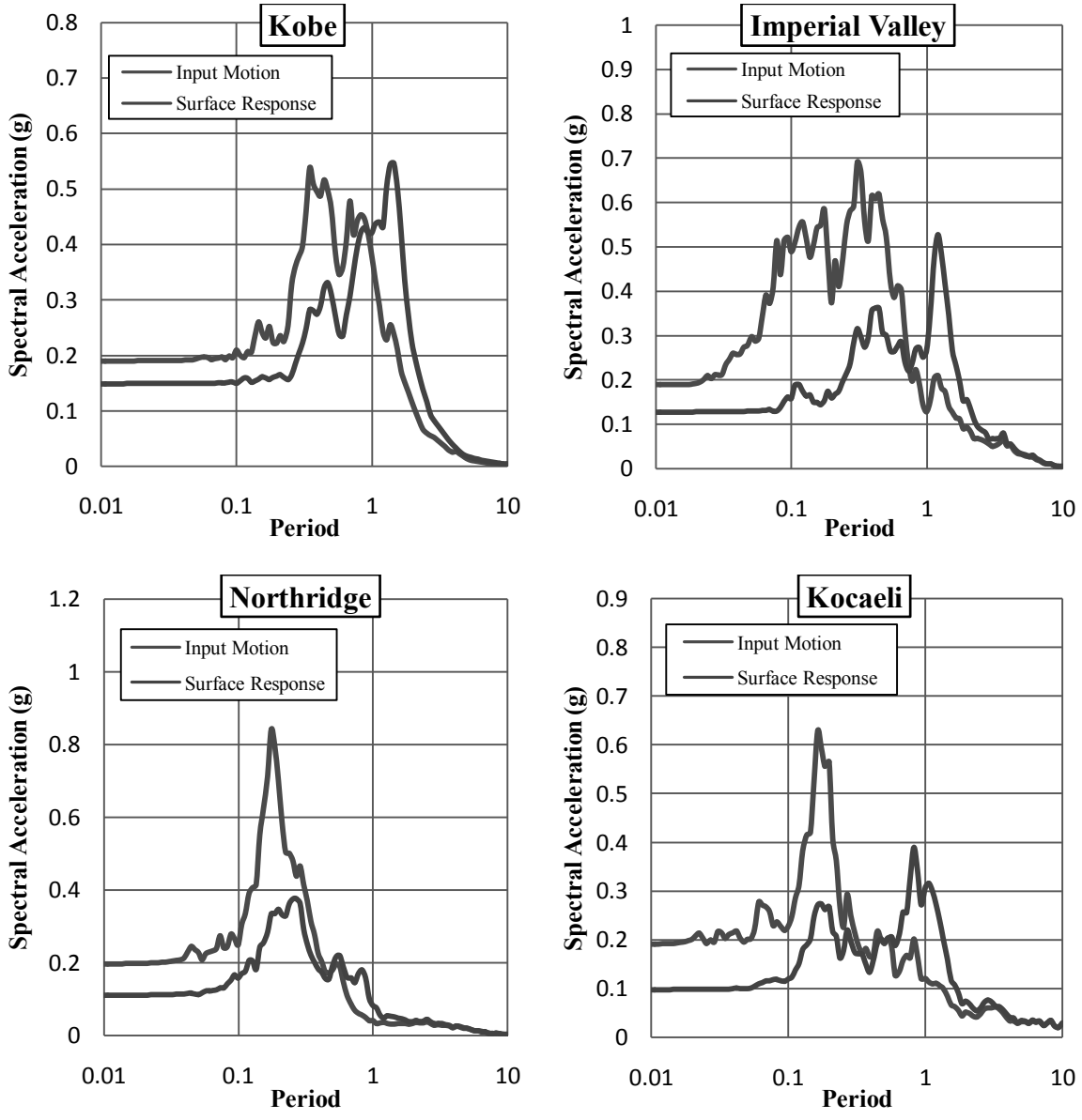


Figure 4.18 Response spectra for the Site-4, Gulsan-2.

**Maximum Peak Ground Acceleration (PGA)**

Maximum Peak Ground Acceleration (PGA) at different depths of four earthquakes for this site is shown in Figure 4.19. PGA at surface and that at bedrock was obtained from the analysis. The peak ground acceleration values at surface were observed to be in the range of 0.97g (Kocaeli) to 0. 149g (Kobe) and that of the bedrock were observed to vary from 0.185g (Kobe) to 0.22 g (Northridge).

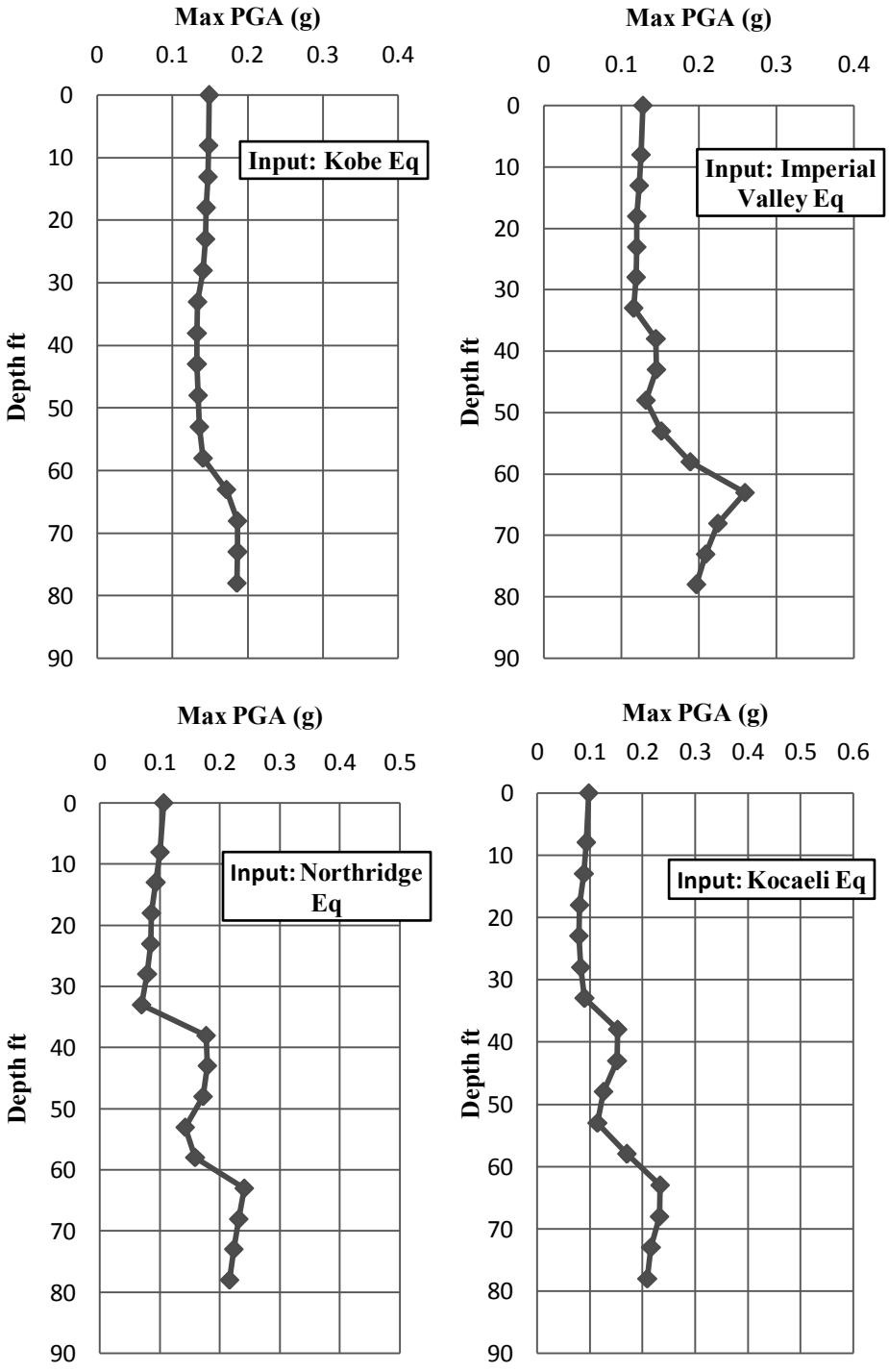


Figure 4.19 Maximum peak ground acceleration for the Site-4, Gulsan-2.

**Site amplification factors**

Amplification Factor (Kobe earthquake) = 0.80

Amplification Factor (Imperial Valley earthquake) = 0.65

Amplification Factor (Northridge earthquake) = 0.49

Amplification Factor (Kocaile earthquake) = 0.47

It was identified that similar to the peak ground acceleration values, the variation of amplification factor was within 0.47 (Kacoeli) to 0.80 (Kobe).

The comparison of PSA is given in Figure 4.20 and the comparison of mean and standard deviation for surface PSA is given in Figure 4.21.

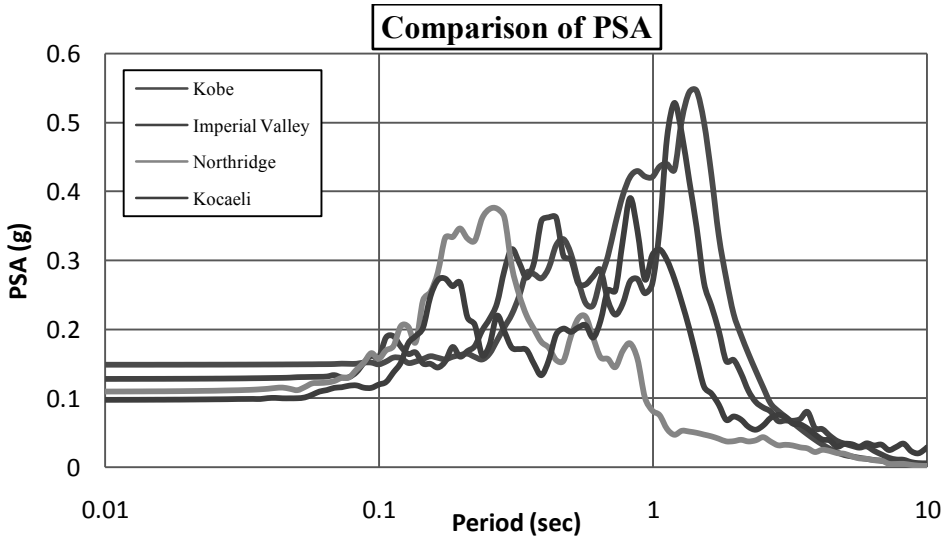


Figure 4.20 Comparison of PSA for different input Motion for the Site-4, Gulsan-2.

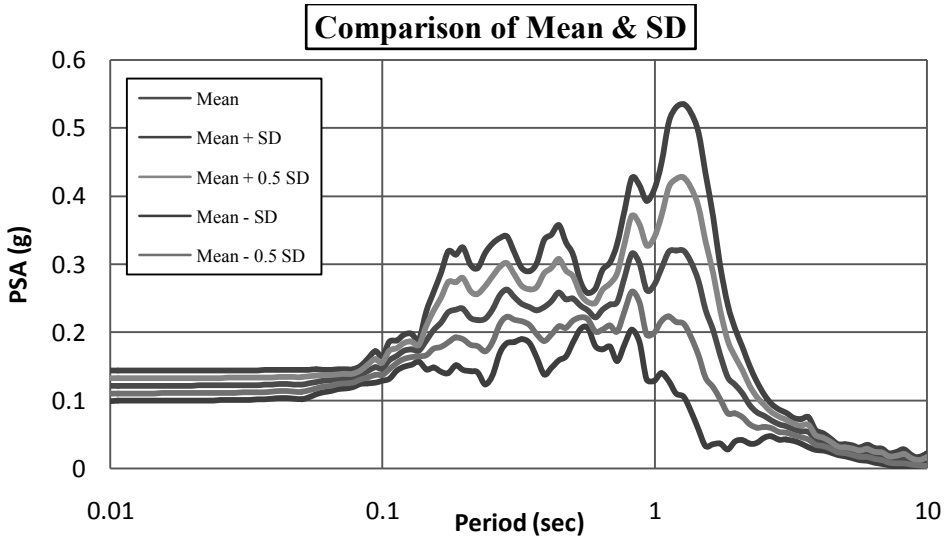


Figure 4.21 Comparison of mean and standard deviation for surface PSA for the Site-4, Gulshan-2.

### 4.2.5 Ground Response Analysis of Site-5

This site was situated at Kamrangichor. The test was performed at 31st October, 2014. A 100ft borehole was done and test performed near 68 ft.

**Response Spectra**

Response spectra of four earthquakes are shown in Figure 4.22. Among the four earthquakes, Kobe earthquake produces highest (1.302g) peak spectral acceleration (PSA) for this site and Northridge earthquake produces lowest (0.002g) peak spectral acceleration (PSA). It was observed that initially soil surface response is more than input response for some earthquakes for this site.

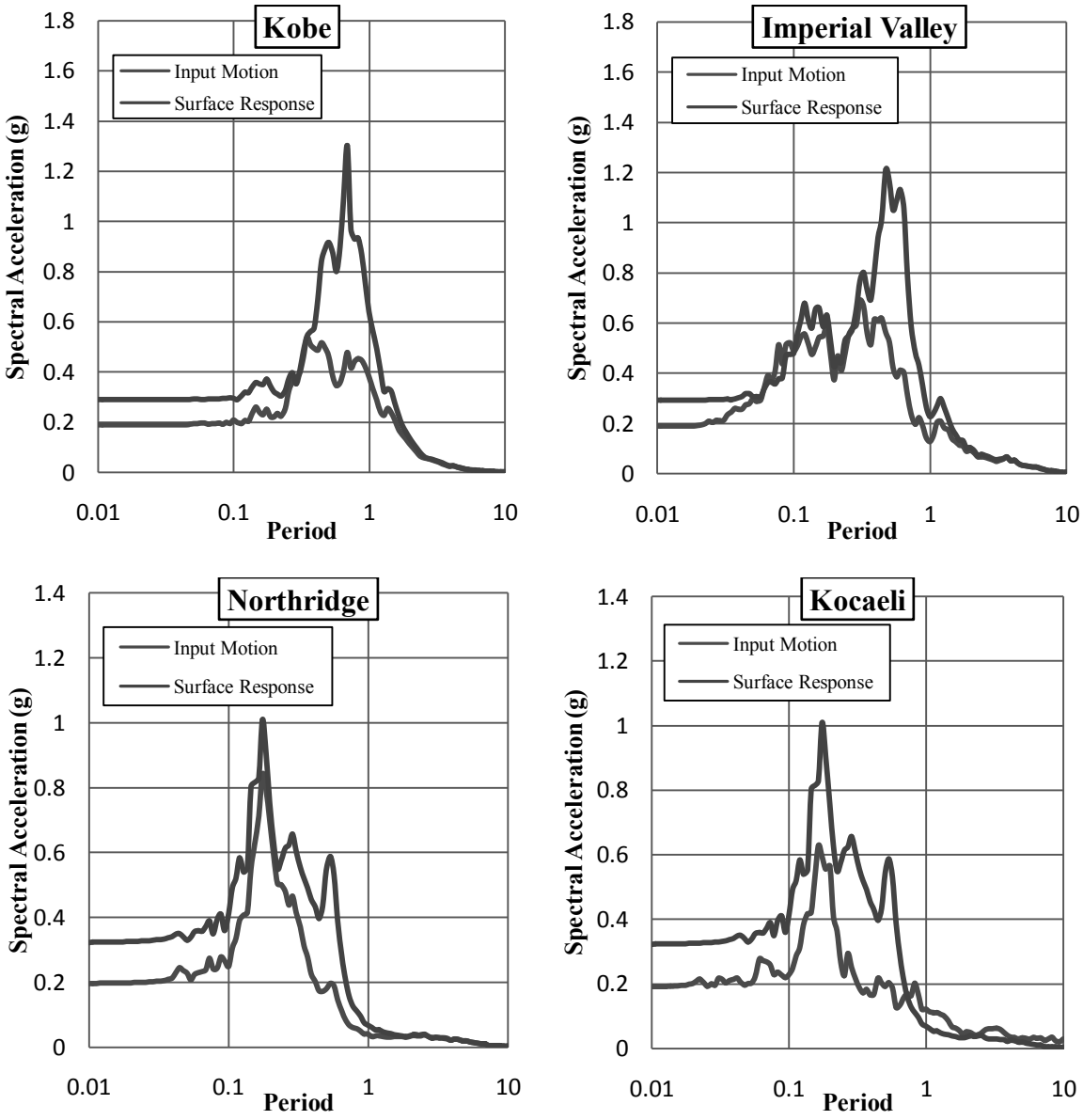


Figure 4.22 Response spectra for the Site-5, Kamrangichor.

**Maximum Peak Ground Acceleration (PGA)**

Maximum Peak Ground Acceleration (PGA) at different depths of four earthquakes for this site is shown in Figure 4.23. PGA at surface and that at bedrock was obtained from the analysis. The peak ground acceleration values at surface were observed to be in the range of 0.27g (Kocaeli) to 0. 32g (Northridge) and that of the bedrock were observed to vary from 0.182g (Kobe) to 0.190 g (Kocaeli).

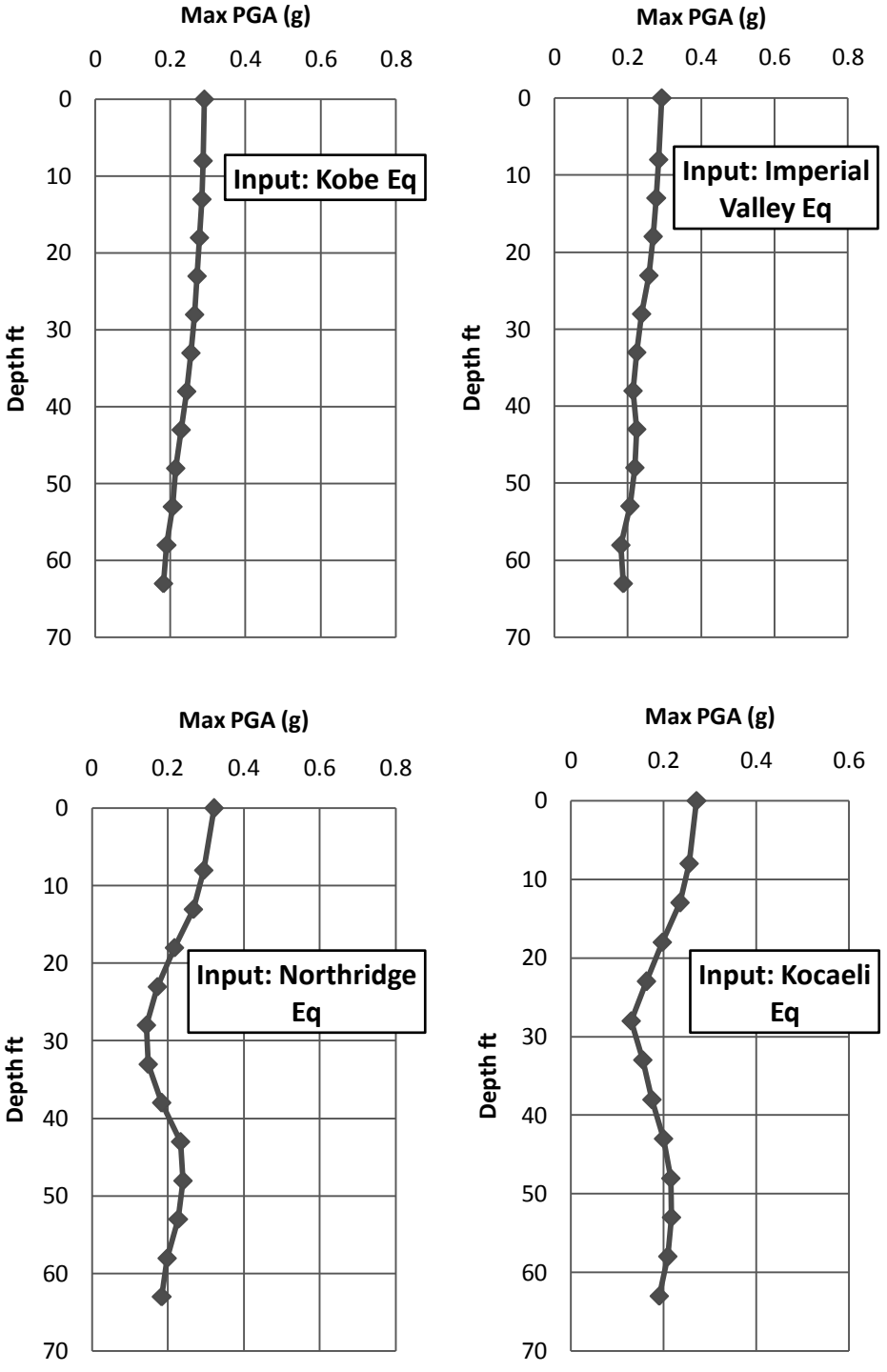


Figure 4.23 Maximum peak ground acceleration for the Site-5, Kamrangichor.

**Site amplification factors**

Amplification Factor (Kobe earthquake) = 1.59

Amplification Factor (Imperial Valley earthquake) = 1.57

Amplification Factor (Northridge earthquake) = 1.74

Amplification Factor (Kocaile earthquake) = 1.43

It was identified that similar to the peak ground acceleration values, the variation of amplification factor was within 1.43 (Kacoeli) to 1.74 (Northridge).

The comparison of PSA is given in Figure 4.24 and the comparison of mean and standard deviation for surface PSA is given in Figure 4.25.

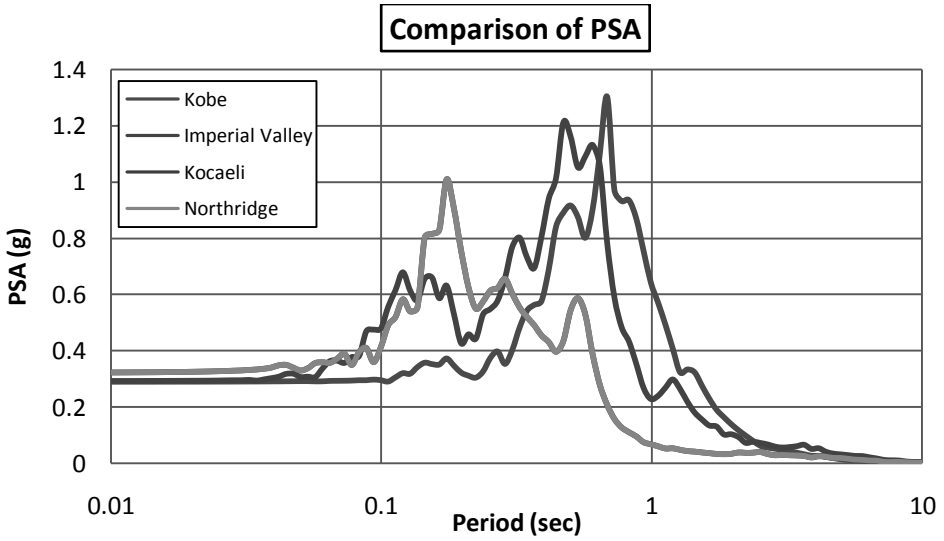


Figure 4.24: Comparison of PSA for different input Motion for the Site-5, Kamrangichor.

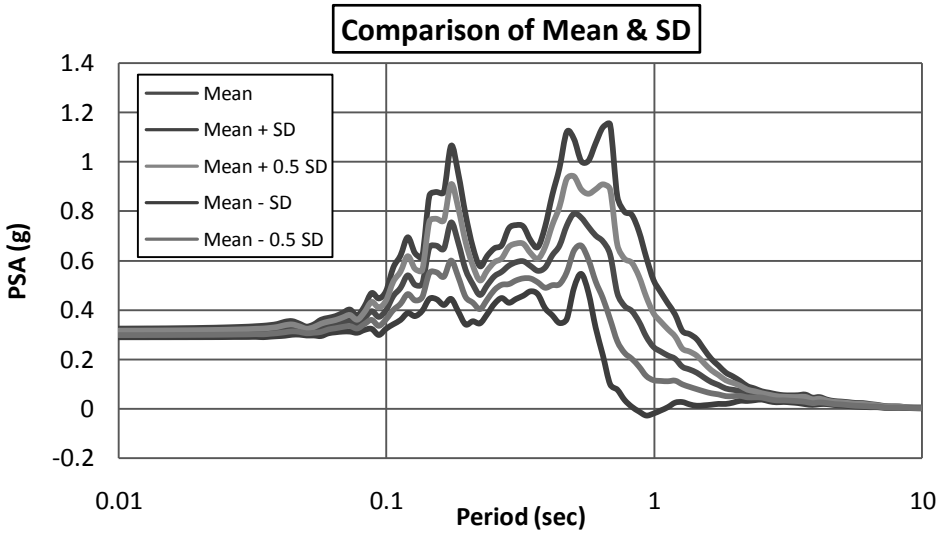


Figure 4.25: Comparison of Mean and Standard deviation for surface PSA for the Site-5, Kamrangichor.

### 4.2.6 Ground Response Analysis of Site-6

This site was situated at South Kafrul beside Kafrul Pagoda. This test was at 8th July, 2014. A 100ft borehole was done and test performed near 65ft.

**Response Spectra**

Response spectra of four earthquakes are shown in Figure 4.26. Among the four earthquakes, Kobe earthquake produces highest (1.00g) peak spectral acceleration (PSA) for this site and Northridge earthquake produces lowest (0.002g) peak spectral acceleration (PSA). It was observed that initially soil surface response is more than input response for some earthquakes for this site.

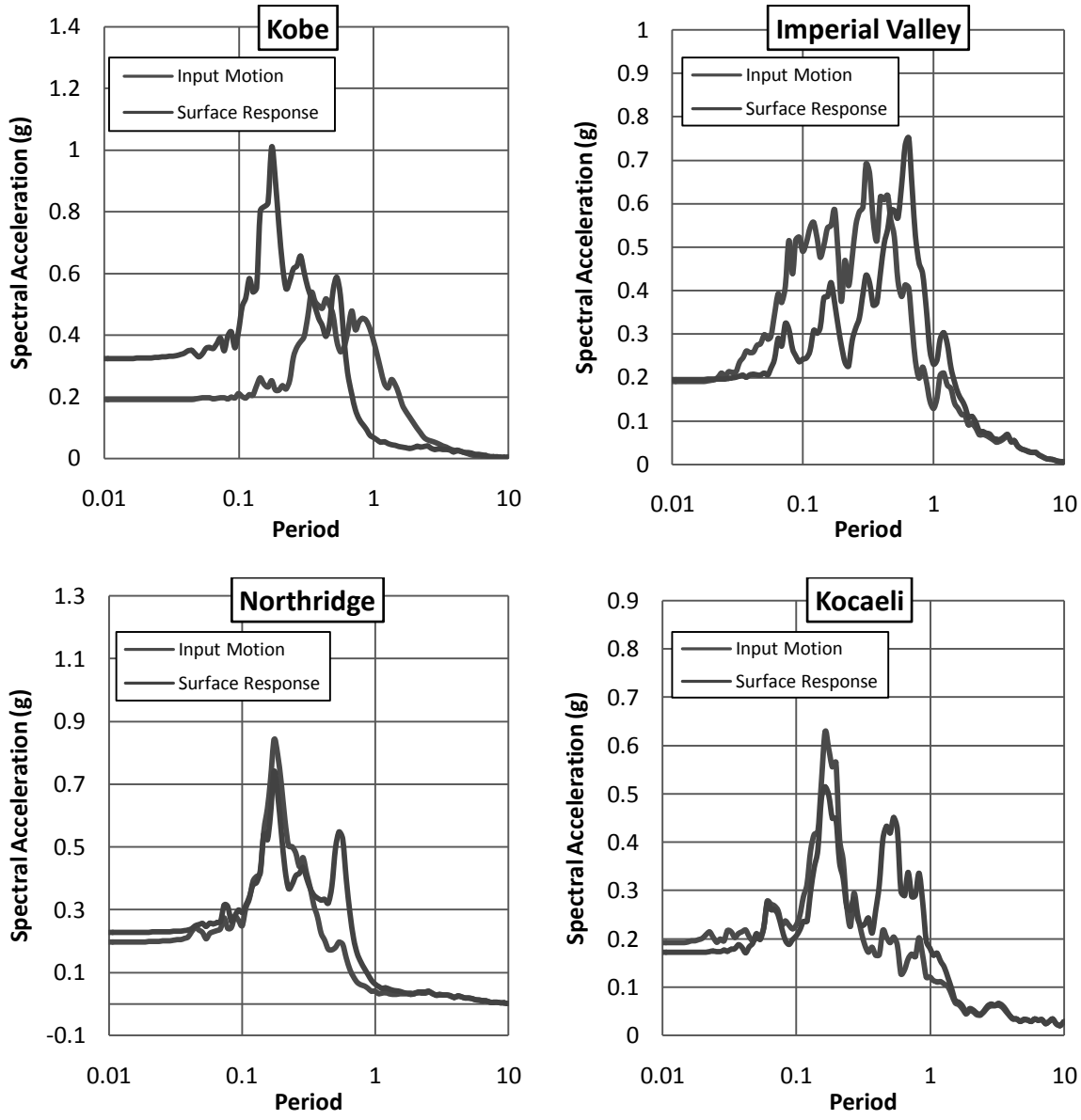


Figure 4.26 Response spectra for the Site-6, South Kafrul.

**Maximum Peak Ground Acceleration (PGA)**

Maximum Peak Ground Acceleration (PGA) at different depths of four earthquakes for this site is shown in Figure 4.27. PGA at surface and that at bedrock was obtained from the analysis. The peak ground acceleration values at surface were observed to be in the range of 0.17g (Kocaeli) to 0. 23g (Northridge) and that of the bedrock were observed to vary from 0.179g (Kobe) to 0.20 g (Imperial Valley). The impedance in the acceleration values can be observed. Such as, a sudden rise within few meters can cause considerable damage to the sub and super structure resulting in huge loss.

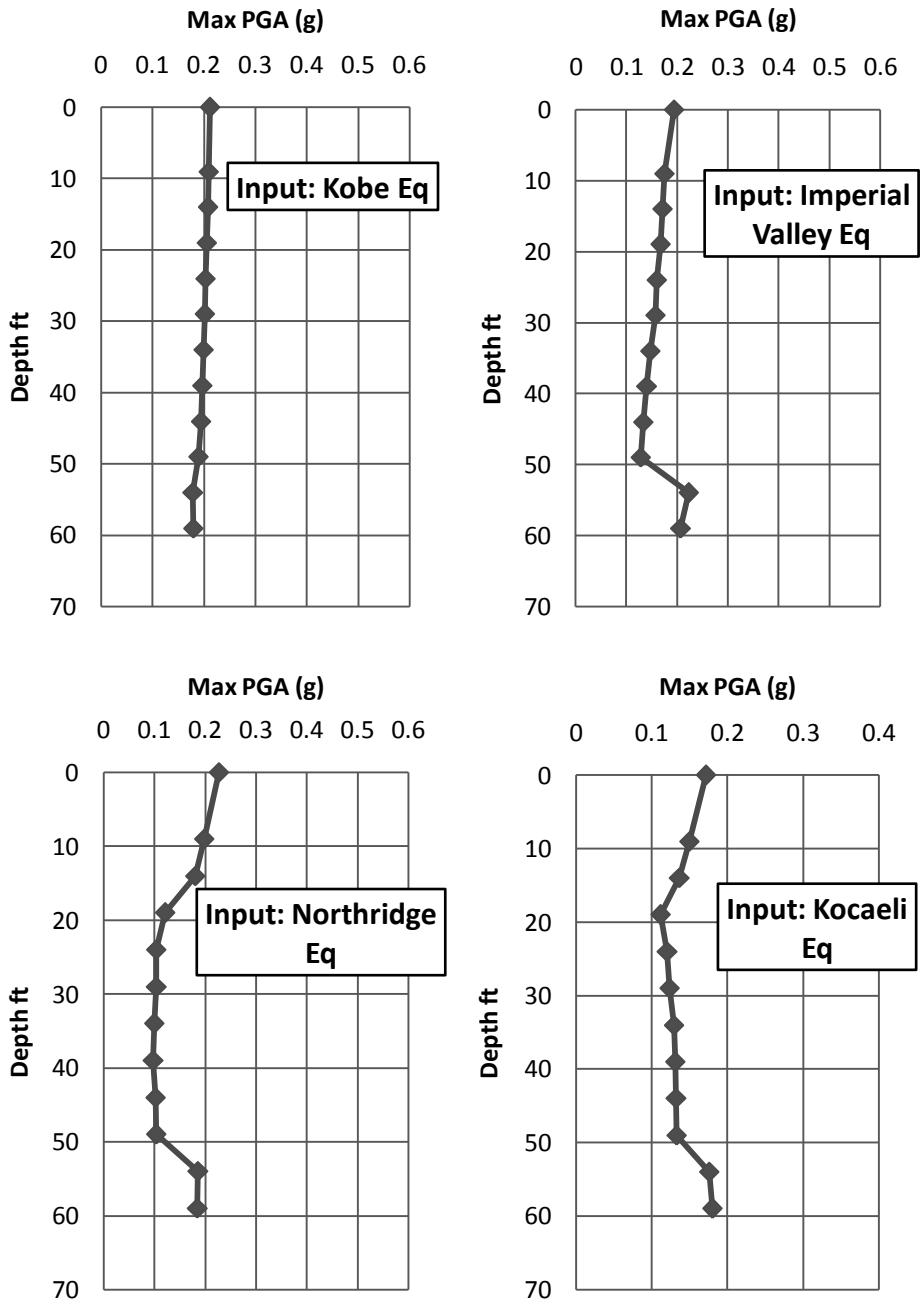


Figure 4.27 Maximum peak ground acceleration for the Site-6, South Kafrul.

**Site amplification factors**

Amplification Factor (Kobe earthquake) = 1.178

Amplification Factor (Imperial Valley earthquake) = 0.93

Amplification Factor (Northridge earthquake) = 1.23

Amplification Factor (Kocaile earthquake) = 0.95

It was identified that similar to the peak ground acceleration values, the variation of amplification factor was within 0.93 (Imperial Valley) to 1.23 (Northridge).

The comparison of PSA is given in Figure 4.28 and the comparison of mean and standard deviation for surface PSA is given in Figure 4.29.

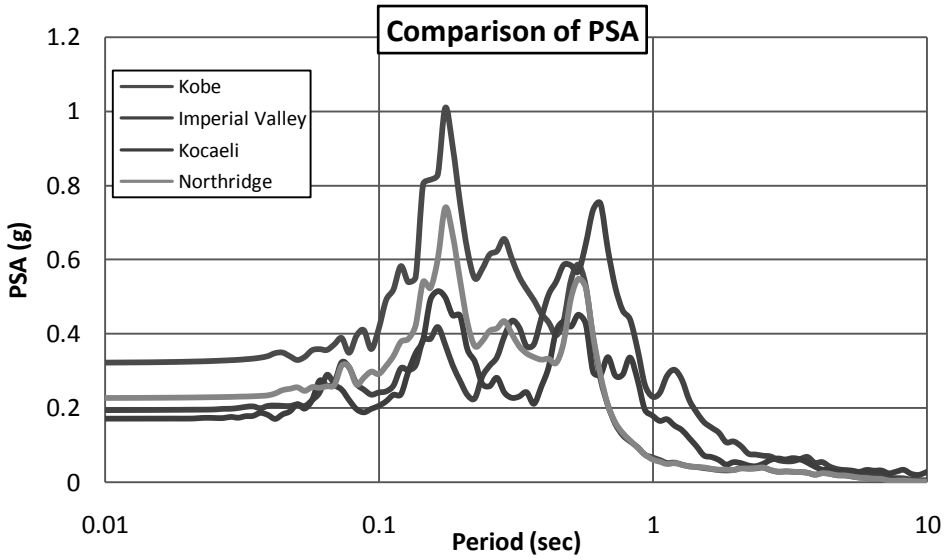


Figure 4.28 Comparison of PSA for different input motion for the Site-6, South Kafrul.

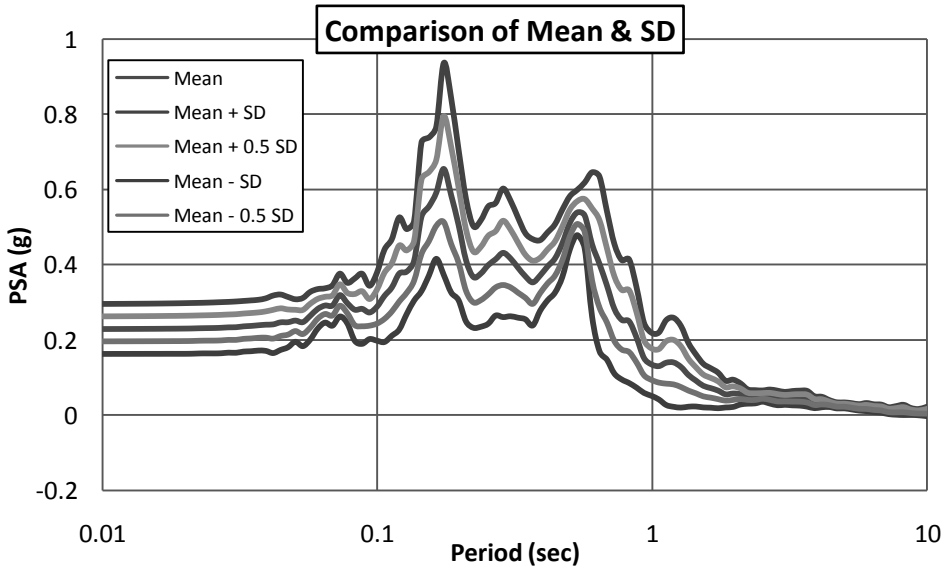


Figure 4.29 Comparison of mean and standard deviation for surface PSA for the Site-6, South Kafrul.

### 4.2.7 Ground Response Analysis of Site-7

This site was situated at Maniknagar beside Islamic University. This test was performed at 8th July, 2014. A 100ft borehole was done and test performed near 65ft.

**Response Spectra**

Response spectra of four earthquakes are shown in Figure 4.30. Among the four earthquakes, Northridge earthquake produces highest (0.73g) peak spectral acceleration (PSA) for this site and Kocaeli earthquake produces lowest (0.002g) peak spectral acceleration (PSA). It was observed that initially soil surface response is less than input response for some earthquakes for this site.

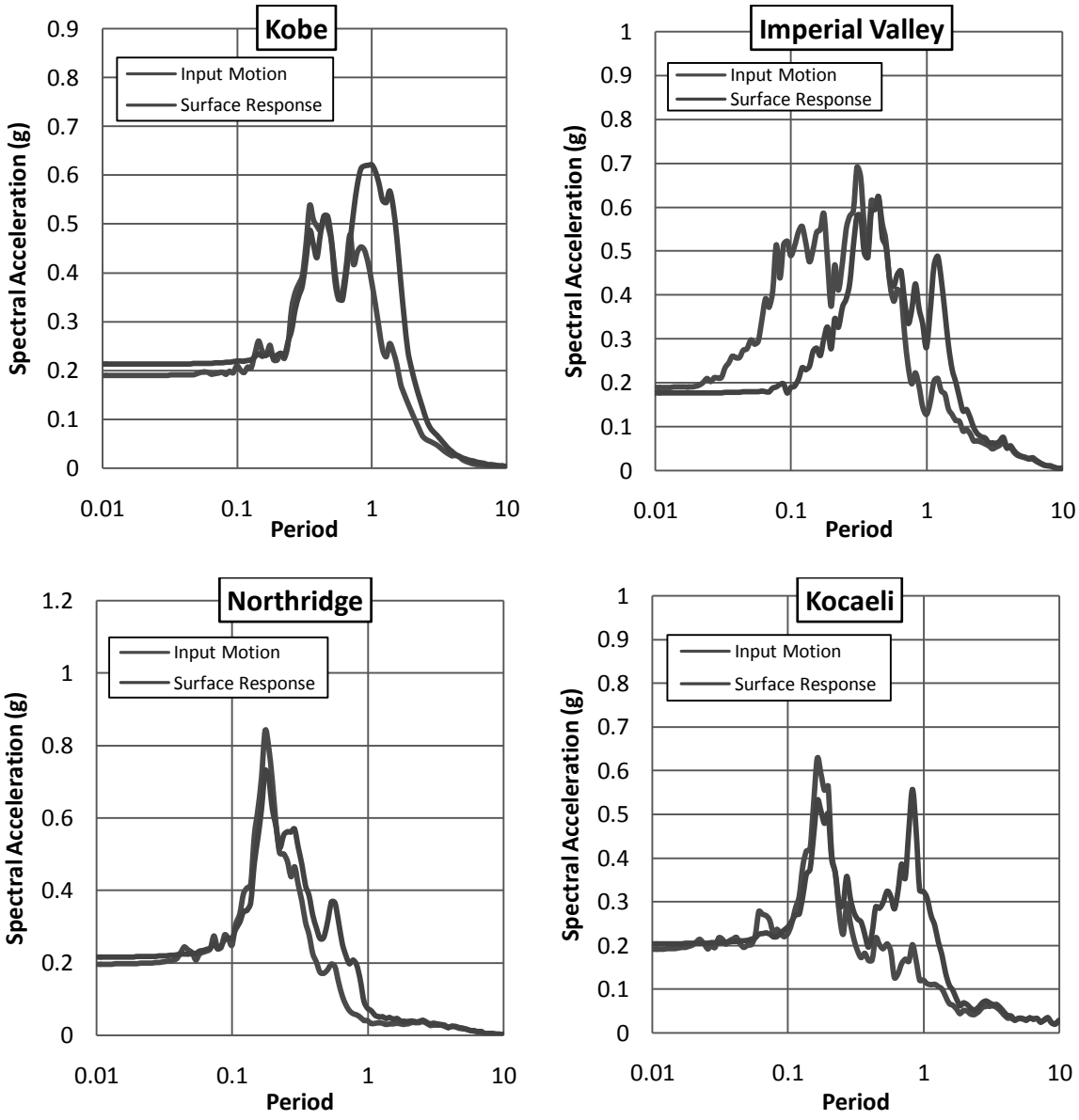


Figure 4.30 Response spectra for the Site-7, Maniknagar.

**Maximum Peak Ground Acceleration (PGA)**

Maximum Peak Ground Acceleration (PGA) at different depths of four earthquakes for this site is shown in Figure 4.31. PGA at surface and that at bedrock was obtained from the analysis. The peak ground acceleration values at surface were observed to be in the range of 0.17g (Imperial Valley) to 0. 21g (Kobe) and that of the bedrock were observed to vary from 0.178g (Kocaeli) to 0.185 g (Northridge).

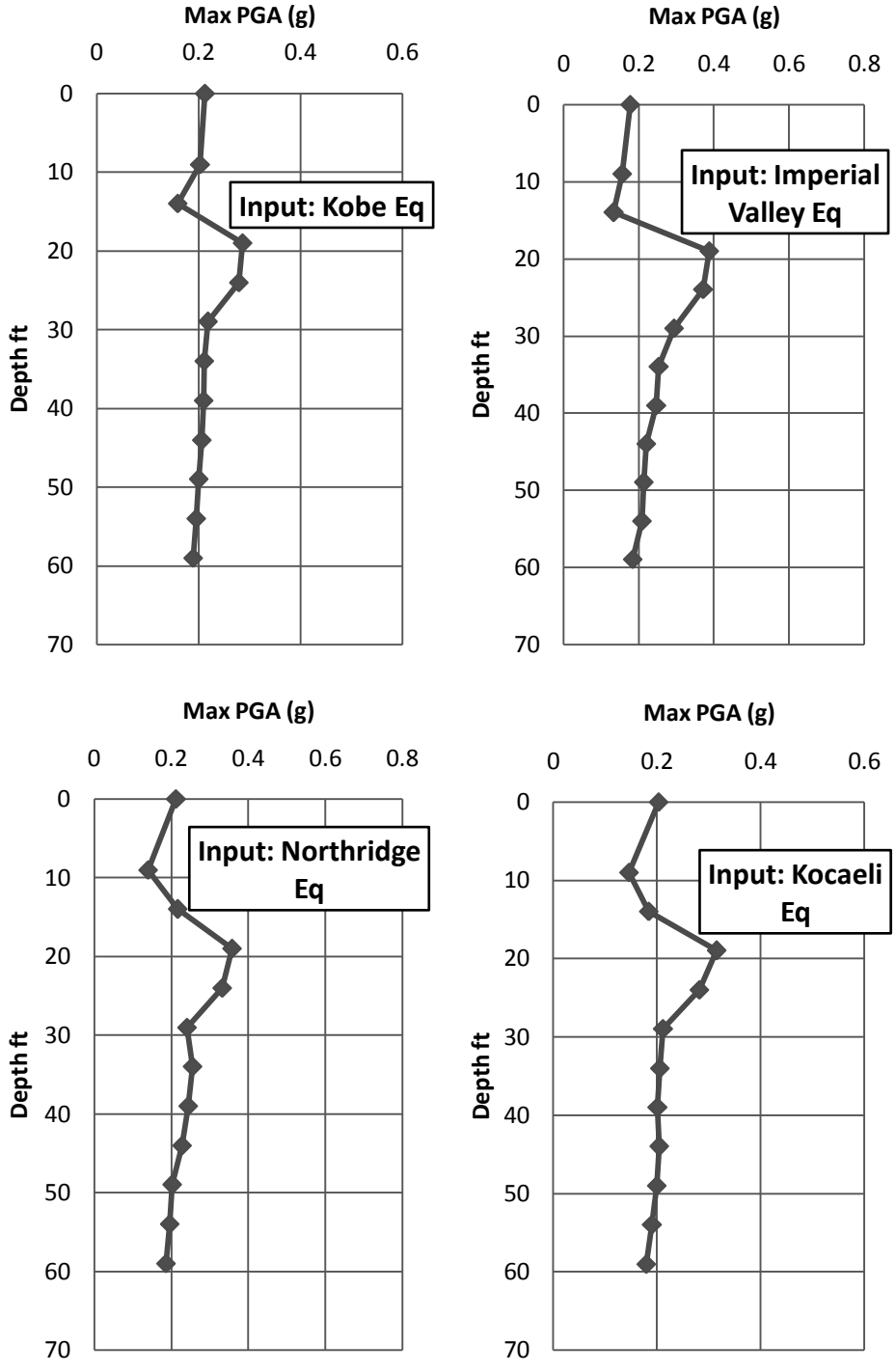


Figure 4.31 Maximum peak ground acceleration for the Site-7, Maniknagar.

**Site amplification factors**

Amplification Factor (Kobe earthquake) = 1.13

Amplification Factor (Imperial Valley earthquake) = 0.96

Amplification Factor (Northridge earthquake) = 1.15

Amplification Factor (Kocaile earthquake) = 1.14

It was identified that similar to the peak ground acceleration values, the variation of amplification factor was within 0.96 (Imperial Valley) to 1.15 (Northridge).

The comparison of PSA is given in Figure 4.32 and the comparison of mean and standard deviation for surface PSA is given in Figure 4.33.

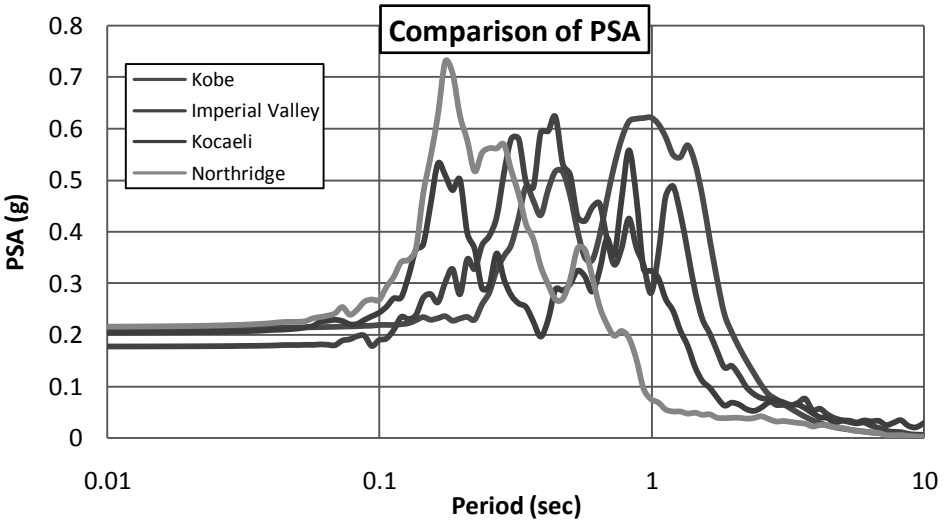


Figure 4.32 Comparison of PSA for different input motion for the Site-7, Maniknagar.

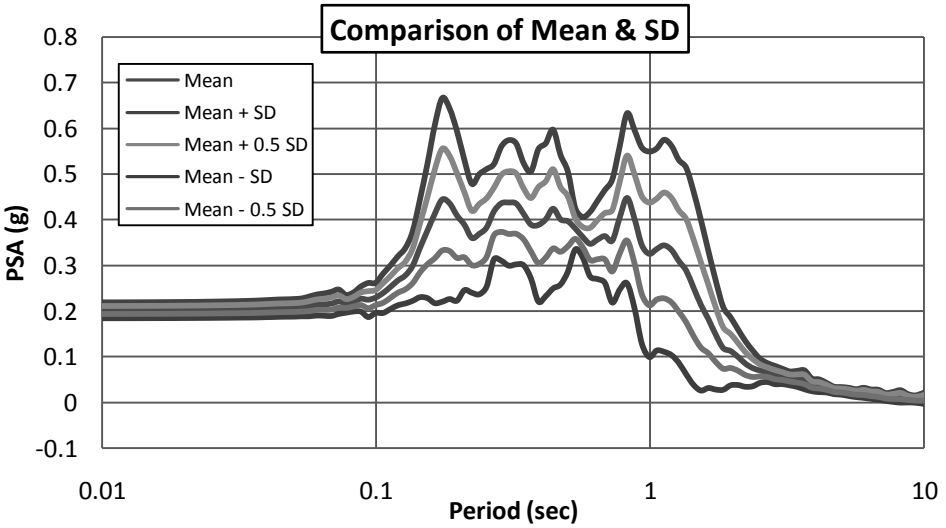


Figure 4.33 Comparison of mean and standard deviation for surface PSA for the Site-7 Maniknagar.

### 4.2.8 Ground Response Analysis of Site-8

This site was situated just before the internal steel bridge of Aftabnagar. This test was performed at 17th April, 2014. A 100ft borehole was done and test performed near 60ft.

**Response Spectra**

Response spectra of four earthquakes are shown in Figure 4.34. Among the four earthquakes, Kobe earthquake produces highest (0.60g) peak spectral acceleration (PSA) for this site and Northridge earthquake produces lowest (0.002g) peak spectral acceleration (PSA). It is observed that initially soil surface response was less than input response for some earthquakes for this site.

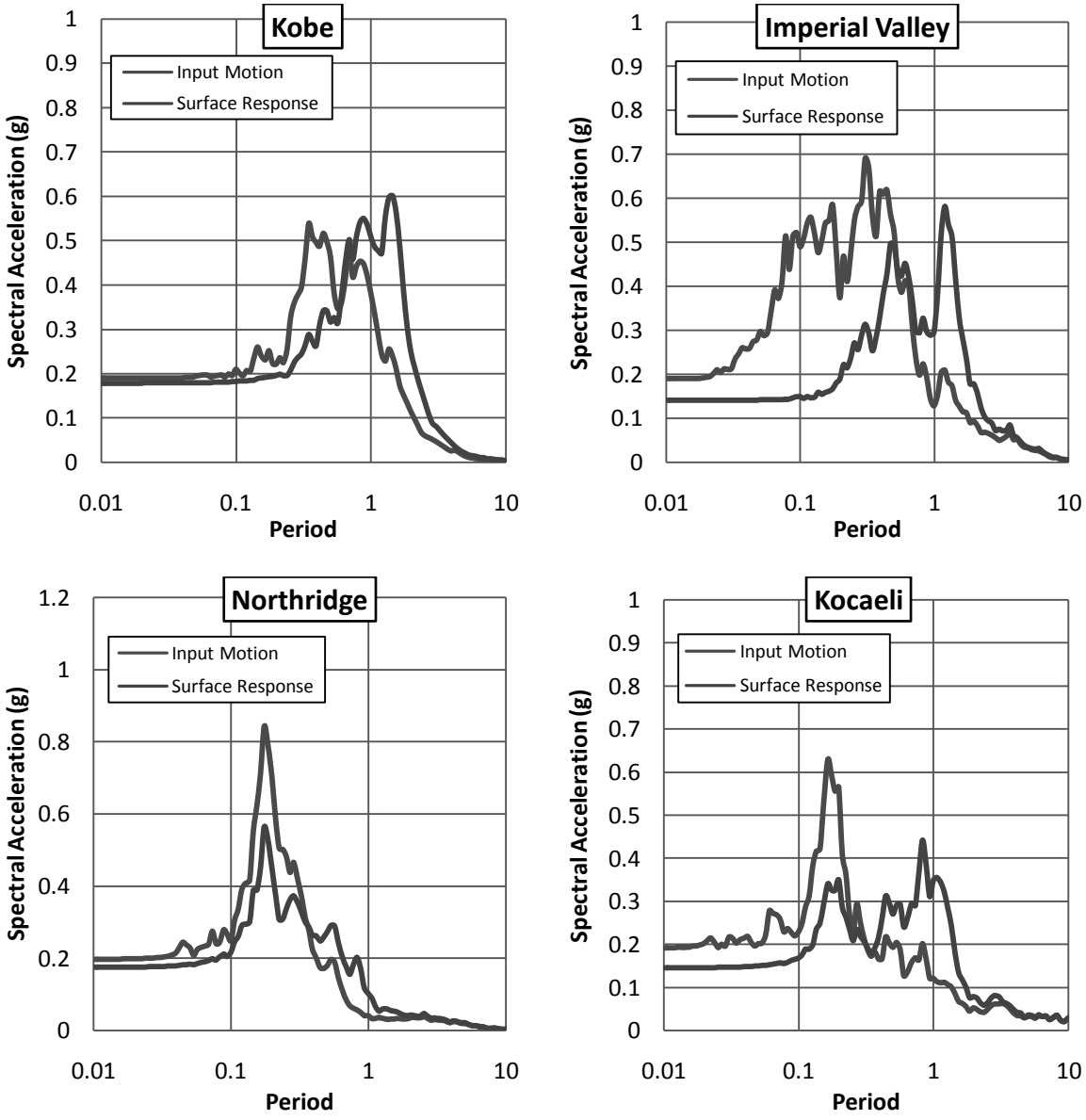


Figure 4.34 Response Spectra for the Site Maniknagar.

**Maximum Peak Ground Acceleration (PGA)**

Maximum Peak Ground Acceleration (PGA) at different depths of four earthquakes for this site is shown in Figure 4.35. PGA at surface and that at bedrock was obtained from the analysis. The peak ground acceleration values at surface were observed to be in the range of 0.14g (Imperial Valley) to 0. 18g (Kobe) and that of the bedrock were observed to vary from 0.17g (Kobe) to 0.19 g (Kocaeli).

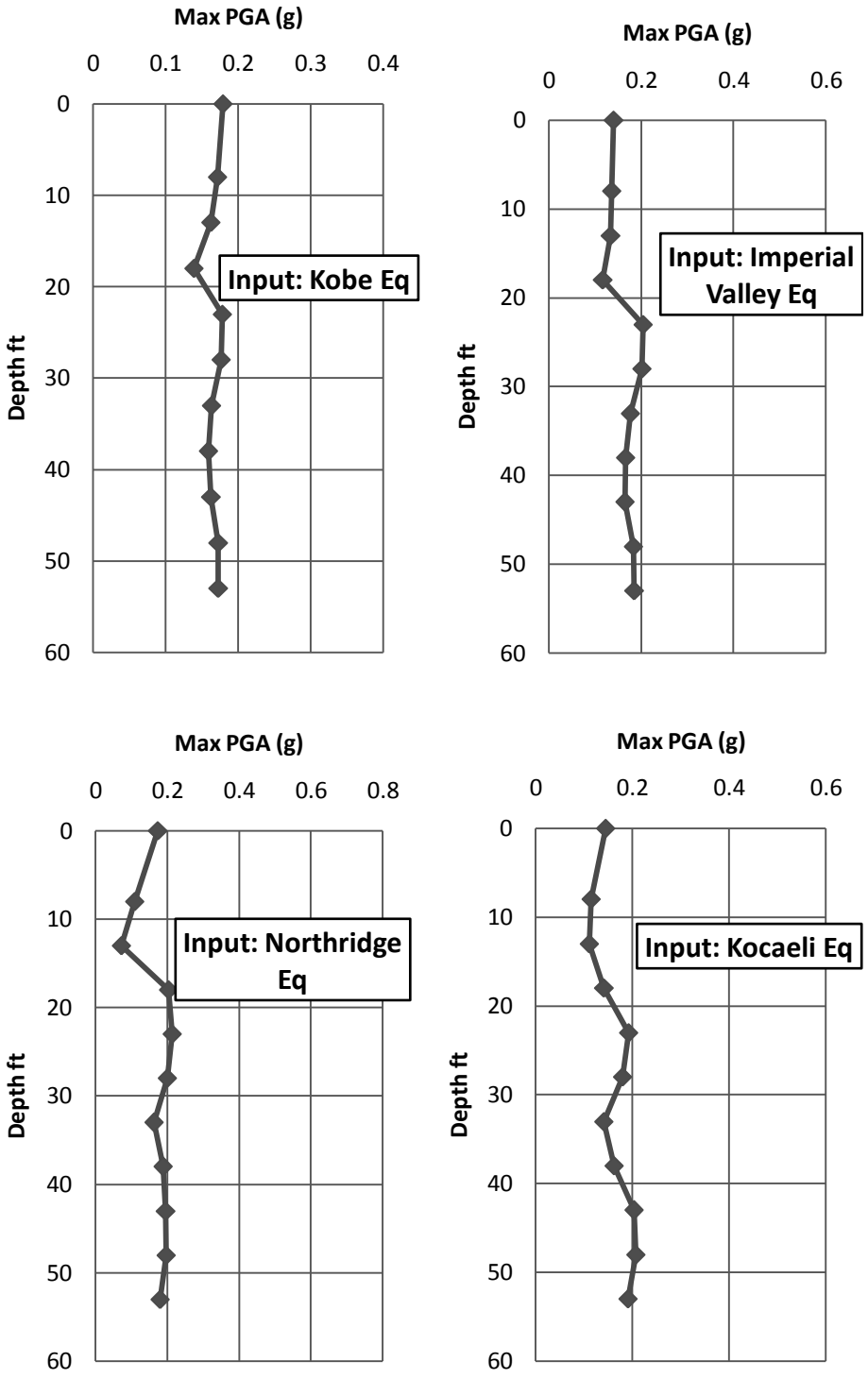


Figure 4.35 Maximum peak ground acceleration for the Site-8, Maniknagar.

**Site amplification factors**

Amplification Factor (Kobe earthquake) = 1.03

Amplification Factor (Imperial Valley earthquake) = 0.76

Amplification Factor (Northridge earthquake) = 0.96

Amplification Factor (Kocaile earthquake) = 0.75

It was identified that similar to the peak ground acceleration values, the variation of amplification factor was within 0.75 (Kocaeli) to 1.03 (Kobe).

The Comparison of PSA is given in Figure 4.36 and the comparison of mean and standard deviation for surface PSA is given in Figure 4.37.

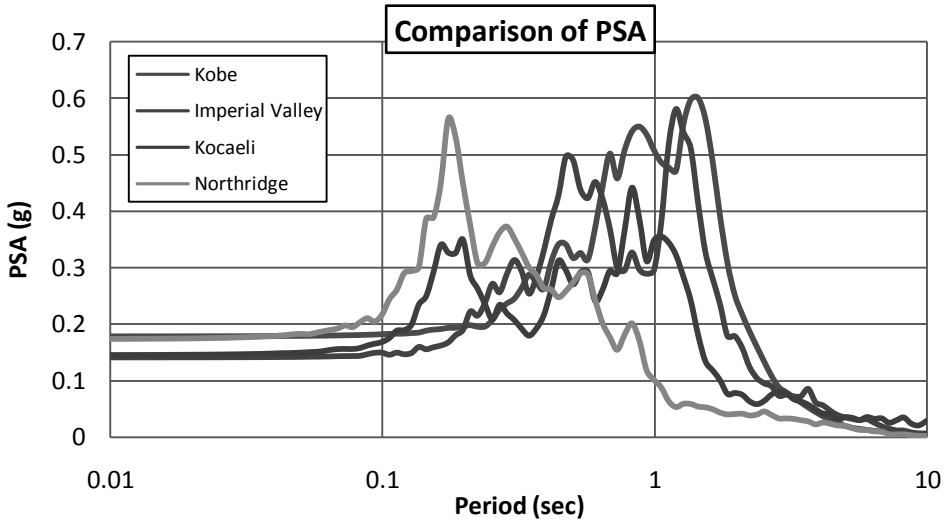


Figure 4.36 Comparison of PSA for different input motion for the Site-8, Maniknagar.

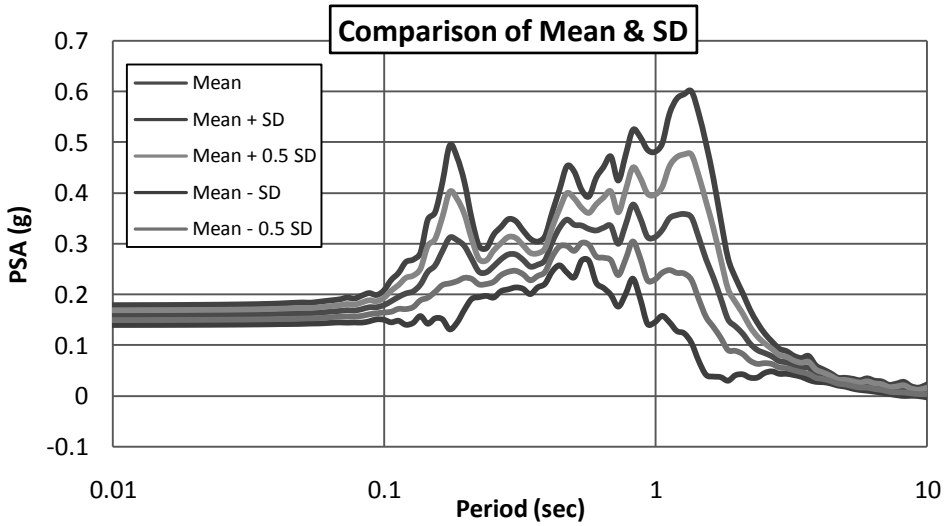


Figure 4.37 Comparison of mean and standard deviation for surface PSA for the Site-8, Maniknagar.

### 4.2.9 Ground Response Analysis of Site-9

This site was situated just beside the gate of the Lake city Concord. The test was performed at 31st October, 2014. A 100ft borehole was done and test performed near 53ft.

**Response Spectra**

Response spectra of four earthquakes are shown in Figure 4.38. Among the four earthquakes, Imperial Valley earthquake produces highest (1.14g) peak spectral acceleration (PSA) for this site and Northridge earthquake produces lowest (0.002g) peak spectral acceleration (PSA). It was observed that initially soil surface response was more than input response for some earthquakes for this site.

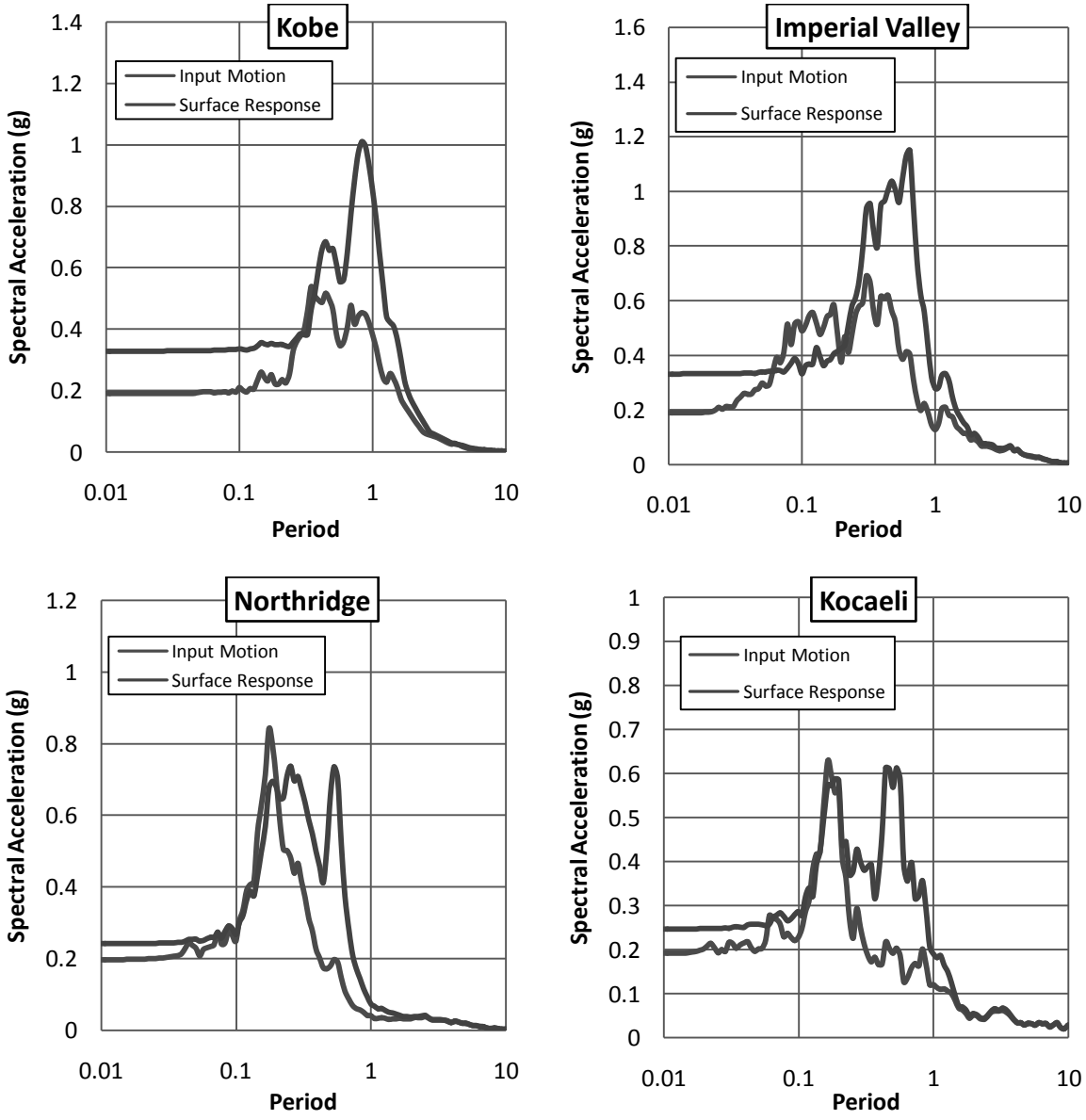


Figure 4.38 Response spectra for the Site-9 Lake City Concord, Khilkhet.

**Maximum Peak Ground Acceleration (PGA)**

Maximum Peak Ground Acceleration (PGA) at different depths of four earthquakes for this site is shown in Figure 4.39. PGA at surface and that at bedrock was obtained from the analysis. The peak ground acceleration values at surface were observed to be in the range of 0.24g (Northridge) to 0. 32g (Kobe) and that of the bedrock were observed to vary from 0.09g (Kocaeli) to 0.153 g (Kobe).

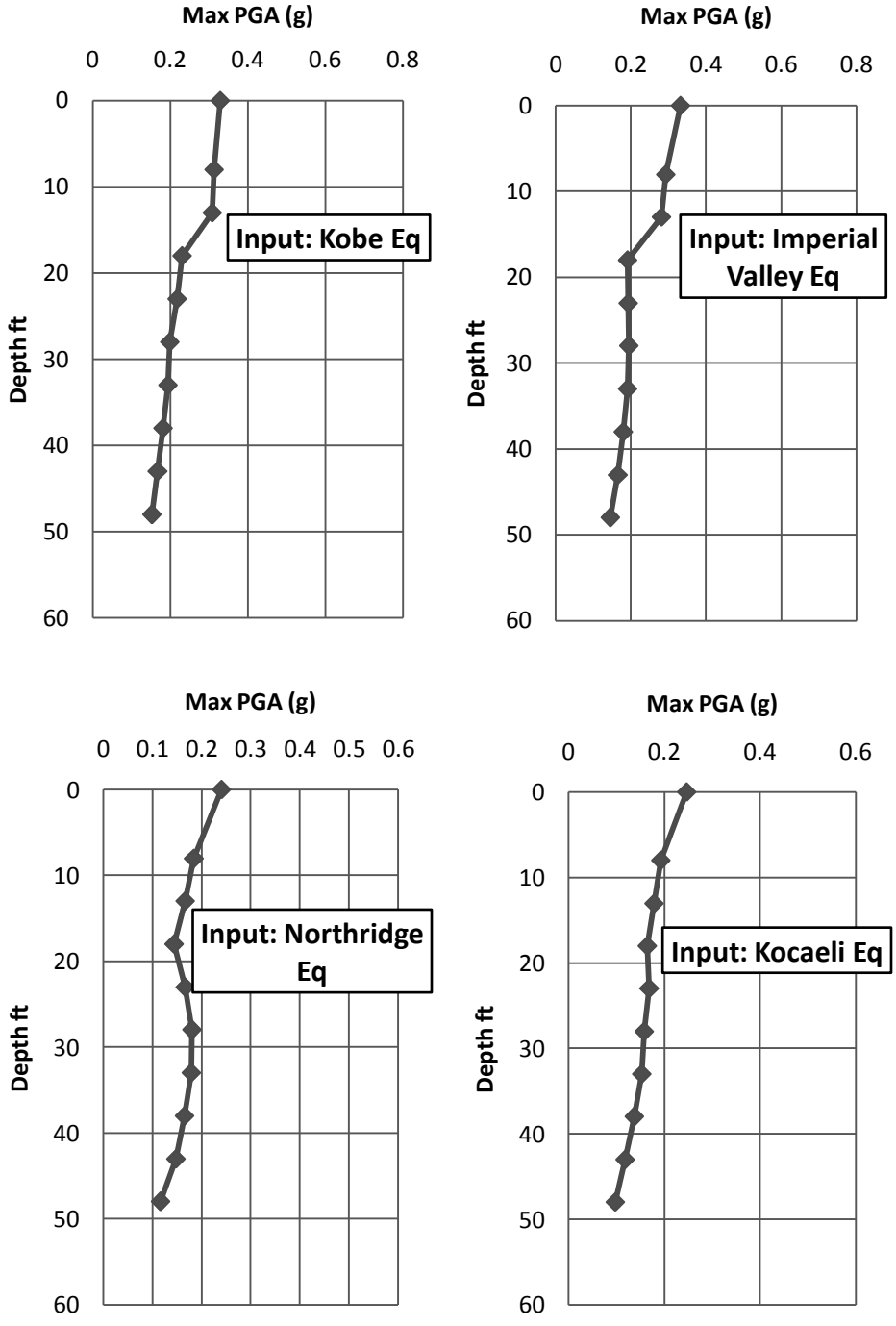


Figure 4.39 Maximum peak ground Acceleration for the Site-9, Lake City Concord, Khilkhet.

**Site amplification factors**

Amplification Factor (Kobe earthquake) = 2.16

Amplification Factor (Imperial Valley earthquake) = 2.29

Amplification Factor (Northridge earthquake) = 2.07

Amplification Factor (Kocaile earthquake) = 2.52

It was identified that similar to the peak ground acceleration values, the variation of amplification factor was within 2.07 (Kocaeli) to 2.52 (Kobe).

The Comparison of PSA is given in Figure 4.40 and the comparison of mean and standard deviation for surface PSA is given in Figure 4.41.

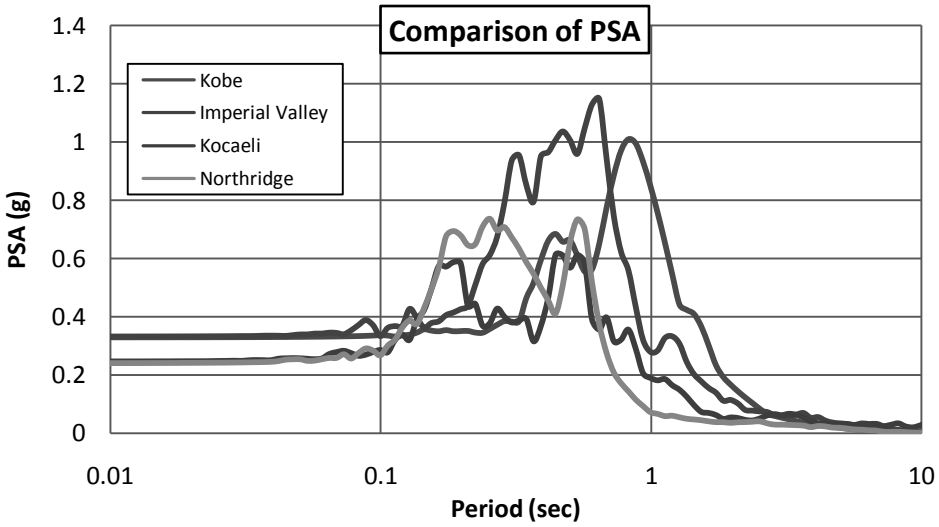


Figure 4.40: Comparison of PSA for different input motion for the Site-9, Lake City Concord, Khilkhet.

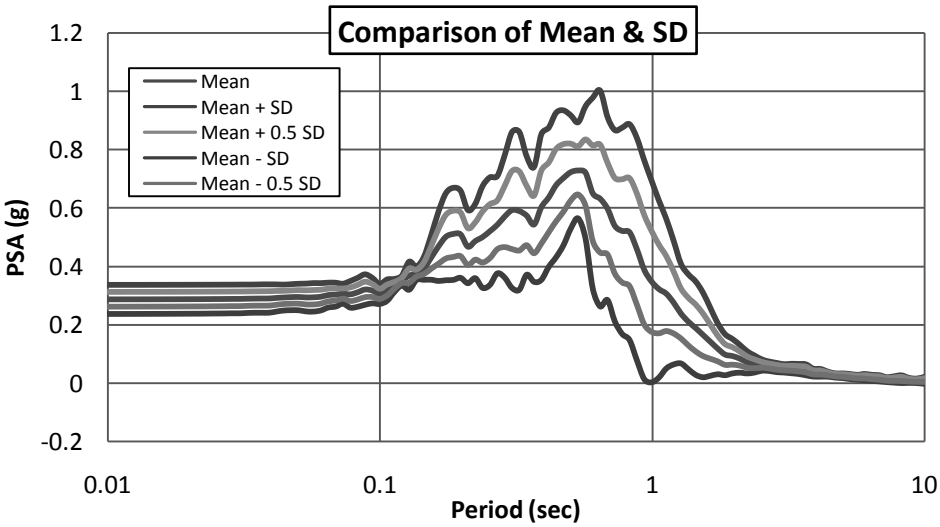


Figure 4.41: Comparison of mean and standard deviation for surface PSA for the Site-9, Lake City Concord, Khilkhet.

### 4.2. 10. Ground Response Analysis of Site-10

**Response Spectra**

Response spectra of four earthquakes are shown in Figure 4.42. Among the four earthquakes, Imperial Valley earthquake produces highest (1.90g) peak spectral acceleration (PSA) for this site and Northridge earthquake produces lowest (0.002g) peak spectral acceleration (PSA). It was observed that initially soil surface response was more than input response s for this site.

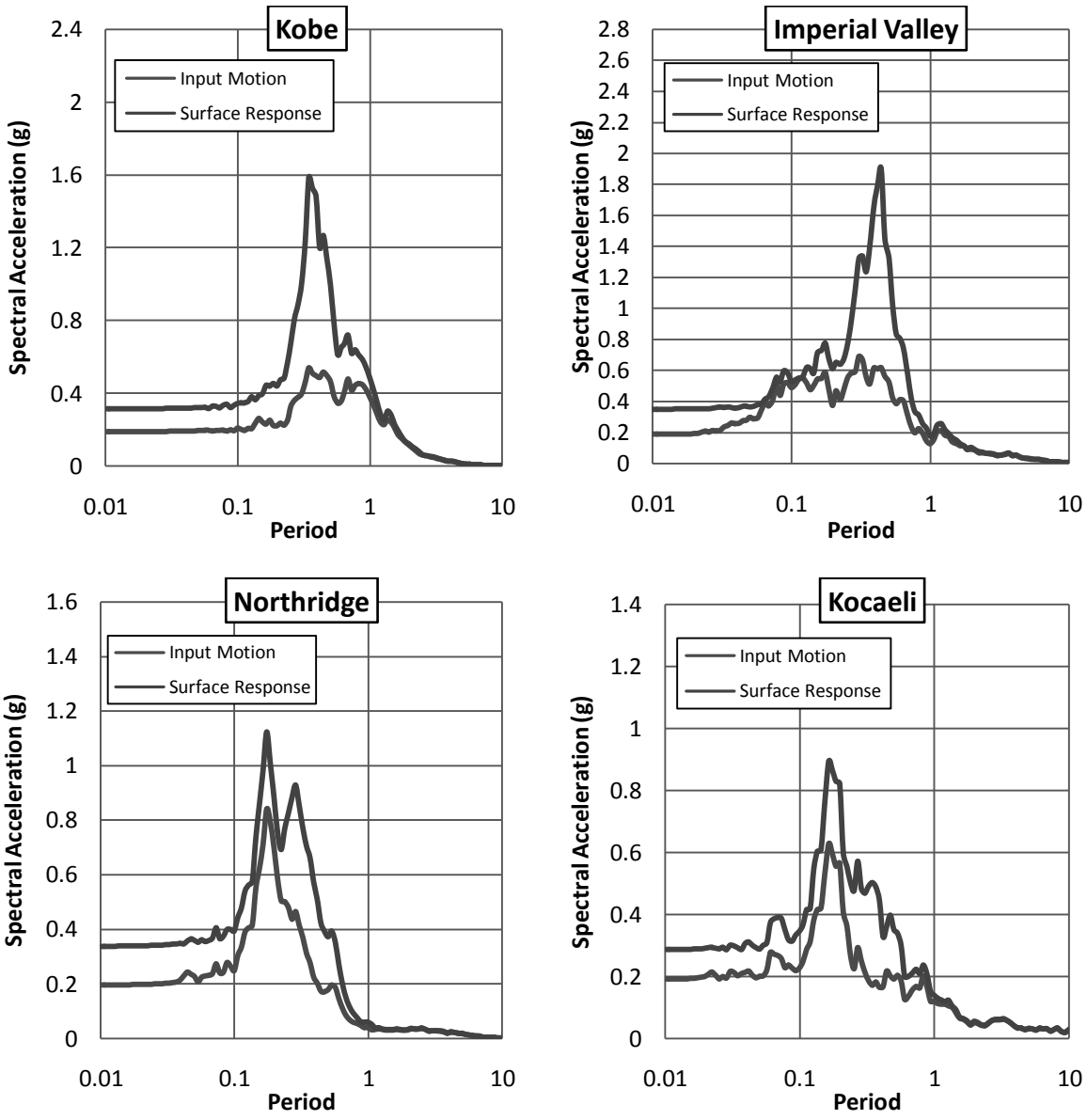


Figure 4.42 Response spectra for the Site-10, RHD, Tejgaon

.

**Maximum Peak Ground Acceleration (PGA)**

Maximum Peak Ground Acceleration (PGA) at different depths of four earthquakes for this site is shown in Figure 4.43. PGA at surface and that at bedrock was obtained from the analysis. The peak ground acceleration values at surface were observed to be in the range of 0.29g (Kocaeli) to 0. 35g (Imperial Valley) and that of the bedrock were observed to vary from 0.182g (Imperial Valley) to 0.102g (Kobe).

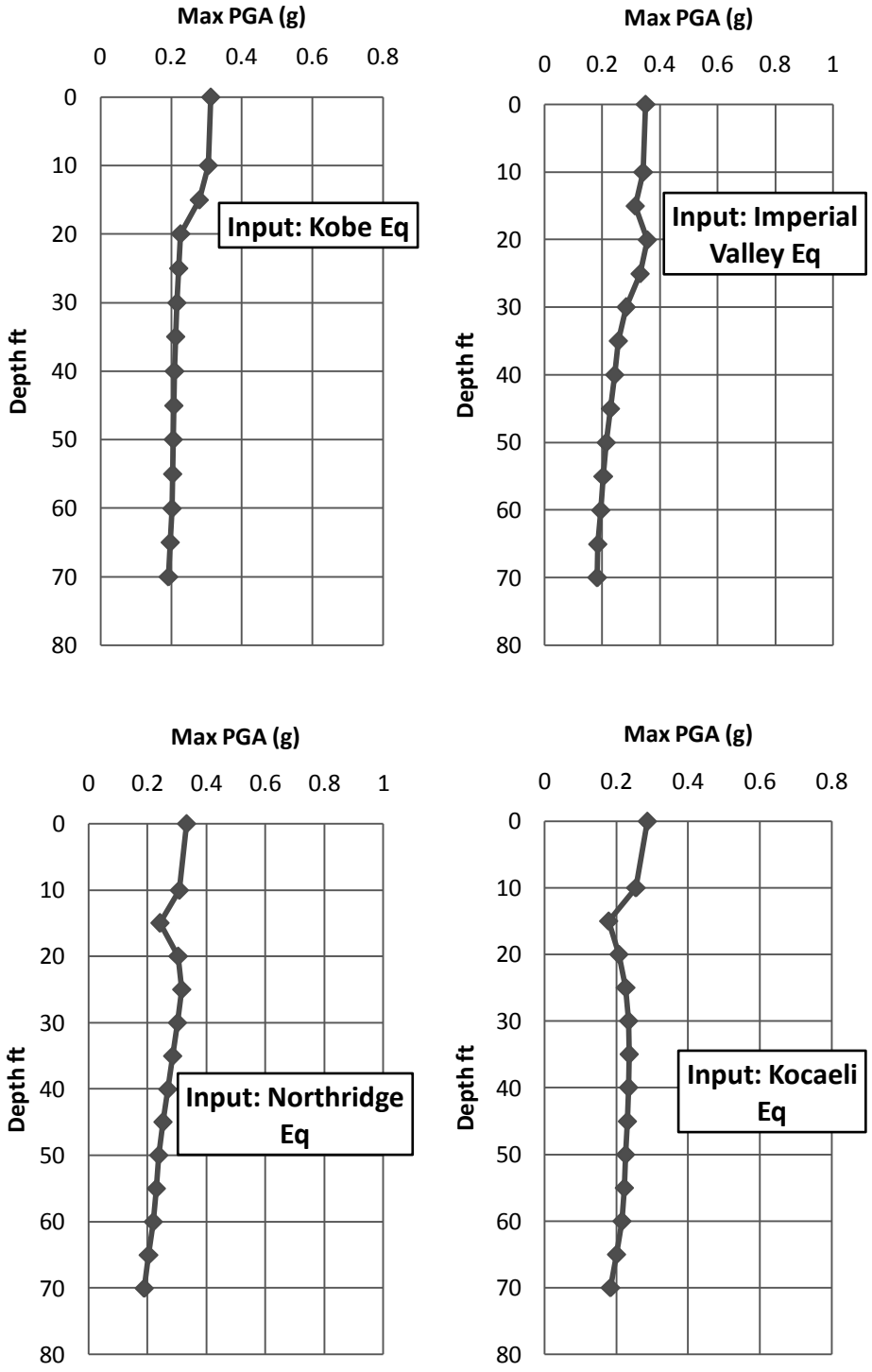


Figure 4.43 Maximum peak ground Acceleration for the Site-10, RHD, Tejgaon

**Site amplification factors:**

Amplification Factor (For Kobe earthquake) = 1.62

Amplification Factor (For Imperial Valley earthquake) = 1.92

Amplification Factor (For Northridge earthquake) = 1.76

Amplification Factor (For Kocaile earthquake) = 1.55

It was identified that similar to the peak ground acceleration values, the variation of amplification factor was within 1.55 (Kocaeli) to 1.92 (Imperial Valley).

The Comparison of PSA is given in Figure 4.44 and the comparison of mean and standard deviation for surface PSA is given in Figure 4.45.

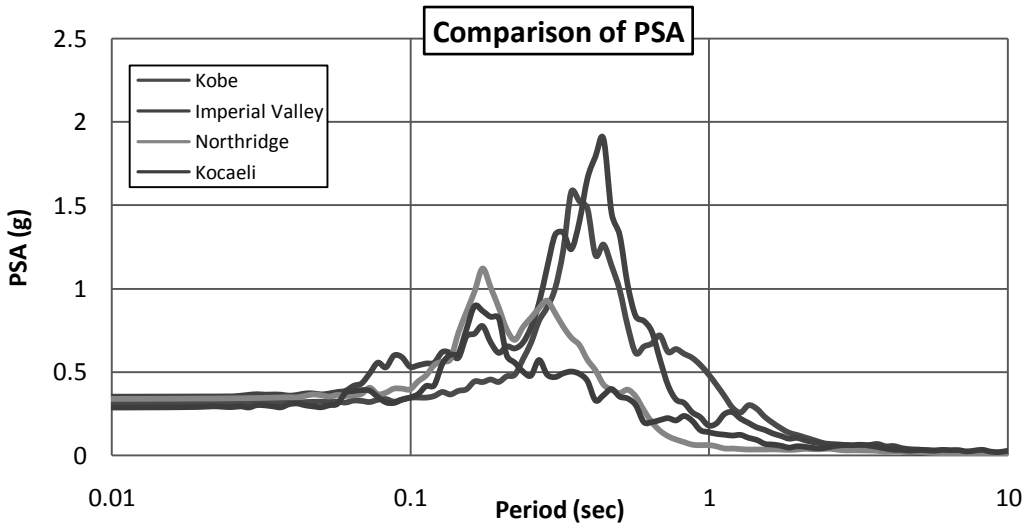


Figure 4.44 Comparison of PSA for different input motion for the Site-10, RHD, Tejgaon

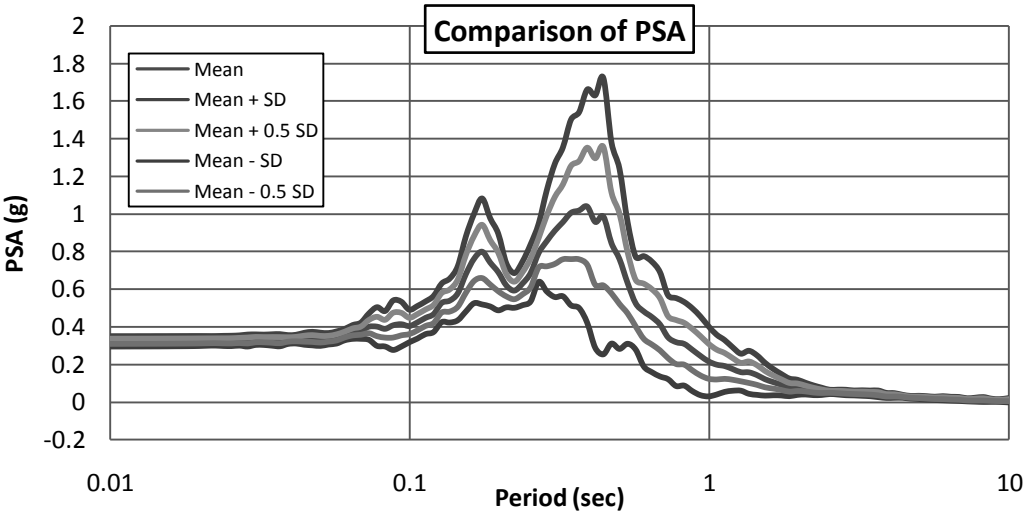


Figure 4.45 Comparison of mean and standard deviation for surface PSA for the Site-10, RHD, Tejgaon

### 4.2.11. Ground Response Analysis of Site-11

**Response Spectra**

Response spectra of six earthquakes are shown in Figure 4.46. Among the four earthquakes, Kobe earthquake produces highest (1.14g) peak spectral acceleration (PSA) for this site and Northridge earthquake produces lowest (0.003g) peak spectral acceleration (PSA). It was observed that initially soil surface response is more than input response for this site.

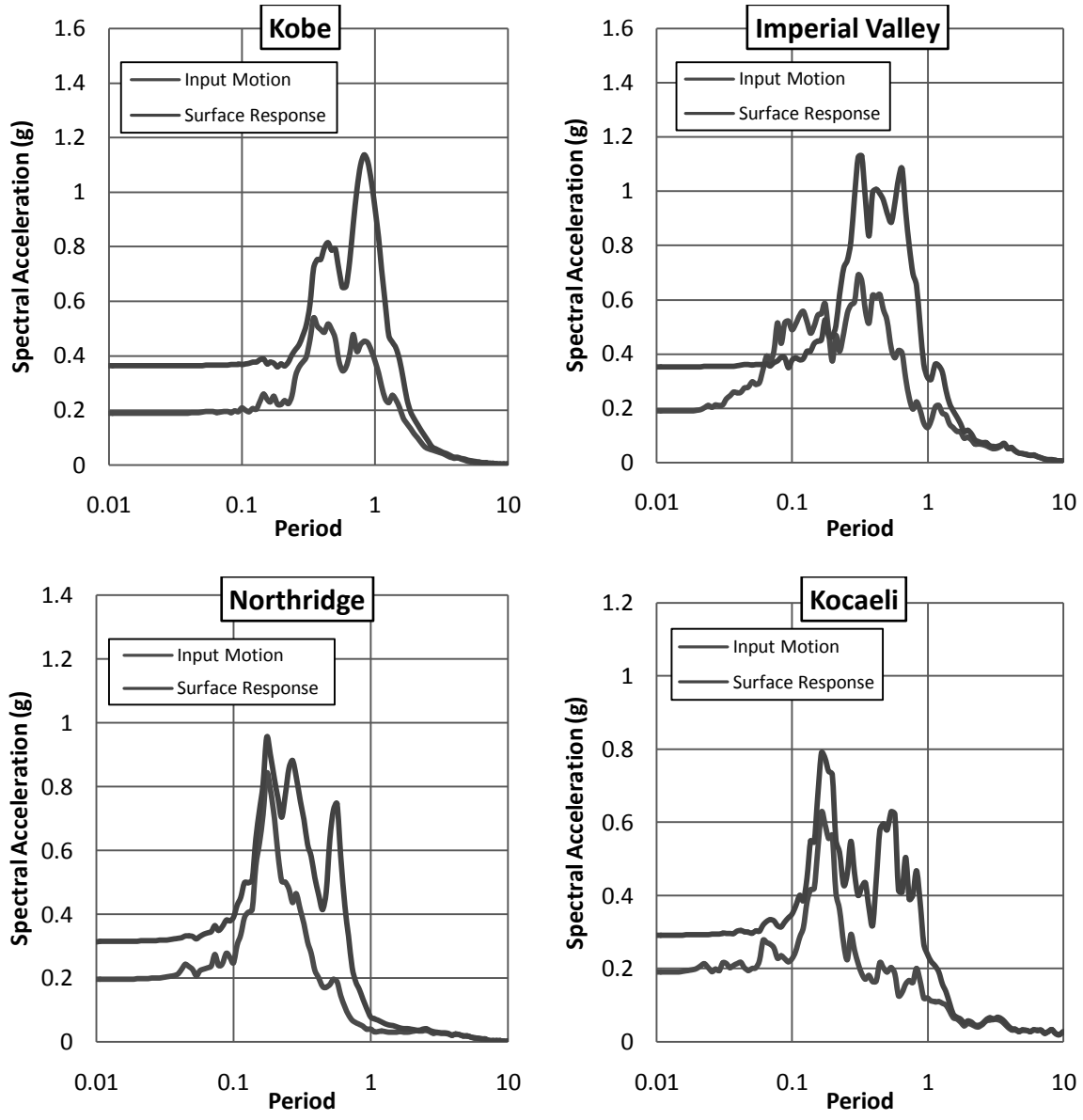


Figure 4.46 Response spectra for the Site Site-11, Mehernagar Uttara

.

**Maximum Peak Ground Acceleration (PGA)**

Maximum Peak Ground Acceleration (PGA) at different depths of four earthquakes for this site is shown in Figure 4.47. PGA at surface and that at bedrock was obtained from the analysis. The peak ground acceleration values at surface were observed to be in the range of 0.29g (Kocaeli) to 0. 36g (Kobe) and that of the bedrock were observed to vary from 0.17g (Kocaeli) to 0.18g (Kobe).

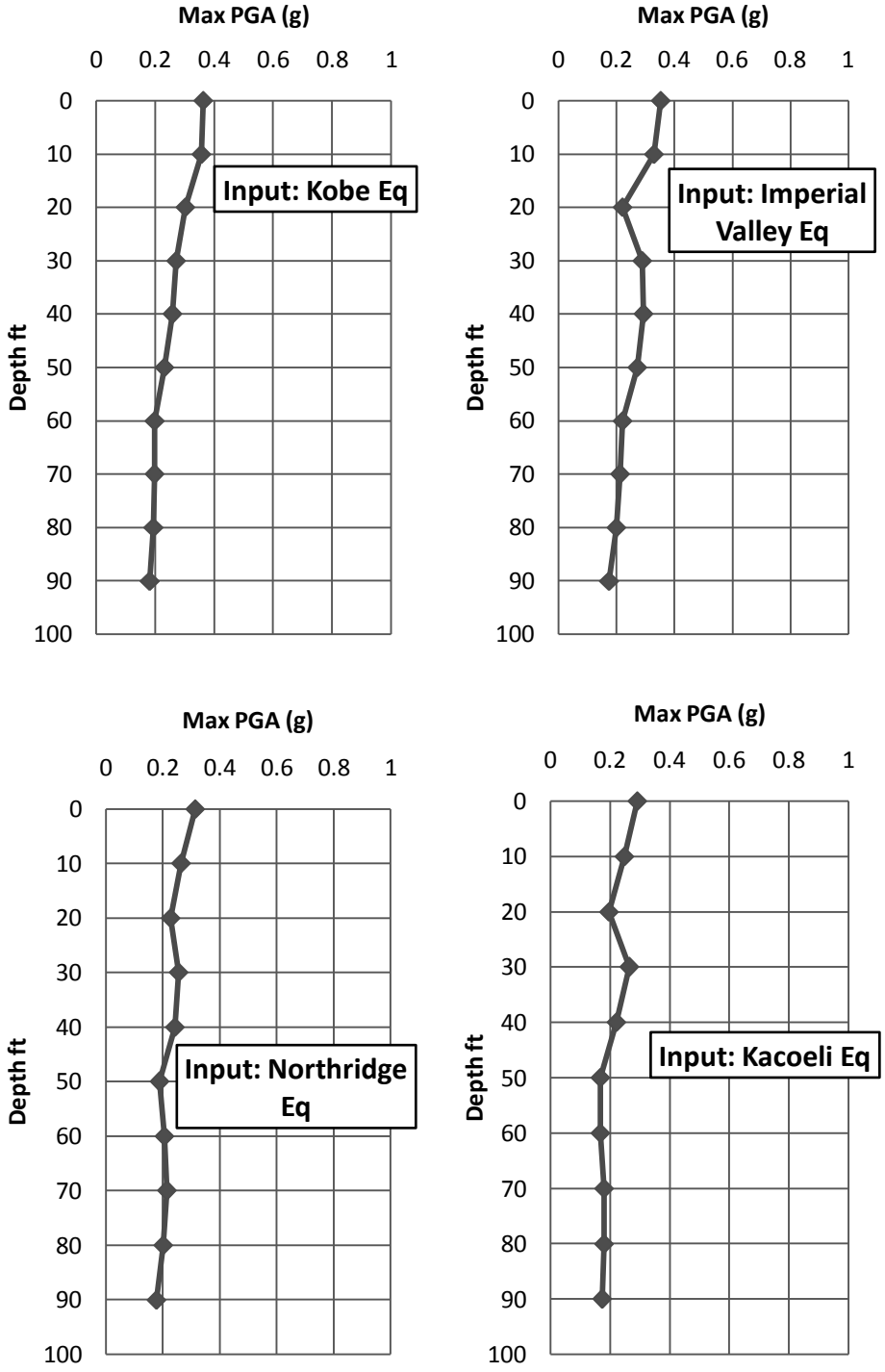


Figure 4.47 Maximum peak ground acceleration for the Site-11, Mehernagar Uttara

**Site amplification factors:**

Amplification Factor (Kobe earthquake) = 1.99

Amplification Factor (Imperial Valley earthquake) = 2.01

Amplification Factor (Northridge earthquake) = 1.76

Amplification Factor (Kocaile earthquake) = 1.68

It was identified that similar to the peak ground acceleration values, the variation of amplification factor was within 1.68 (Kocaeli) to 2.01 (Imperial Valley).

The Comparison of PSA is given in Figure 4.48 and the comparison of mean and standard deviation for surface PSA is given in Figure 4.49.

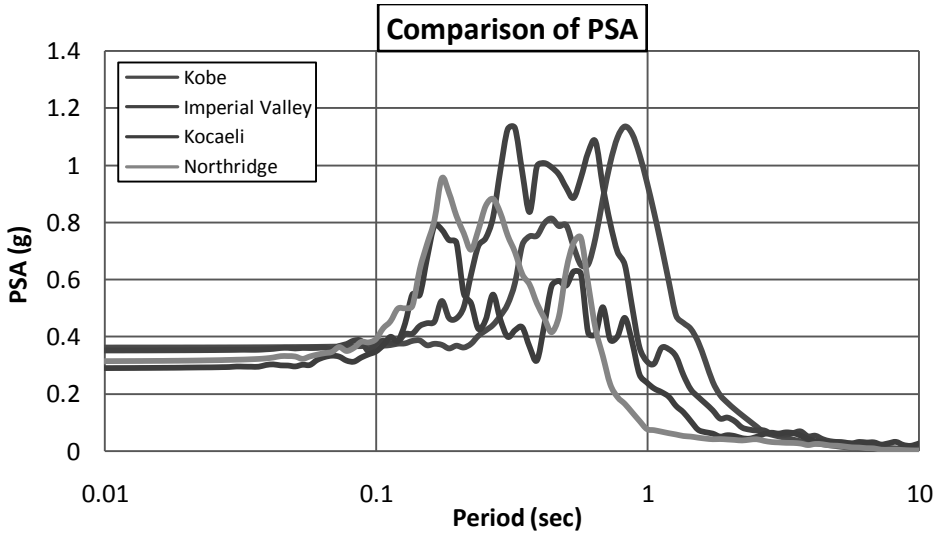


Figure 4.48 Comparison of PSA for different input motion for the Site-11, Mehernagar Uttara.

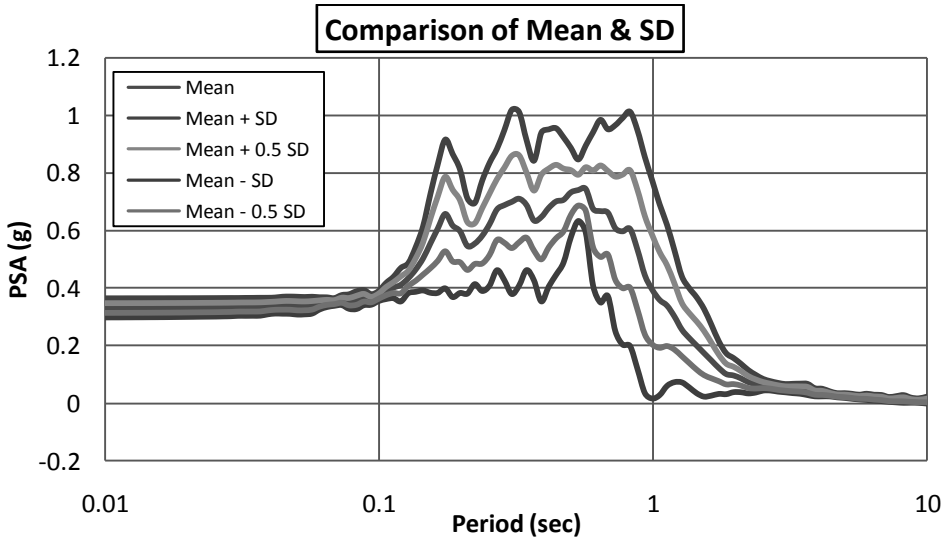


Figure 4.49 Comparison of mean and standard deviation for surface PSA for the Site-11, Mehernagar Uttara.

### 4.2.12. Ground Response Analysis of Site-12

**Response Spectra**

Response spectra of six earthquakes are shown in Figure 4.50. Among the four earthquakes, Kobe earthquake produces highest (0.53g) peak spectral acceleration (PSA) for this site and Northridge earthquake produces lowest (0.002g) peak spectral acceleration (PSA). It was observed that initially soil surface response is less than input response for this site.

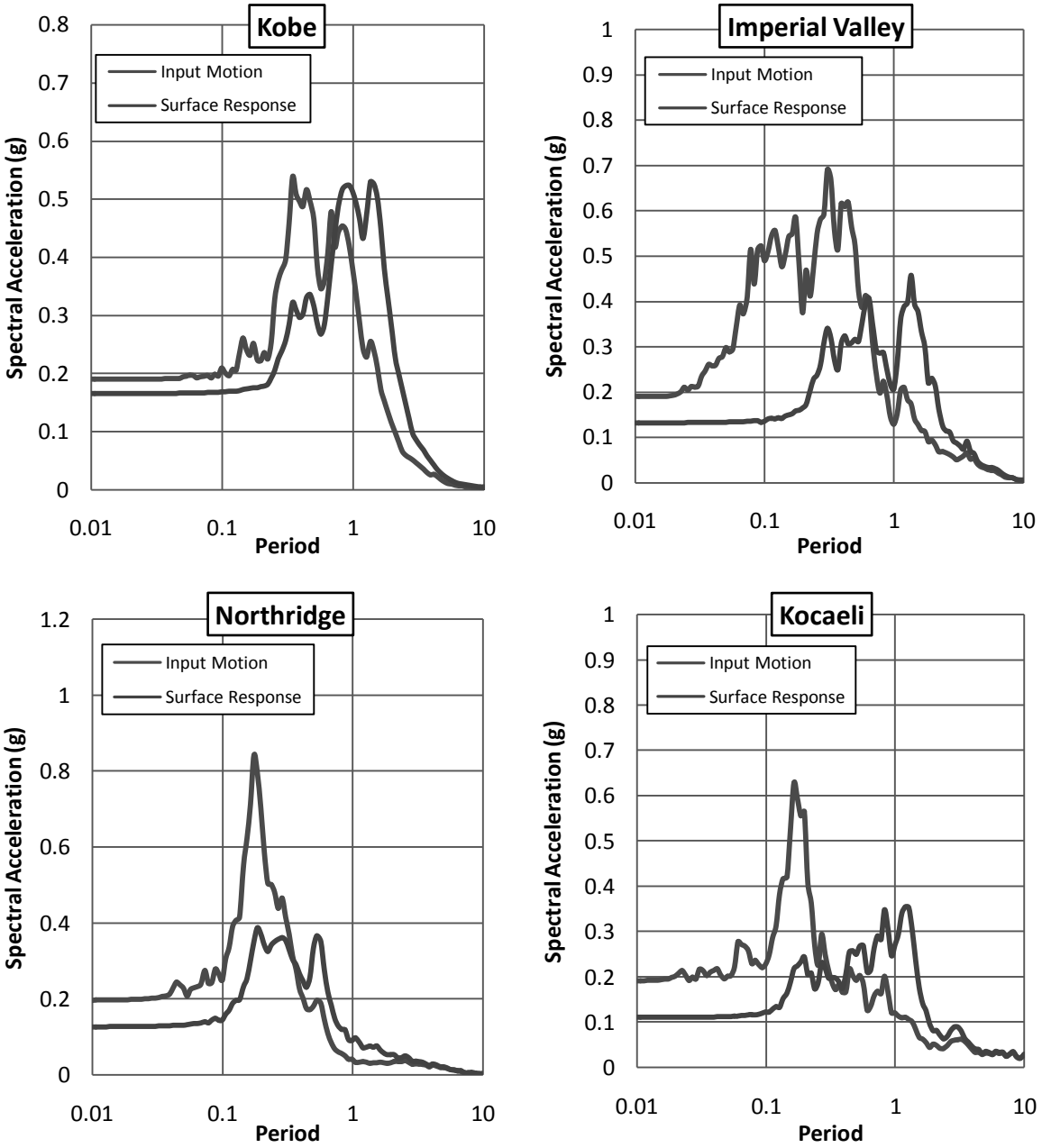


Figure 4.50 Response spectra for the Site-12, Ashulia, Jubok Project

.

**Maximum Peak Ground Acceleration (PGA)**

Maximum Peak Ground Acceleration (PGA) at different depths of four earthquakes for this site is shown in Figure 4.51. PGA at surface and that at bedrock was obtained from the analysis. The peak ground acceleration values at surface were observed to be in the range of 0.11g (Kocaeli) to 0. 17g (Kobe) and that of the bedrock were observed to vary from 0.17g (Kocaeli) to 0.20g (Imperial Valley).

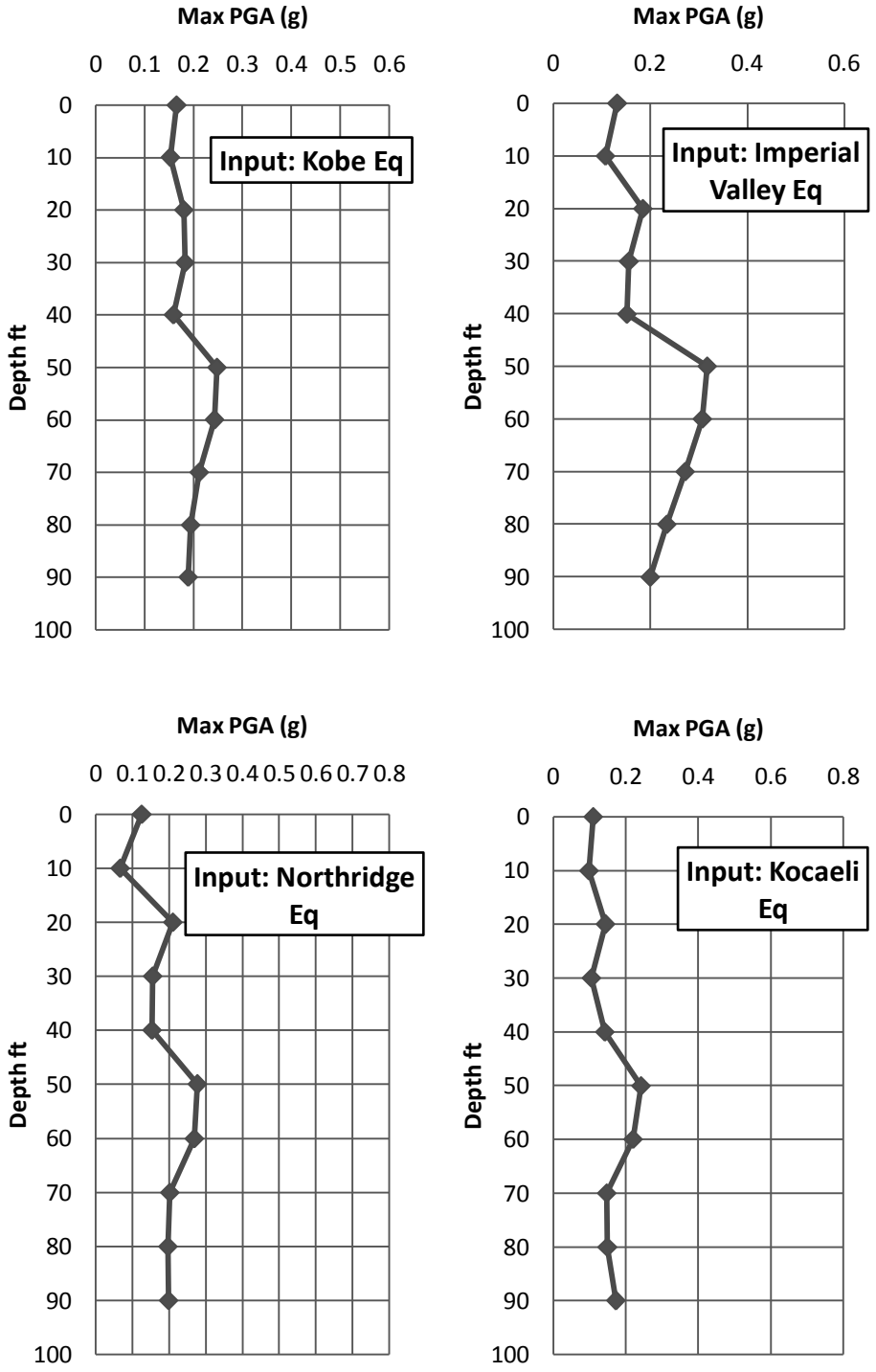


Figure 4.51 Maximum peak ground acceleration for the Site-12, Ashulia, Jubok Project

**Site amplification factors:**

Amplification Factor (For Kobe earthquake) = 0.86

Amplification Factor (For Imperial Valley earthquake) = 0.66

Amplification Factor (For Northridge earthquake) = 0.63

Amplification Factor (For Kocaile earthquake) = 0.64

It was identified that similar to the peak ground acceleration values, the variation of amplification factor was within 0.63 (Northridge) to 0.86 (Kobe).

The Comparison of PSA is given in Figure 4.52 and the comparison of mean and standard deviation for surface PSA is given in Figure 4.53.

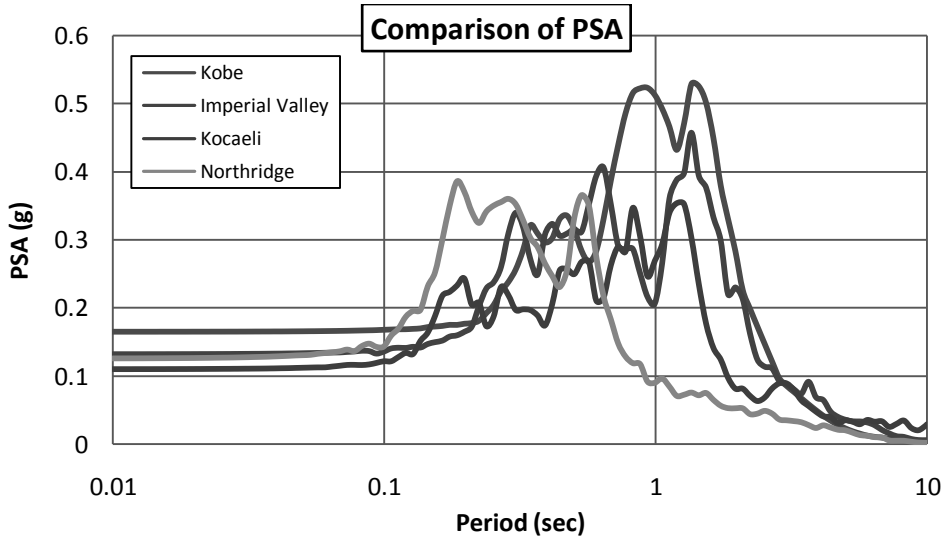


Figure 4.52 Comparison of PSA for different input motion for the Site-12, Mehernagar Uttara.

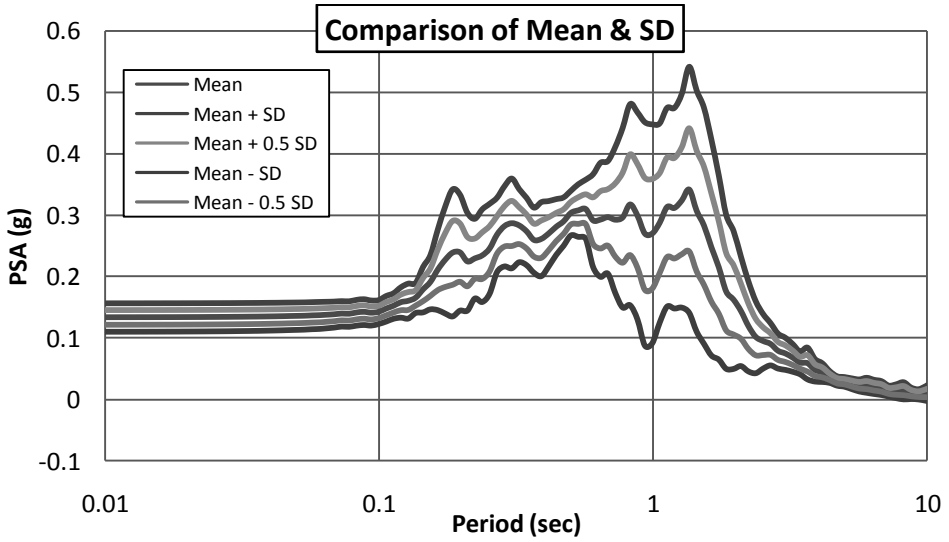


Figure 4.53 Comparison of mean and standard deviation for surface PSA for the Site-12, Ashulia, Jubok Project

### 4.2.13. Ground Response Analysis of Site-13

**Response Spectra**

Response spectra of four earthquakes are shown in Figure 4.54. Among the four earthquakes, Imperial Valley earthquake produces highest (1.54g) peak spectral acceleration (PSA) for this site and Northridge earthquake produces lowest (0.003g) peak spectral acceleration (PSA). It was observed that initially soil surface response is more than input response for this site.

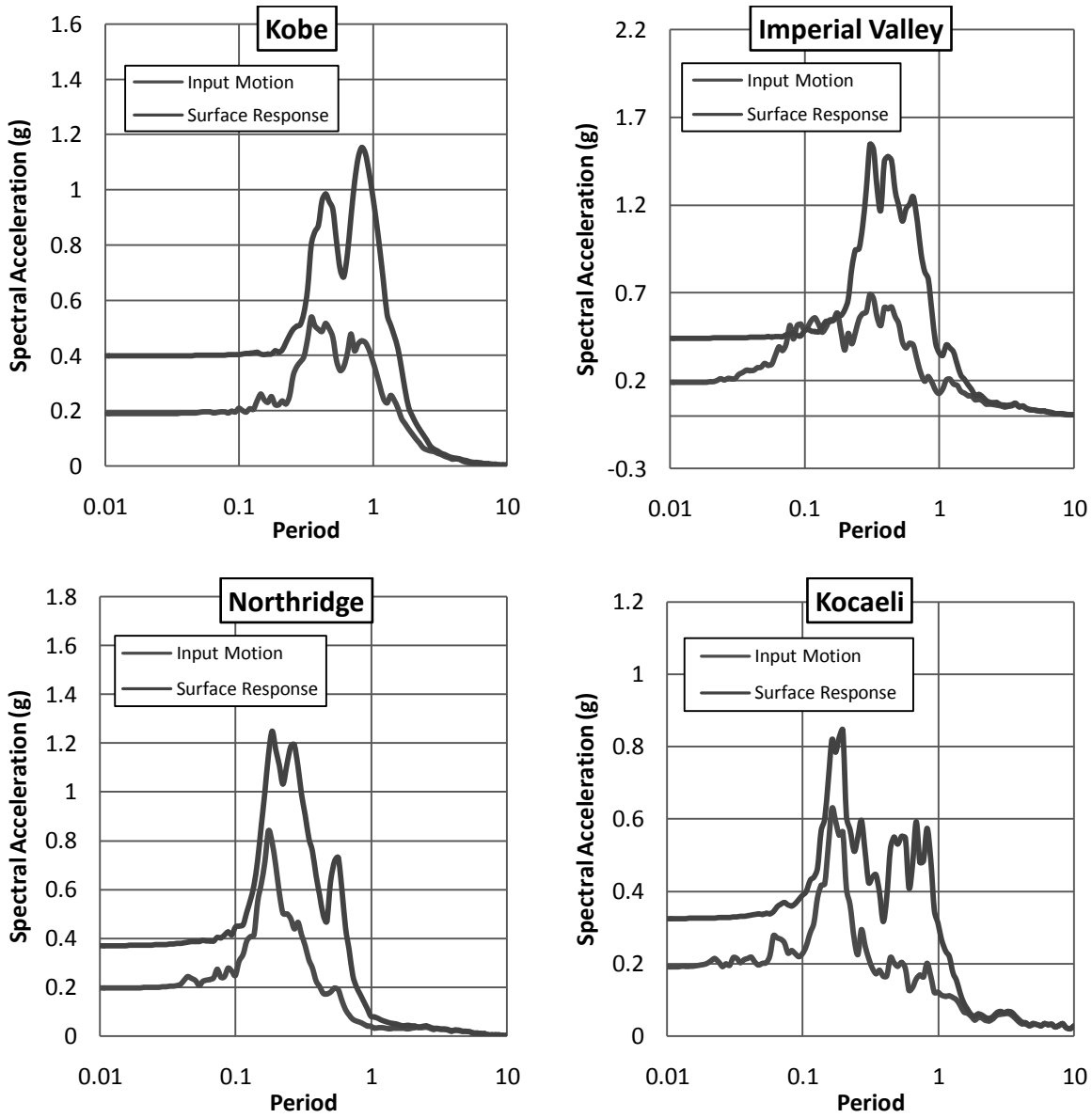


Figure 4.54 Response spectra for the Site-13, Mirpur-1, Avenue-2

**Maximum Peak Ground Acceleration (PGA)**

Maximum Peak Ground Acceleration (PGA) at different depths of four earthquakes for this site is shown in Figure 4.55. PGA at surface and that at bedrock was obtained from the analysis. The peak ground acceleration values at surface were observed to be in the range of 0.32g (Kocaeli) to 0. 44g (Imperial Valley) and that of the bedrock were observed to vary from 0.14g (Imperial Valley) to 0.17g (Kobe).

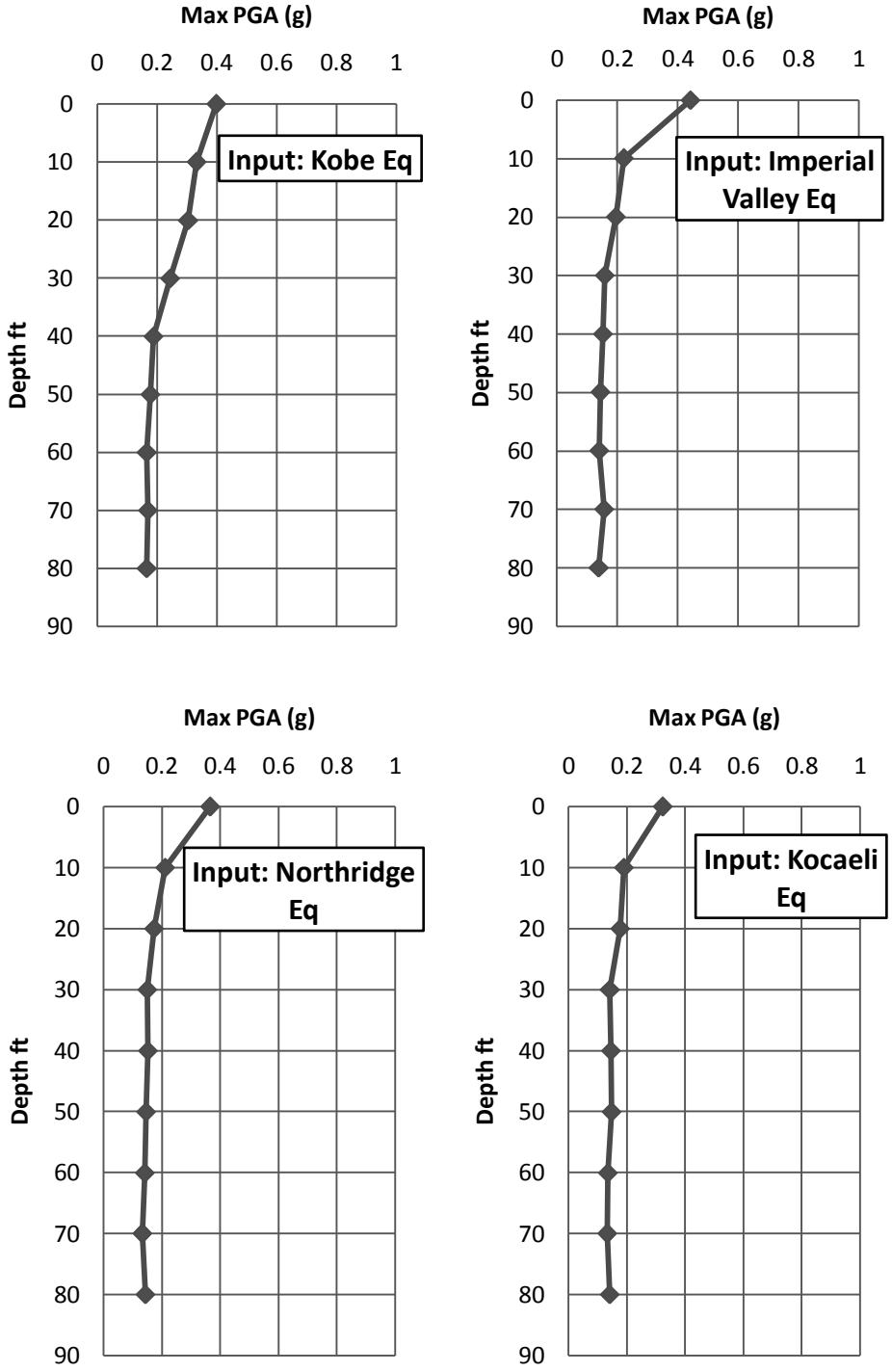


Figure 4.55 Maximum peak ground acceleration for the Site-13, Mirpur-1, Avenue-2

**Site amplification factors:**

Amplification Factor (Kobe earthquake) = 2.39

Amplification Factor (Imperial Valley earthquake) = 3.18

Amplification Factor (Northridge earthquake) = 2.54

Amplification Factor (Kocaile earthquake) = 2.29

It was identified that similar to the peak ground acceleration values, the variation of amplification factor was within 2.29 (Kocaile earthquake) to 3.18 (Imperial Valley).

The Comparison of PSA is given in Figure 4.56 and the comparison of mean and standard deviation for surface PSA is given in Figure 4.57.

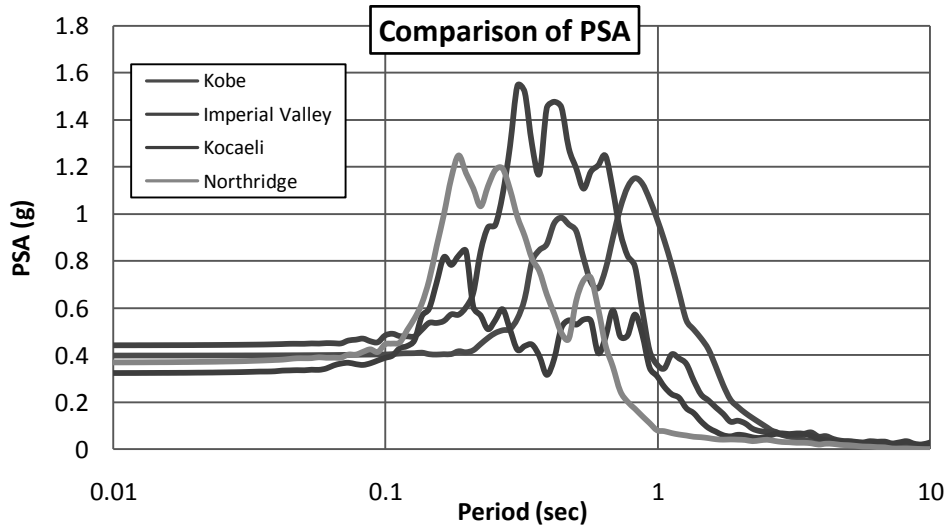


Figure 4.56 Comparison of PSA for different input motion for the Site-13, Mirpur-1, Avenue-2.

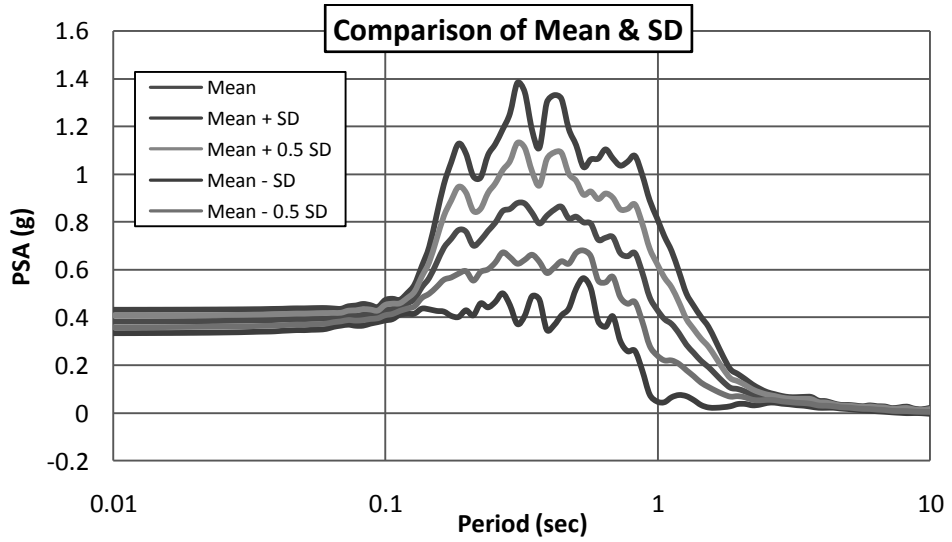


Figure 4.57 Comparison of Mean and Standard deviation for surface PSA for the Site-13, Mirpur-1, Avenue-2

### 4.2.14 Ground Response Analysis of Site-14

**Response Spectra:**

Response spectra of four earthquakes are shown in Figure 4.58. Among the four earthquakes, Imperial Valley earthquake produces highest (1.81g) peak spectral acceleration (PSA) for this site and Northridge earthquake produces lowest (0.002g) peak spectral acceleration (PSA). It was observed that initially soil surface response is more than input response for this site.

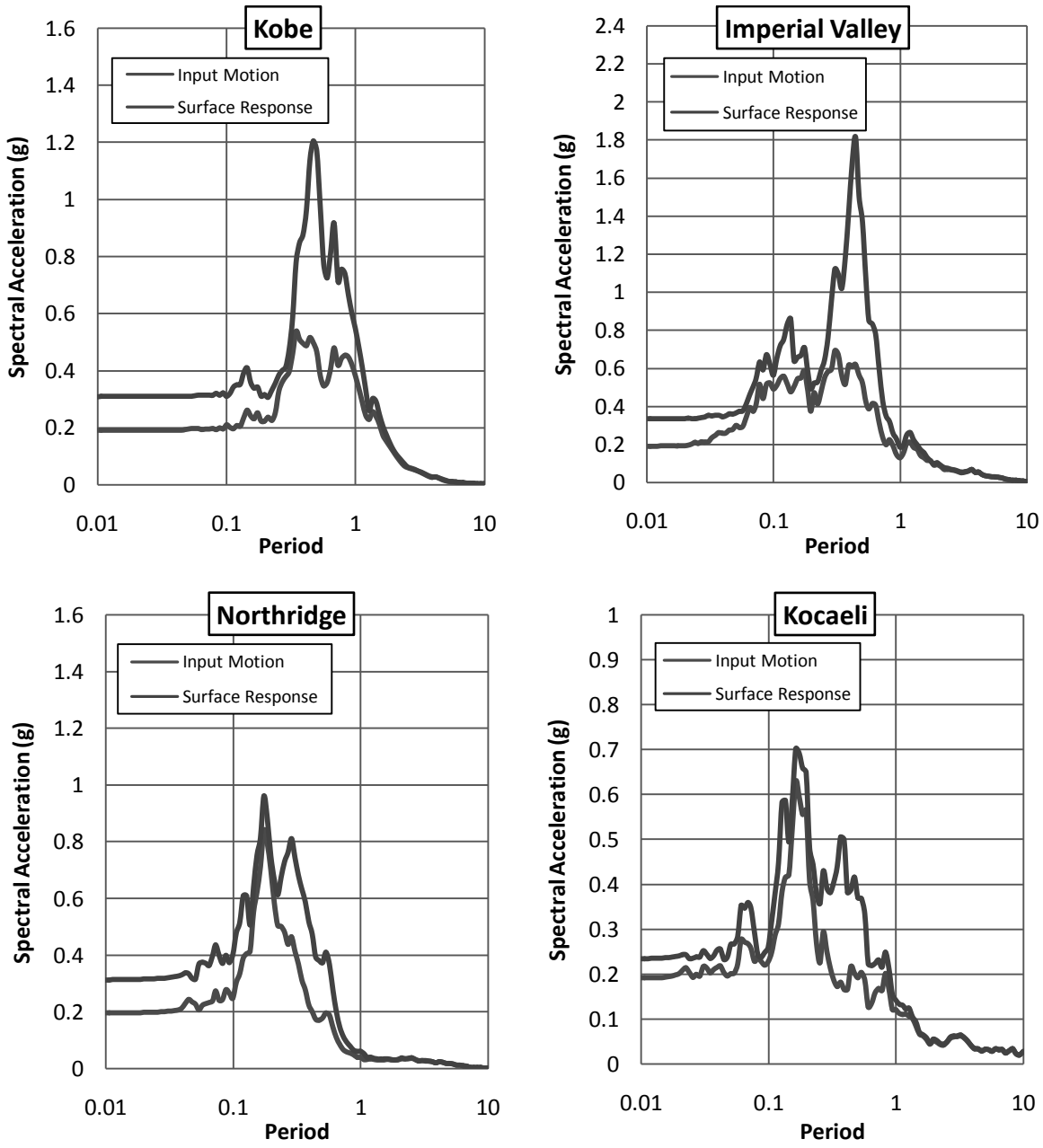


Figure 4.58 Response spectra for the Site-14, Akash Nagar, Mohammadpur, Beribadh

**Maximum Peak Ground Acceleration (PGA)**

Maximum Peak Ground Acceleration (PGA) at different depths of four earthquakes for this site is shown in Figure 4.59. PGA at surface and that at bedrock was obtained from the analysis. The peak ground acceleration values at surface were observed to be in the range of 0.23g (Kocaeli) to 0. 33g (Imperial Valley) and that of the bedrock were observed to vary from 0.14g (Kocaeli) to 0.21g (Kobe).

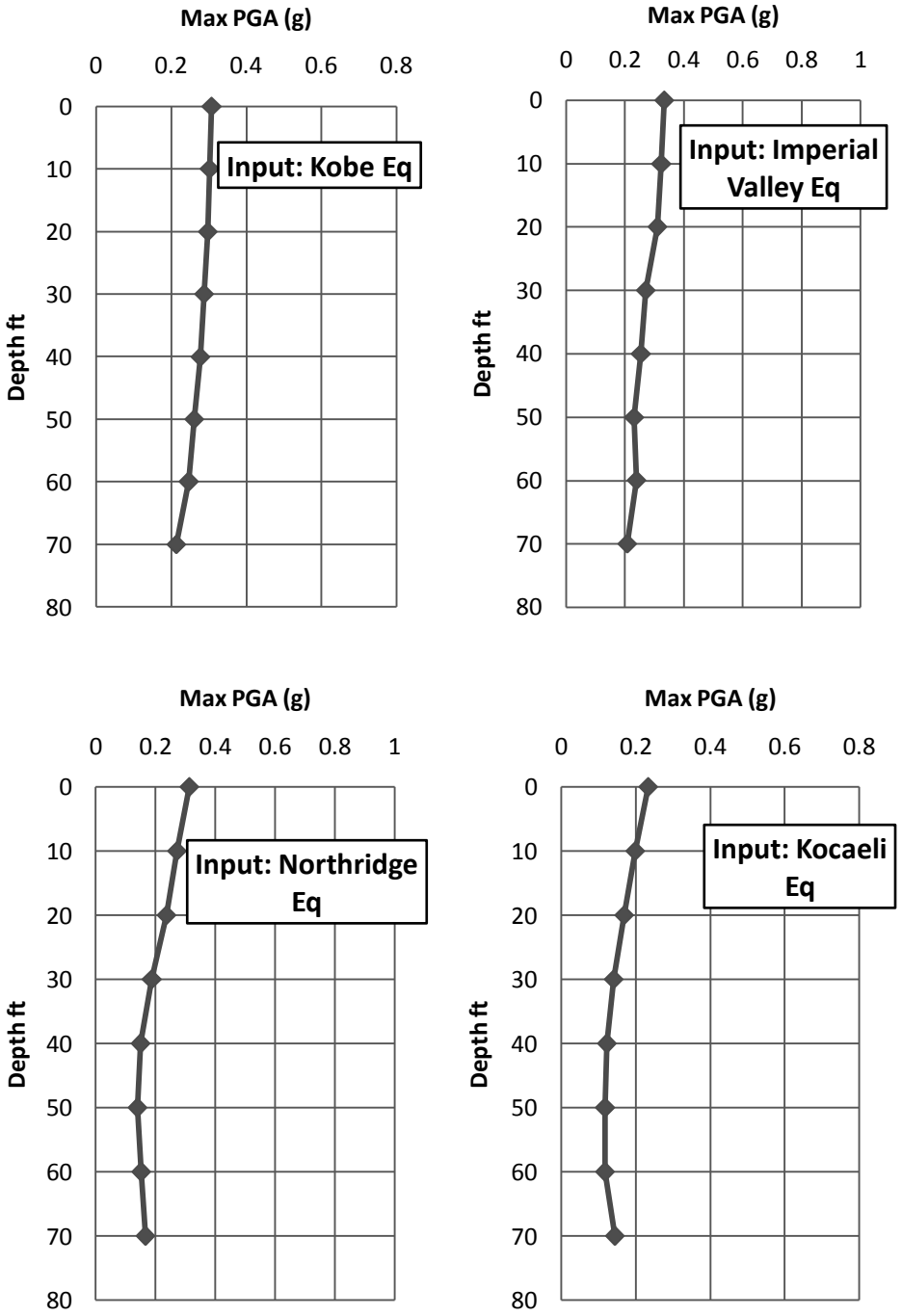


Figure 4.59 Maximum peak ground acceleration for the Site-14, Akash Nagar, Mohammadpur, Beribadh

**Site amplification factors:**

Amplification Factor (Kobe earthquake) = 1.44

Amplification Factor (Imperial Valley earthquake) = 1.61

Amplification Factor (Northridge earthquake) = 1.88

Amplification Factor (Kocaile earthquake) = 1.63

It was identified that similar to the peak ground acceleration values, the variation of amplification factor was within 1.44 (Kobe earthquake) to 1.88 (Northridge).

The Comparison of PSA is given in Figure 4.60 and the comparison of mean and standard deviation for surface PSA is given in Figure 4.61.

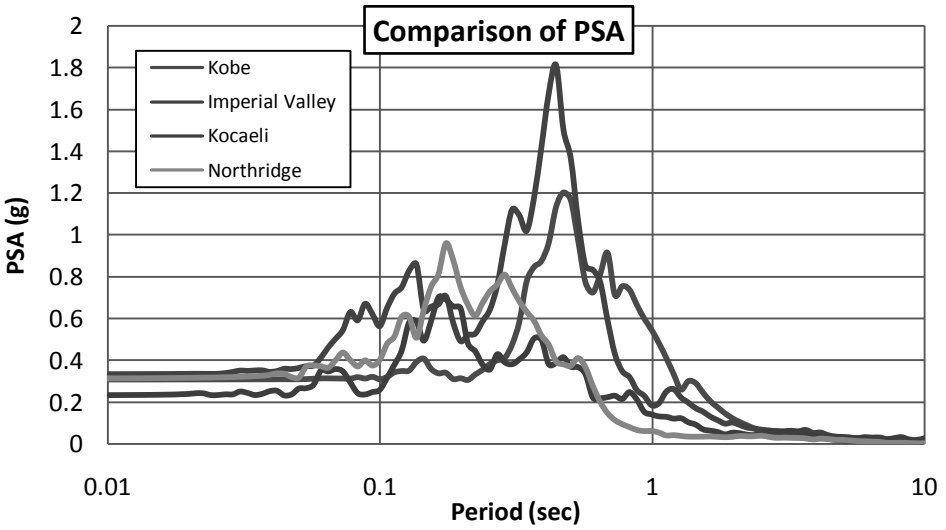


Figure 4.60 Comparison of PSA for different input motion for the Site-14 Akash Nagar, Mohammadpur, Beribadh

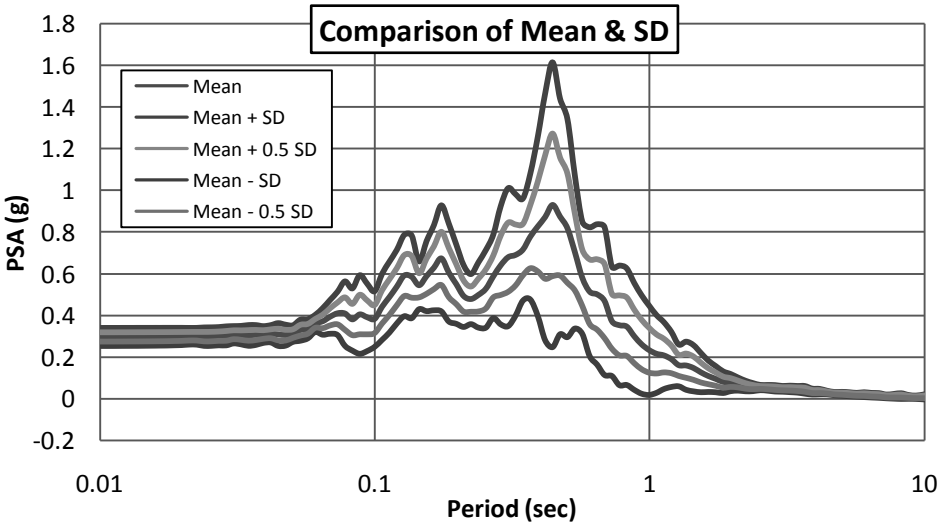


Figure 4.61 Comparison of mean and standard deviation for surface PSA for the Site-14, Akash Nagar, Mohammadpur, Beribadh

### 4.2.15. Ground Response Analysis of Site-15

**Response Spectra**

Response spectra of four earthquakes are shown in Figure 4.62. Among the four earthquakes, Imperial Valley earthquake produces highest (0.53g) peak spectral acceleration (PSA) for this site and Northridge earthquake produces lowest (0.002g) peak spectral acceleration (PSA). It was observed that initially soil surface response is less than input response for this site.

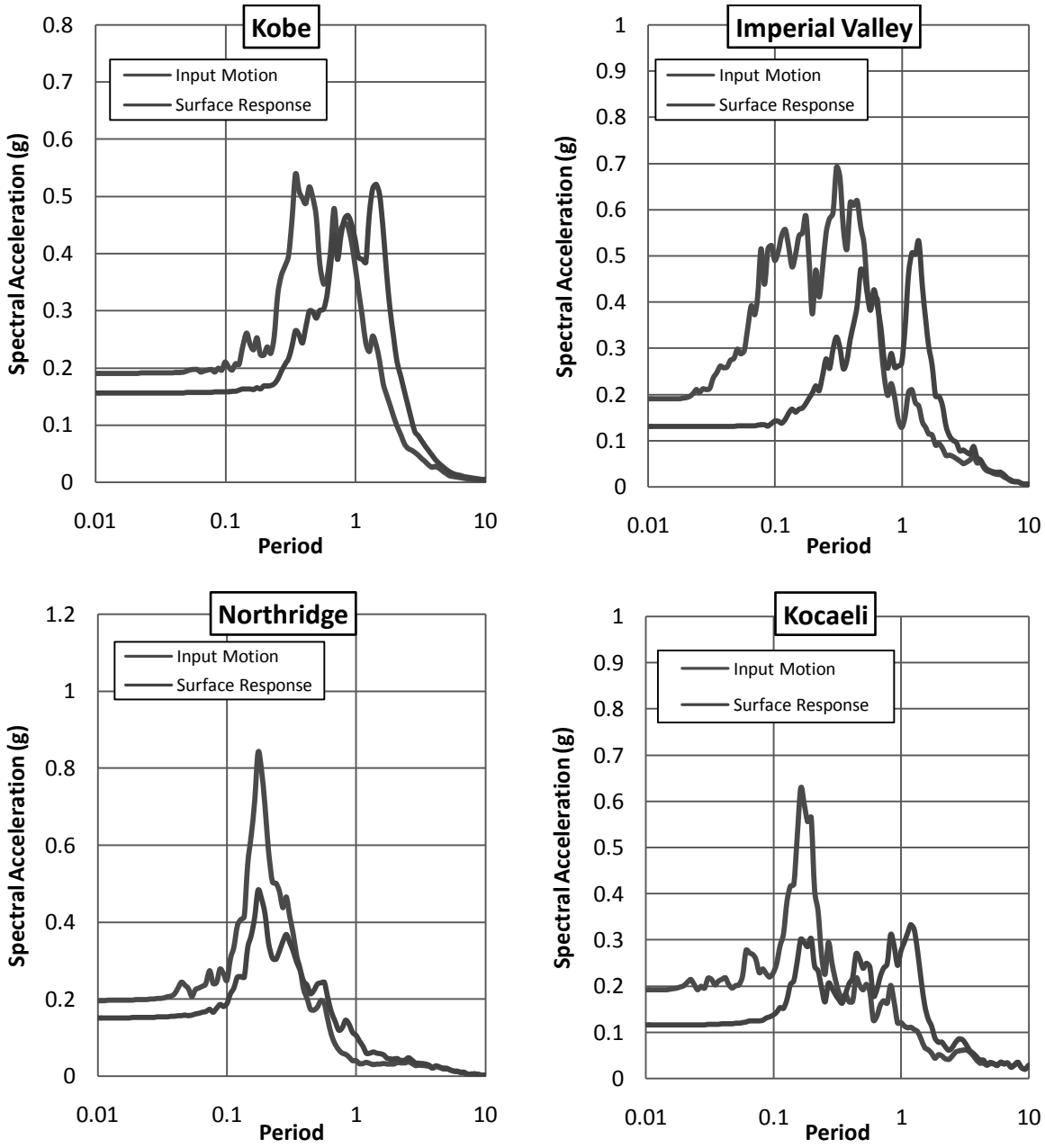


Figure 4.62 Response spectra for the Site-15, United City Project, Beraidh

**Maximum Peak Ground Acceleration (PGA)**

Maximum Peak Ground Acceleration (PGA) at different depths of four earthquakes for this site is shown in Figure 4.63. PGA at surface and that at bedrock was obtained from the analysis. The peak ground acceleration values at surface were observed to be in the range of 0.12g (Kocaeli) to 0. 16g (Kobe) and that of the bedrock were observed to vary from 0.19g (Kobe) to 0.23g (Northridge).

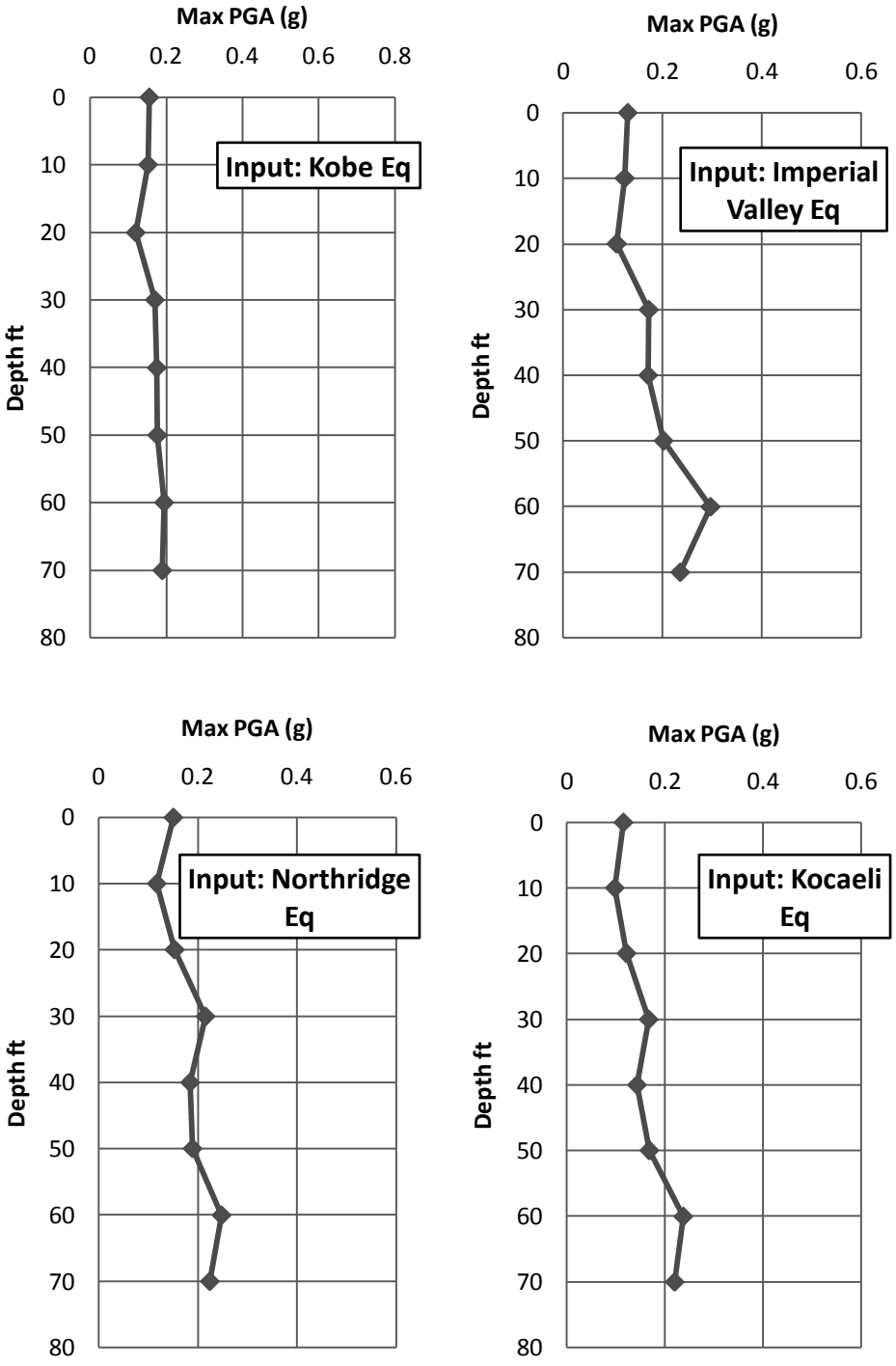


Figure 4.63 Maximum peak ground acceleration for the Site-15, United City Project, Beraidh

**Site amplification factors**

Amplification Factor (Kobe earthquake) = 0.82

Amplification Factor (Imperial Valley earthquake) = 0.55

Amplification Factor (Northridge earthquake) = 0.67

Amplification Factor (Kocaile earthquake) = 0.52

It was identified that similar to the peak ground acceleration values, the variation of amplification factor was within 0.55 (Imperial Valley) to 0.82 (Kobe).

The Comparison of PSA is given in Figure 4.64 and the comparison of mean and standard deviation for surface PSA is given in Figure 4.65.

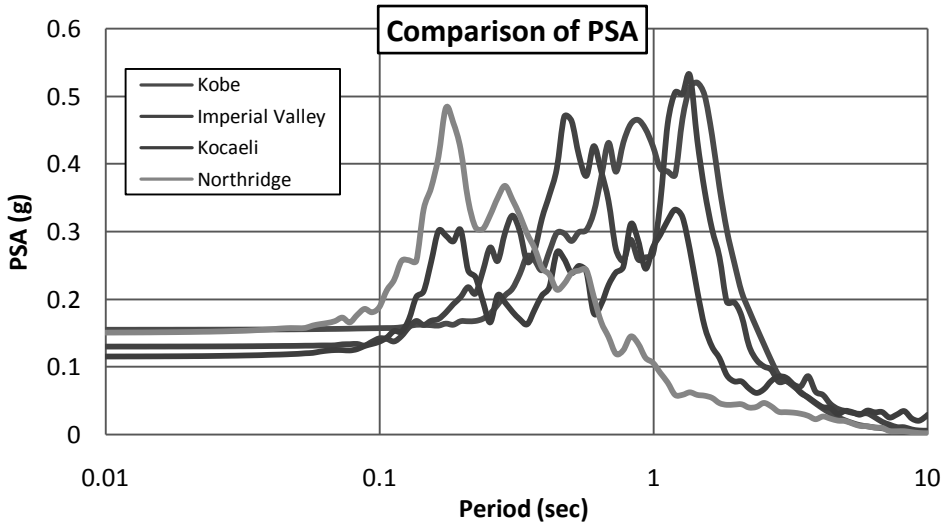


Figure 4.64 Comparison of PSA for different input motion for the Site-15, United City Project, Beraidh

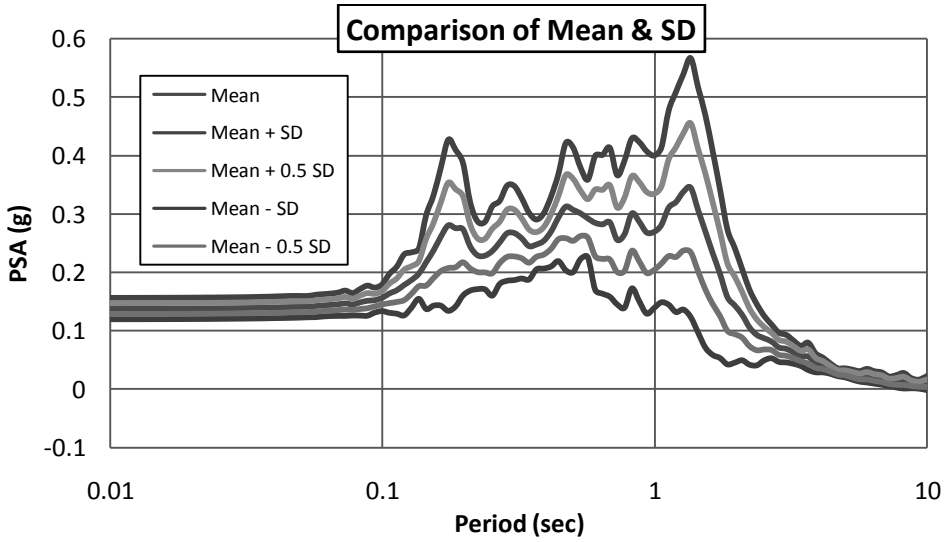


Figure 4.65 Comparison of mean and standard deviation for surface PSA for the Site-15, United City Project, Beraidh.

### 4.2.16. Ground Response Analysis of Site-16

**Response Spectra**

Response spectra of four earthquakes are shown in Figure 6.66. Among the four earthquakes, Imperial Valley earthquake produces highest (2.46g) peak spectral acceleration (PSA) for this site and Northridge earthquake produces lowest (0.002g) peak spectral acceleration (PSA). It was observed that initially soil surface response is much more than input response for this site.

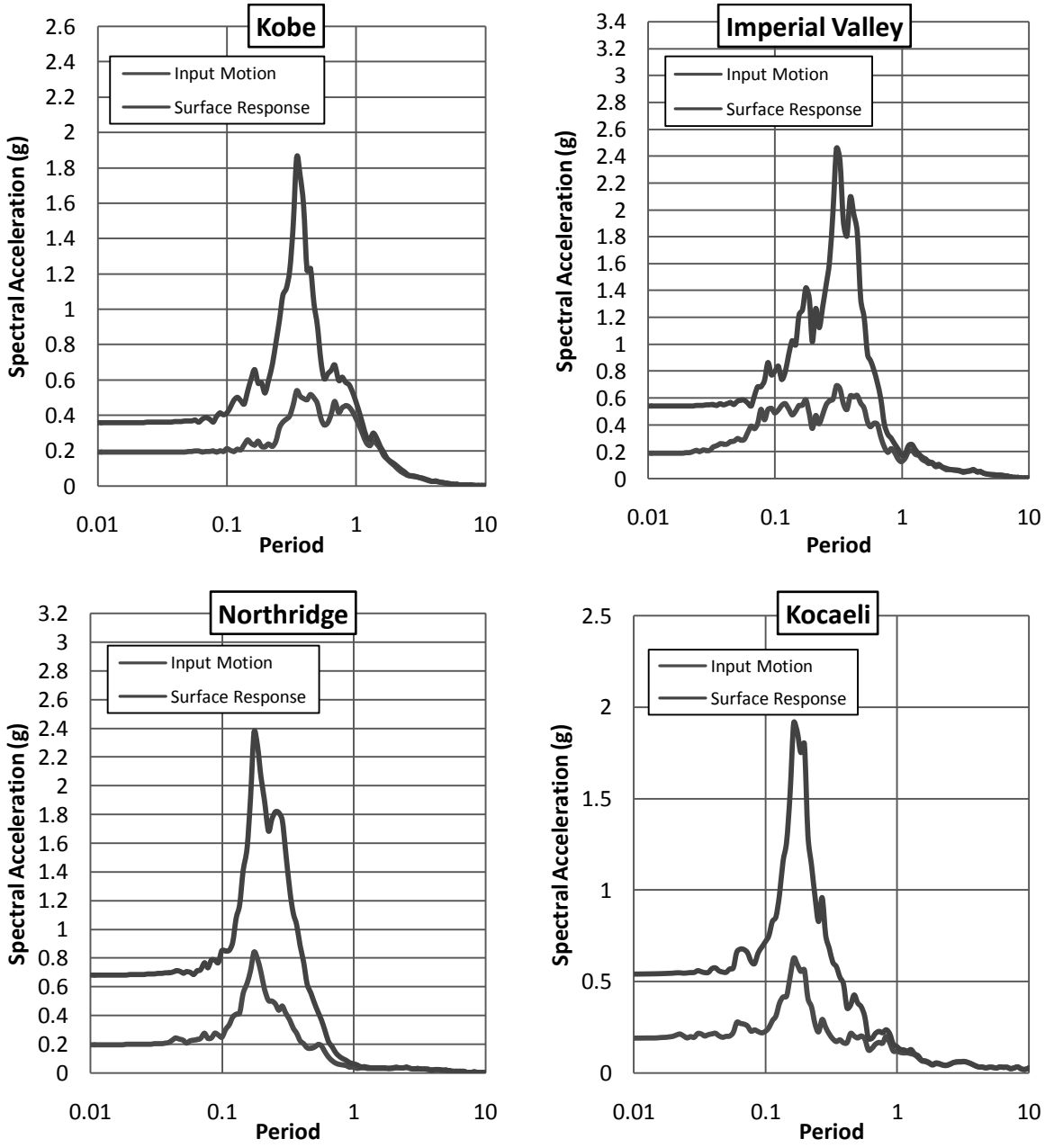


Figure 4.66 Response spectra for the Site-16, East Nandipara

**Maximum Peak Ground Acceleration (PGA)**

Maximum Peak Ground Acceleration (PGA) at different depths of four earthquakes for this site is shown in Figure 4.67. PGA at surface and that at bedrock was obtained from the analysis. The peak ground acceleration values at surface were observed to be in the range of 0.36g (Kobe) to 0. 66g (Northridge) and that of the bedrock were observed to vary from 0.14g (Northridge) to 0.21g (Imperial Valley).

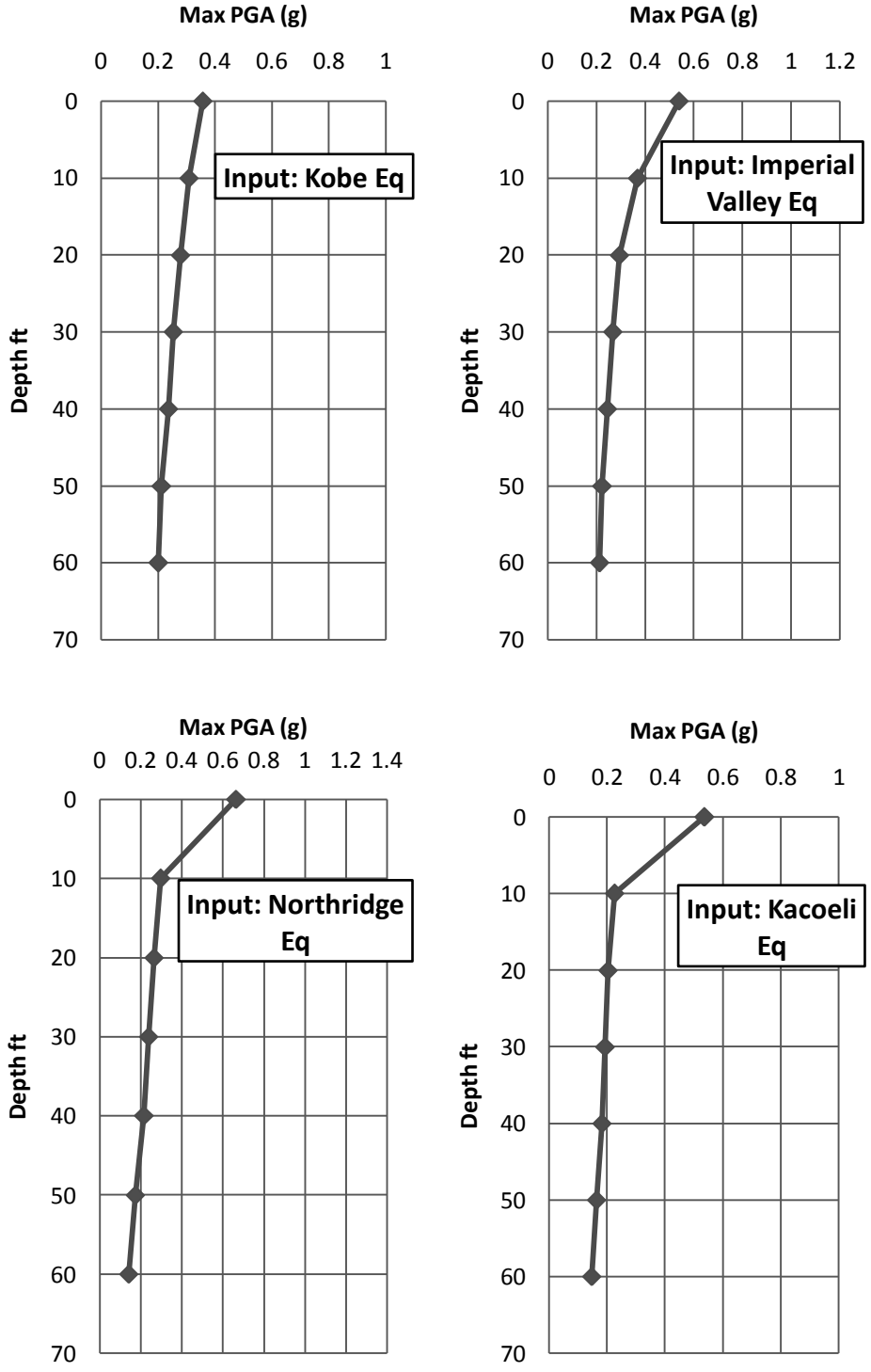


Figure 4.67 Maximum peak ground acceleration for the Site-16, East Nandipara

**Site amplification factors**

Amplification Factor (Kobe earthquake) = 1.77

Amplification Factor (Imperial Valley earthquake) = 2.53

Amplification Factor (Northridge earthquake) = 4.69

Amplification Factor (Kocaile earthquake) = 3.65

It was identified that similar to the peak ground acceleration values, the variation of amplification factor was within 1.77 (Kobe) to 4.69 (Northridge).

The Comparison of PSA is given in Figure 4.68 and the comparison of mean and standard deviation for surface PSA is given in Figure 4.69.

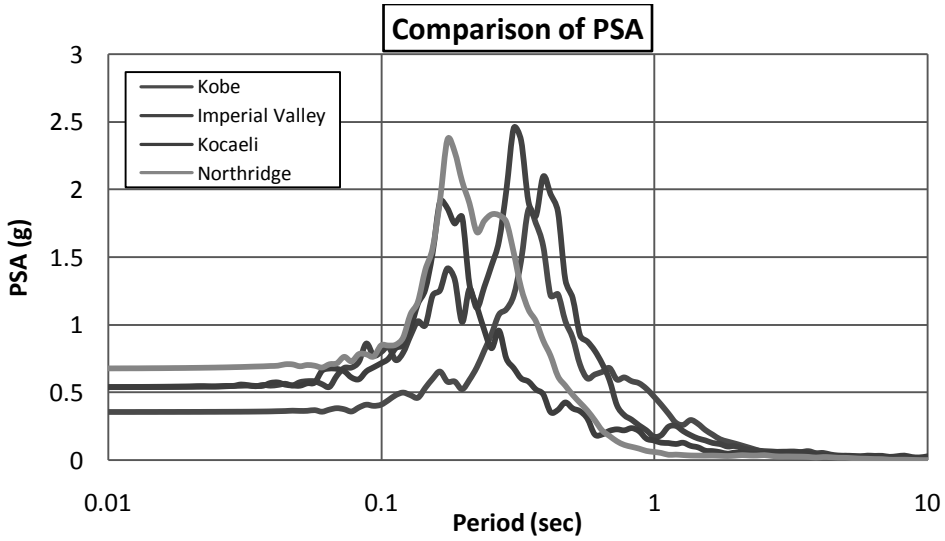


Figure 4.68 Comparison of PSA for different input motion for the Site-16, East Nandipara

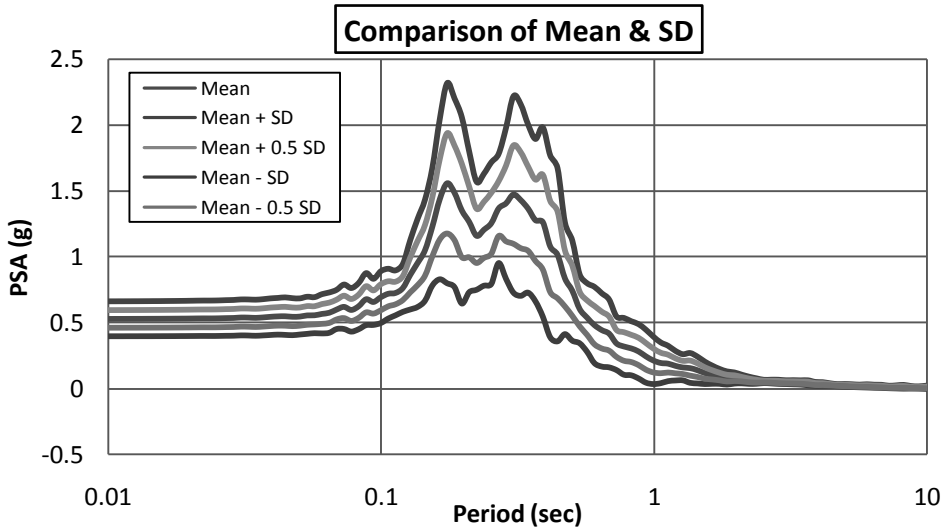


Figure 4.69 Comparison of mean and standard deviation for surface PSA for the Site-16, East Nandipara

### 4.2.17. Ground Response Analysis of Site-17

**Response Spectra**

Response spectra of four earthquakes are shown in Figure 4.70. Among the four earthquakes, Imperial Valley earthquake produces highest (0.77g) peak spectral acceleration (PSA) for this site and Northridge earthquake produces lowest (0.002g) peak spectral acceleration (PSA). It was observed that initially soil surface response was more than input response for some earthquakes for this site.

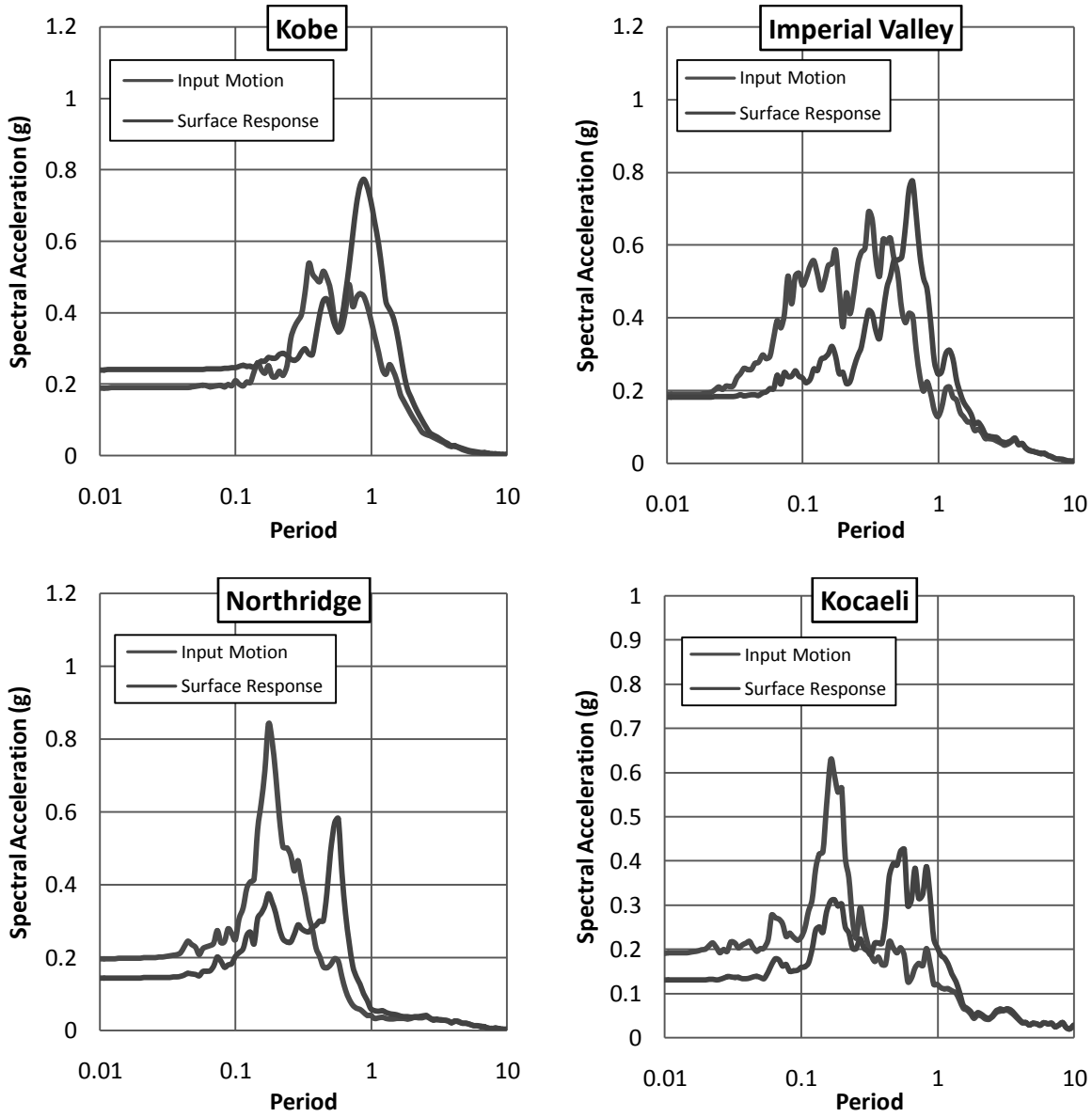


Figure 4.70 Response spectra for the Site-17, Asian City, Dokhinkhan

**Maximum Peak Ground Acceleration (PGA)**

Maximum Peak Ground Acceleration (PGA) at different depths of four earthquakes for this site is shown in Figure 4.71. PGA at surface and that at bedrock was obtained from the analysis. The peak ground acceleration values at surface were observed to be in the range of 0.13g (Kocaeli) to 0. 24g (Kobe) and that of the bedrock were observed to vary from 0.17g (Kobe) to 0.21g (Imperial Valley).

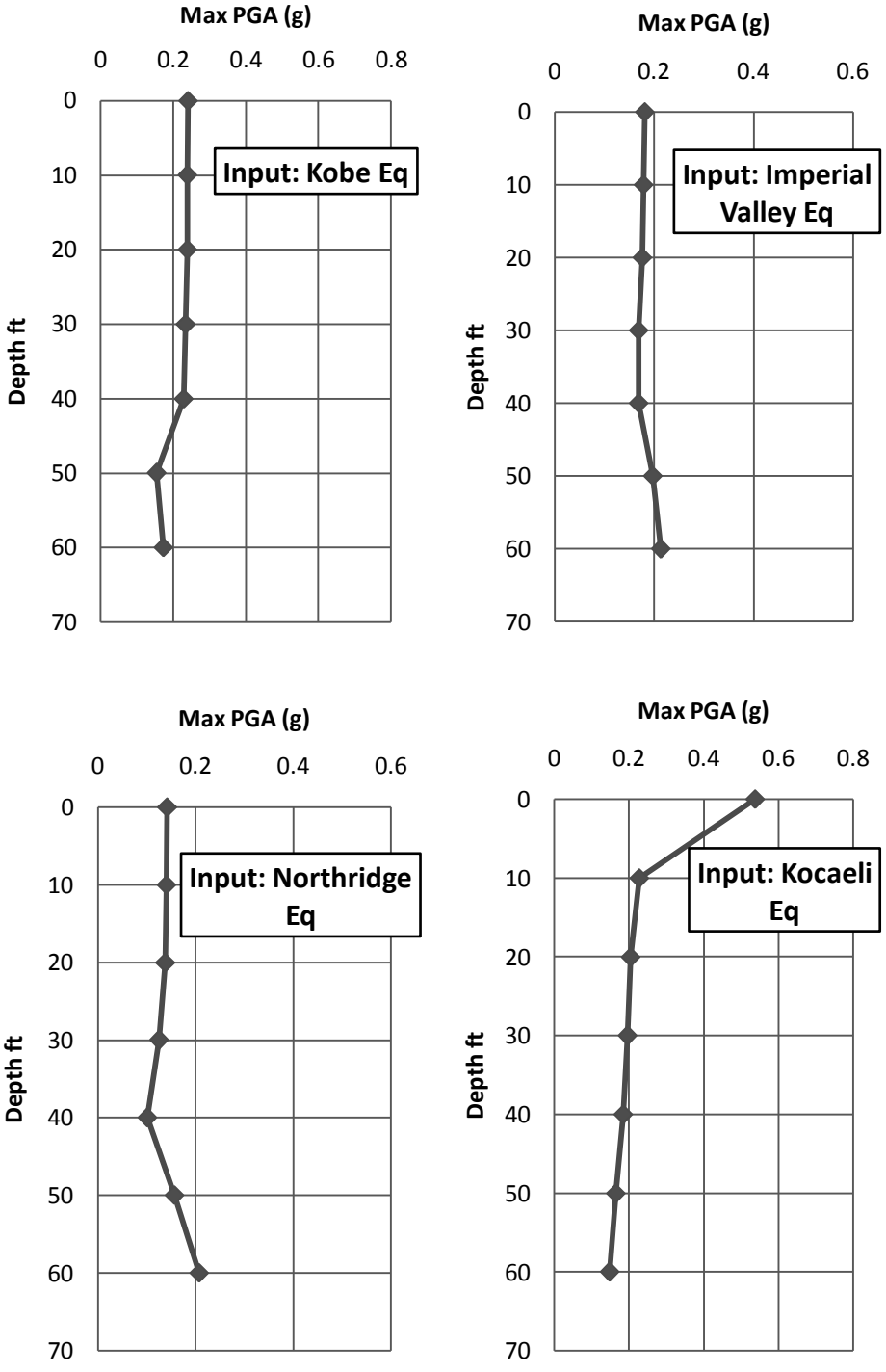


Figure 4.71 Maximum peak ground acceleration for the Site-17, Asian City, Dokhinkhan

**Site amplification factors:**

Amplification Factor (Kobe earthquake) = 1.39

Amplification Factor (Imperial Valley earthquake) = 0.85

Amplification Factor (Northridge earthquake) = 0.68

Amplification Factor (Kocaile earthquake) = 0.67

It was identified that similar to the peak ground acceleration values, the variation of amplification factor was within 0.67 (Kocaile) to 1.39 (Kobe).

The Comparison of PSA is given in Figure 4.72 and the comparison of mean and standard deviation for surface PSA is given in Figure 4.73.

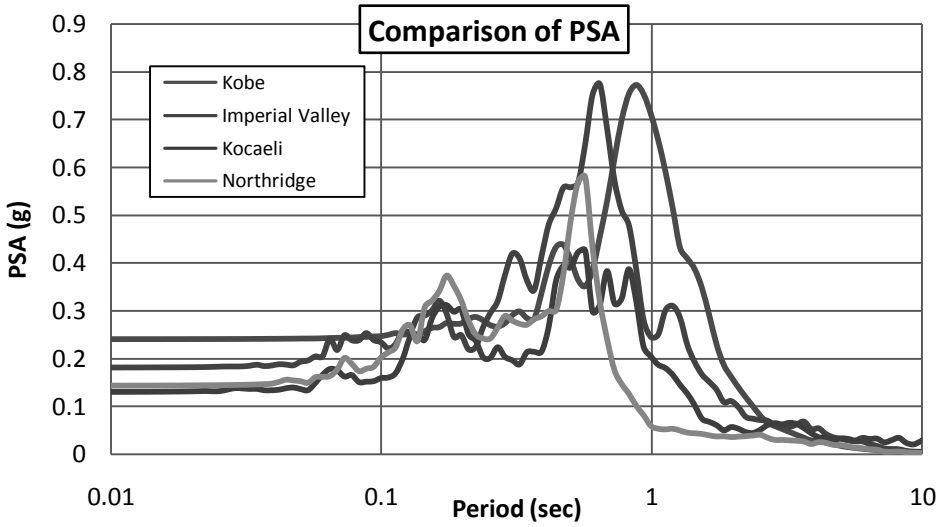


Figure 4.72 Comparison of PSA for different input motion for the Site-17, Asian City, Dokhinkhan

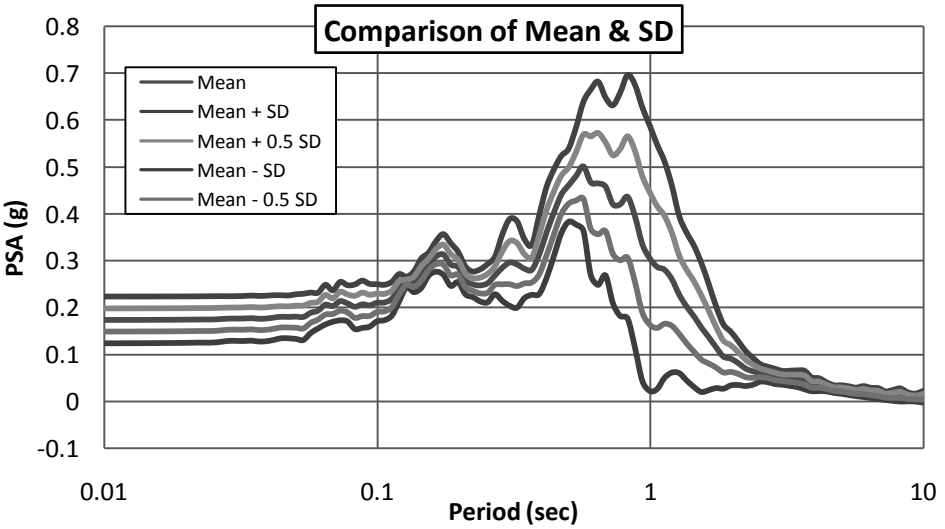


Figure 4.73 Comparison of mean and standard deviation for surface PSA for the Site-17, Asian City, Dokhinkhan

## 4.3 Result Summary

The highest and lowest values of Peak Spectral Acceleration at different locations, Maximum PGA of surface soil at different locations and Maximum PGA of Bedrock at different locations are shown in Table 4.1, Table 4.2 and Table 4.3. Table 4.4 shows the Site amplification factor at different locations.

Table 4.1 Peak Spectral Acceleration at different locations

| Sl. No. | Location | Maximum PGA | |
|---|---|---|---|
| | | Lowest | Highest |
| 1 | JIDPUS, BUET | 0.002g (Northridge) | 1.103g (Imperial Valley) |
| 2 | MIST, Mirpur | 0.002g (Kocaeli) | 1.47g (Northridge) |
| 3 | Hazaribag | 0.002g (Northridge) | 1.20g (Imperial Valley) |
| 4 | Gulshan 2 | 0.002g (Northridge) | 0.546g (Kobe) |
| 5 | Kamrangichor | 0.002g (Northridge) | 1.302g (Kobe) |
| 6 | Dakhin Kafrul | 0.002g (Northridge) | 1.00g (Kobe) |
| 7 | Maniknagar | 0.002g (Kocaeli) | 0.73g (Northridge) |
| 8 | Aftabnagar | 0.002g (Northridge) | 0.60g (Kobe) |
| 9 | Lake City Concord, Khilkhet | 0.002g (Northridge) | 1.14g (Imperial Valley) |
| 10 | RHD, Tejgaon | 0.002g (Northridge) | 1.90g (Imperial Valley) |
| 11 | Mehernagar Uttara | 0.003g (Northridge) | 1.14g (Kobe) |
| 12 | Ashulia, Jubok Project | 0.002g (Northridge) | 0.53g (Kobe) |
| 13 | Mirpur-1, Avenue-2 | 0.003g (Northridge) | 1.54g (Imperial Valley) |
| 14 | Akash Nagar, Mohammadpur, Beribadh | 0.002g (Northridge) | 1.81g (Imperial Valley) |
| 15 | United City Project, Beraidh | 0.002g (Northridge) | 0.53g (Imperial Valley) |
| 16 | East Nandipara | 0.002g (Northridge) | 2.46g (Imperial Valley) |
| 17 | Asian City, Dokhinkhan | 0.002g (Northridge) | 0.77g (Imperial Valley) |

Table 4.2 Maximum PGA of surface soil at different locations

| Sl. No. | Location | Maximum PGA | |
|---|---|---|---|
| | | Lowest | Highest |
| 1 | JIDPUS, BUET | 0.157g (Kocaeli) | 0. 281g (Kobe) |
| 2 | MIST, Mirpur | 0. 272g (Northridge) | 0.194g (Imperial Valley) |
| 3 | Hazaribag | 0.28g (Imperial Valley) | 0. 36g (Kobe) |
| 4 | Gulshan 2 | 0.97g (Kocaeli) | 0. 149g (Kobe) |
| 5 | Kamrangichor | 0.27g (Kocaeli) | 0. 32g (Northridge) |
| 6 | Dakhin Kafrul | 0.17g (Kocaeli) | 0. 23g (Northridge) |
| 7 | Maniknagar | 0.17g (Imperial Valley) | 0. 21g (Kobe) |
| 8 | Aftabnagar | 0.14g (Imperial Valley) | 0. 18g (Kobe) |
| 9 | Lake City Concord, Khilkhet | 0.24g (Northridge) | 0. 32g (Kobe) |
| 10 | RHD, Tejgaon | 0.29g (Kocaeli) | 0. 35g (Imperial Valley) |
| 11 | Mehernagar Uttara | 0.29g (Kocaeli) | 0. 36g (Kobe) |
| 12 | Ashulia, Jubok Project | 0.11g (Kocaeli) | 0. 17g (Kobe) |
| 13 | Mirpur-1, Avenue-2 | 0.32g (Kocaeli) | 0. 44g (Imperial Valley) |
| 14 | Akash Nagar, Mohammadpur, Beribadh | 0.23g (Kocaeli) | 0. 33g (Imperial Valley) |
| 15 | United City Project, Beraidh | 0.12g (Kocaeli) | 0. 16g (Kobe) |
| 16 | East Nandipara | 0.36g (Kobe) | 0. 66g (Northridge) |
| 17 | Asian City, Dokhinkhan | 0.13g (Kocaeli) | 0. 24g (Kobe) |

Table 4.3 Maximum PGA of Bedrock at different locations

| Sl. No. | Location | Maximum PGA | |
|---|---|---|---|
| | | Lowest | Highest |
| 1 | JIDPUS, BUET | 0.181g (Kobe) | 0.189 g (Northridge) |
| 2 | MIST, Mirpur | 0.179g (Kocaeli) | 0.196 g (Imperial Valley) |
| 3 | Hazaribag | 0.183g (Kobe) | 0.184 g (Northridge) |
| 4 | Gulsan 2 | 0.185g (Kobe) | 0.22 g (Northridge) |
| 5 | Kamrangichor | 0.182g (Kobe) | 0.190 g (Kocaeli) |
| 6 | Dakhin Kafrul | 0.179g (Kobe) | 0.20 g (Imperial Valley) |
| 7 | Maniknagar | 0.178g (Kocaeli) | 0.185 g (Northridge) |
| 8 | Aftabnagar | 0.17g (Kobe) | 0.19 g (Kocaeli) |
| 9 | Lake City Concord, Khilkhet | 0.09g (Kocaeli) | 0.153 g (Kobe) |
| 10 | RHD, Tejgaon | 0.182g (Imperial Valley) | 0.102g (Kobe) |
| 11 | Mehernagar Uttara | 0.17g (Kocaeli) | 0.18g (Kobe) |
| 12 | Ashulia, Jubok Project | 0.17g (Kocaeli) | 0.20g (Imperial Valley) |
| 13 | Mirpur-1, Avenue-2 | 0.14g (Imperial Valley) | 0.17g (Kobe) |
| 14 | Akash Nagar, Mohammadpur, Beribadh | 0.14g (Kocaeli) | 0.21g (Kobe) |
| 15 | United City Project, Beraidh | 0.19g (Kobe) | 0.23g (Northridge) |
| 16 | East Nandipara | 0.14g (Northridge) | 0.21g (Imperial Valley) |
| 17 | Asian City, Dokhinkhan | 0.17g (Kobe) | 0.21g (Imperial Valley). |

Table 4.4 Site amplification factor at different locations

| Sl. No. | Location | Amplification Factors | | | |
|---|---|---|---|---|---|
| | | Kobe | Imperial valley | Northridge | Kocaeli |
| 1 | JIDPUS, BUET | 1.547 | 1.192 | 1.066 | 0.856 |
| 2 | MIST, Mirpur | 1.09 | 0.99 | 1.49 | 1.28 |
| 3 | Hazaribag | 1.96 | 1.56 | 1.80 | 1.64 |
| 4 | Gulshan 2 | 0.80 | 0.65 | 0.49 | 0.47 |
| 5 | Kamrangichor | 1.59 | 1.57 | 1.74 | 1.43 |
| 6 | Dakhin Kafrul | 1.178 | 0.93 | 1.23 | 0.95 |
| 7 | Maniknagar | 1.13 | 0.96 | 1.15 | 1.14 |
| 8 | Aftabnagar | 1.03 | 0.76 | 0.96 | 0.75 |
| 9 | Lake City Concord, Khilkhet | 2.16 | 2.29 | 2.07 | 2.52 |
| 10 | RHD, Tejgaon | 1.62 | 1.92 | 1.76 | 1.55 |
| 11 | Mehernagar Uttara | 1.99 | 2.01 | 1.76 | 1.68 |
| 12 | Ashulia, Jubok Project | 0.86 | 0.66 | 0.63 | 0.64 |
| 13 | Mirpur-1, Avenue-2 | 2.39 | 3.18 | 2.54 | 2.29 |
| 14 | Akash Nagar, Mohammadpur, Beribadh | 1.44 | 1.61 | 1.88 | 1.63 |
| 15 | United City Project, Beraidh | 0.82 | 0.55 | 0.67 | 0.52 |
| 16 | East Nandipara | 1.77 | 2.53 | 4.69 | 3.65 |
| 17 | Asian City, Dokhinkhan | 1.39 | 0.85 | 0.68 | 0.67 |

Amplification map of Dhaka was prepared for four input earthquake motion- Kobe earthquake, Imperial Valley earthquake, Northridge earthquake and Kacaeli earthquake.

Amplification map s of different earthquake input motions are shown below in Figure 4.74 (Kobe); Figure 4.75 (Imperial Valley); Figure 4.76 (Northridge) and Figure 4.77 (Kocaeli).

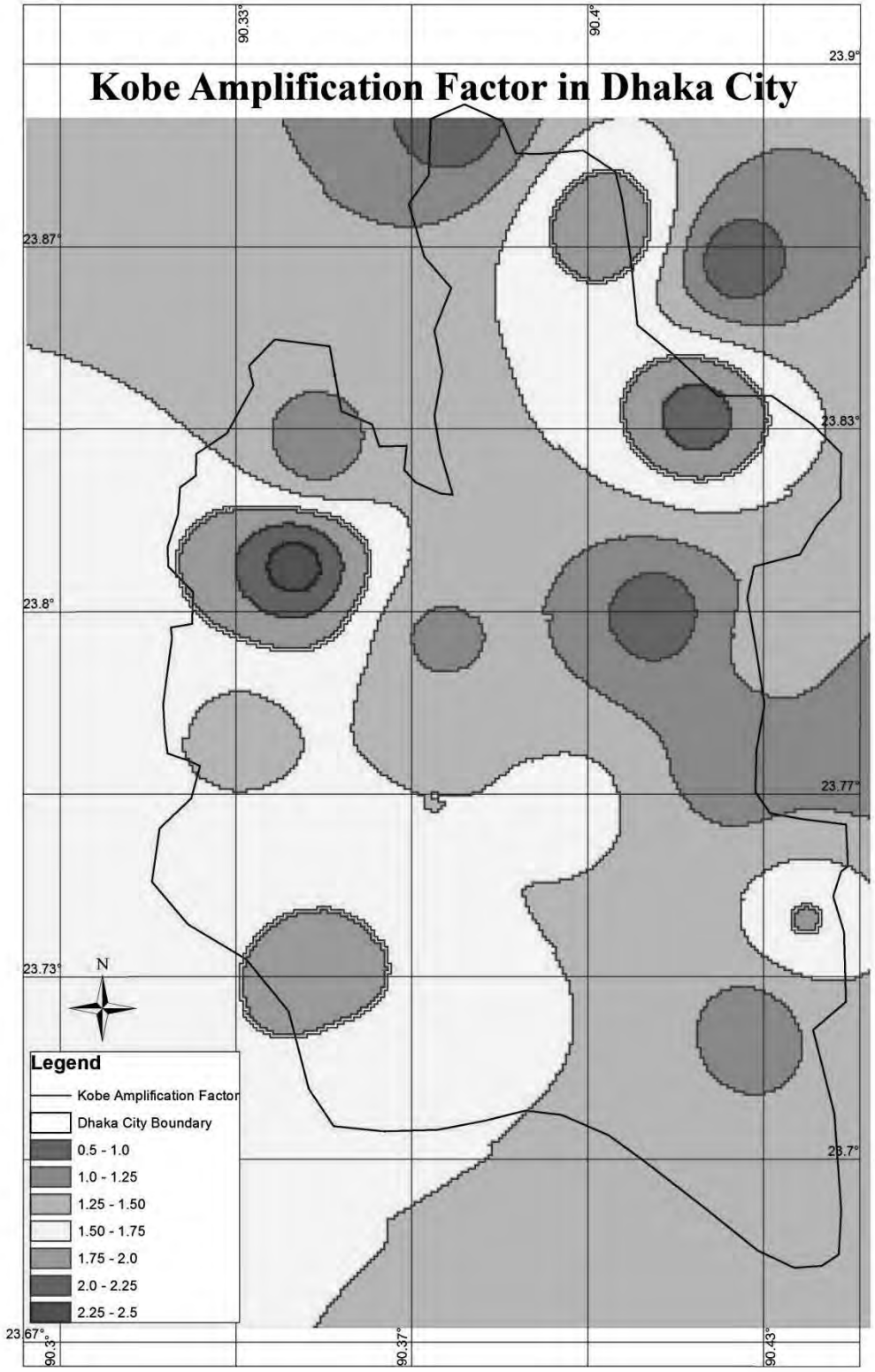


Figure 4.74 Amplification map for Kobe Earthquake

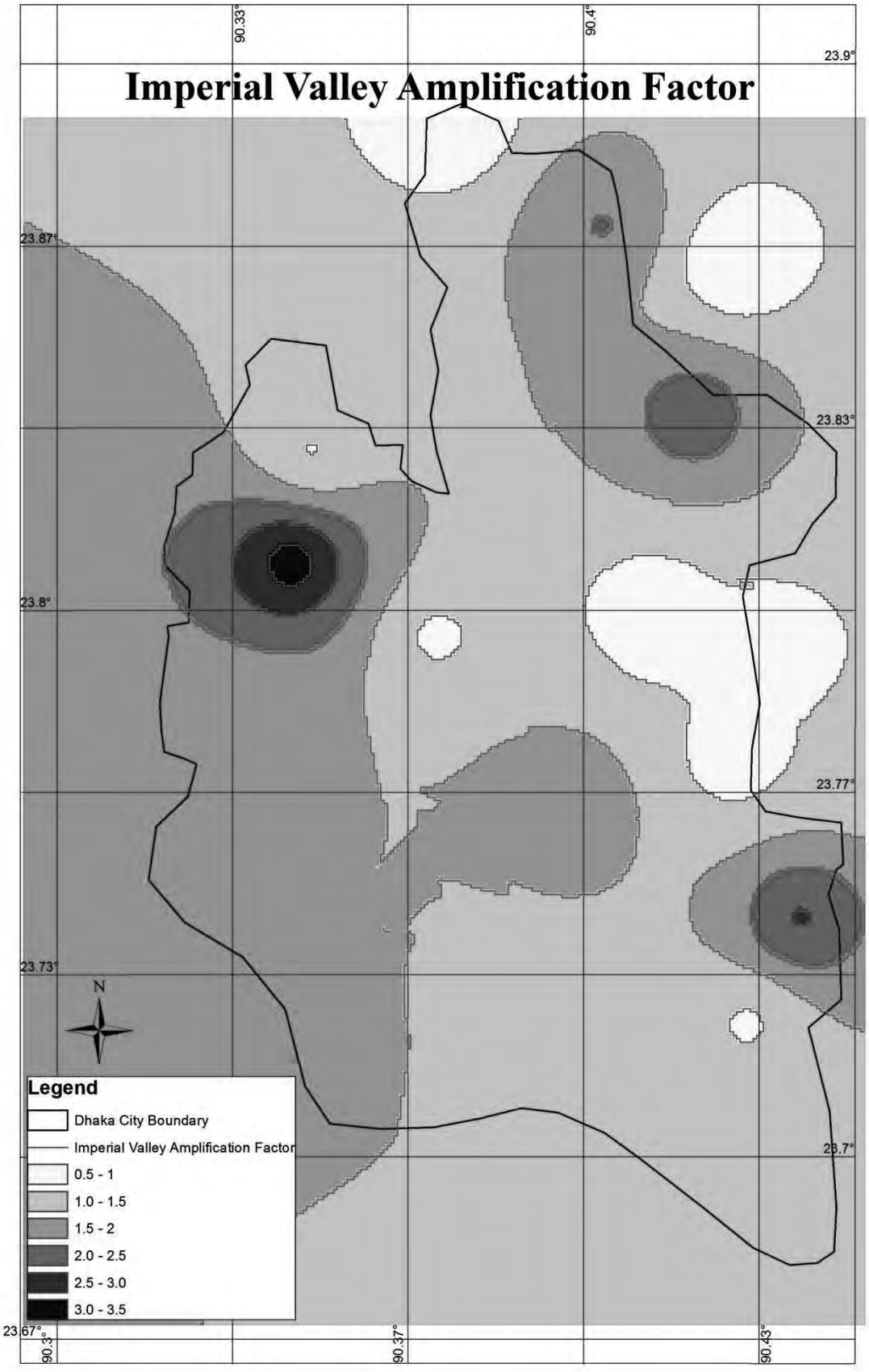


Figure 4.75 Amplification map for Imperial Valley Earthquake

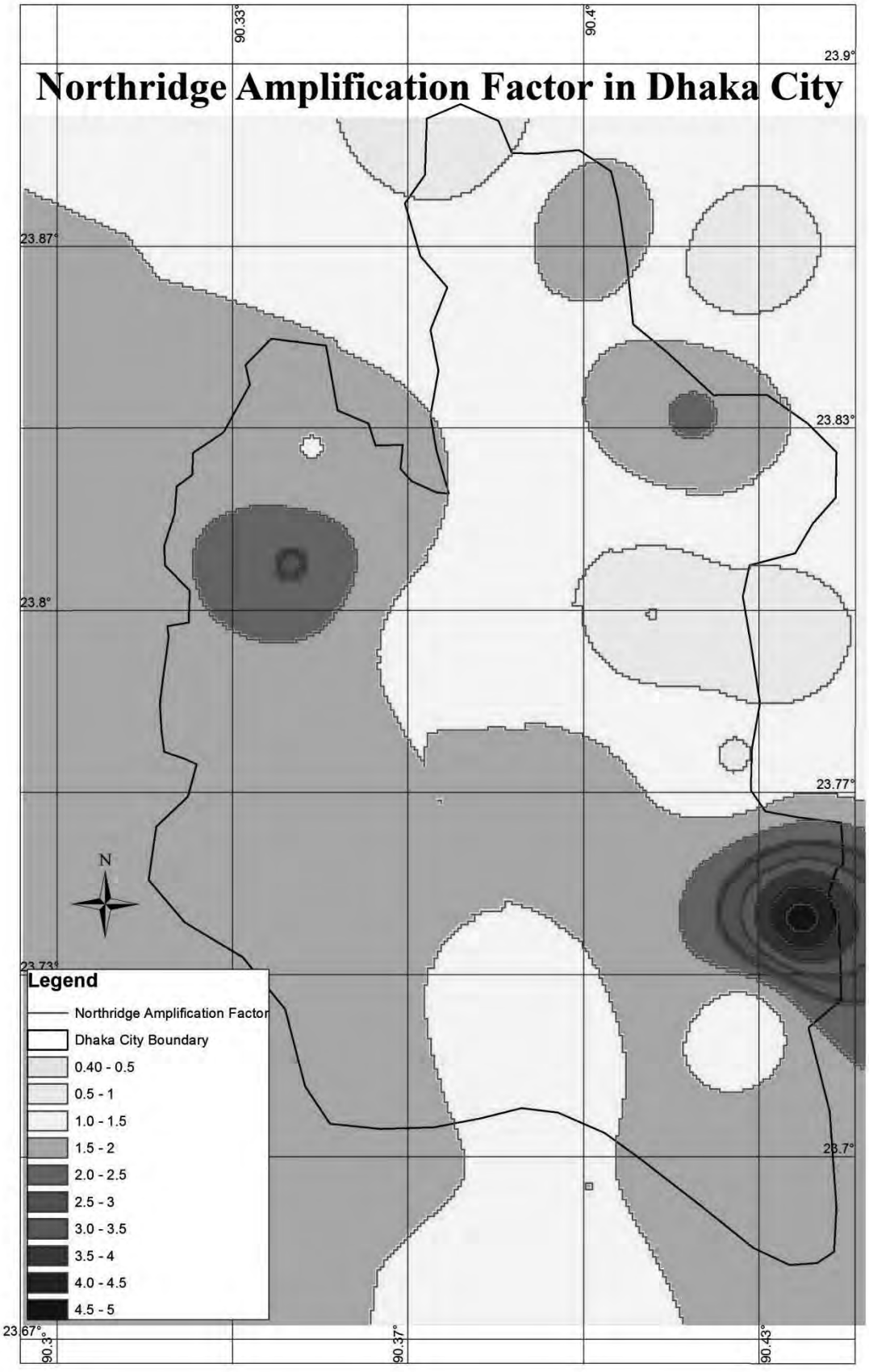


Figure 4.76 Amplification map for Northridge Earthquake.

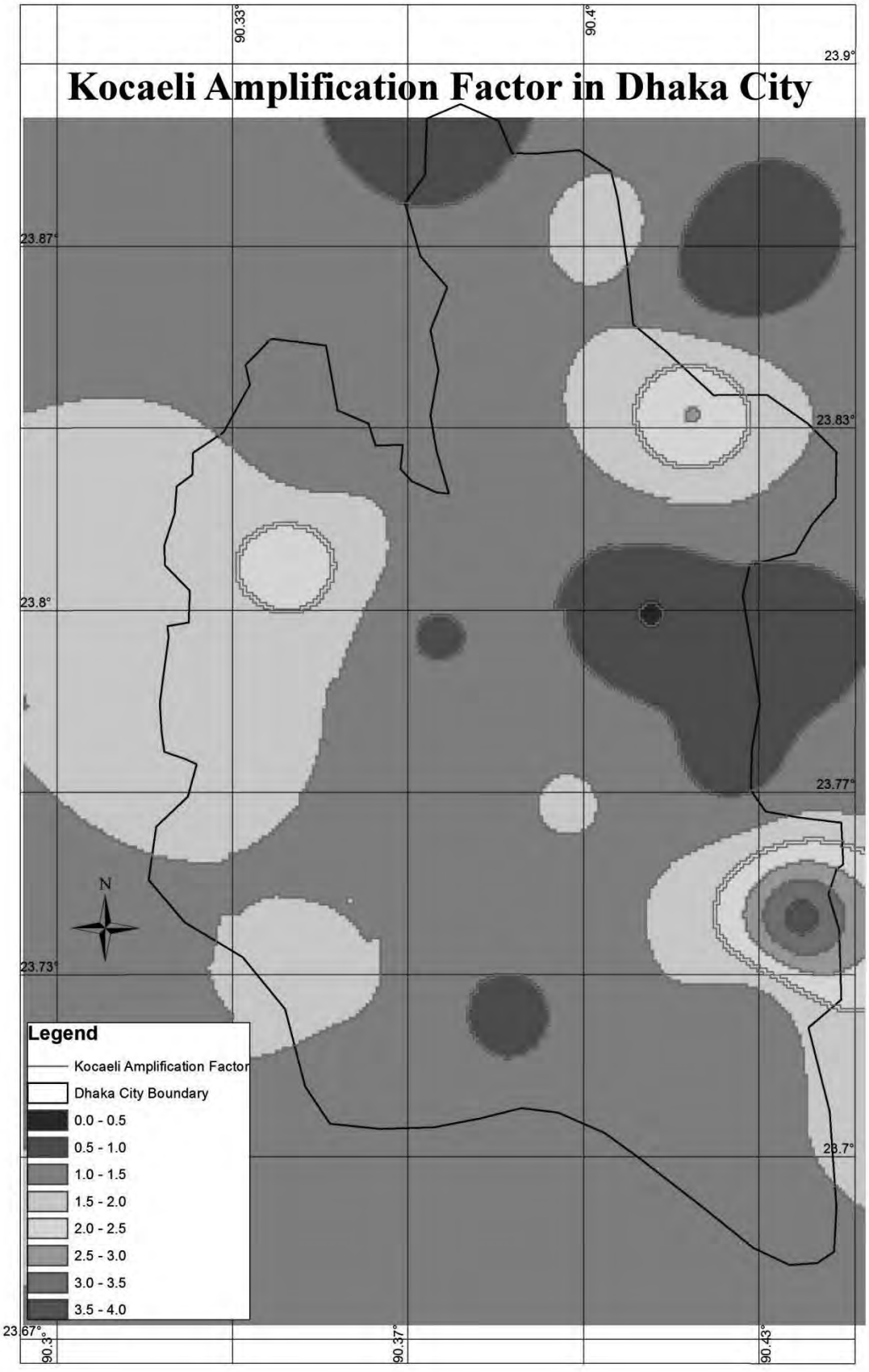


Figure 4.77 Amplification map for Kocaeli Earthquake.

## 4.4 Concluding Remarks

In the seismic hazard assessment of any area, ground response analysis is an important step. To evaluate and remediate geotechnical and structural hazards, response of a site to seismic shaking is required. Dhaka city has varied geological formations. Site specific ground response analysis has been carried out to evaluate the effects of alluvium and to estimate its dynamic effects. For site specific ground response analysis, three basic input parameters that are essential are input ground motion; shear wave velocity profile and dynamic soil characteristics (e.g., strain dependent modulus reduction and damping behavior and cyclic strength curves). One dimensional soil response evaluation tool DEEPSOIL (Hashash et al., 2011), was selected for the analysis. Equivalent linear analysis in frequency domain was the form of analysis selected to obtain ground response. Thickness (m), unit weight (kN/m3) and shear velocity (m/sec) were the inputs given. , The Imperial Valley earthquake, The Kobe Earthquake, The Kocaeli Earthquake, The Northridge earthquake were used as the input ground motion due to the absence of recorded data.

# CHAPTER FIVE
# CONCLUSIONS AND RECOMMENDATIONS

## 5.1 General

The main purpose of the present study was to use the Suspension PS Logging to estimate the seismic wave velocity of ten selected areas of Dhaka City and to estimate the ground response analysis of seventeen locations including those ten using the shear wave velocities. Soil models for those seventeen locations were developed based on field SPT values and shear-wave velocities Equivalent linear analysis was carried out using a computer program DEEPSOIL.

In the ground response analyses, the Imperial Valley earthquake on October 15, 1979; the Kobe Earthquake on January 17, 1995 (Mb-7.2); the Kocaeli Earthquake on August 17, 1999(Mb-7.4) and the Northridge earthquake of Los Angeles were selected as the input ground motion. Following section elaborate comment based on the above analysis. The scope of future research relevant to present study is also stated.

## 5.2 Conclusion

From the PS Logging tests and detailed site response analysis of the selected seventeen areas of the city, following conclusions can be summarized:

- The maximum shear wave velocity was 2488ft/s at site, RHD, Tejgaon and the minimum shear wave velocity was 136 ft/s at JIDPUS, BUET.
- Imperial Valley earthquake produced the highest (2.46g) peak spectral acceleration (PSA) for East Nandipara site and Northridge earthquake produced the lowest (0.002g) peak spectral acceleration (PSA) for most of the sites.
- The peak ground acceleration values at surface were observed to be in the range of 0.11g (Kocaeli) for the Ashulia Jubok Project site to as high as 0.66g (Northridge) for the East Nandipara site and that of the bedrock were observed to vary from 0.09g (Kocaeli) for Lake City Concord site to 0.23g (Northridge) for the United City Project site.

- The amplification factor of different locations were found in the range of 0.47 (Kocaeli) for the Gulsan-2 site to as high as 4.69 (Northridge) for the East Nandipara site.

A correlation was suggested using 189 set of data of depth, SPT N value and shear wave velocity. Considering $V_S$ as the dependent variable, following correlation was obtained:

$$\mathbf{Vs = 169\ N^{0.2638}\ D^{0.2396}}\ [r^2 = 0.45]$$

Where,

Vs =Shear Wave Velocity, ft/s

N = Standard Penetration Number, and

D = Depth, ft.

### 5.3 Recommendations for future Research

The testing program and empirical analysis conducted under the present study has led to many questions and subsequent future research interests. The areas of future research have been listed below followed by brief comments:

a) A study may be undertaken to prepare guidelines for mitigation of seismic hazards of reclaimed areas.
b) A study may be conducted to determine the suitable ground improvement techniques for such areas.
c) The correlation developed from the present study is done by using 189 sets of data. Using more data correlation can be refined.
d) Deep boreholes can be drilled and the depth of bedrock and its profile can be identified. This would also be useful to check the accuracy of the collected data.
e) The Imperial Valley earthquake, The Kobe Earthquake, The Kocaeli Earthquake, The Northridge earthquake were used as input motion for the calculation of PGA of Dhaka city due to unavailability of any recorded seismic data in the area. Artificial accelerogram could be generated for the soil conditions in the city and can be analyzed.
f) Ground response analysis may be performed in the reclaimed areas of Bangladesh based on Suspension PS Logging Test and other methods.

g) A study may be conducted to make a GIS Map of Bangladesh based on shear wave velocity.

h) PS Logging test may be conducted to develop a surface PGA map of Bangladesh based on shear wave velocity.

# REFERENCE


1. Ali, M.H and Choudhury, J.R (1992) –Tectonics and Earthquake Occurrence in Bangladesh", 36th Annual Convention, IEB, Dhaka.
2. Ansary, M. A; Noor, M. A. and Rashid, M. A. (2004) –Site amplification characteristics of Dhaka city", Journal of Civil Engineering (IEB), 32 (1) pp-5.
3. Molnar, S., Cassidy, J.F., Monahan, P. A. and Dosso1, S. E., –Comparison Of Geophysical Shear-Wave Velocity Methods" in Ninth Canadian Conference on Earthquake Engineering Ottawa, Ontario, Canada, 26-29 June, 2007, pp. 390-391.
4. Luna, R. and Jadi, H., –Determination Of Dynamic Soil Properties Using Geophysical Methods" presented at International Conference on the Application of Geophysical and NDT Methodologies to Transportation Facilities and Infrastructure, St. Louis, MO, December 2000.
5. Inazaki, T., –Relationship between S-Wave Velocities and Geotechnical Properties of Alluvial Sediments" in 19th EEGS Symposium on the Application of Geophysics to Engineering and Environmental Problems, Apr. 2006.
6. Perez-Santisteban, I., Garcia-Mayordomo, J., Martin, A. M., Carbo, A., (2011 ) –Comparison among SASW, ReMi and PS-Logging techniques: Application to a railway embankment" in journal of applied geophysics, Vol 1; pp. 59-64.
7. Chen, M.H., Wen, K. L., Loh, C. H. and Nigbor, R. L., –Experience of Suspension P-S Logging Method and Empirical Formula of Shear Wave Velocities in Taiwan" presented at - U.S.-Taiwan Workshop on Soil Liquefaction, Mar 2, 2012.
8. Biringen, E. and Davie, J., –Assessment of dynamic and static characteristics of igneous bedrock by means of suspension P-S logging and uniaxial compressive strength tests" in –2011 Pan-Am CGS Geotechnical Conference" October 2-6, 2011.
9. Asten, M. W. an Boore, D. M., –Comparison of Shear-Velocity Profiles of Unconsolidated Sediments near the Coyote Borehole (CCOC) Measured With Fourteen Invasive and Non-Invasive Methods", U.S. Geological Survey Open-File Report 2005-1169.
10. Perez-Santisteban, I., Garcia-Mayordomo, J., Martin, A. M., Carbo, A., –Comparison among SASW, ReMi and PS-Loggong techniques: Application to a railway embankment" in journal of applied geophysics, Vol 1; pp. 59-64, 2011.
11. Urban Geology of Dhaka, Bangladesh, Atlas Of Urban Geology, Volume 11.
12. Rashid, A. (2000), "Seismic Microzonation of Dhaka City based on site

amplification and liquefaction", M. Engg. Thesis, Department of Civil Engineering, BUET, Dhaka, Bangladesh.

**13.** Islam, M. R (2005). "Seismic Loss Estimation for Sylhet City, M. Sc. Engg. Thesis, Department of Civil Engineering, BUET, Dhaka, Bangladesh.

**14.** Masud, M. A. (2007), "Earthquake Risk Analysis for Chittagong", M. Engg. Thesis, Department of Civil Engineering, BUET, Dhaka, Bangladesh.

**15.** Rizvi M. S. (2014) –Site Amplification of the selected areas of Dhaka City Based on Shear Wave Velocity", M. Sc. Engg. Thesis, Department of Civil Engineering, BUET, Dhaka, Bangladesh.

**16.** Rahman Md. Saidur (2011) –Applicability of H/V Microtremor Technique for site Response Analysis in Dhaka City", M. Sc. Engg. Thesis, Department of Civil Engineering, BUET, Dhaka, Bangladesh.

**17.** http://www.floyd.k12.va.us/itrt/pwrpnts/geography/Earthquakes.ppt.

**18.** U.S Geological Survey, National Seismic Hazard Maps (2012).

**19.** E. E. Schmitz, Mayor, –Eatrhquakes", (1906).

**20.** Luna, R. and H. Jadi, (2000) "Determination of Dynamic Soil Properties Using Geophysical Methods," Proceedings of the First International Conference on the Application of Geophysical and NDT Methodologies to Transportation Facilities and Infrastructure, St. Louis, MO.

**21.** Emad Y. Sharif; Anis A. Al Bis; Mahmoud K. Harb, –An Application of Geophysical Techniques For Determining Dynamic Properties of The Ground In Dubailand Area, Uae", Arab Center For Engineering Studies (ACES-Dubai).

**22.** –Engineering Geological Mapping of Dhaka, Chittagong and Sylhet City Corporation Area of Bangladesh", (June, 2009), Comprehensive Disaster Management Program (CDMP), Ministry of Disaster Management and Relief.

**23.** Bangladesh National Building Code (BNBC), 1993.

**24.** Manne, A. (2013). "Site Characterization and Ground Response Analysis for Vijayawada urban", MSc. Engg. Thesis, Earthquake Engineering Research Centre, International Institute of Information Technology Hyderabad, India.

**25.** Afkhami A.; –Reliability and Applicability of SPT Correlations with Shear Wave Velocity"; Novo Tech Software Ltd., Vancouver, Canada.

**26.** Maheswari U., Boominathan and Dodagoudar; –Development of Empirical Correlation between Shear Wave Velocity and Standard Penetration Resistance In

Soils Of Chennai City."; The 14th World Conference on Earthquake Engineering; October 12-17, 2008, Beijing, China.

**27.** Marto A., Soon T. C., Kasim F., Suhatril M.; "A Correlation of Shear Wave Velocity and Standard Penetration Resistance"; EJGE, Vol. 18 [2013], Bund. C; P-463-471.

**28.** Shooshpashaa , H. Mola-Abasia, A. Jamalianb, Ü. Dikmenc, M. Salahib; "Validation and application of empirical Shear wave velocity models based on standard penetration test"; Computational Methods in Civil Engineering, Vol.4 No.1 (2013) 25-41.

**29.** Hashash, Y.M.A, Groholski, D.R., Phillips, C. A., Park, D and Musgrove, M. (2011) DEEPSOIL 4.0, User Manual and Tutorial. 98 p.

**30.** System Reference Manual 2007, Crosshole And Downhole Seismic Test, Freedom Data PC with WINGEO Software Version 2.1, Olson Instruments

**31.** T. Yajai, Nondestructive Evaluation for Geophysical Engineering, Nondestructive Evaluation (NDE) Users Seminar, Olson Engineering, Inc.

**32.** Kramer, S.L. (1996), Geotechnical Earthquake Engineering, Upper Saddle River, New Jersey, USA.

**33.** Cramer, C. H., and Real, C. R. (1992). A statistical analysis of submitted site-effects predictions for the weak-motion blind prediction test conducted at the Turkey Flat, USA, site effects test area near Parkfield, California. InProceedings of the International Symposium on the Effects of Surface Geology on Seismic Motion, March, 1992, Odawara, Japan.Vol. 2, 15-20).

**34.** Marto A, Soon T. C., Kasim F., "A Correlation of Shear Wave Velocity and Standard Penetration Resistance", Vol. 18 [2013], Bund. C, EJGE.

# Appendix A

## Shear Wave velocities at different Locations

**Table A-1: Site-1-BUET JIDPUS:**

| Depth ft | Geophone-1 | | | Geophone-2 | | | S wave Velocity ft/s |
|---|---|---|---|---|---|---|---|
| | Arrival time μs | Arrival time sec | Distance ft | Arrival time μs | Arrival time sec | Distance ft | |
| 6 | 32880 | 0.03288 | 15.86 | 40740 | 0.04074 | 16.93 | 136 |
| 11 | 39560 | 0.03956 | 16.93 | 44980 | 0.04498 | 19.28 | 433 |
| 16 | 39340 | 0.03934 | 19.28 | 43604 | 0.043604 | 22.51 | 758 |
| 21 | 45760 | 0.04576 | 22.51 | 48640 | 0.04864 | 26.30 | 1316 |
| 26 | 48200 | 0.0482 | 26.30 | 62220 | 0.06222 | 30.44 | 295 |
| 31 | 54440 | 0.05444 | 30.44 | 57740 | 0.05774 | 34.81 | 1324 |
| 36 | 59840 | 0.05984 | 34.81 | 64180 | 0.06418 | 39.33 | 1041 |
| 41 | 66340 | 0.06634 | 39.33 | 69280 | 0.06928 | 43.95 | 1572 |
| 46 | 69300 | 0.0693 | 43.95 | 76460 | 0.07646 | 48.65 | 656 |
| 51 | 75920 | 0.07592 | 48.65 | 79400 | 0.0794 | 53.40 | 1366 |
| 56 | 80100 | 0.0801 | 53.40 | 85940 | 0.08594 | 58.20 | 821 |
| 61 | 81540 | 0.08154 | 58.20 | 90600 | 0.0906 | 63.02 | 533 |
| 66 | 102720 | 0.10272 | 63.02 | 109620 | 0.10962 | 67.87 | 703 |
| 71 | 94580 | 0.09458 | 67.87 | 101240 | 0.10124 | 72.74 | 731 |
| 76 | 95300 | 0.0953 | 72.74 | 99100 | 0.0991 | 77.63 | 1286 |
| 81 | 101120 | 0.10112 | 77.63 | 104780 | 0.10478 | 82.53 | 1339 |

**Table A-2: Site-2-MIST:**

| Depth ft | Geophone-1 | | | Geophone-2 | | | S wave Velocity ft/s |
|---|---|---|---|---|---|---|---|
| | Arrival time μs | Arrival time sec | Distance ft | Arrival time μs | Arrival time sec | Distance ft | |
| 8.66 | 19020 | 0.01902 | 7.60468 | 24940 | 0.02494 | 10.92846 | 561 |
| 13.66 | 26240 | 0.02624 | 10.92846 | 35140 | 0.03514 | 15.19971 | 480 |
| 18.66 | 29780 | 0.02978 | 15.19971 | 35540 | 0.03554 | 19.81492 | 801 |
| 23.66 | 36500 | 0.0365 | 19.81492 | 43100 | 0.0431 | 24.58111 | 722 |
| 28.66 | 43980 | 0.04398 | 24.58111 | 49760 | 0.04976 | 29.42501 | 838 |
| 33.66 | 48600 | 0.0486 | 29.42501 | 52820 | 0.05282 | 34.31372 | 1158 |
| 38.66 | 59820 | 0.05982 | 34.31372 | 71800 | 0.0718 | 39.23049 | 410 |
| 43.66 | 67780 | 0.06778 | 39.23049 | 74540 | 0.07454 | 44.16595 | 730 |
| 48.66 | 72140 | 0.07214 | 44.16595 | 83200 | 0.0832 | 49.11447 | 447 |
| 53.66 | 77600 | 0.0776 | 49.11447 | 82320 | 0.08232 | 54.07246 | 1050 |
| 58.66 | 88800 | 0.0888 | 54.07246 | 93500 | 0.0935 | 59.03754 | 1056 |
| 63.66 | 95460 | 0.09546 | 59.03754 | 99360 | 0.09936 | 64.00806 | 1274 |
| 68.66 | 101360 | 0.10136 | 64.00806 | 107280 | 0.10728 | 68.98283 | 840 |
| 73.66 | 100100 | 0.1001 | 68.98283 | 104540 | 0.10454 | 73.96101 | 1121 |
| 78.66 | 111760 | 0.11176 | 73.96101 | 115560 | 0.11556 | 78.94195 | 1311 |

**Table A-3: Site-3-Hazaribag:**

| Depth ft | Geophone-1 | | | Geophone-2 | | | S wave Velocity ft/s |
|---|---|---|---|---|---|---|---|
| | Arrival time μs | Arrival time sec | Distance ft | Arrival time μs | Arrival time sec | Distance ft | |
| 10 | 9580 | 0.00958 | 15.8114 | 17380 | 0.01738 | 18.0278 | 284 |
| 15 | 19520 | 0.01952 | 18.0278 | 28730 | 0.02873 | 21.2132 | 346 |
| 20 | 61192 | 0.061192 | 21.2132 | 69620 | 0.06962 | 25 | 450 |
| 25 | 63140 | 0.06314 | 25 | 73420 | 0.07342 | 29.1548 | 405 |
| 30 | 73940 | 0.07394 | 29.1548 | 83250 | 0.08325 | 33.541 | 472 |
| 35 | 77430 | 0.07743 | 33.541 | 83720 | 0.08372 | 38.0789 | 722 |
| 40 | 81100 | 0.0811 | 38.0789 | 92070 | 0.09207 | 42.72 | 424 |
| 45 | 95780 | 0.09578 | 42.72 | 98990 | 0.09899 | 47.4342 | 1469 |
| 50 | 99990 | 0.09999 | 47.4342 | 110630 | 0.11063 | 52.2015 | 449 |
| 55 | 115120 | 0.11512 | 52.2015 | 119970 | 0.11997 | 57.0088 | 992 |
| 60 | 132300 | 0.1323 | 57.0088 | 139350 | 0.13935 | 61.8466 | 687 |
| 65 | 146850 | 0.14685 | 61.84658 | 150658 | 0.15066 | 66.70832 | 1277 |
| 70 | 153270 | 0.15327 | 66.70832 | 157550 | 0.15755 | 71.58911 | 1140 |
| 75 | 166030 | 0.16603 | 71.58911 | 169855 | 0.16986 | 76.48529 | 1280 |
| 80 | 184330 | 0.18433 | 76.48529 | 188338 | 0.18834 | 81.3941 | 1225 |

**Table A-4: Site-4-Gulshan 2:**

| Depth D ft | Geophone-1 | | | Geophone-2 | | | S wave Velocity ft/s |
|---|---|---|---|---|---|---|---|
| | Arrival time μs | Arrival time sec | Distance ft | Arrival time μs | Arrival time sec | Distance ft | |
| 8 | 19890 | 0.01989 | 6.708204 | 24840 | 0.02484 | 10 | 665 |
| 13 | 24900 | 0.0249 | 10 | 30320 | 0.03032 | 14.31782 | 797 |
| 18 | 29080 | 0.02908 | 14.31782 | 36200 | 0.0362 | 18.97367 | 654 |
| 23 | 36820 | 0.03682 | 18.97367 | 40640 | 0.04064 | 23.76973 | 1256 |
| 28 | 40660 | 0.04066 | 23.76973 | 47310 | 0.04731 | 28.63564 | 732 |
| 33 | 46660 | 0.04666 | 28.63564 | 54280 | 0.05428 | 33.54102 | 644 |
| 38 | 61020 | 0.06102 | 33.54102 | 73310 | 0.07331 | 38.47077 | 401 |
| 43 | 75750 | 0.07575 | 38.47077 | 79420 | 0.07942 | 43.41659 | 1348 |
| 48 | 75860 | 0.07586 | 43.41659 | 83860 | 0.08386 | 48.37355 | 620 |
| 53 | 87930 | 0.08793 | 48.37355 | 97730 | 0.09773 | 53.33854 | 507 |
| 58 | 100890 | 0.10089 | 53.33854 | 111760 | 0.11176 | 58.30952 | 457 |
| 63 | 105390 | 0.10539 | 58.30952 | 117010 | 0.11701 | 63.28507 | 428 |
| 68 | 121920 | 0.12192 | 63.28507 | 131640 | 0.13164 | 68.26419 | 512 |
| 73 | 121140 | 0.12114 | 68.26419 | 127880 | 0.12788 | 73.24616 | 739 |
| 78 | 127880 | 0.12788 | 73.24616 | 131640 | 0.13164 | 78.23043 | 1326 |
| 83 | 125640 | 0.12564 | 78.23043 | 131640 | 0.13164 | 83.21658 | 831 |

**Table A-5: Site-5-Kamrangichor:**

| Depth D ft | Geophone-1 | | | Geophone-2 | | | S wave Velocity ft/s |
|---|---|---|---|---|---|---|---|
| | Arrival time ms | Arrival time sec | Distance ft | Arrival time ms | Arrival time sec | Distance ft | |
| 8 | 12790 | 0.01279 | 3.354102 | 20030 | 0.02003 | 8.13941 | 661 |
| 13 | 31150 | 0.03115 | 13.08625 | 37140 | 0.03714 | 18.06239 | 845 |
| 18 | 17870 | 0.01787 | 8.13941 | 24120 | 0.02412 | 13.08625 | 791 |
| 23 | 92260 | 0.09226 | 38.02959 | 98270 | 0.09827 | 43.02615 | 831 |
| 28 | 97880 | 0.09788 | 43.02615 | 103880 | 0.10388 | 48.02343 | 833 |
| 33 | 104000 | 0.104 | 48.02343 | 110640 | 0.11064 | 53.02122 | 753 |
| 38 | 110640 | 0.11064 | 53.02122 | 118140 | 0.11814 | 58.01939 | 666 |
| 43 | 128640 | 0.12864 | 58.01939 | 135380 | 0.13538 | 63.01785 | 742 |
| 48 | 158640 | 0.15864 | 63.01785 | 163880 | 0.16388 | 68.01654 | 954 |
| 53 | 151880 | 0.15188 | 68.01654 | 157880 | 0.15788 | 73.01541 | 833 |
| 58 | 155380 | 0.15538 | 73.01541 | 160880 | 0.16088 | 78.01442 | 909 |
| 63 | 160140 | 0.16014 | 78.01442 | 164640 | 0.16464 | 83.01355 | 1111 |

**Table A-6: Site-6-Kafrul, Cantonment:**

| Depth D ft | Geophone-1 | | | Geophone-2 | | | S wave Velocity ft/s |
|---|---|---|---|---|---|---|---|
| | Arrival time μs | Arrival time sec | Distance ft | Arrival time μs | Arrival time sec | Distance ft | |
| 8.5 | 24910 | 0.02491 | 7.38241 | 31150 | 0.03115 | 10.7005 | 532 |
| 13.5 | 30470 | 0.03047 | 10.7005 | 35830 | 0.03583 | 14.9833 | 799 |
| 18.5 | 40920 | 0.04092 | 14.9833 | 48570 | 0.04857 | 19.6087 | 605 |
| 23.5 | 50200 | 0.0502 | 19.6087 | 56350 | 0.05635 | 24.3824 | 776 |
| 28.5 | 70950 | 0.07095 | 24.3824 | 74590 | 0.07459 | 29.2318 | 1332 |
| 33.5 | 75220 | 0.07522 | 29.2318 | 80600 | 0.0806 | 34.1248 | 909 |
| 38.5 | 84543 | 0.084543 | 34.12477 | 88970 | 0.08897 | 39.04485 | 1100 |
| 43.5 | 98270 | 0.09827 | 39.04485 | 102563 | 0.102563 | 43.98295 | 1150 |
| 48.5 | 116550 | 0.11655 | 43.983 | 121440 | 0.12144 | 48.9336 | 1012 |
| 53.5 | 106170 | 0.10617 | 48.9336 | 115950 | 0.11595 | 53.8934 | 507 |
| 58.5 | 93770 | 0.09377 | 53.8934 | 98540 | 0.09854 | 58.86 | 1041 |
| 63.5 | 99265 | 0.099265 | 58.86 | 103339 | 0.10334 | 63.83181 | 1220 |

**Table A-7: Site-7-Maniknagar:**

| Depth D ft | Geophone-1 | | | Geophone-2 | | | S wave Velocity ft/s |
|---|---|---|---|---|---|---|---|
| | Arrival time μs | Arrival time sec | Distance ft | Arrival time μs | Arrival time sec | Distance ft | |
| 8.5 | 40990 | 0.04099 | 9.19239 | 48760 | 0.04876 | 12.0208 | 364 |
| 13.5 | 61360 | 0.06136 | 12.0208 | 74260 | 0.07426 | 15.9531 | 305 |
| 18.5 | 67940 | 0.06794 | 15.9531 | 85140 | 0.08514 | 20.3593 | 256 |
| 23.5 | 90980 | 0.09098 | 20.3593 | 100460 | 0.10046 | 24.99 | 488 |
| 28.5 | 109920 | 0.10992 | 24.99 | 121500 | 0.1215 | 29.7405 | 410 |
| 33.5 | 100510 | 0.10051 | 29.7405 | 109220 | 0.10922 | 34.5615 | 554 |
| 38.5 | 108770 | 0.10877 | 34.5615 | 114510 | 0.11451 | 39.4271 | 848 |
| 43.5 | 115890 | 0.11589 | 39.4271 | 123760 | 0.12376 | 44.3227 | 622 |
| 48.5 | 123010 | 0.12301 | 44.3227 | 129760 | 0.12976 | 49.2392 | 728 |
| 53.5 | 130140 | 0.13014 | 49.2392 | 135380 | 0.13538 | 54.171 | 941 |
| 58.5 | 130130 | 0.13013 | 54.171 | 135050 | 0.13505 | 59.1143 | 1005 |
| 63.5 | 138380 | 0.13838 | 59.1143 | 142880 | 0.14288 | 64.0664 | 1100 |

**Table A-8: Site-8-Aftabnagar:**

| Depth D ft | Geophone-1 | | | Geophone-2 | | | S wave Velocity ft/s |
|---|---|---|---|---|---|---|---|
| | Arrival time μs | Arrival time sec | Distance ft | Arrival time μs | Arrival time sec | Distance ft | |
| 7.5 | 27120 | 0.02712 | 7.60 | 37600 | 0.0376 | 10.92 | 317 |
| 12.5 | 23260 | 0.02326 | 10.92 | 33780 | 0.03378 | 15.19 | 406 |
| 17.5 | 39220 | 0.03922 | 15.19 | 55400 | 0.0554 | 19.81 | 285 |
| 22.5 | 49600 | 0.0496 | 19.81 | 66620 | 0.06662 | 24.58 | 280 |
| 27.5 | 56640 | 0.05664 | 24.58 | 66160 | 0.06616 | 29.42 | 509 |
| 32.5 | 71320 | 0.07132 | 29.42 | 83940 | 0.08394 | 34.31 | 387 |
| 37.5 | 70440 | 0.07044 | 34.31 | 82500 | 0.0825 | 39.23 | 408 |
| 42.5 | 86620 | 0.08662 | 39.23 | 99000 | 0.099 | 44.16 | 399 |
| 47.5 | 92440 | 0.09244 | 44.16 | 104040 | 0.10404 | 49.11 | 427 |
| 52.5 | 98200 | 0.0982 | 49.11 | 106940 | 0.10694 | 54.07 | 567 |
| 57.5 | 108360 | 0.10836 | 54.07 | 119020 | 0.11902 | 59.034 | 466 |

**Table A-9: Site-9-Khilkhet:**

| Depth D ft | Geophone-1 | | | Geophone-2 | | | S wave Velocity ft/s |
|---|---|---|---|---|---|---|---|
| | Arrival time μs | Arrival time sec | Distance ft | Arrival time μs | Arrival time sec | Distance ft | |
| 8 | 30830 | 0.03083 | 4.87 | 42490 | 0.04249 | 8.87 | 343 |
| 13 | 44460 | 0.04446 | 8.87 | 51460 | 0.05146 | 13.55 | 669 |
| 18 | 52170 | 0.05217 | 13.55 | 63950 | 0.06395 | 18.40 | 412 |
| 23 | 59660 | 0.05966 | 18.40 | 67640 | 0.06764 | 23.32 | 616 |
| 28 | 66990 | 0.06699 | 23.32 | 74840 | 0.07484 | 28.26 | 630 |
| 33 | 74440 | 0.07444 | 28.26 | 79570 | 0.07957 | 33.22 | 967 |
| 38 | 81680 | 0.08168 | 33.22 | 88290 | 0.08829 | 38.19 | 752 |
| 43 | 87180 | 0.08718 | 38.19 | 93550 | 0.09355 | 43.17 | 781 |
| 48 | 94700 | 0.0947 | 43.17 | 102170 | 0.10217 | 48.15 | 667 |
| 53 | 100860 | 0.10086 | 48.15 | 109910 | 0.10991 | 53.14 | 551 |

**Table A-10: Site-10-RHD, Tejgaon:**

| Depth ft | Geophone-1 | | | Geophone-2 | | | S wave Velocity ft/s |
|---|---|---|---|---|---|---|---|
| | Arrival time μs | Arrival time sec | Distance ft | Arrival time μs | Arrival time sec | Distance ft | |
| 10 | 9400 | 0.0094 | 7.49 | 14520 | 0.01452 | 11.45 | 773 |
| 15 | 13680 | 0.01368 | 11.45 | 21300 | 0.0213 | 16.01 | 597 |
| 20 | 16400 | 0.0164 | 16.01 | 25980 | 0.02598 | 20.76 | 497 |
| 25 | 24380 | 0.02438 | 20.76 | 30800 | 0.0308 | 25.62 | 756 |
| 30 | 34340 | 0.03434 | 25.62 | 39800 | 0.0398 | 30.52 | 897 |
| 35 | 41660 | 0.04166 | 30.52 | 45820 | 0.04582 | 35.44 | 1184 |
| 40 | 48900 | 0.0489 | 35.44 | 52200 | 0.0522 | 40.39 | 1499 |
| 45 | 54780 | 0.05478 | 40.39 | 57820 | 0.05782 | 45.35 | 1631 |
| 50 | 70680 | 0.07068 | 45.35 | 73400 | 0.0734 | 50.31 | 1826 |
| 55 | 65840 | 0.06584 | 50.31 | 67840 | 0.06784 | 55.28 | 2486 |
| 60 | 78880 | 0.07888 | 55.28 | 80880 | 0.08088 | 60.26 | 2488 |
| 65 | 82020 | 0.08202 | 60.26 | 85000 | 0.085 | 65.24 | 1671 |
| 70 | 88400 | 0.0884 | 65.24 | 91220 | 0.09122 | 70.22 | 1767 |
| 75 | 99460 | 0.09946 | 70.22 | 102400 | 0.1024 | 75.21 | 1696 |

# Appendix B

**(Shear Wave velocities and SPT N Values at different Locations)**

**Table B-1: Site-1-BUET JIDPUS:**

| Depth ft | SPT N Value | Shear Wave Velocity ft/s |
|---|---|---|
| 5 | 2 | 136 |
| 10 | 5 | 433 |
| 15 | 14 | 758 |
| 20 | 18 | 1316 |
| 25 | 9 | 295 |
| 30 | 10 | 1324 |
| 35 | 14 | 1041 |
| 40 | 21 | 1572 |
| 45 | 20 | 656 |
| 50 | 30 | 1366 |
| 55 | 30 | 821 |
| 60 | 32 | 533 |
| 65 | 45 | 703 |
| 70 | 37 | 731 |
| 75 | 34 | 1286 |
| 80 | 22 | 1339 |

**Table B-2: Site-2-MIST:**

| Depth ft | SPT N Value | Shear Wave Velocity ft/s |
|---|---|---|
| 8.66 | 4 | 561 |
| 13.66 | 3 | 480 |
| 18.66 | 2 | 801 |
| 23.66 | 3 | 722 |
| 28.66 | 4 | 838 |
| 33.66 | 5 | 1158 |
| 38.66 | 5 | 410 |
| 43.66 | 5 | 730 |
| 48.66 | 6 | 447 |
| 53.66 | 7 | 1050 |
| 58.66 | 10 | 1056 |
| 63.66 | 8 | 1274 |
| 68.66 | 9 | 840 |
| 73.66 | 8 | 1121 |
| 78.66 | 10 | 1311 |

**Table B-3: Site-3-Hazaribag:**

| Depth ft | SPT N Value | Shear Wave Velocity ft/s |
|---|---|---|
| 10 | 1 | 284 |
| 15 | 1 | 346 |
| 20 | 2 | 450 |
| 25 | 2 | 405 |
| 30 | 4 | 472 |
| 35 | 10 | 722 |
| 40 | 14 | 424 |
| 45 | 8 | 1469 |
| 50 | 18 | 449 |
| 55 | 25 | 992 |
| 60 | 30 | 687 |
| 65 | 28 | 1277 |
| 70 | 31 | 1140 |
| 75 | 40 | 1280 |
| 80 | 46 | 1225 |

**Table B-4: Site-4-Gulshan 2:**

| Depth ft | SPT N Value | Shear Wave Velocity ft/s |
|---|---|---|
| 8 | 14 | 665 |
| 13 | 8 | 797 |
| 18 | 9 | 654 |
| 23 | 13 | 1256 |
| 28 | 16 | 732 |
| 33 | 18 | 644 |
| 38 | 19 | 401 |
| 43 | 34 | 1348 |
| 48 | 40 | 620 |
| 53 | 42 | 507 |
| 58 | 46 | 457 |
| 63 | 48 | 428 |
| 68 | 49 | 512 |
| 73 | 50 | 739 |
| 78 | 50 | 1326 |
| 83 | 50 | 831 |

**Table B-5: Site-5-Kamrangichor:**

| Depth ft | SPT N Value | Shear Wave Velocity ft/s |
|---|---|---|
| 8 | 8 | 661 |
| 13 | 10 | 845 |
| 18 | 11 | 791 |
| 23 | 15 | 831 |
| 28 | 20 | 831 |
| 33 | 28 | 833 |
| 38 | 32 | 753 |
| 43 | 42 | 666 |
| 48 | 50 | 742 |
| 53 | 50 | 954 |
| 58 | 48 | 833 |
| 63 | 48 | 909 |
| 68 | 50 | 1111 |

**Table B-6: Site-6-Kafrul, Cantonment:**

| Depth ft | SPT N Value | Shear Wave Velocity ft/s |
|---|---|---|
| 9 | 13 | 532 |
| 14 | 12 | 799 |
| 19 | 14 | 605 |
| 24 | 35 | 776 |
| 29 | 33 | 1332 |
| 34 | 36 | 909 |
| 39 | 50 | 1100 |
| 44 | 50 | 1150 |
| 49 | 43 | 1012 |
| 54 | 44 | 507 |
| 59 | 50 | 1041 |
| 64 | 50 | 1220 |

**Table B-7: Site-7-Maniknagar:**

| Depth ft | SPT N Value | Shear Wave Velocity ft/s |
|---|---|---|
| 9 | 2 | 364 |
| 14 | 3 | 305 |
| 19 | 5 | 256 |
| 24 | 9 | 488 |
| 29 | 15 | 410 |
| 34 | 17 | 554 |
| 39 | 23 | 848 |
| 44 | 30 | 622 |
| 49 | 35 | 728 |
| 54 | 33 | 941 |
| 59 | 28 | 1005 |
| 64 | 32 | 1100 |

**Table B-8: Site-8-Aftabnagar:**

| Depth ft | SPT N Value | Shear Wave Velocity ft/s |
|---|---|---|
| 8 | 3 | 317 |
| 13 | 6 | 406 |
| 18 | 7 | 285 |
| 23 | 6 | 280 |
| 28 | 5 | 509 |
| 33 | 7 | 387 |
| 38 | 8 | 408 |
| 43 | 12 | 399 |
| 48 | 15 | 427 |
| 53 | 11 | 567 |
| 58 | 12 | 466 |

**Table B-9: Site-9-Khilkhet:**

| Depth ft | SPT N Value | Shear Wave Velocity ft/s |
|---|---|---|
| 8 | 4 | 343 |
| 13 | 8 | 669 |
| 18 | 7 | 412 |
| 23 | 8 | 616 |
| 28 | 10 | 630 |
| 33 | 11 | 967 |
| 38 | 12 | 752 |
| 43 | 12 | 781 |
| 48 | 14 | 667 |
| 53 | 31 | 551 |

**Table B-10: Site-10-RHD, Tejgaon:**

| Depth ft | SPT N Value | Shear Wave Velocity ft/s |
|---|---|---|
| 10 | 15 | 773 |
| 15 | 12 | 597 |
| 20 | 8 | 497 |
| 25 | 8 | 756 |
| 30 | 20 | 897 |
| 35 | 32 | 1184 |
| 40 | 41 | 1499 |
| 45 | 43 | 1631 |
| 50 | 44 | 1826 |
| 55 | 46 | 2486 |
| 60 | 51 | 2488 |
| 65 | 50 | 1671 |
| 70 | 50 | 1767 |
| 75 | 50 | 1696 |

**Table B-11: Site-11-Mehernagar Uttara:**

| Depth ft | SPT N Value | Shear Wave Velocity ft/s |
|---|---|---|
| 10 | 2 | 561 |
| 20 | 3 | 495 |
| 30 | 2 | 502 |
| 39 | 5 | 758 |
| 49 | 15 | 820 |
| 59 | 35 | 830 |
| 69 | 36 | 1122 |
| 79 | 50 | 1332 |
| 89 | 58 | 1056 |
| 98 | 39 | 1706 |

**Table B-12: Site-12-Ashulia, Jubok Project:**

| Depth ft | SPT N Value | Shear Wave Velocity ft/s |
|---|---|---|
| 10 | 1 | 285 |
| 20 | 2 | 236 |
| 30 | 4 | 400 |
| 39 | 2 | 410 |
| 49 | 1 | 361 |
| 59 | 17 | 948 |
| 69 | 30 | 731 |
| 79 | 28 | 712 |
| 89 | 52 | 1000 |
| 98 | 60 | 1246 |

**Table B-13: Site-13-Mirpur-1, Avenue-2:**

| Depth ft | SPT N Value | Shear Wave Velocity ft/s |
|---|---|---|
| 10 | 2 | 302 |
| 20 | 10 | 610 |
| 30 | 12 | 633 |
| 39 | 18 | 626 |
| 49 | 20 | 984 |
| 59 | 23 | 840 |
| 69 | 28 | 774 |
| 79 | 29 | 912 |
| 89 | 31 | 754 |

**Table B-14: Site-14-Akash Nagar, Mohammadpur, Beribadh:**

| Depth ft | SPT N Value | Shear Wave Velocity ft/s |
|---|---|---|
| 10 | 10 | 676 |
| 20 | 22 | 1109 |
| 30 | 21 | 1168 |
| 39 | 22 | 1302 |
| 49 | 27 | 1214 |
| 59 | 22 | 1394 |
| 69 | 30 | 1050 |
| 79 | 35 | 1050 |

**Table B-15: Site-15-United City Project, Beraidh:**

| Depth ft | SPT N Value | Shear Wave Velocity ft/s |
|---|---|---|
| 10 | 2 | 462 |
| 20 | 5 | 312 |
| 30 | 1 | 305 |
| 39 | 1 | 430 |
| 49 | 1 | 492 |
| 59 | 1 | 443 |
| 69 | 40 | 804 |
| 79 | 10 | 1000 |

Table B-16: **Site-16-**Eas Nandipara:

| Depth ft | SPT N Value | Shear Wave Velocity ft/s |
|---|---|---|
| 10 | 5 | 413 |
| 20 | 15 | 790 |
| 30 | 11 | 1096 |
| 39 | 29 | 1410 |
| 49 | 35 | 1345 |
| 59 | 19 | 1102 |
| 69 | 21 | 1220 |

Table B-17: **Site-17-**Asian City, Dokhinkhan:

| Depth ft | SPT N Value | Shear Wave Velocity ft/s |
|---|---|---|
| 10 | 45 | 1309 |
| 20 | 40 | 2037 |
| 30 | 30 | 1200 |
| 39 | 21 | 1174 |
| 49 | 22 | 656 |
| 59 | 22 | 649 |
| 69 | 39 | 886 |